COO-4041-12
Distribution Category UC-64

BIOFOULING AND CORROSION STUDIES

FINAL REPORT

PART I

May 1, 1976 to December 31, 1977

by

L. M. MAHALINGAM

This work was supported by the Department of Energy, Solar Energy Division, under Contract No. EY-76-S-02-4041.

DISCLAIMER

DOE/ET/20310--12

DE83 001012

DOE/ET/20310--12

COO-4041-12

Distribution Category UC-64

BIOFOULING AND CORROSION STUDIES

FINAL REPORT

PART I

May 1, 1976 to December 31, 1977

MASTER

by

L. M. MAHALINGAM

J. G. Fetkovich, Program Manager

Carnegie-Mellon University
Pittsburgh, PA 15213

This work was supported by the Department of Energy, Solar Energy Division, under Contract No. EY-76-S-02-4041.

CONTENTS

List of Figures

ABSTRACT

This report describes the work done by the Biofouling Research Group at Carnegie-Mellon University (CMU) during the period May 1, 1976 to December 31, 1977. This work was carried out for the Energy Research and Development Administration under the Ocean Thermal Energy Conversion (OTEC) program. During this period the University of Hawaii was a subcontractor to CMU and contributed to our field experiments at Hawaii. Three sets (seven total) of biofouling experiments were conducted. Two of these sets were done in the Pacific Ocean at Keahole Point, Hawaii, and one was in the Caribbean at St. Croix, Virgin Islands. Data and results from these experiments are presented and discussed. Heat transfer, biological, and metallurgical measurements are presented. A brief account of the data analysis procedures, and an assessment of the hardware performance are given. We conclude the report with suggestions and recommendations to improve the quality of the current efforts in the OTEC Biofouling, Corrosion and Materials program.

1. INTRODUCTION

This report summarizes the results and recommendations of the group based on the work carried out for the Energy Research and Development Administration (ERDA) during the period May 1, 1976 to December 31, 1977. Under normal operating conditions, both in the evaporator and in the condensor of an OTEC plant, there will be a temperature drop of about 1°C between the flowing sea water and the heat exchanger surface. It is expected that the sea water side of the heat exchanger surface will suffer biofouling, chemical corrosion and scaling. Prior to this work, no data relevant to these problems existed under conditions closely approximating those in an OTEC heat exchanger. We had developed a novel technique to measure the heat transfer coefficient with a small ΔT ($\sim$1°C) and with high precision (better than 1%). Part of the power of this technique is that it does not involve absolute calibration of thermometers or power sources. Thus, it can be used in remote locations for long periods of time. The necessary apparatus and procedures were subjected to extensive laboratory tests and found it to be satisfactory. This was the situation at the beginning of the contract period.

By December 31, 1977, field experiments had been successfully completed in three independent operations: two in the Pacific and one in the Caribbean. In these experiments, conducted for periods up to 20 weeks, various parameters, such as geographical location, heat exchanger material, heat exchanger surface preparation and flow velocity were varied. The first cleaning experiments were carried out as well. To date these results form the core of the available thermal data relevant to the OTEC heat exchanger design.

Some progress has been made in understanding the nature and origin of the fouling film causing the thermal resistance. However, there is no consensus about the nature of the film. More coordinated thermal, biological and metallurgical investigations are needed.

During this period we also played a major role in preparing and disseminating information about this device and training other interested research groups. These included personnel of the University of Hawaii, the Pacific Northwest Laboratories (PNL) of Battelle, the National Data Buoy Office (NDBO) of the National Oceanic and Atmospheric Administration (NOAA), the David Taylor Naval Ship Research and Development Center (NSRDC) of the U.S. Navy and Tracor Marine.

In this document we discuss three sets of experiments: aboard the moored research vessel NOII at Keahole Point, Hawaii, on a submerged buoy at Keahole Point, and aboard a navy barge off St. Croix, Virgin Islands. Two kinds of simulated heat exchanger tubes were used: aluminum and titanium. Two nominal flow velocities were used: 3 ft/sec and 6 ft/sec. We refer to these experiments by the shorthand notation: xyn, where x is a letter (N, B or S) representing the location of the experiment, y is a letter (A or T) representing the material of the heat exchanger tube, and n is a number (3 or 6) representing the nominal flow velocity. Thus, experiment BA3 refers to the run on the submerged buoy using an aluminum heat exchanger tube with a nominal flow velocity of 3 ft/sec.

2. HAWAII OPERATION

The satisfactory performance of the CMU heat transfer monitoring device under extensive laboratory tests indicated that this technique could be employed in the field to evaluate the effects of fouling, corrosion and scaling on the thermal performance of the simulated OTEC heat exchangers. At this stage, it was desired to develop a field version of this device which would be easier to use than the laboratory test unit. However, ERDA pressed for biofouling data urgently to meet the program goals, so the laboratory version was used in the field. The first opportunity to conduct field experiments was realized in collaborative efforts with the University of Hawaii in early 1976.

2.1. Experimental Data. The experiments were conducted in the Pacific Ocean off the coast of Keahole Point on the leeward side of the Big Island of Hawaii. The site is about 1100 feet from shore where the depth is about 250 feet (Fig. 2.1). Because of the location (close to the beach and on the leeward side of the island), the water is not believed to be typical of open ocean waters[1]. The level of biological activity in these waters is high. In one water characterization measurement, the bacterial count was 20,000/ml[2].

2.1.1. Noi'i Data. In early 1976, attempts were made to lay a submarine cable between submerged, buoy-mounted experimental units and a shore-based data acquisition system. However, an accident destroyed the cable and the attempt was aborted. It was found that the acquisition of a new submarine cable with the required properties would take many months. Because of ERDA's expressed urgency in acquiring the initial biofouling data, it was decided to run a preliminary experiment using equipment mounted on a vessel moored at the same site, thus eliminating the need of the submarine cable.

In the summer of 1976, the research vessel Noi'i of the University of Hawaii was moored at the site with two CMU heat transfer units set up as shown in Fig. 2.2.

These heat transfer monitor units, designed to measure precisely the thermal resistance, R_f, of the fouling layer in a simulated OTEC heat exchanger tube, are described in detail in another report[1]. Each unit was designed around a simulated heat exchanger tube 1 inch in diameter and 8-1/2 feet in length (Fig. 2.3). Each unit was connected to a pump which was located on the downstream side of the heat exchanger pipe (Fig. 2.4). The sea water was brought to the experimental units through approximately 40 feet of 2 inch reinforced plastic hose, from a depth of 20 feet. Both heat exchanger pipes were Al 6061-T6. One pipe, used with a flow velocity of 6 ft/sec, was used as received from the supplier, except that the surface was gently swabbed with acetone to remove grease and dirt. The other, used with a 3 ft/sec flow, was scrubbed clean with a nylon bristle brush and commercial cleanser (100 strokes). The flow through the heat exchanger pipes was continuous except during certain maintenance operations as tabulated in Tables 2.6 and 2.7. These pump shut-downs were typically an hour long. In addition, on data-taking days (Tables 2.1 and 2.2), the flow was stopped in the appropriate unit for a period of about 20 minutes (made up of four five-minute periods) to measure the zero reading of the flow meter.

The experiment involved measuring the heat transfer coefficient* from the inside wall of the heat exchanger pipe to the flowing sea water about once a week. This measurement is accomplished by repeating the measurements about 16 times on a typical data-taking day. Such repetition helps to check the reproducibility of the result, to assess the size of the random error and to improve the precision of the measured value. The analyzed results are presented in Tables 2.1 and 2.2. The same data are presented graphically in Fig. 2.5 where the thermal resistance of the fouling layer is plotted as a function of time. The typical precision in the measurement of h during the Noi'i operation is about 1-2% (Tables 2.1 and 2.2).

- - - - - - - - - -

*See Ref. 4 for details on how this is done.

In a clean tube, the value of h depends on the flow velocity as well as on water temperature. For ease of comparison, each value of h is normalized to a nominal temperature ($70^{\circ}F$) and flow velocity (the velocity corresponding to the chosen nominal value). The measured thermal resistance (1/h) is calculated and the difference between (1/h) and the initial value of (1/h) gives R_f. This is a measure of the thermal resistance on the seawater side of the heat exchanger pipe due to biological fouling, chemical precipitation from seawater (scale) and corrosion products. The tables contain a column labeled t_f which is an average thickness of this layer calculated assuming that it has the same thermal conductivity as sea water.

2.1.2. Buoy Data. As soon as a replacement submarine cable was obtained, preparations for sub-surface buoy experiments were started. The buoy was positioned about 50 feet under the surface in about 250 feet of water at about the same location as the Noi'i experiments were done. Fig. 2.6 shows the buoy in place while divers are mounting the experimental units on it. Also mounted on the buoy is the required electronics, such as switching relays and signal amplifiers. This electronics package acts as a slave to the master electronics placed in a shelter on the shore. Armored cable about 1500' feet long connects the beach-based electronics to the buoy electronics.

2.1.3. Cleaning Tests.

In February 1977, the Buoy Series I experiments were started with three simulated heat exchanger tubes. Two of these were Al 6061-T6 and one was Ti Grade 2. One Al 6061-T6 was operated at a nominal flow of 3 ft/sec and another at 6 ft/sec (actually about 7 ft/sec). The titanium pipe was operated at a nominal flow of 6 ft/sec (actually about 6.4 ft/sec). Before submersion, the waterside surfaces of all the pipes were treated in the same manner, i.e., scrubbed with a nylon bristle brush and commercial cleanser (100 strokes). In the experiments, the sea water was taken directly into the pipe through a fish screen. Thus the

pressure drop experienced by the fouling organisms before they encountered the heat transfer surface is only the frictional head of the flow and is about 3 feet of water.

As in the Noi'i experiments, we took 16 h measurements from each experimental unit once a week. Tables 2.3, 2.4 and 2.5 summarize the data for these three experiments. The corresponding thermal resistance values are plotted in Fig. 2.9. For each of the entries under column (h) in Tables 2.3, 2.4 and 2.5, two errors are quoted. The values given in parentheses are the statistical errors on the mean of the accepted cooling curves. Thus these numbers represent what the apparatus is capable of in relative precision. The other error is an estimate of the systematic error in velocity measurement. It is set at 1% based on calibration experiments on the Ramapo Mark V flow meters used in the apparatus. All subsequent error calculations (the errors quoted on R_f and t_f) are based on this assigned error of 1%.

As Fig. 2.9 shows, the Ti unit functioned for 10.6 weeks until its pump failed. The remaining two pumps stopped for an unknown period of time between 11.4 and 12.6 weeks. These pump stoppages apparently caused the structure exhibited by the data between 11.4 weeks and 16 weeks. The problems related to these flow stoppages are discussed in Section 6.4 and 7.4. Also, as shown in Fig. 2.9, the two Al 6061-T6 pipes were cleaned at 16.1 weeks and then allowed to refoul.

The cleaning results are presented in Fig. 2.9. First consider the 6 ft/sec experimental unit. At week 16.3, just before cleaning, R_f was 25.0 ± 1.4 (in units of Fig. 2.9). After one (back-and-forth) pass of the M.A.N. brush, R_f fell to -2.7 ± 1.2. After a total of six passes, R_f was reduced to -8.2 ± 1.2. The apparent negative values of R_f are due to equipment failure causing uncertainty in the flow velocity[3]. Next consider the 3 ft/sec unit. It had R_f = 34.7 ± 2.7 before cleaning. After one pass of the brush, R_f was reduced

to 44.6 ± 6.6 and after 11 passes to 29.8 ± 2.7. It was noted by the divers that there were barnacles visible inside this pipe. The cleaning was halted by the divers for fear that one of the barnacles might be dislodged and damage the flow meter and the pump.

As Fig. 2.9 shows, R_f increased rapidly and roughly linearly in both units after cleaning. It should be noted that the cleaning data were obtained after pump stoppages for lengths of time on the order of a few days. These stoppages might have affected the fouling film and thus the preliminary cleaning results presented here should be viewed with caution.

2.1.4. Biological Study. George Harvey of Pan Pacific Laboratories led a biofouling study at Keahole Point that centered on direct observations of the "fouling layer." This work was arranged to be done in conjunction with our heat transfer measuring experiments on board the Noi'i. Examined were: sea water samples; the Al pipes used for our experiments on board the Noi'i; glass slides that were submerged for different lengths of time; glass slides and sections of Al and Ti pipe that were in the flow downstream of the test units for different lengths of time.

The study indicates that bacteria and diatoms were the main components of the early biofouling in these tests. On the interior of the aluminum pipes used in the thermal experiments, there appear to be two layers of fouling. The layer closer to the pipe is scale which may have some bacteria in it. The layer closer to the flowing water is made of living organisms, their products, and particulate inorganic material. A large amount of glass in the form of fragments, fibers and spheres was found in these deposits. Local volcanic activity is believed to be the source of this glass. The section of titanium pipe showed only one layer of fouling, of biological material.

The report by George Harvey is Appendix A of this report.

Similar studies were conducted during our Buoy Series I experiments, but we are not in a position to report on the results of that work.

2.2. Hardware.

2.2.1. Basic Hardware Features - Design Document. During late 1976, an extensive document[4] was prepared for ERDA on the theory and practice of the high precision heat transfer monitor developed by our group. This document covers all the basic design details of the mechanical and electrical aspects of the device. It also covers the design details of the buoy-based slave electronics and the shore-based master electronics used in the buoy experiments. The document includes industry standard drawings, which detail the construction procedures, material requirements, recommended suppliers, quality assurance tests and assembly checklists. The design document is the primary source for details on the hardware.

2.2.2. Manual Data Acquisition System. A manual data acquisition system* for heat transfer monitoring device was designed, tested and extensively used in the laboratory. It was designed to be useful in a laboratory-like application, i.e., non-remote operation, and to be used as a back-up system if the primary data acquisition system should malfunction.

The system is shown in block-diagram form in Fig. 2.12. The three data signals, namely thermopile, thermistor and flow meter voltages from the experimental unit are available at the input end of the scanner. Under the control of the teletype interface (PS 91), the scanner sequentially switches these three signals to the low voltage Digital Multimeter (DMM). The output of the DMM is channelled to the teletype through the interface. The teletype generates a printout and a paper tape.

- - - - - - - - - -

*Appendix D of Reference 4 discusses this system in detail.

2.2.3. Automated Data Acquisition System. From early 1976, it was planned to design and build an automated data acquisition system to be operated with the heat transfer monitoring device. The designed system was based on an Intel 8080 microprocessor (μP). Here, we give a brief overview of this microprocessor-based system.

Under program control, the μP can run a series of cooling curves, acquire the raw data, dump it out on command and do preliminary analysis of the raw data. This automated system is shown in block diagram form in Fig. 2.13. The three data signals (namely thermocouple, thermistor and flow meter signals) arrive from the buoy electronics (Buoy Control*) to the shore-based beach electronics (Beach Control*) in the form of frequency-modulated pulses. The three counters shown count the signals simultaneously for a period of 1 second every 2 seconds. Each datum so digitized requires 2 bytes (8 bit long byte) of memory for storage. The μP system has 5K (5 x 1024) of random-access memory (RAM) and is adequate to store the data collected during one cooling curve.

Further, the μP system has 5K of read-only memory (ROM). The program that performs tasks such as controlling the experiment, acquiring the data, and reducing the data is stored in a little over 2K of ROM. The Intel 8080 monitor system and the floating-point arithmetic package (for real arithmetic) each requires 1K of ROM. The semi-processed data and the results of preliminary analysis are output to the teletype yielding a printout and a punched paper tape for further analysis.

Collecting the data using this facility proceeds as follows. The operator selects with the beach control the experimental unit he wants to run. Using the teletype, the operator types in the starting address of the program in the μP, then types in title and date, desired option to have a raw data dump, number of times cooling curve measurements are to be repeated, coefficients required to

- - - - - - - - - -

*See Ref. 4 for detailed design.

convert the flow meter data to flow velocity and thermistor data to temperature, and an approximate value for the time constant. The μP, through a 1-bit control signal to the beach electronics, turns on the heater. The heater is kept on for a period of about 10 time constants. Then the μP, through the same 1-bit control signal, turns off the heater. The signals are sampled once in 2 seconds and stored in RAM. The temperature of the block and the operating sequence during the cooling curve are as indicated in Fig. 2.14. Data are collected and stored during the 10th time constant (which is also the last) of the heating period and for the ten subsequent time constants (during thermal decay). After a long time, the thermopile output reaches an asymptotic value corresponding to a zero temperature differential between the reference and heater blocks.

The "analysis window" starts ten seconds after the heater is turned off and lasts one time constant. The time slots during the 9th and 10th time constants during decay are designated as the 1st and 2nd "asymptotic windows." The program averages the thermocouple reading during the 2nd asymptotic window, subtracts this value from each thermocouple reading during the analysis window, and computes the natural logarithm of each of these values. These zero-corrected logarithms of thermocouple decay data are later analyzed to yield a time constant. The μP program also computes the averages and rms deviations of the velocity and the temperature during the analysis window and the 1st and 2nd asymptotic windows. This temperature and velocity information is needed for normalization of results. This information is also useful in assessing the reliability of the time constant evaluated from the cooling curve. The μP also outputs an approximate time constant (based on just two decay points in the analysis window) to help the operator check the operational status of the experimental unit. The μP then repeats this process of running cooling curves, collecting, semi-processing and outputting the data a specific number of times.

After laboratory tests, the automated system was installed during September 1977, at Keahole Point and field tested. Data acquisition proceeded with the manual DMM-based system and the automated μP-based system being used in parallel.

These data were independently least-squares fitted to evaluate the time constant, τ. A rough estimate of τ is also available from the two-point evaluation mentioned above. All three of these values of τ agree within the errors. For example, in one test, involving ten cooling curves, the average and the error on the average for the time constants are (22.93 ± 0.19) seconds, (23.30 ± 0.35) seconds, and (23.38 ± 0.34) seconds, respectively. Since September 1977, the μP system has been in operation and is performing satisfactorily.

This automated data acquisition system has many advantages over the manual one. Acquiring about 16 cooling curves from an experimental unit using the manual data acquisition system used to tie up five to eight hours of operator time. The automated system reduces the amount of operator time needed to less than an hour. Furthermore, automated operation has increased the reliability and quality of the data because it has essentially eliminated human error (particularly the errors related to repetitious operations).

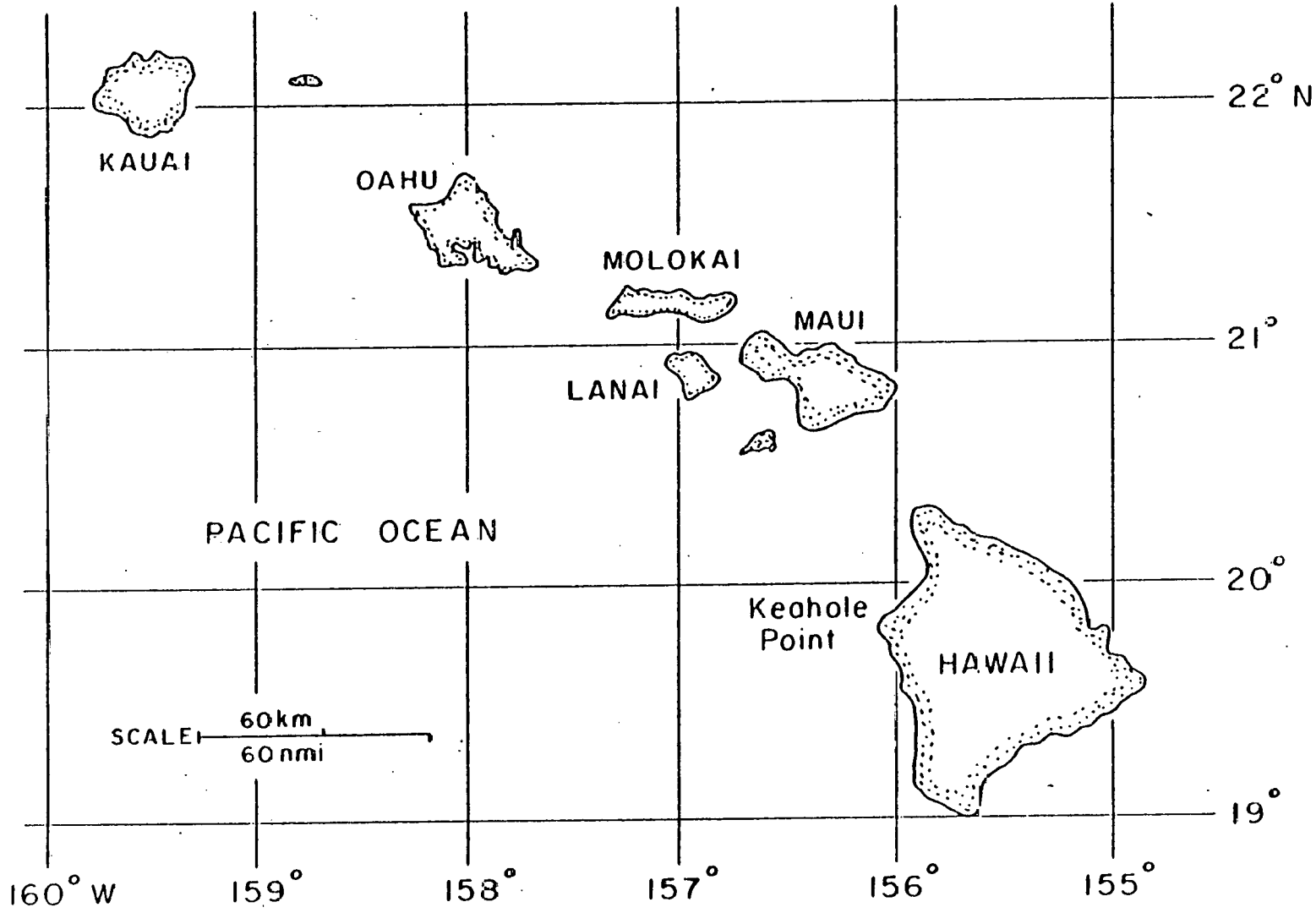

2.1 Map of Hawaiian Islands

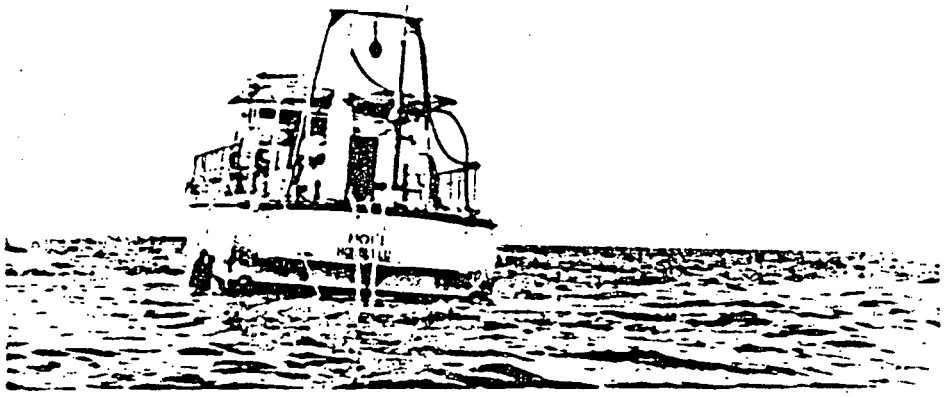

Figure 2.2 NA3 and NA6 experiments on the research vessel Noi'i moored in Pacific waters at Keahole Point, Hawaii.

LIST OF MATERIAL

ITEM	NO REQD	ORDERING INFORMATION	MATERIAL	SPEC	DETAIL DWG NO	VENDOR - PART NO	REMARKS	WT
1	1	HEAT EXCHANGER HOUSING			D-401			
2	1	TOP PVC PLATE (UP STREAM)			B-202			
3	1	BOTTOM PVC PLATE			B-215			
4	1	SIDE PVC PLATE			B-214			
5	1	FLOW PIPE CONNECTOR			C-300			
6	1	FLOW PIPE - TITANIUM			B-205			
	1	FLOW PIPE - ALUMINUM			B-206			
8	1	COPPER REFERENCE BLOCK			B-216			
9	2	HEATER BLOCK			B-217			
10	1	THERMOCOUPLE HEATER BLOCK			B-218			
11	1	CLAMP RING			B-204			
12	1	FLOW METER			B-219			
13	1	MICARTA DISC			B-208			
14	1	TOP SEAL PLATE			B-200			
	1	FLOW PIPE SUPPORT ASSEMBLY			D-400			
16	1	PIPE ASSEMBLY			C-301			
17	1	BOTTOM SEAL PLATE			B-201			
18	3	GASKET 6" I.P.S. - 1/8" THICK	NEOPRENE	COM'L.	-	PLASTIC PIPING SYS #15119	SEE NOTE "A"	
19	2	GASKET 1¼" I.P.S. - 1/8" THICK	NEOPRENE	COM'L.	-	PLASTIC PIPING SYS #15112	SEE NOTE "A"	
20	1	"O" RING - 1 5/8" I.D. x 3/16" WIDE	BUNA N	COM'L.	-	PARKER - #2-323	SEE NOTE "B"	
21	1	"O" RING - 1¼" I.D. x 3/16" WIDE	BUNA N	COM'L.	-	PARKER - #2-322	SEE NOTE "B"	
22	1	"O" RING - 1 5/8" I.D. x 3/16" WIDE	BUNA N	COM'L.	-	PARKER - #2-326	SEE NOTE "B"	

ITEM	NO REQD	ORDERING INFORMATION	MATERIAL	SPEC	DETAIL DWG NO	VENDOR - PART NO	REMARKS	WT
23	21	3/4"-10 x 4½" LG HEX HD BOLT	STN STL	COM'L	-			
24	3	3/4"-10 x 4¾" LG HEX HD BOLT	STN STL	COM'L	-			
25	24	3/4"-10 HEX NUT	STN STL	COM'L	-			
26	24	3/4" LOCKWASHER	STN STL	COM'L	-			
27	48	3/4" FLATWASHER	STN STL	COM'L	-			
28	8	1/4"-20 x 1½" LG T-READED ROD	STN STL	COM'L	-			
29	5	1/4"-20 x 3¼" LG T-READED ROD	STN STL	COM'L	-			
30	9	1/4"-20 x 1¾" LG SOC HD CAP SCR.	STN STL	COM'L	-			
31	3	5/16"-18 x 1" LG SOC HD CAP SCR.	STN STL	COM'L	-			
32	12	1/2"-13 x 2¼" LG HEX HD BOLT	STN STL	COM'L	-			
33	12	1/2"-13 HEX NUT	STN STL	COM'L	-			
34	12	1/2" FLATWASHER	STN STL	COM'L	-			
35	8	1/4" FLATWASHER	STN STL	COM'L	-			
36	22	1/4"-20 HEX NUT	STN STL	COM'L	-			
37	1	PIN CONNECTOR					SEE NOTE "C"	
38	1	THERMISTOR MOUNT			B-222			
39	1	THERMISTOR			B-222			
40	1	HOSE CLAMP # 28	STN STL	COM'L	-			
41	A.R.	PVC PRIMER					E-Z WELD	SEE NOTE "D"
42	A.R.	PVC CEMENT					E-Z WELD	SEE NOTE "D"

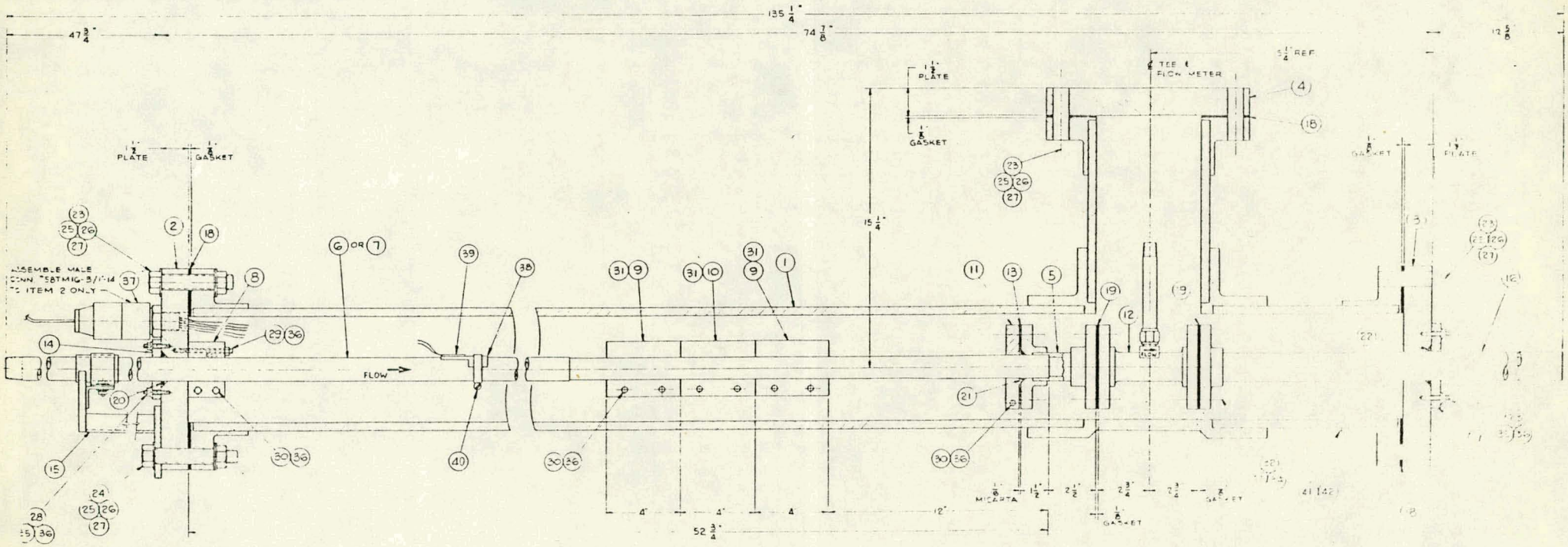

NOTES

"A" PLASTIC PIPING SYSTEMS - 50 PLAINFIELD, N.J. 07080 OR APPD EQUAL

"B" PARKER SEAL COMPANY - CULVER CITY, CALIF. 90230 OR APPD. EQUAL

"C" ELECTRO - PARAMOUNT, CALIF. 90723 OR APPD EQUAL
5 PINS - 10 CONTACTS (2 CONTACTS PER PIN)
ONE POLARIZING PIN
MALE - "SETMIG-3/1"-14 THD
FEMALE - "SIFIOF
CAPTIVE CPLG INCLUDED

"D" PCI INDUSTRIES INC - RIVIERA BEACH, FLORIDA OR APPD EQUAL

2.3 Cross-sectional view of the heat transfer monitor

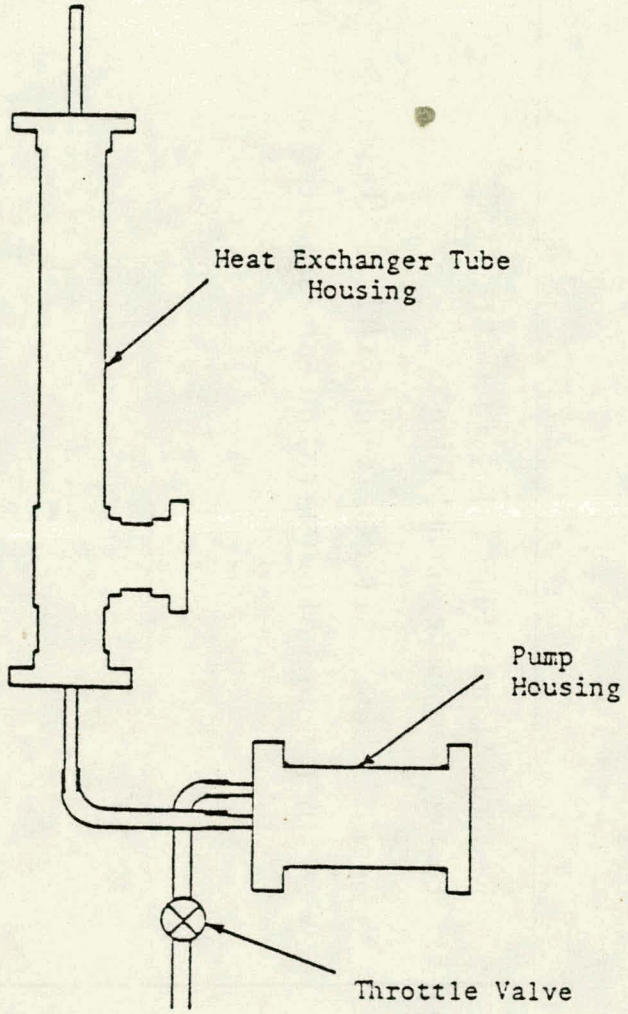

2.4 Heat Transfer Monitoring Unit showing pump attached

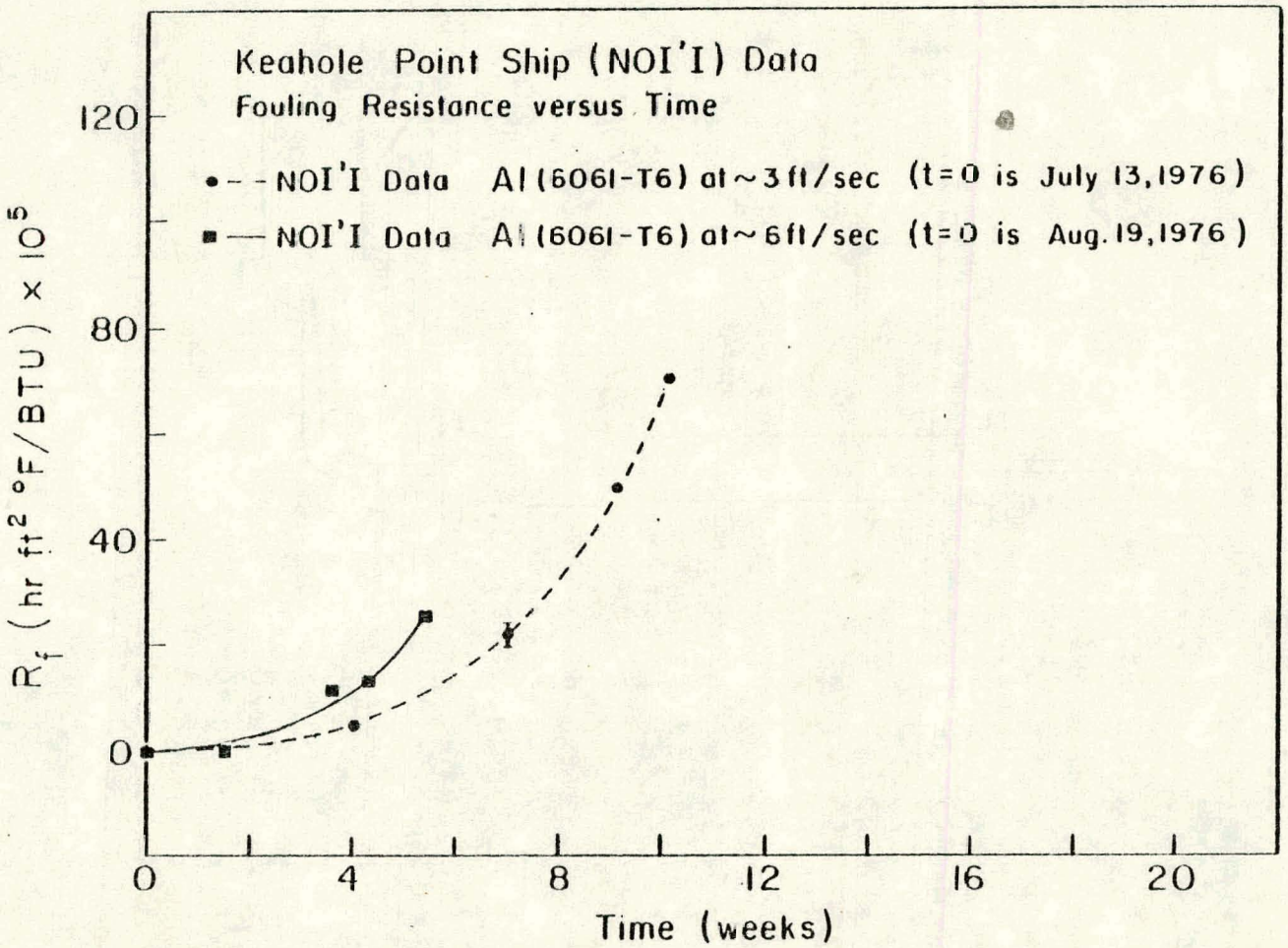

2.5 Thermal Resistance (R_f) vs. Time for Noi'i experiments at Keahole Point

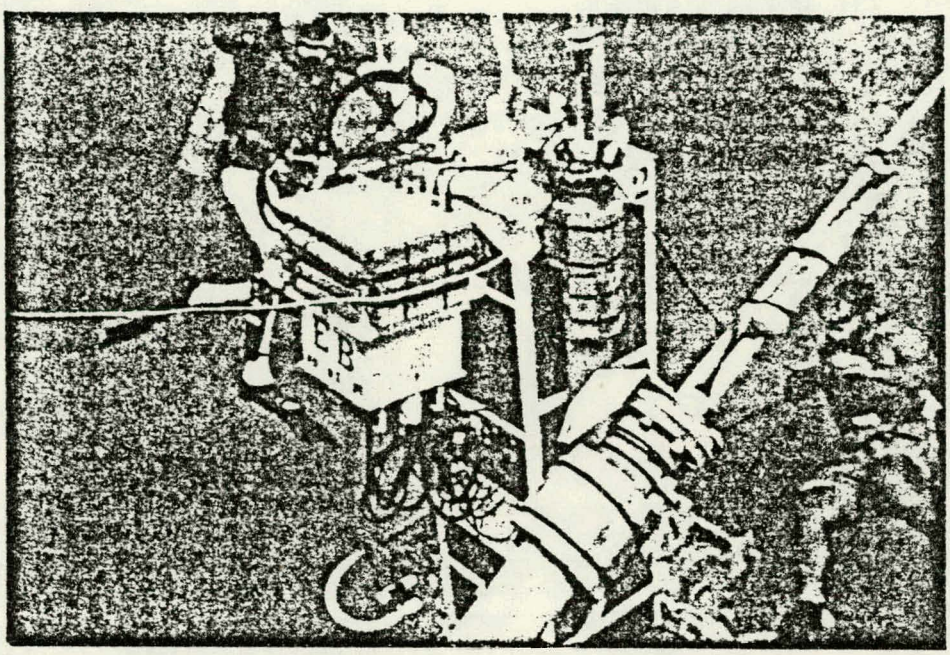

Figure 2.6 Divers mounting experimental units to submerged buoy.

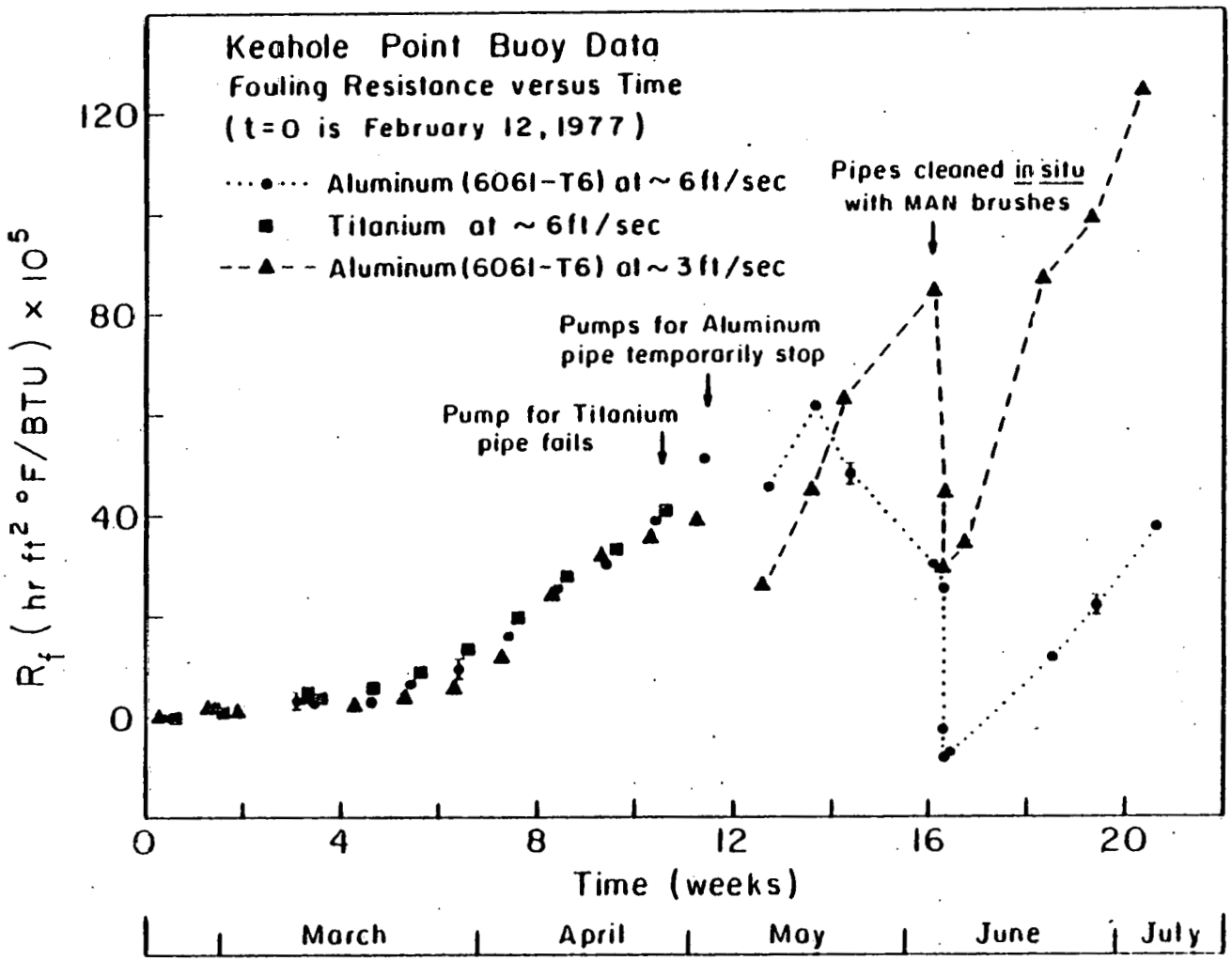

2.9 Thermal Resistance (R_f) vs. Time for Buoy Series I experiments at Keahole Point

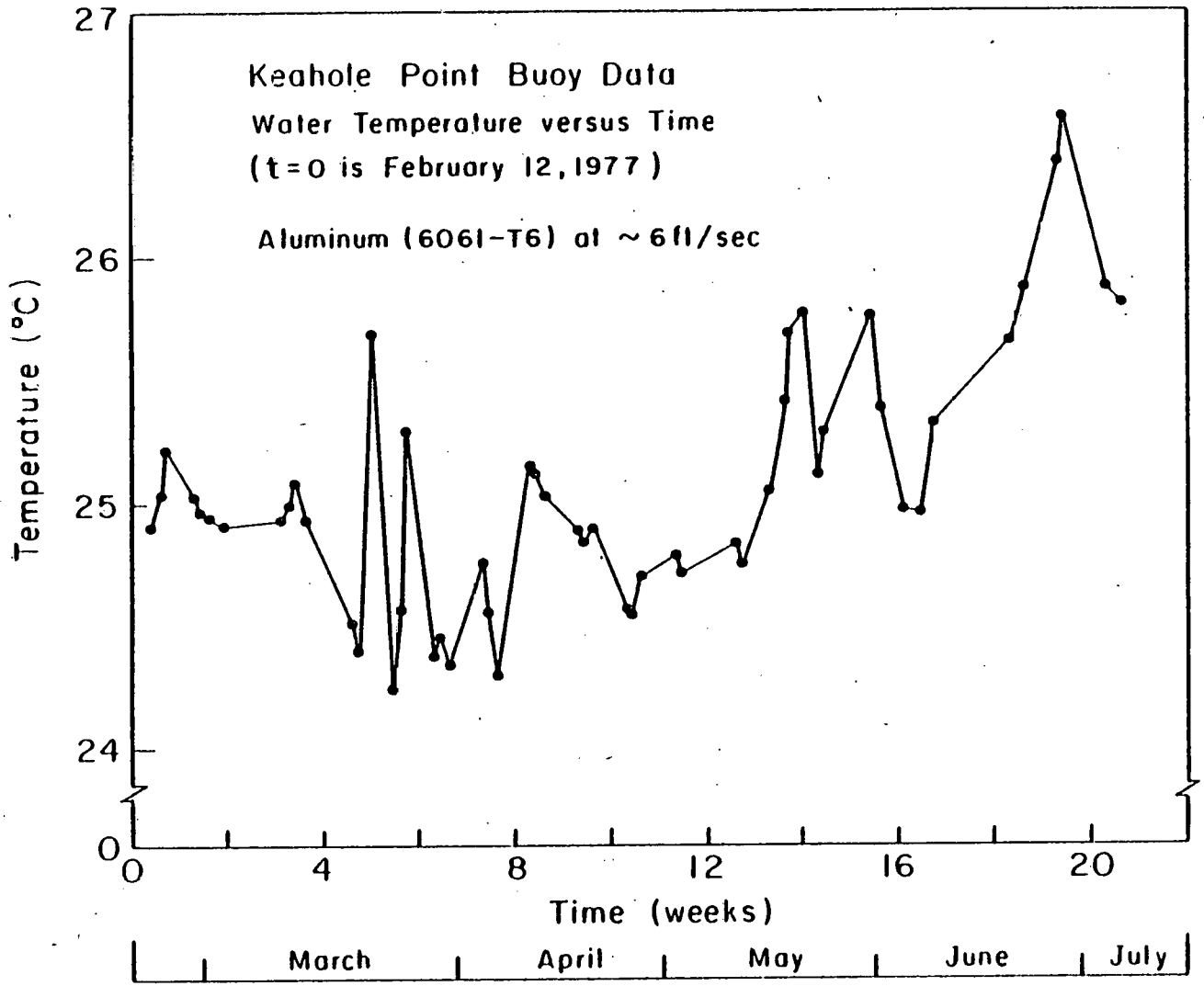

2.10 Water Temperature vs. Time for Buoy Series I experiments at Keahole Point

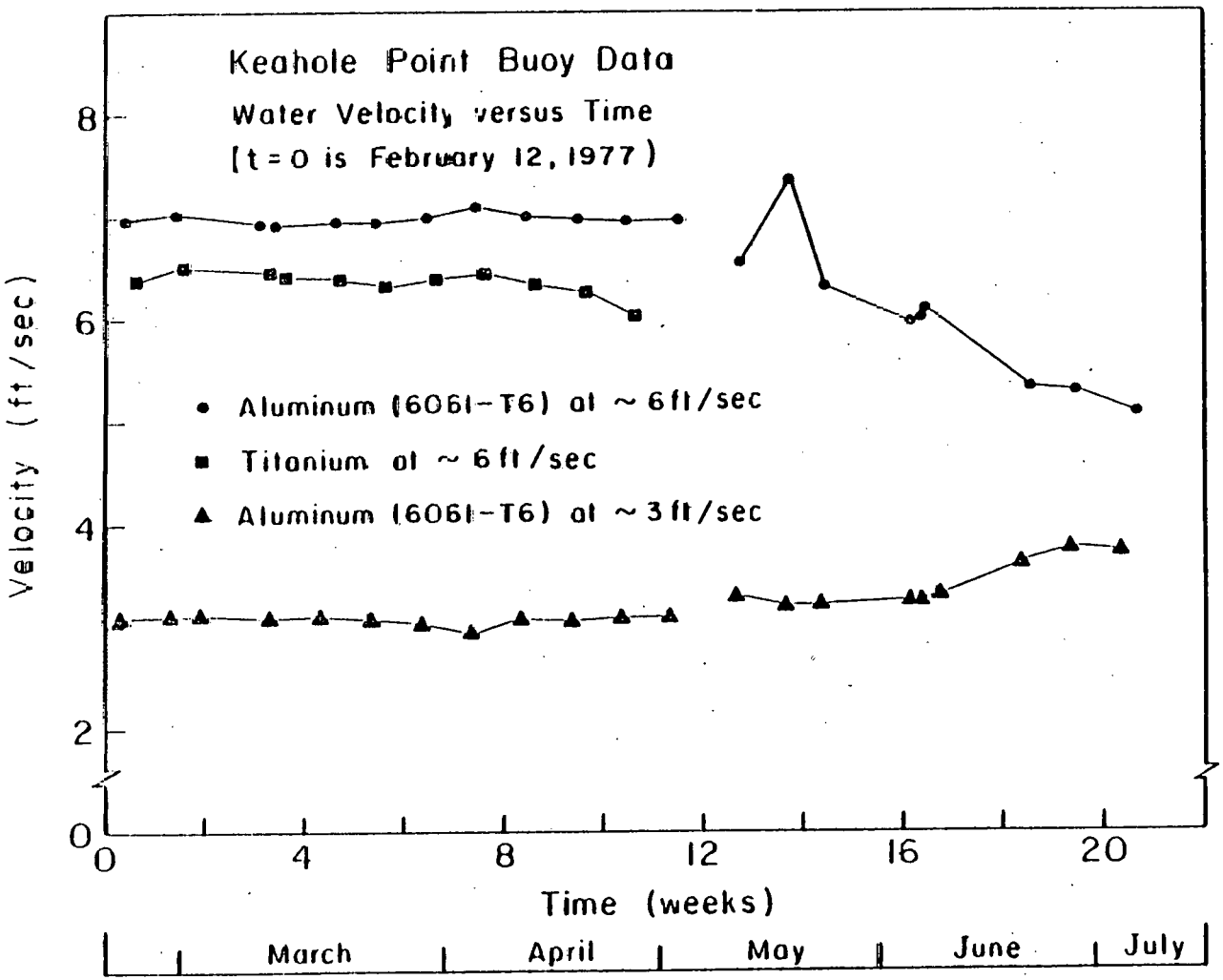

2.11 Flow Velocity vs. Time for Buoy Series I experiments at Keahole Point

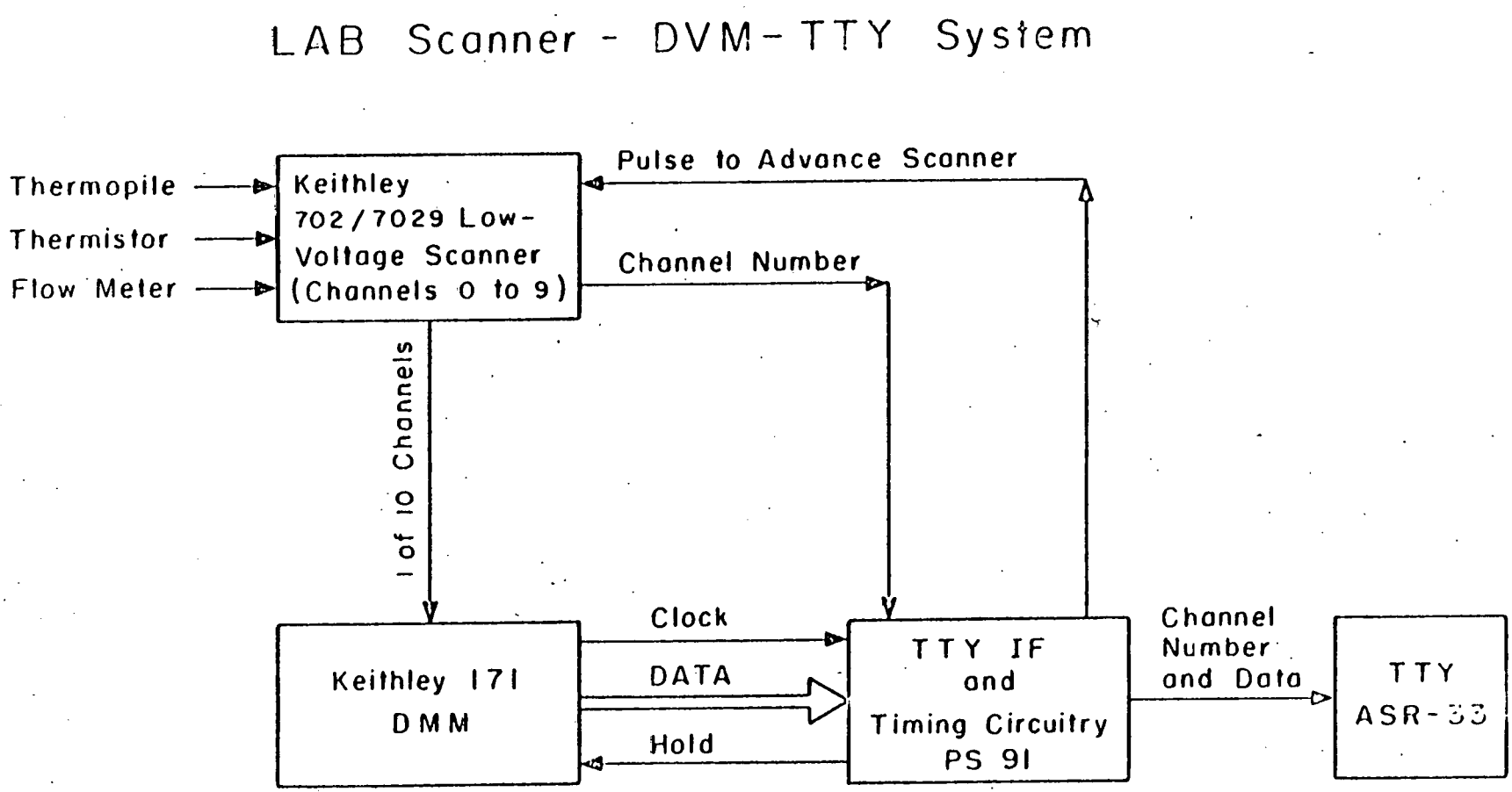

2.12 Block Diagram-Manual Data Acquisition System

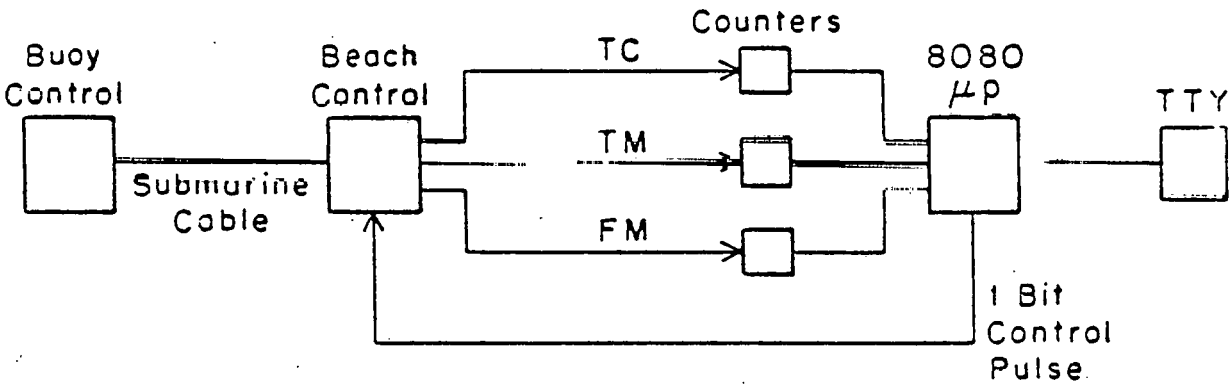

2.13 Block Diagram-Automated Data Acquisition System

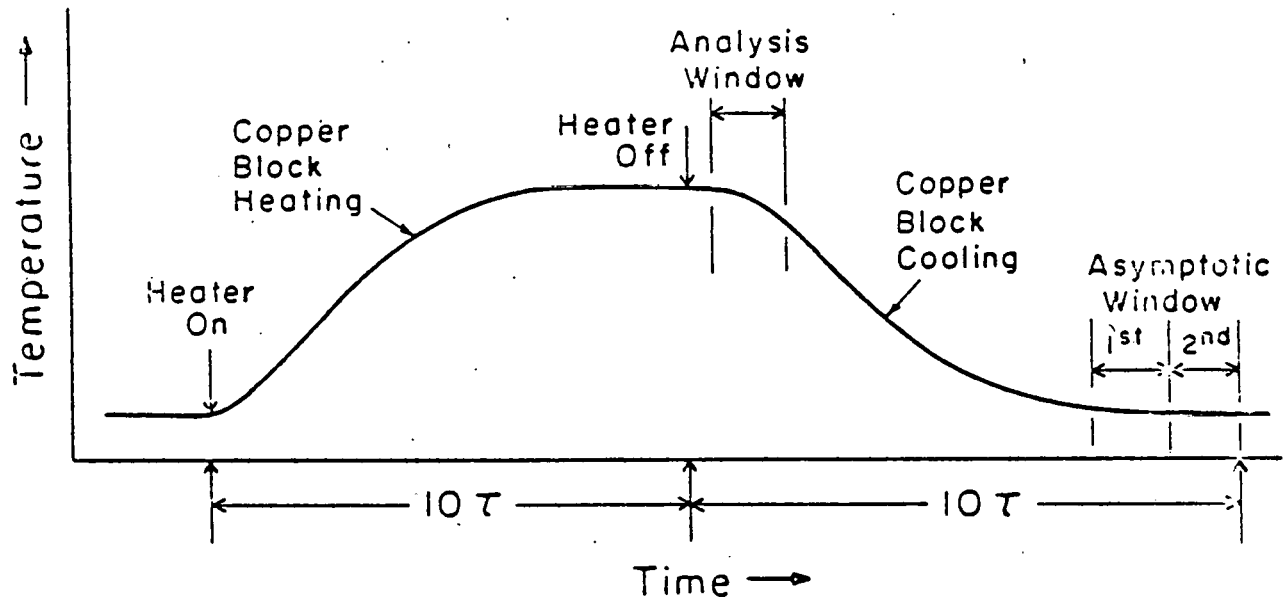

2.14 Time-Temperature relation during cooling curve measurement

TABLE 2.1

SUMMARY OF DATA FOR NAS EXPERIMENT

Nominal Flow Velocity: 3.0 ft/sec

Material: Aluminum (6061-T6)

Starting Time: July 13, 1976
Data Normalized to 70°F, 3 ft/sec

Time (Weeks)	$\langle h \rangle^{*}$ $\left(\frac{BTU}{hr\ ft^2\ ^oF}\right)$	$\Delta\langle(\frac{1}{h})\rangle = R_f$ $\left(\frac{hr\ ft^2\ ^oF}{BTU}\right) \times 10^5$	t_f (μm)
0	627.2 ± 8.0	0.0 ± 2.8	0.0 ± 3.0
4.0	608.8 ± 7.3	4.9 ± 2.8	5.2 ± 3.0
7.0	551.6 ± 4.3	21.9 ± 2.4	23.4 ± 2.6
9.1	478.8 ± 3.3	49.5 ± 2.4	52.8 ± 2.6
10.1	435.4 ± 3.7	70.2 ± 2.8	74.9 ± 3.0

* The errors quoted on <h> are on the mean and based on the reproducibility of the measurement.

TABLE 2.2

SUMMARY OF DATA FOR NA6 EXPERIMENT

Nominal Flow Velocity: 6.0 ft/sec

Material: Aluminum (6061-T6)

Starting Time: August 19, 1976
Data Normalized to 70°F, 6 ft/sec

Time (Weeks)	$\langle h \rangle^*$ $\left(\frac{\text{BTU}}{\text{hr ft}^2\ ^\circ\text{F}}\right)$	$\Delta\langle\left(\frac{1}{h}\right)\rangle = R_f$ $\left(\frac{\text{hr ft}^2\ ^\circ\text{F}}{\text{BTU}}\right) \times 10^5$	t_f (μm)
0	1083.9 ± 30.0	0.0 ± 3.7	0.0 ± 4.0
1.6	1079.0 ± 12.9	0.4 ± 2.8	0.4 ± 3.0
3.6	963.1 ± 11.1	11.5 ± 2.9	12.3 ± 3.1
4.3	946.6 ± 24.6	13.3 ± 3.7	14.2 ± 4.0
5.4	848.0 ± 14.9	25.6 ± 3.3	27.3 ± 3.5

* The errors quoted on <h> are on the mean and based on the reproducibility of the measurement.

TABLE 2.3

SUMMARY OF DATA FOR BA3 EXPERIMENT

Nominal Flow Velocity: 3.0 ft/sec

Material: Aluminum (6061-T6)

Starting Time: February 12, 1977
Data Normalized to 70°F, 3 ft/sec

Time (Weeks)	$\langle h \rangle^*$ $\left(\frac{BTU}{hr\ ft^2\ ^oF}\right)$	$\Delta\langle 1/h \rangle \equiv R_f$ $\left(\frac{hr\ ft^2\ ^oF}{BTU}\right) \times 10^5$	t_f (μm)
0.3	680 ± 7 (5)	0.0 ± 2.1	0.0 ± 2.2
1.3	671 ± 7 (1)	2.0 ± 2.1	2.1 ± 2.2
1.9	673 ± 7 (4)	1.6 ± 2.1	1.7 ± 2.2
3.3	661 ± 7 (1)	4.1 ± 2.1	4.4 ± 2.2
4.3	670 ± 7 (3)	2.3 ± 2.1	2.5 ± 2.2
5.3	662 ± 7 (1)	3.9 ± 2.1	4.2 ± 2.2
6.3	654 ± 7 (2)	5.8 ± 2.1	6.2 ± 2.2
7.3	629 ± 6 (3)	12.0 ± 2.2	12.8 ± 2.3
8.3	584 ± 6 (2)	24.2 ± 2.3	25.8 ± 2.5
9.3	559 ± 6 (1)	31.9 ± 2.3	34.1 ± 2.5
10.3	548 ± 5 (4)	35.6 ± 2.3	38.0 ± 2.5
11.3	538 ± 5 (2)	39.0 ± 2.4	41.6 ± 2.6
12.6	578 ± 6 (2)	25.9 ± 2.3	27.7 ± 2.5
13.6	523 ± 5 (4)	45.0 ± 2.4	28.0 ± 2.6
14.3	478 ± 5 (4)	63.0 ± 2.6	67.3 ± 2.8
16.1 (before cleaning)	432 ± 4 (2)	84.7 ± 2.7	90.4 ± 2.9
16.3 (after 1 pass)	522 ± 18	44.6 ± 6.6	47.6 ± 7.0
16.3 (after 11 passes)	566 ± 8	29.8 ± 2.7	31.8 ± 2.9
16.7	553 ± 6 (2)	34.0 ± 2.3	36.3 ± 2.5
18.3	427 ± 4 (1)	87.0 ± 2.7	92.9 ± 2.9
19.3	406 ± 4 (2)	99.0 ± 2.9	105.7 ± 3.1
20.3	368 ± 4 (1)	125.0 ± 3.1	133.4 ± 3.3

* The errors quoted on $\langle h \rangle$ are on the mean. The values given in the parentheses are based on the reproducibility of the measurement. The other error is an assigned value of 1% and due to the fact that our knowledge of flow velocity is limited. Errors on R_f and t_f are computed based on the 1% assigned error on h.

TABLE 2.4

SUMMARY OF DATA FOR BA6 EXPERIMENT

Nominal Flow Velocity: 6.0 ft/sec

Material: Aluminum (6061-T6)

Starting Time: February 12, 1977
Data Normalized to 70°F, 6 ft/sec

Time (Weeks)	$\langle h \rangle^*$ $\left(\frac{\text{BTU}}{\text{hr ft}^2\ ^\circ\text{F}}\right)$	$\Delta\langle 1/h \rangle \equiv R_f$ $\left(\frac{\text{hr ft}^2\ ^\circ\text{F}}{\text{BTU}}\right) \times 10^5$	t_f (μm)
0.4	1155 ± 12 (2)	0.0 ± 1.3	0.0 ± 1.4
1.4	1129 ± 11 (1)	2.0 ± 1.3	2.1 ± 1.4
3.1	1115 ± 11 (1)	3.1 ± 1.3	3.3 ± 1.4
3.4	1120 ± 11 (1)	2.7 ± 1.3	2.9 ± 1.4
4.6	1116 ± 11 (2)	3.0 ± 1.3	3.2 ± 1.4
5.4	1073 ± 11 (3)	6.6 ± 1.3	7.0 ± 1.4
6.4	1041 ± 10 (1)	9.5 ± 1.3	10.1 ± 1.4
7.4	975 ± 10 (1)	16.0 ± 1.3	17.1 ± 1.4
8.4	891 ± 9 (2)	25.6 ± 1.4	27.3 ± 1.5
9.4	858 ± 9 (3)	30.0 ± 1.5	32.0 ± 1.6
10.4	797 ± 8 (3)	38.9 ± 1.6	41.5 ± 1.7
11.4	726 ± 7 (4)	51.2 ± 1.7	54.7 ± 1.8
12.7	758 ± 8 (5)	45.4 ± 1.6	48.5 ± 1.7
13.7	673 ± 7 (2)	61.9 ± 1.7	66.1 ± 1.8
14.4	741 ± 7 (2)	48.4 ± 1.6	51.7 ± 1.7
16.1	858 ± 9 (2)	30.0 ± 1.4	32.0 ± 1.5
16.3 (before cleaning)	896 ± 9 (1)	25.0 ± 1.4	26.7 ± 1.5
16.3 (after 1 pass)	1192 ± 22	-2.7 ± 1.2	-2.9 ± 1.3
16.3 (after 6 passes)	1276 ± 13 (4)	-8.2 ± 1.2	-8.9 ± 1.3
16.4	1263 ± 13 (7)	-7.4 ± 1.2	-7.9 ± 1.3
18.3	1019 ± 10 (6)	11.3 ± 1.3	12.3 ± 1.4
19.4	912 ± 9 (5)	21.9 ± 1.4	23.4 ± 1.5
20.6	803 ± 8 (1)	37.9 ± 1.5	40.5 ± 1.6

* The errors quoted on $\langle h \rangle$ are on the mean. The values given in the parentheses are based on the reproducibility of the measurement. The other error is an assigned value of 1% and due to the fact that our knowledge of flow velocity is limited. Errors on R_f and t_f are computed based on the 1% assigned error on h.

TABLE 2.5

SUMMARY OF DATA FOR BT6 EXPERIMENT

Nominal Flow Velocity: 6.0 ft/sec
Material: Titanium (Grade 2)
Starting Time: February 12, 1977
Data Normalized to 70°F, 6 ft/sec

Time (Weeks)	$\langle h \rangle^*$ $\left(\frac{BTU}{hr\ ft^2\ ^oF}\right)$	$\Delta\langle 1/h \rangle \equiv R_f$ $\left(\frac{hr\ ft^2\ ^oF}{BTU}\right) \times 10^5$	t_f (μm)
0.6	1132 ± 11 (2)	0.0 ± 1.3	0.0 ± 1.4
1.6	1117 ± 11 (4)	1.2 ± 1.3	1.3 ± 1.4
3.3	1070 ± 11 (2)	5.2 ± 1.3	5.6 ± 1.4
3.6	1076 ± 11 (3)	4.6 ± 1.3	4.9 ± 1.4
4.7	1062 ± 11 (1)	5.9 ± 1.3	6.3 ± 1.4
5.6	1026 ± 10 (2)	9.2 ± 1.3	9.8 ± 1.4
6.6	980 ± 10 (1)	13.7 ± 1.3	14.6 ± 1.4
7.6	925 ± 9 (2)	19.8 ± 1.4	21.1 ± 1.5
8.6	859 ± 9 (1)	28.1 ± 1.5	30.0 ± 1.6
9.6	820 ± 8 (1)	33.6 ± 1.5	35.9 ± 1.6
10.6	773 ± 8 (2)	41.4 ± 1.6	44.2 ± 1.7

* The errors quoted are on the mean. The values given in the parentheses are based on the reproducibility of the measurement. The other error is an assigned value of 1% due to the limits on our knowledge of flow velocity. Errors on R_f and t_f are computed based on the 1% assigned error on h.

TABLE 2.6

LOG OF PUMP STOPPAGES FOR NA3 EXPERIMENT

Date 1976	Time (Weeks)	Length of Time Pumping was Stopped	Reason
July 15	0.3	65 min.	oil change
July 15	0.3	1-30 min.	extension cord to pump disconnected
July 18	0.7	48 min.	generator off
July 20	1.0	45 min.	oil change-generator
July 24	1.6	90 min.	generator repairs
July 25	1.7	30 min.	generator repairs
July 30	2.4	3 hr.	tank replaced; exhaust line wrapped
Aug. 1	2.7	20 min.	out of fuel
Aug. 2	2.9	30 min.	replace leaking tank
Aug. 13	4.4	60 min.	oil and filter change-generator
Aug. 27	6.4	70 min.	oil check-generator
Sept. 2	7.3	60 min.	oil change-generator
Sept. 13	8.9	?	breaker tripped
Sept. 22	10.1	<40 min.	generator tripped out
Sept. 27	10.9	?	oil change

TABLE 2.7

LOG OF PUMP STOPPAGES FOR NA6 EXPERIMENT

Date 1976	Time (Weeks)	Length of Time Pumping was Stopped	Reason
Aug. 27	1.1	70 min.	oil check-generator; necessary to reprime pump
Aug. 30	1.6	60 min.	flow valve left closed
Sept. 2	2.0	60 min.	oil change-generator
Sept. 13	3.6	?	breaker tripped; necessary to reprime pump
Sept. 13	3.6	?	lost prime during FMZ reading
Sept. 22	4.9	<40 min.	generator tripped out; necessary to reprime pump
Sept. 26	5.4	≤20 min.	lost prime when taking inflow samples
Sept. 27	5.6	?	oil change

SECTION 2 REFERENCES

1. K. H. Bathen, R. M. Kamins, D. Kornreich and J. E. T. Moncur of University of Hawaii, "An Evaluation of Oceanographic and Socio-Economic Aspects of a Nearshore Ocean Thermal Energy Conversion Pilot Plant in Subtropical Hawaiian Waters," submitted to National Science Foundation - RANN (April, 1975), p. 3.1-23.

2. Appendix A of this report.

3. J. G. Fetkovich, G. N. Grannemann, L. M. Mahalingam and D. L. Meier, "Degradation of Heat Transfer Rates Due to Biofouling and Corrosion at Keahole Point, Hawaii," Proceedings of the Ocean Thermal Energy Conversion (OTEC) Biofouling and Corrosion Symposium, edited by R. H. Gray (Pacific Northwest Laboratory, Seattle, WA, 1978), pp. 374-375.

4. J. G. Fetkovich, C. W. Fette, R. W. Findley, G. N. Grannemann, L. M. Mahalingam, D. L. Meier and P. D. Runco, "A System for Measuring the Effect of Fouling and Corrosion on Heat Transfer Under Simulated OTEC Conditions," DOE Report No. C00-4041-10, (1976).

3. ST. CROIX OPERATION

In the summer of 1977, biofouling studies were carried out on board a U.S. Navy Research and Development barge moored in about 12,000 feet of water, roughly seven miles north of the coast of St. Croix in the U.S. Virgin Islands (Fig. 3.1). The water here was characteristic of tropical water in the mixed layer. Unlike near Keahole Point, the St. Croix site was biologically typical of the open ocean. Water samples collected during the experiments showed bacterial populations below 10 cells/ml[1], much less than at Keahole Point.

The St. Croix operation was a collaborative effort among Carnegie-Mellon University, the University of Miami and Tracor Marine. Our group was responsible for the heat transfer measurements. Tracor Marine operated the barge for the U.S. Navy and provided the general field facilities and support. The University of Miami conducted the corrosion studies[2], microbiological studies[3] and water characterization measurements[3]. In this section, we will report on the thermal measurements.

3.1. Experimental Data. Heat transfer measurements were taken from two heat exchanger pipes, each of Al 6061-T6 (1 inch inner diameter, sch 40). Fig. 3.2 shows the experiments in progress with the two experimental units in their protective housings and mounted on the barge. Water was pumped to the units through flexible plastic tubing from a depth of 60 feet at nominal velocities of 3 ft/sec for one experiment and 6 ft/sec for the other. The pumps were located on the downstream side of the heat exchanger pipes. Before installation, the interior surface of each Al pipe was prepared by treating it with a 10% solution of NaOH at ambient temperature and then thoroughly rinsing the surface. It may be noted that this was a different method of surface preparation compared to those used in Hawaii. This method of surface preparation is believed to remove the heat treated oxide layer from the heat exchanger pipe surface and to enable the formation of a uniform oxide layer under controlled conditions[4].

Water temperature at the site during the 10-week experimental period was between 25C and 28.6C as shown in Fig. 3.3. Short-term temperature fluctuations (rms deviation) were of the order of 0.01C. The flow through each of the heat exchanger pipes was continuous during the 10-week experimental period. It was adjusted once, as shown in Fig. 3.4, which shows the flow velocity throughout the 10-week experimental period. Short-term velocity fluctuations were of the order of 0.2 ft/sec and 0.3 ft/sec for nominal flow of 3 ft/sec and 6 ft/sec, respectively. The short-term velocity variations experienced in these experiments were higher than those in the sub-surface buoy experiments at Hawaii (typically 0.01 ft/sec for a nominal flow of 6 ft/sec).

As in Hawaii, 16 heat transfer rate measurements were taken for each experimental unit about once a week. The values of h were then normalized to 70°F and to the appropriate nominal flow velocity. Table 3.1 summarizes h and R_f values for the 6 ft/sec aluminum pipe and Table 3.2 for the 3 ft/sec pipe. As seen from Tables 3.1 and 3.2, the precision of measurement of h is within 1%. The R_f data as a function of time are presented in a graphical form in Fig. 3.5.

3.2. Hardware. The heat transfer devices used in the St. Croix operation were similar to those employed in Hawaii. However, certain new features were incorporated to improve the modularity of the equipment and the quality of signals from them. Each pipe housing was fitted with a "pipe electronics" unit which contains pre-amplifiers and power supplies in order to bring the low level signals from the thermopile, flow meter and thermistor to the 0-10 V level before transmission.

Once the heat transfer experimental unit is assembled and put into operation, one has no access to the pipe electronics without interrupting the experiment. Therefore, high reliability was a major design criterion.

Another feature was the improved data acquisition system. It is very similar to the manual data acquisition system discussed in Sec. 2.2.2. Design details

of both the pipe electronics and the data acquisition system are given in a separate report[5].

The system performed satisfactorily during the entire experimental period. No flow stoppages occurred during the experiments at St. Croix and no problems arose with the flow meters. Upon disassembly the units were found to be free of macrofoulers. Presumably the constant flow prevented macrofoulers from attaching, as happened during the Buoy Series I experiments, where flow stoppages did occur.

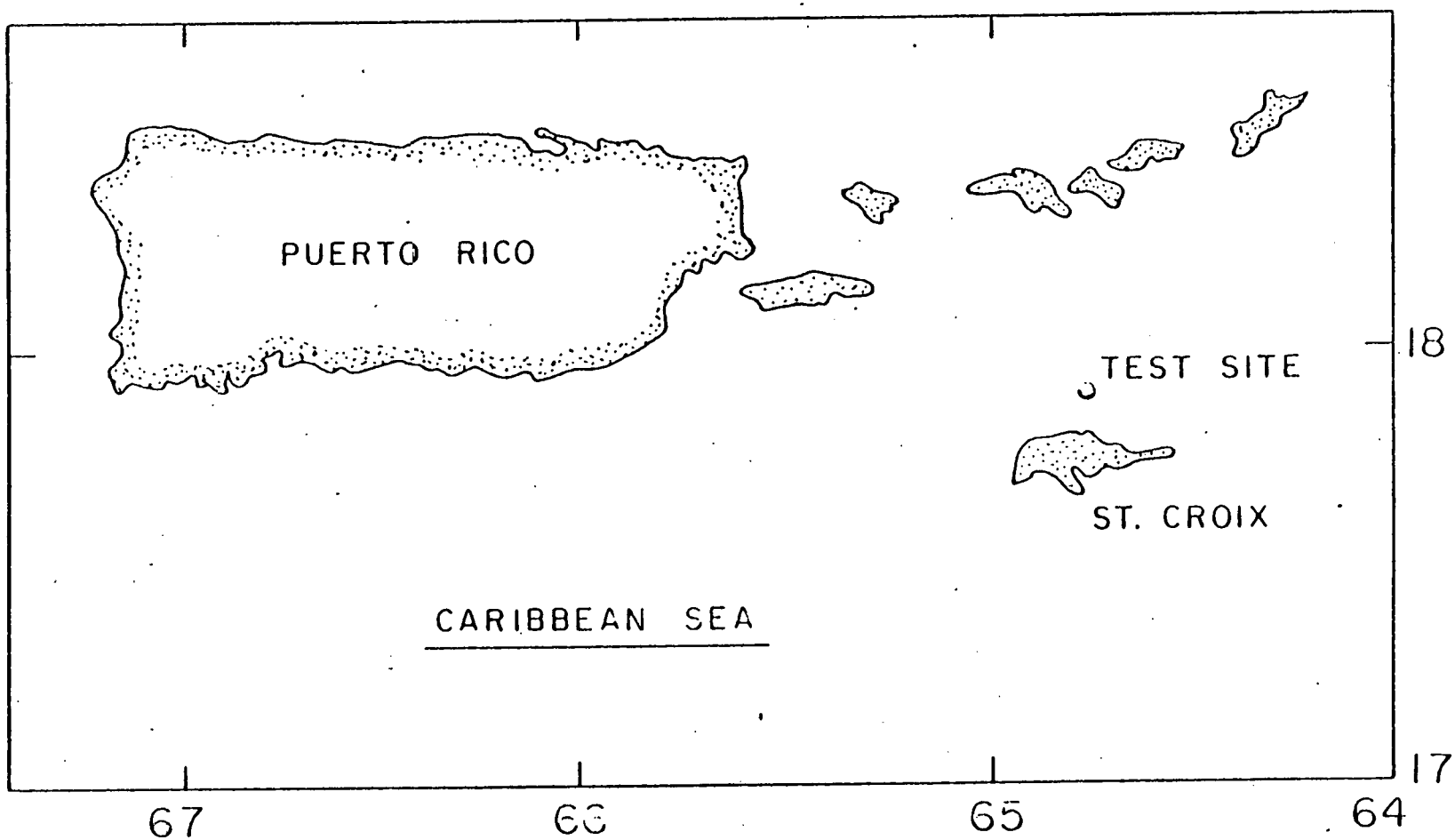

3.1 Location of the test site for the St. Croix operation

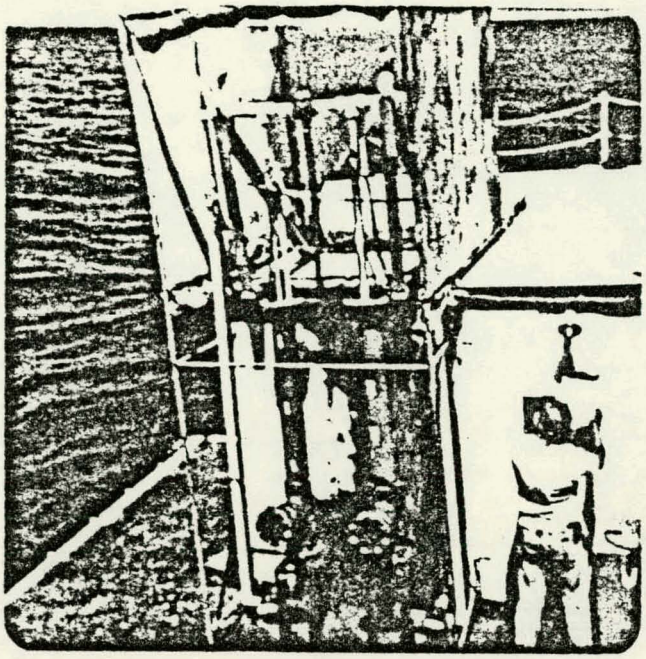

Figure 3.2 SA3 and SA6 biofouling experiments on board a U.S. Navy barge.

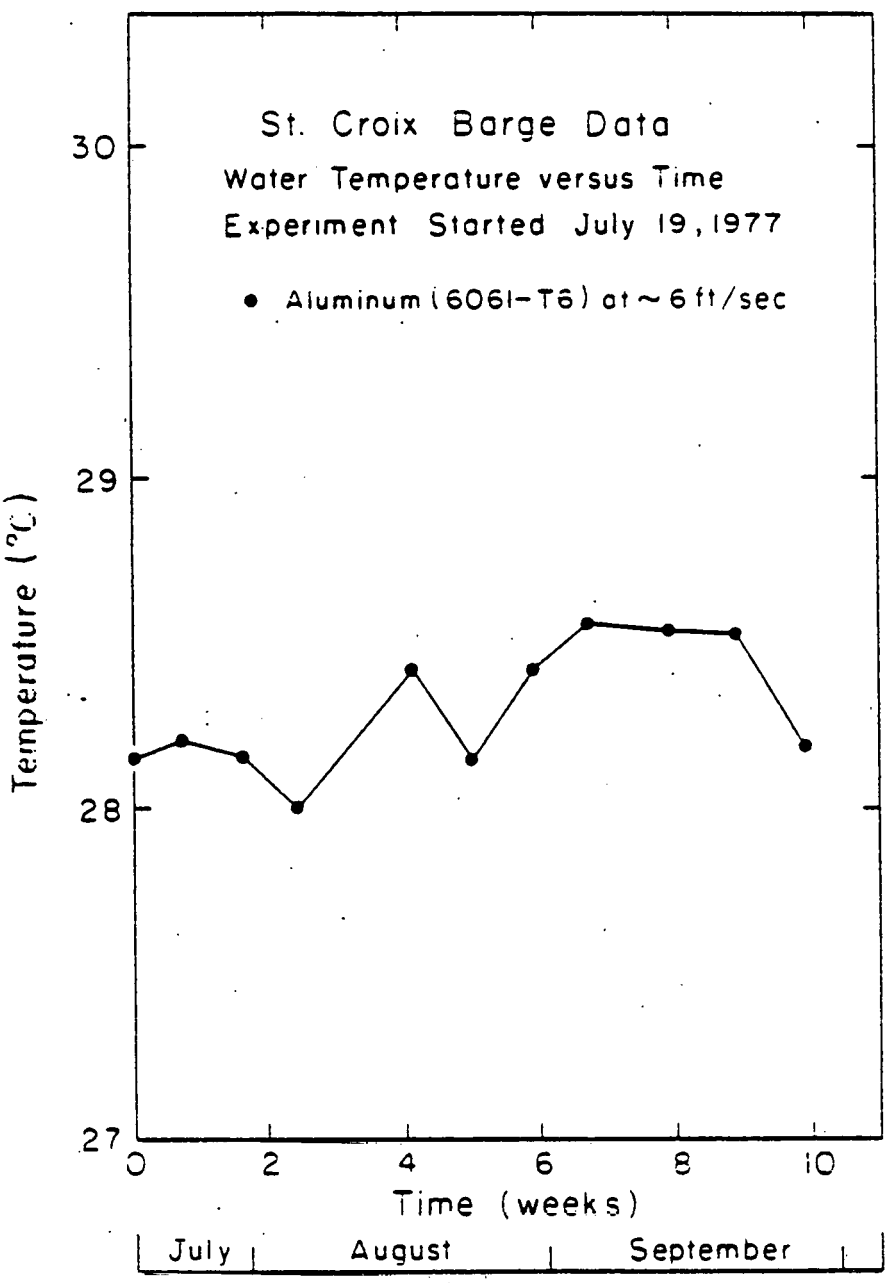

3.3 Water Temperature vs. Time for St. Croix experiments

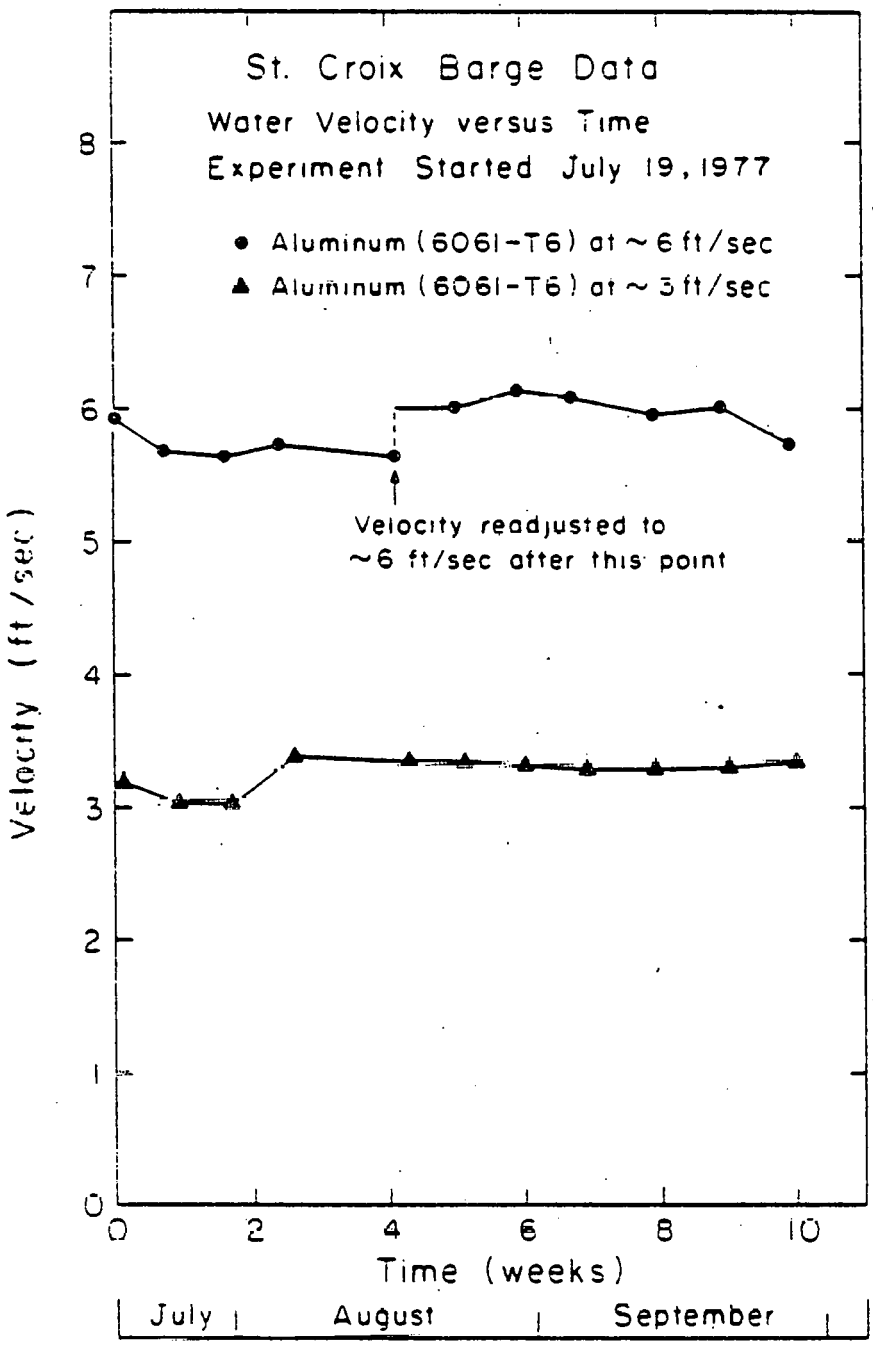

3.4 Water Velocity vs. Time for St. Croix experiments

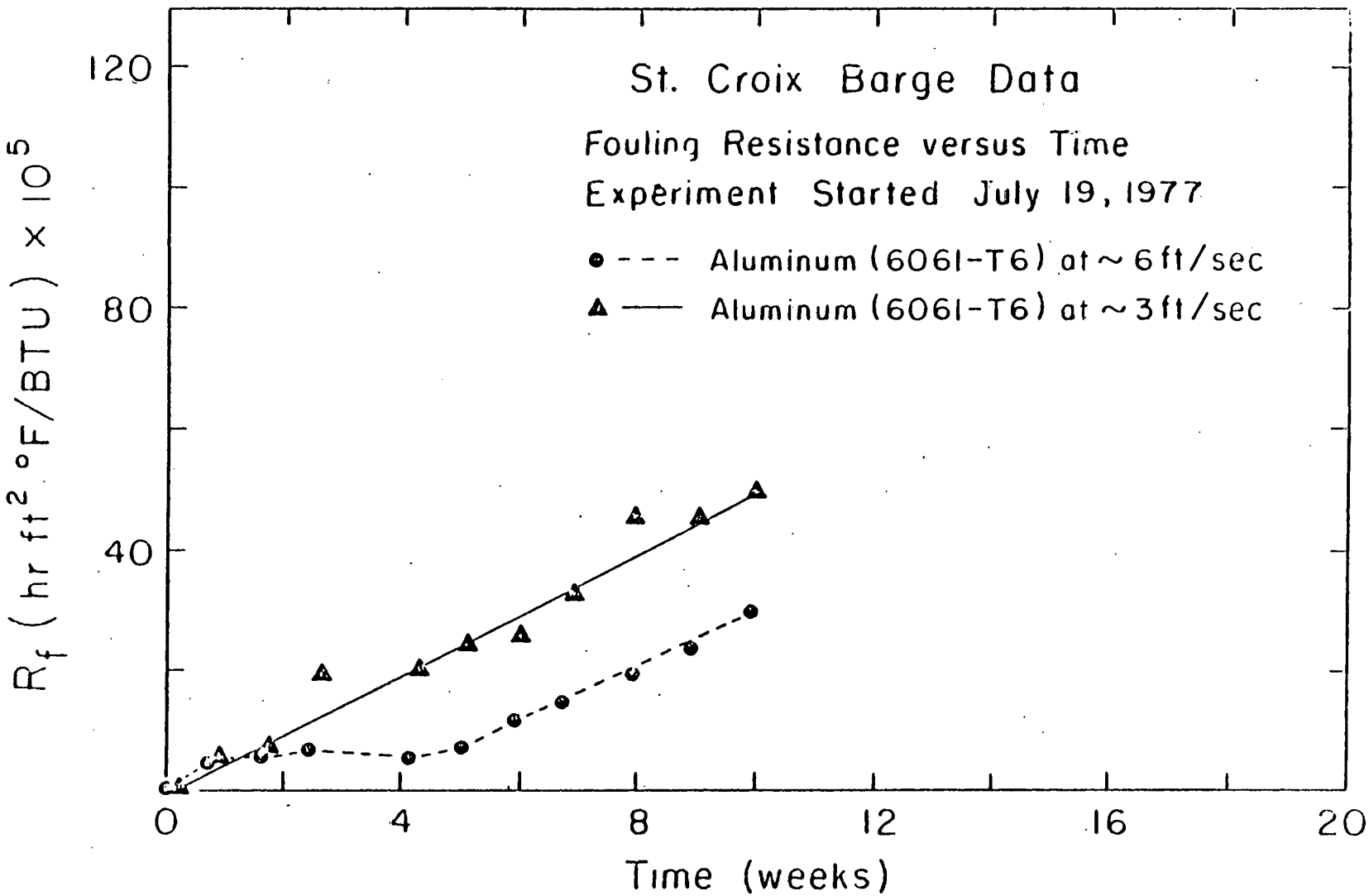

3.5 Thermal Resistance (R_f) vs. Time for St. Croix experiments

TABLE 5.1

SUMMARY OF DATA FOR SA6 EXPERIMENT

Nominal Flow Velocity: 6.0 ft/sec.

Material: Aluminum (6061-T6)

Starting Time: July 19, 1977
Data Normalized to 70°F, 6 ft/sec.

Time (Weeks)	$\langle h \rangle$ * $\left(\frac{BTU}{hr\ ft^2\ ^oF}\right)$	$\Delta\langle 1/h \rangle \equiv R_f$ $\left(\frac{hr\ ft^2\ ^oF}{BTU}\right) \times 10^5$	t_f (μm)
0.0	1178 ± 6	0.0 ± 0.7	0.0 ± 0.7
0.7	1122 ± 5	4.2 ± 0.6	4.5 ± 0.6
1.6	1107 ± 9	5.5 ± 0.8	5.9 ± 0.9
2.4	1090 ± 6	6.9 ± 0.7	7.4 ± 0.7
4.1	1106 ± 15	5.6 ± 1.3	6.0 ± 1.4
5.0	1086 ± 11	7.2 ± 1.0	7.7 ± 1.1
5.9	1036 ± 6	11.6 ± 0.7	12.4 ± 0.7
6.7	1005 ± 6	14.8 ± 0.6	15.8 ± 0.6
7.9	958 ± 4	19.5 ± 0.6	20.8 ± 0.6
8.9	921 ± 4	23.7 ± 0.7	25.3 ± 0.7
9.9	871 ± 3	30.0 ± 0.6	32.0 ± 0.6

* Errors quoted on h are on the mean and based on the repeatability of the measurement. Errors on R_f and t_f are computed from these errors on h.

TABLE 3.2

SUMMARY OF DATA FOR SA3 EXPERIMENT

Nominal Flow Velocity: 3.0 ft/sec.
Material: Aluminum (6061-T6)
Starting Time: July 19, 1977
Data Normalized to 70°F, 3 ft/sec.

Time (Weeks)	$\langle h \rangle$* $\left(\frac{BTU}{hr\ ft^2\ ^oF}\right)$	$\Delta\langle 1/h \rangle \equiv R_f$ $\left(\frac{hr\ ft^2\ ^oF}{BTU}\right) \times 10^5$	t_f (μm)
0.1	643 ± 2	0.0 ± 0.8	0.0 ± 0.9
0.9	622 ± 3	5.4 ± 1.0	5.8 ± 1.1
1.7	615 ± 4	7.1 ± 1.2	7.6 ± 1.3
2.6	571 ± 2	19.6 ± 1.0	20.9 ± 1.1
4.3	569 ± 3	20.3 ± 1.2	21.7 ± 1.3
5.1	556 ± 3	24.3 ± 0.8	25.9 ± 0.9
6.0	551 ± 1	26.0 ± 0.8	27.8 ± 0.9
6.9	531 ± 1	32.9 ± 0.6	35.1 ± 0.6
7.9	498 ± 1	45.2 ± 0.6	48.3 ± 0.6
9.0	498 ± 5	45.5 ± 2.1	48.6 ± 2.2
10.0	487 ± 4	49.7 ± 1.7	53.1 ± 1.8

* Errors quoted on h are on the mean and based on the repeatability of the measurement. Errors on R_f and t_f are computed from these errors on h.

SECTION 3 REFERENCES

1. J. Hirshman, D. L. Meier, R. S. C. Munier and B. F. Taylor, "Introduction to the St. Croix Biofouling and Corrosion Study," Proceedings of the Ocean Thermal Energy Conversion (OTEC) Biofouling and Corrosion Symposium, edited by R. H. Gray (Pacific Northwest Laboratory, Seattle, WA, 1978), p. 337.

2. H. L. Craig, Jr., R. S. C. Munier and J. Morse, "Corrosion Results from a 72-day Field Test of Simulated OTEC Aluminum Heat Exchanger Surfaces at St. Croix, U.S.V.I.," Proceedings of: The Fifth Ocean Thermal Energy Conversion Conference, edited by A. Lavi and T. N. Veziroglu (Clean Energy Research Institute, University of Miami, Miami, FL, 1978), pp. VIII-148-VIII-192.

3. R. P. Aftring, D. G. Capone, L. Duguay, J. W. Fell, I. M. Master and B. F. Taylor, "Biofouling and Site Characterization Studies in an Ocean Thermal Energy Conversion (OTEC) Experiment at St. Croix, U.S. Virgin Islands," Proceedings of: The Fifth Ocean Thermal Energy Conversion Conference, edited by A. Lavi and T. N. Veziroglu (Clean Energy Research Institute, University of Miami, Miami, FL, 1978), pp. VIII-45-VIII-72.

4. H. L. Craig, Jr., J. Nelson and R. S. C. Munier, "Cleaning Procedures for Aluminum Pipe and Tubing for Biofouling and Corrosion Experiments," Proceedings of the Ocean Thermal Energy Conversion (OTEC) Biofouling and Corrosion Symposium, edited by R. H. Gray (Pacific Northwest Laboratory, Seattle, WA, 1978), pp. 277-286.

5. R. W. Findley and D. L. Meier, "Design Report for PS-10S Data Acquisition System for Biofouling Studies of Heat Exchangers in Seawater," DOE Report No. C00-4041-6, (1977).

4. CORROSION STUDIES

In late 1977, we conducted some metallurgical measurements on heat exchanger pipe samples from the Noi'i, Buoy Series I, and St. Croix experiments.

Some of the objectives of this study were to understand the nature of the "fouling film"; its composition, its origin and the grain boundary structure at the interface of the "fouling film" and the heat exchanger pipe. Two different materials, Al 6061-T6 and Ti (Grade 2), were studied. Metallurgical techniques employed were metallography and the associated optical microscopy, scanning electron microscopy (SEM) and the associated electron excited x-ray energy analysis (E/EDAX), x-ray diffraction (XRD) and secondary ion mass spectroscopy (SIMS).

A more detailed report covering this investigation appears as Appendix B. In this section, we present a brief overview.

4.1. Samples. Samples from seven field experiments were studied. Six of the samples were Al 6061-T6 and one was Ti (Grade 2). There was one Al sample from each of the following experiments: NA3, NA6, BA3, BA6, SA3, and SA6. The Ti sample was from the BT6 experiment. It was not investigated in as much detail as the Al samples. At the conclusion of the experiments mentioned above, the heat exchanger pipes were drained and allowed to dry in the air. Samples were sectioned from the pipes and preserved in plastic bags until studied.

4.2. Fouling Film Thickness. For metallographic examination, approximately 0.25 in long sections of the heat exchanger pipe samples were cut. An approximately 400Å thick film of Au - 10% Pd alloy was deposited by vacuum deposition on these ring-shaped sections of pipe. This was followed by electrodeposition of ~20 μm of Ni. These sections were then ground, polished and optically examined under a stereo microscope. The thickness of the "fouling film" was measured both under the microscope and from the photographic record. For each sample, approximately 25 readings were taken around the ring and averaged. Table 4.1

presents the results of the fouling film thickness measurements from the micrographs as well as values calculated from the thermal measurements. The optical measurements are in rough agreement with the thermal measurements in most cases. However, Craig et al. reported a fouling film thickness of 1 to 6 μm for their analysis of St. Croix samples[1] using a weight loss technique. This differs seriously with our thickness measurements and points to the need to identify satisfactory techniques for such investigation. Further, there is an unresolved issue of relating dry-film thickness (obtained by metallurgical techniques) to that of wet-film (the thickness that actually exists during thermal measurements).

4.3. Nature of Fouling Film. Since it is anticipated that corrosion of the metal surface will be related to its grain structure, all samples were treated with an etchant to develop the grain boundary structure. Subsequently, they were examined optically. Although all the Al samples meet the standard specifications for 6061-T6 pipe, there were considerable variations in their response to the etchant, in the distribution and the size of grains and in the impurity inclusions. It was felt that such large variations are more closely related to the variations in the manufacturing procedures of Al 6061-T6 pipes than to any differences in their corrosion history.

The deposit material was studied using SEM over a wide range of magnifications. The "fouling film" exhibited typically a cracked, loosely adherent structure. Figures 4.1 and 4.2 show the typical matrix structure at two different magnifications. Biological materials such as diatoms, mollusk shells and stringy amorphous material seem to be anchored onto the matrix coating. Figures 4.3 and 4.4 show such bio-mass attachment.

As the samples were examined under SEM, the deposit material was analyzed by E/EDAX. Elements from Na and above on the periodic table were identified by this technique and their relative strengths were determined semi-quantitatively. All Al samples show that the "fouling film" has a high Al content, strongly

indicating that the film may have a chemical, rather than biological, origin. However, there is evidence to support the alternative view that the "fouling film" is biological in origin. This is discussed in Section 7.3.

In an attempt to identify the chemical constituents of the "fouling layer," some of the samples were subjected to SIMS. Also, some deposit material was carefully scraped off the pipe surfaces and analyzed by XRD using a Debye-Scherrer camera. The XRD work revealed a low degree of crystallinity for the material. The results of EDAX, SIMS and XRD, taken together, indicate that for the Al samples, the average deposit has Al and Ca as major components, Mg and organic material as minor components, and Si, Na and Cl as trace elements.

4.4. Recommendations. This investigation suggests some improvements needed in biofouling experiments and some features one would like to include in similar metallurgical investigations in the future.

- There is a great need to select alloys of Al that have better material control during the manufacturing process in terms of their resistance to corrosion.
- One would like to include within the realm of biofouling research a method to estimate the rate of metal loss in the heat exchanger pipes due to corrosion and erosion. It may be necessary to maintain control cross-sections cut from the heat exchanger pipe prior to the beginning of thermal measurements.
- Post-experimental techniques for measuring the thickness of the dry film need to be reviewed and correct techniques identified.
- The relation of dry-film thickness to wet-film thickness has to be resolved.
- An effort to assess the maximum rate of etch pit penetration must be instituted.

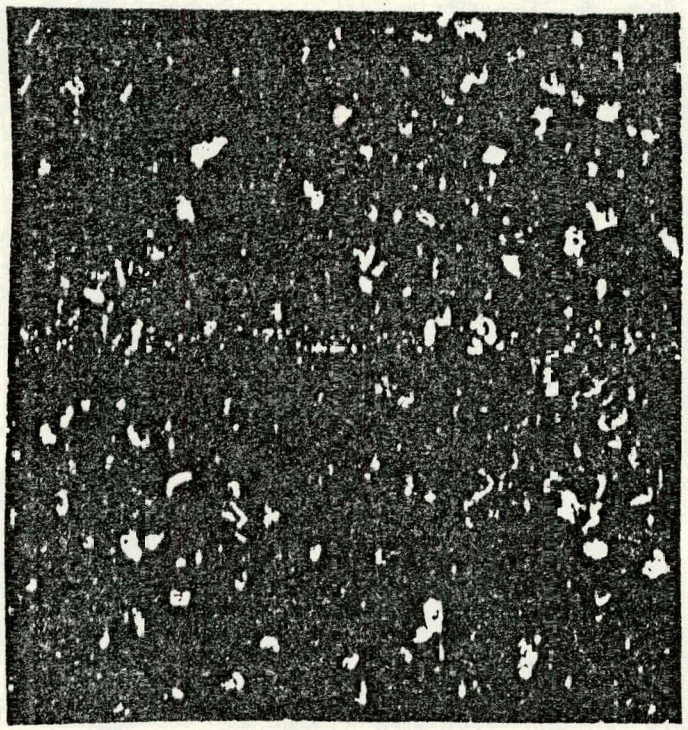

Figure 4.1 Typical Al 6061-T6 heat exchanger pipe surface under SEM at a magnification of 100. The sample is from NA6 experiment.

Figure 4.2 Fouled heat exchanger pipe surface under SEM at a magnification of 1000. The sample is from NA6 experiment.

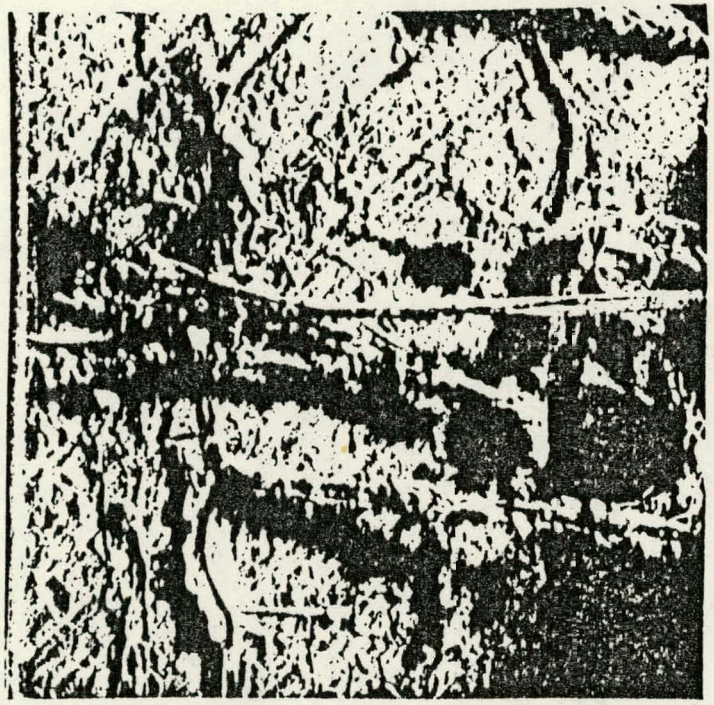

Figure 4.3 Biological material attached to the fouled heat exchanger surface. SEM picture of a sample from BA3 experiment at a magnification of 100.

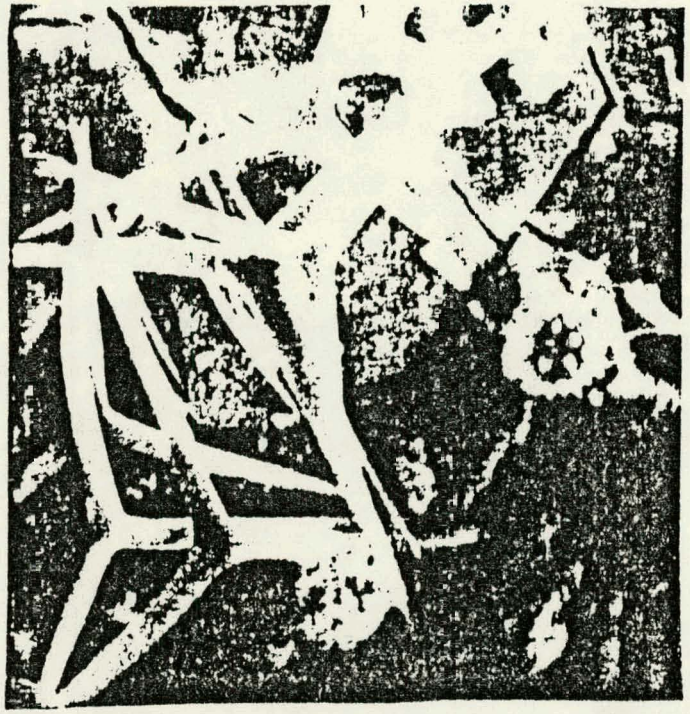

Figure 4.4 Biological material attached to the fouled heat exchanger pipe surface. SEM picture of a sample from BA3 experiment at a magnification of 3000.

TABLE 4.1

COMPARISON OF MICROGRAPH AND THERMAL MEASUREMENT OF FOULING LAYER THICKNESS: AL 6061-T6 SAMPLES

Experiment	Film Thickness (Micrograph) μm*	Film Thickness (Thermal) μm**
NA3	10 - 15	75
NA6	30 - 35	27
BA3	35 - 55+	133
BA6	35 - 40+	41
SA3	15 - 20	53
SA6	35 - 40	32

* Samples dried before examination

** Calculated from final value of R_f assuming that the thermal conductivity of fouling film is same as that of water.

\+ Sample handling after removal from buoy may have removed significant amounts of fouling material.

SECTION 4 REFERENCES

1. H. L. Craig, Jr., R. S. C. Munier and J. Morse, "Corrosion Results from a 72-day Field Test of Simulated OTEC Aluminum Heat Exchanger Surfaces at St. Croix, U.S.V.I.," Proceedings of: The Fifth Ocean Thermal Energy Conversion Conference, edited by A. Lavi and T. N. Veziroglu (Clean Energy Research Institute, University of Miami, Miami, FL, 1978), pp. VIII-148 - VIII-192.

5. DATA ANALYSIS

The thermal resistance of the fouling film is determined at any time by measuring the heat transfer coefficient (h) and comparing with h at the beginning of the experimental period (h_o). The thermal resistance is then computed as $R_f = 1/h - 1/h_o$. In this section, we will discuss data-taking and analysis.

5.1. Taking Data. At the beginning of the experiment, the heat transfer coefficient to the flowing sea water is determined at various velocities, usually in the range of 2 ft/sec to 10 ft/sec. These data are used to construct the Wilson plot (1/h vs. $v^{-.8}$) for the experimental unit. This helps to assure the integrity of the experimental unit, and it also yields a value for the heat transfer coefficient at time $t = 0_x(h_o)$.

After the flow has begun through the heat exchanger pipe, the normal procedure for taking heat transfer data proceeds in the following manner. Heater power is applied to heat the heater blocks (Fig. 2.3) for a period of about ten thermal time constants of the system. This raises the temperature of the copper cylinder to its asymptotic value (~1°C above the temperature of the flowing water). The heater power is then turned off. The output of the thermopile, thermistor and the flow meter are then recorded as functions of time for about ten time constants. This time record of the heat decay is defined as a cooling curve. During this time, almost all of the heat stored in the heater cylinder is removed through the inside surface of the heat exchanger pipe to the flowing water, and the output of the thermopile reaches its asymptotic value. This procedure is repeated a number of times (usually 16) in succession on the same day, to increase the precision of the result. This forms the core of the biofouling data. The analysis procedures used to determine the time constant from the cooling curve, the heat transfer coefficient from the time constant and the thermal resistance from the heat transfer data are presented next.

5.2. Analyzing Data. Processing the heat transfer data proceeds through many stages. Even before the experiment is started, the relationship that converts the time constant, τ, to the heat transfer coefficient, h, is developed for an experimental unit. This is accomplished by the program HTAU[1]. The input to this program is of two kinds: the geometric details (such as the i.d. of the heat exchanger pipe, the o.d. of the heat exchanger pipe at the location where the heater cylinders are clamped, and the o.d. of the heater cylinders) and the physical properties (such as heat capacity, thermal conductivity and density) of the heat exchanger pipe and the heater cylinder. The output of this program is the functional relationship between τ and h for that particular experimental unit, assuming a single path for heat flow (namely from the inside surface of the heat exchanger pipe to the flowing water). This program needs to be run only once for an experimental unit and is done before any cooling curves are analyzed.

Extracting a time constant from the cooling curve is done next. Here we use two distinct procedures: a two-parameter fit and a three-parameter fit. The program package, HTCOEF, uses the two-parameter fit.

In the absence of any fluctuations in the temperature of the flowing water, the output of the thermopile during thermal decay has the exponential structure,

$$V_{TC}(t) = [V_{TC}(t=0) - V_{TC}(t=\infty)] \exp(-t/\tau) + V_{TC}(t=\infty), \qquad (5.1)$$

Where $V_{TC}(t=0)$ and $V_{TC}(t=\infty)$ are the output voltages of the thermopile at the beginning of heat decay and in the asympototic region, respectively. Thus Eq. 5.1 has three unknown parameters, $V_{TC}(t=0)$, $V_{TC}(t=\infty)$ and τ. In the two-parameter fit, the parameter $V_{TC}(t=\infty)$ is determined experimentally by averaging the output of the thermopile in the asymptotic region leaving $V_{TC}(t=0)$ and τ as unknown parameters to be determined from the cooling curve. Thus,

granting $V_{TC}(t=\infty)$ to be a known parameter, Eq. 5.1 can be rewritten as,

$$\ln [V_{TC}(t) - V_{TC}(t=\infty)] = \ln [V_{TC}(t=0) - V_{TC}(t=\infty)] - t/\tau. \qquad (5.2)$$

Equation 5.2 has the structure of a linear equation, and a simple linear regression of the heat decay data (suitably weighted) yields the desired parameter τ.

However, the experimental determination of $V_{TC}(t=\infty)$ could be in error for the following two reasons. Fluctuations in the temperature of the flowing water before and during the asymptotic region would introduce uncertainties in the $V_{TC}(t=\infty)$ as seen in Fig. 5.3. A cooling curve that was terminated early would also yield an unreliable estimate of $V_{TC}(t=\infty)$. Situations like these can be handled with the three-parameter fit in which all three parameters, $V_{TC}(t=0)$, $V_{TC}(t=\infty)$ and τ, are treated as unknowns. The heat decay data are analyzed by a multiparameter minimization procedure, and this is accomplished by the program package PETITE.

The quantity χ^2 is defined as follows:

$$\chi^2 = \sum_i^n [V_{TC}^{expt.}(t) - V_{TC}^{fit}(t)]_i^2 \qquad (5.3)$$

where $V_{TC}^{expt}(t)$ and $V_{TC}^{fit}(t)$ are the experimental and fitted values of the thermopile voltage, and n is the number of experimental points. The function χ^2 is considered as a continuous function of the three unknown parameters. This χ^2 space is searched to find a minimum. The search procedure is initiated by supplying initial guess values for each of the unknown parameters. In practice the results obtained from the previously described 2-parameter fit are used as the starting values. The program package first uses the efficient 'Gradient Search'[2] technique until a minimum of χ^2 is approached. Then it switches over to the 'Grid Search'[2] technique until χ^2 is minimized to the required accuracy.

In our routine data reduction, the cooling curves are processed by the 2 parameter and the 3 parameter procedures successively and the results are checked one against the other.

The extracted time constant τ is then converted to a heat transfer coefficient using the τ-h relationship for that experimental unit derived by HTAU. Then this value of h is corrected for heat losses to the air and up and down the walls of the heat exchanger pipe. The corrected value of h is normalized to a nominal temperature (70°F) and the nominal flow velocity. This is repeated for all the cooling curves for that day and the results are stored. The mean and the error on the mean for various experimentally measured quantities like h, T and V are computed. Next, based on prescribed criteria, the results of individual cooling curves are accepted or rejected. The acceptance criteria are discussed below. The mean and the error on the mean for the quantities h, T and V are once again computed using only the accepted cooling curves.

5.3. Acceptance Criteria. We expect (and have observed in the laboratory) that such cooling curves will be precisely exponential in the absence of variation in ambient conditions. However, if water temperature or flow velocity should vary rapidly enough, deviations from exponential behavior will occur, and will affect the measured values of h, and thus of R_f. We have found that variation variations of velocity, of the magnitude experienced in the field, have little effect. Water temperature fluctuations, however, are more of a problem.

The thermal time constants of the reference and heater cylinders are designed to be approximately the same (differences in their construction details and variations in their assembly procedures introduce small differences). Perfect equality of the two time constants would yield the desirable feature of immunity of the thermopile output to the temperature fluctuations in the flowing water. This makes the thermopile output obey a pure exponential function during the thermal decay. However, if the reference and heater cylinders are not precisely tuned, changes in the temperature of the flowing sea water cause changes in the thermopile output. The relationship between these changes

and the fluctuations in the water temperature are complicated. This effect is illustrated in Fig. 5.1 for one of the cooling curves collected during the Noi'i operation. Figure 2 shows the output of the thermistor and the thermopile for a cooling curve taken during the St. Croix operation. Here, the output of the thermopile, in spite of large fluctuations in the thermistor voltage, is relatively steady. In this case, the two cylinders are tuned well. The ratio of the time constants for the heater and reference cylinders is $\tau_H/\tau_R = 0.97$. Fig. 5.3 shows similar data taken using one of our devices at Keahole Point, during the Buoy Series I operation. As the figure shows, the output of the thermopile is more sensitive to water temperature fluctuations. The ratio of the two time constants in this case is $\tau_H/\tau_n = 1.42$.

Methods of determining the extent of detuning and procedures for tuning the device have been discussed in greater detail in the design document[3].

Since not all test units are perfectly tuned, it is desirable to define an objective set of criteria which will discriminate against data which are seriously influenced by water temperature fluctuations. We expect that the "goodness of fit" of the fitted exponential curve to the experimental data points will be sensitive to this problem. To find out, we compute, for each cooling curve, the FITRMS as a measure of the goodness of fit. Its definition is

$$\text{FITRMS} = (1/n\chi^2)^{1/2}, \tag{5.4}$$

where χ^2 is defined in Eq. 5.3. The FITRMS for a typical data set are tabulated in Table 5.3 and plotted in Fig. 5.5. From Fig. 5.5 it is rather clear that there is a well defined grouping with FITRMS just less than 1 mV, and that the point at 4.2 mV should be rejected. It is not clear, however, precisely where to draw the line, i.e., should some or all of the points between 1 and 2 mV be rejected?

The situation is clarified considerably if we look at a second parameter. Define V_m(fit) to be the fitted value, and V_m(meas) to be the measured value

of the thermocouple output in the asymptotic region (the second asymptotic window of Fig. 2.14). Then let

$$\Delta V_\infty = V_\infty(\text{meas}) - V_\infty(\text{fit}). \qquad (5.5)$$

We expect ΔV_∞ also to be affected by water temperature variations in a detuned system. The values of ΔV_∞ are also tabulated in Table 5.3 and plotted in Fig. 5.6 for the same data set.

Again we see a clustering at $\Delta V_\infty = 0$, but we do not see clear cut-off points in Fig. 5.6 where acceptance criteria might be set. However, a two-dimensional scatter plot of ΔV_∞ vs. FITRMS for the individual points of Table 5.3 shows a clearer separation. This scatter plot, shown in Fig. 5.4, shows a well defined cluster of six points at the lower left, and four points which are, to varying degrees, affected by water temperature variations. This plot shows that, for this particular unit, data points should be accepted if (approximately) $-25<\Delta V_\infty<10$, and FITRMS<1.3.

It should be noted that suitable two-dimensional acceptance criteria on ΔV_∞ and FITRMS will be different for different units because of differences in degrees of detuning. Therefore, when a new experiment is started, a scatter plot like that of Fig. 5.4 should be made for each unit being used (but using more data; perhaps 32 to 64 points). Scrutiny of this scatter plot will allow reasonable limits to be set. Furthermore, observation of the scatter plots early in the experiment will be useful for detecting major problems in the apparatus or procedures. That is, if the acceptable group of points is very much more spread out than those of Fig. 5.4, or if they do not cluster around the point (1, 0), it is a sign that something is seriously wrong.

We point out that most of the data presented in this report were <u>not</u> subjected to the criteria described above because the analysis was not done until after a large amount of data had been analyzed. For these data, Chauvnet's criterion was used. This criterion is that if one is averaging N data

points, one should reject those whose probability of occurrence is less than 1/2N. Since we took, typically, 16 points per day, this corresponds to a 3% probability of occurrence which is equivalent to rejecting those further than two standard deviations from the mean. (It is the 2σ cut which was actually applied.) The effects of applying this cut are shown in Tables 5.1 and 5.2 for the Buoy I and the St. Croix experiments, respectively.

5.4. Errors. The random error on a typical day's measurement of h (average of 16 measurements) are expected to be less than 1%, as indicated in Tables 5.1 and 5.2. We expect even more precision if the acceptance criteria of Sec. 5.3 are used or if the units are precisely tuned. The limitations on the accuracy of the results (h) are due to the systematic errors. We believe the most serious systematic error to be due to the calibration of the flowmeters). Other systematic errors should be well below this. In all cases, therefore, where the random error is less than 1% (almost always) we assign an error of 1% to each measured value of h due to the flowmeter systematics. Clearly, there is no point in taking more than 16 cooling curves per day since doing so would only reduce the random error (which is already small) and would have no effect on the systematic error (which dominates).

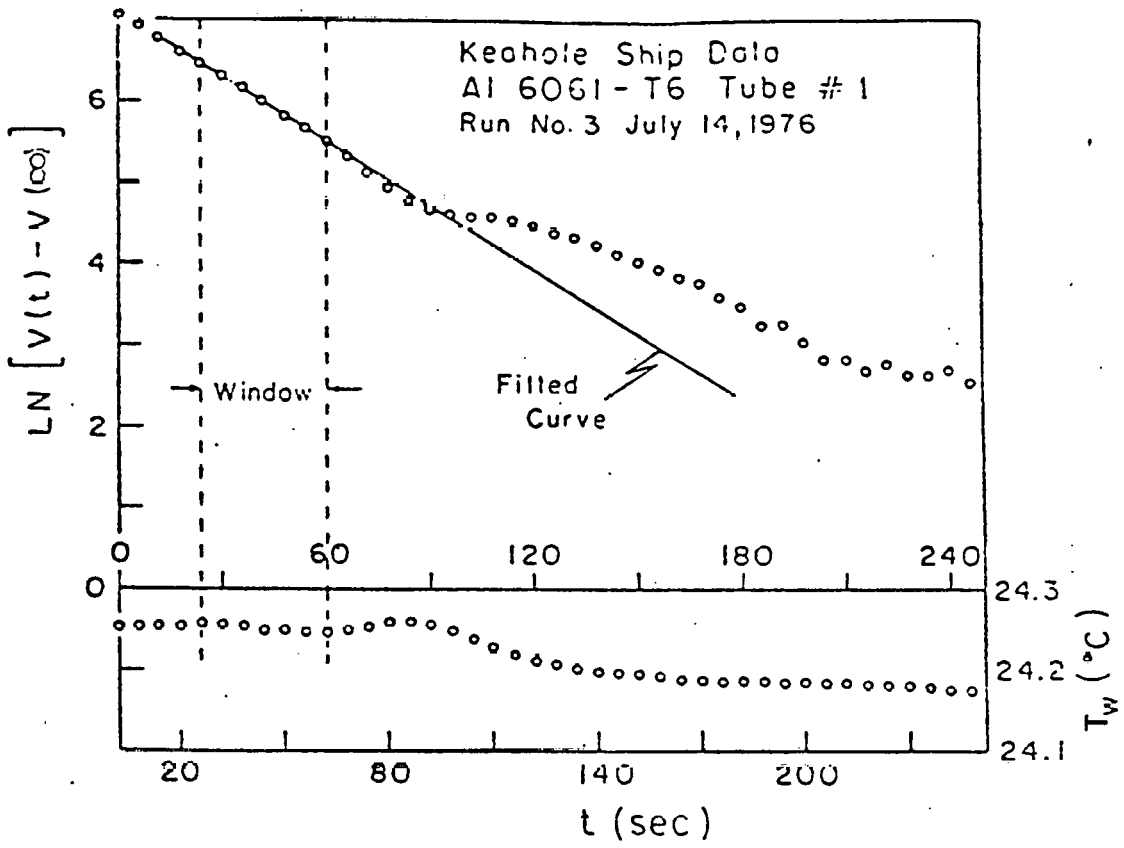

5.1 Correlation between Water Temperature Fluctuations and Deviations of the Thermopile Decay Data from the Fitted Curve

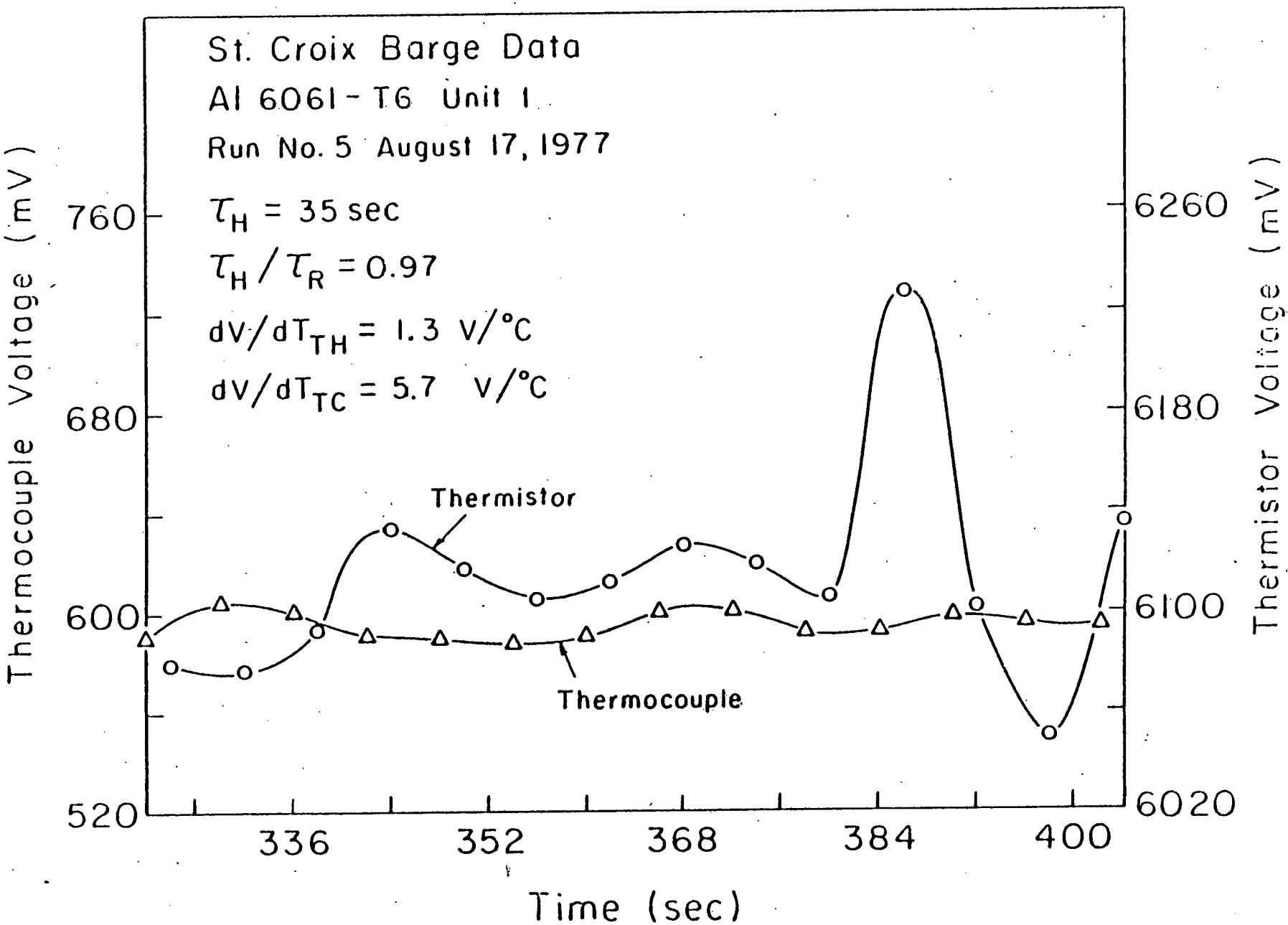

5.2 Correlation between thermopile and thermistor output in the asymptotic region for a well 'tuned' heat transfer unit: SA6 experiment

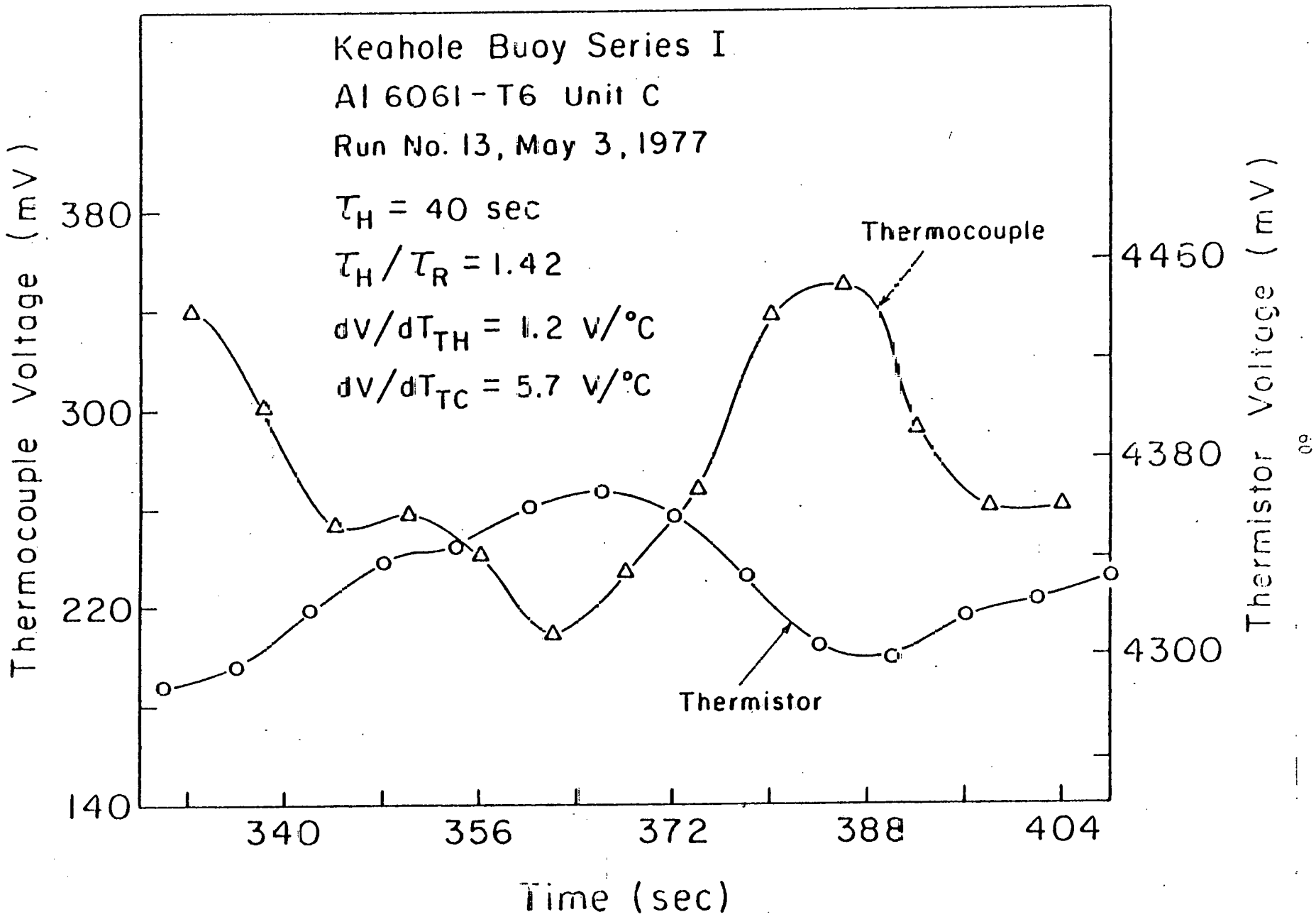

5.3 Correlation between thermopile and thermistor output in the asymptotic region for a poorly 'tuned' heat transfer unit: BA6 experiment

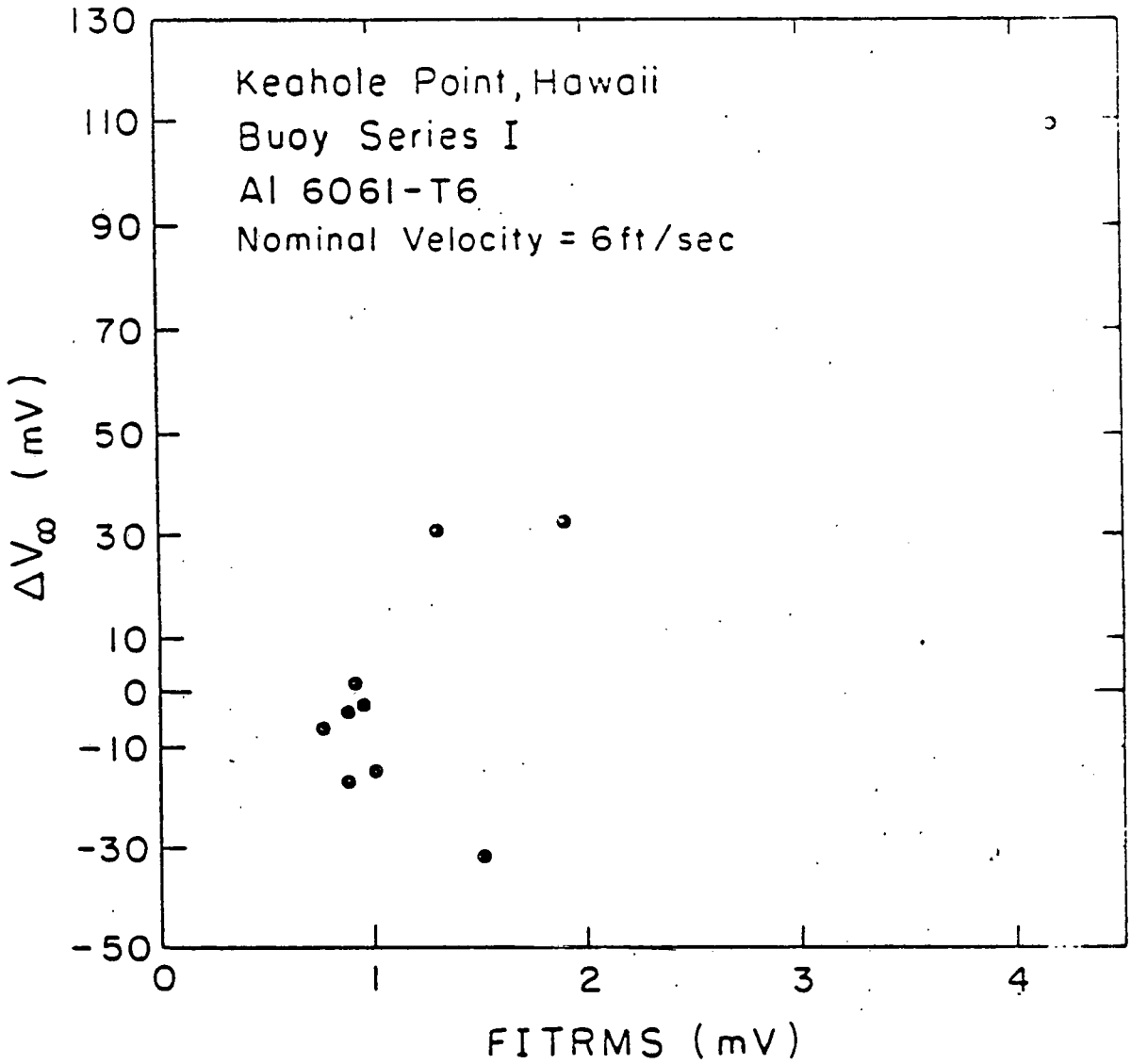

5.4 A scatter plot correlating ΔV_∞ with FITRMS: BA6 experiment

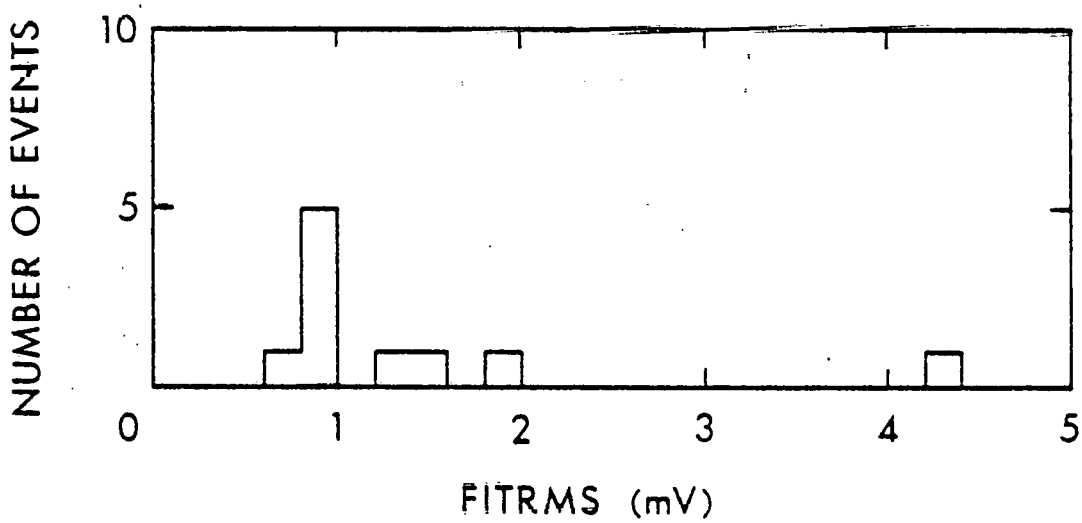

5.5 DISTRIBUTION OF FITRMS: BA6 EXPERIMENT

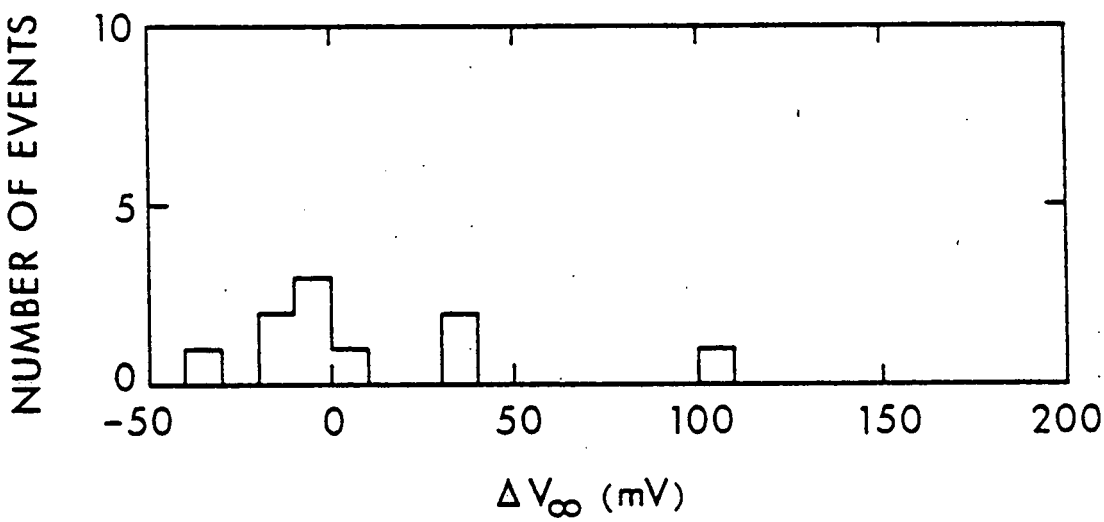

5.6 DISTRIBUTION OF ΔV_∞: BA6 EXPERIMENT

TABLE 5.1

DATA ON THE PERFORMANCE OF THE INTERIM CRITERION
FOR ACCEPTING A COOLING CURVE: BA6 EXPERIMENT
KEAHOLE POINT, BUOY SERIES I

Al 6061-T6 V = 6ft/sec.

Date	Total Number of CCU's	Number of CCU's accepted	<h> for all CCU's	<h>* for accepted CCU's
Mar 8 '77	16	15	1119.0 ± 1.3	1118.3 ± 1.0
Mar 16 '77	16	15	1118.4 ± 3.3	1116.5 ± 2.2
Mar 22 '77	16	15	1070.9 ± 4.1	1073.3 ± 3.1
Mar 29 '77	15	14	1031.8 ± 9.8	1040.6 ± 1.3
Apr 5 '77	14	12	974.8 ± 1.4	974.9 ± 0.9

* The acceptance criterion has been to accept a value of h if it does not differ from the mean by more than 2σ.

TABLE 5.2

DATA ON THE PERFORMANCE OF THE INTERIM CRITERION
FOR ACCEPTING A COOLING CURVE: SA6 EXPERIMENT
ST. CROIX, U.S. VIRGIN ISLANDS

Al 6061-T6 V = 6 ft/sec.

Date	Total Number of CCU's	Number of CCU's accepted	<h> for all CCU's	<h>* for accepted CCU's
July 19 '77	14	14	1177.7 ± 6.5	1177.7 ± 6.5
July 24 '77	13	12	1117.6 ± 6.0	1121.8 ± 4.6
July 30 '77	14	14	1107.0 ± 8.7	1107.0 ± 8.7
Aug 5 '77	14	13	1095.3 ± 8.2	1089.7 ± 6.5
Aug 23 '77	9	9	1085.5 ± 10.8	1085.5 ± 10.8

* The acceptance criterion has been to accept a value of h if it does not differ from the mean by more than 2σ.

TABLE 5.3

ΔV_∞ AND FITRMS: BA6 EXPERIMENT KEAHOLE POINT, BUOY SERIES I

Al 6061-T6 V = 6 ft./sec.

CCU#	FITRMS (mV)	ΔV_∞ (mV)
1	0.89	- 4.8
2	1.31	31.1
3	4.21	108.7
4	0.94	- 4.0
5	0.99	-15.8
6	0.92	1.1
7	1.90	31.9
8	1.50	-32.4
9	0.75	- 8.4
10	0.87	-17.2

SECTION 5 REFERENCES

1. J. G. Fetkovich, C. W. Fette, R. W. Findley, G. N. Grannemann, L. M. Mahalingam, D. L. Meier and P. D. Runco, "A System for Measuring the Effect of Fouling and Corrosion on Heat Transfer Under Simulated OTEC Conditions," DOE Report No. C00-4041-10, (1976), pp. 19-20, 181-204.

2. P. R. Bevington, Data Reduction and Error Analysis for the Physical Sciences, (McGraw-Hill Book Co., New York, 1969), p. 204-246.

3. J. G. Fetkovich, C. W. Fette, R. W. Findley, G. N. Grannemann, L. M. Mahalingam, D. L. Meier and P. Runco, "A System for Measuring the Effect of Fouling and Corrosion on Heat Transfer Under Simulated OTEC Conditions," DOE Report No. C00-4041-10, (1976), pp. 21-27.

6. CHARACTERISTICS AND PERFORMANCE OF THE HEAT TRANSFER MONITORING DEVICE

The design document[1] prepared during late 1976 discusses in detail the theory, construction, assembly, and operating procedures of the heat transfer monitoring device. This document includes results of many of the extensive laboratory tests and some preliminary tests in the ocean. Thus it is the primary source on the hardware features and performance characteristics of the device.

In the last two years, many field experiments have been carried out using these devices, which has increased our understanding of both the characteristics of the device and the biofouling problem. During this period, a considerable effort was made to prepare and disseminate information about this device and to train other groups such as Pacific Northwest Laboratory of Battelle, NSRDC of the U.S. Navy, NDBO of NOAA and the Natural Energy Lab of the University of Hawaii. As new users have come to operate these devices, there is a need to clarify a few of the characteristics.

6.1. Tuning and Immunity to Temperature Fluctuations. In Section 5.3, we discussed how the output from a detuned heat transfer monitoring device would be impaired in the presence of temperature fluctuations. Since temperature fluctuations are prevalent in the ocean, it is natural to ask whether there are ways to obtain reliable measurements in spite of them. There are three ways to handle the problem.

After assembling the device, it is relatively easy to determine the difference between the time constants of the two sets of cylinders (reference and heater). This procedure has been described in the design document[2]. Once the amount of tuning necessary has been determined, it can be achieved in one of many ways. The thermal capacity of the reference cylinder could be changed by using rings of copper that could be clamped to the reference

cylinder. The thermal resistance of the contact between the pipe and the cylinders could be changed in several ways. These include preparing the contact areas of the heat exchanger pipe and the cylinders to different degrees of smoothness, and using varying amounts of high thermal conductivity grease between copper cylinders and the heat exchanger pipe. In general, we do not recommend these procedures since they are an inconvenience and it has been demonstrated that the system, when properly assembled, works quite well as is. NSRDC, in their experiments, have manipulated the torque values with which the cylinders are clamped to the pipe. We <u>most strongly</u> advise against this. There is reason to believe that differential expansion or contraction due to long-term water temperature variations and/or vibrations can cause unseen changes in the thermal resistance of the contact between cylinders and pipe if the cylinders are clamped with a torque less than the design value. Of course, using much greater than the design-value torque risks damage to the apparatus.

Another scheme involves analytically handling the temperature fluctuations in the thermal decay equation. We present the equations below. Let $T_H(t)$, $T_R(t)$ and $T_W(t)$ be the temperatures at time t of the heater cylinders, the reference cylinder, and the flowing seawater. Let τ_H and τ_R be the thermal time constants of the heater cylinder set and the reference cylinder respectively. Then Equations 6.1 and 6.2 describe the time dependent behavior of $T_H(t)$ and $T_R(t)$ in the presence of temperature fluctuations in the seawater.

$$\frac{d}{dt} T_H(t) = -\frac{1}{\tau_H} [T_H(t) - T_W(t)] \tag{6.1}$$

$$\frac{d}{dt} T_R(t) = -\frac{1}{\tau_R} [T_R(t) - T_W(t)] \tag{6.2}$$

Solutions to these first order differential equations can be written as

$$T_H(t) = T_{H_o} e^{-t/\tau_H} + \int_o^t T_W(t') \frac{d}{dt'} \left[e^{-(t-t')/\tau_H} \right] dt'$$

$$T_R(t) = T_{R_o} e^{-t/\tau_R} + \int_o^t T_W(t') \frac{d}{dt'} \left[e^{-(t-t')/\tau_R} \right] dt'$$

where T_{H_o} and T_{R_o} are the temperatures of the heater cylinders and the reference cylinder at time t=0. Since the output of the thermopile is proportional to the difference in the temperature between the heater and reference cylinders, we can write

$$V_{TC}(t) = K \Delta T(t) + V_{TC}^{offset} \qquad (6.3)$$

where $\Delta T(t)$ is $T_H(t) - T_R(t)$,
K is a constant of proportionality and V_{TC}^{offset} is the thermopile offset voltage. For the determination of $T_W(t)$, the thermistor data acquired during thermal decay is used. The cooling curve data could thus be fitted to Eq. 6.3. This involves a five parameter fitting procedure. We have not attempted to use this procedure.

As indicated above, we do not recommend that any turning procedures be used as standard practice. Our experience has shown that, because the two cylinders were designed to be approximately tuned, water temperature fluctuations are not a serious problem. Since typically only a few of each day's 16 measurements usually need to be rejected, such rejection of bad data is by far the easiest solution.

6.2. Velocity Fluctuations and Their Effects. In operating the device in the field, another potential problem was encountered: fluctuations in the velocity of flow through the heat exchanger pipe due to wave action in the ocean. The size of the fluctuations depends both on the roughness of the sea and the mode of operation of the device (sub-surface or above-surface, with or without velocity regulators, etc.). For the experiments attached to

the buoy (at Keahole Point, Hawaii), the fluctuations were small, of the order of 0.2% for the 6 ft/sec experiment as shown in Fig. 6.1. The experiments operated on board the ship Noi'i and on board the moored barge had higher velocity fluctuations. They were largest for the St. Croix experiments, of the order of 5% for the 6 ft/sec experiment and 7% for the 3 ft/sec experiment and are shown as histogram plots in Fig. 6.2.

It is relevant to ask whether these velocity fluctuations registered by the flow meter are real and in what way they impair the quality of the heat transfer data. The flow meter employed in this investigation employs a target on the end of an arm whose flexure in response to flow velocity is measured by a strain gauge. Flexure due to inertial forces arising from motion of the device could cause apparent velocity fluctuations. The measured average velocity should not be seriously affected by such an effect. That this is happening is indicated by two pieces of evidence. Using a large number of cooling curves collected during buoy experiments and St. Croix experiments, we carried out a correlation study. It showed no correlation between the size of the velocity fluctuations and the deviations in the measured thermal time constants. Thus the apparent flow fluctuations do not seem to affect the average.

Figure 6.3 features scatter plots of h before and after velocity normalization for a set of cooling curves collected on one day on board the barge at St. Croix. As seen, there is a great dispersion (about a factor of 2) in the plot of h after velocity normalization. This implies that the true flow velocity is more constant in time than the flow meter indicates.

6.3. Integrity and Durability of the System Hardware. Most mechanical, electrical, and electronics hardware used in the biofouling studies performed satisfactorily. There were a few failures due to poor performance of the material and poor design features. Solutions were developed to handle these failures.

Polyvinyl chloride (PVC) as a material for building the housing for the heat exchanger pipe unit and for the pump unit proved to be very reliable in all sub-surface experiments. The housings were designed to work at a submergence depth of up to 100 feet, but in all buoy experiments they were subjected to only about 50 feet of water. In above-surface applications, if desired, the protective housings could be built at a lower cost and designed for easier assembly since pressure requirements are absent.

In the assembly of the protective housings and in the plumbing of the heat transfer measuring device, three different make-and-break seals (neoprene gaskets, rubber 'o' rings, and teflon 'o' rings) were used. When these seals were made with care, they performed very reliably. No one of the seven biofouling experiments conducted during this period had any problems resulting from these seals.

Materials, design, and construction of the heater (to elevate the temperature of the copper block), the thermopile (to monitor the temperature differential) and the thermistor (to monitor the temperature of seawater) seem satisfactory.

In the original design, the reference cylinder also served the function of clamping the heat exchanger pipe to the top plate of the protective housing (see Fig. 2.3). Later, a separate cylinder of the same dimensions as the reference cylinder was installed as a clamp. This helps to improve the reliability of the thermopile by reducing mechanical handling.

In the Noi'i and Buoy Series I experiments, low level (μV and mV) data signals were handled. Subsequently, each experimental unit was fitted with "pipe electronics" to convert all the data signals to the 0-10 V level before handling. This was put into practice for the St. Croix operation and subsequently has been a standard practice. This feature has made each experimental unit more modular and improved the noise quality of the data signals.

During the reporting period, three data acquisition systems were constructed and operated in conjunction with the biofouling experiments. Two of these were manual. One was operated as a back-up system at Keahole Point and the other was operated at St. Croix. The third one was a microprocessor-based system operated with the Buoy Series II experiments (which began during December 1977). Each of these systems performed well.

Joule heating generated in the motor windings of the pump while it is in continuous operation is removed by tapping part of the seawater from the discharge end of the pump and circulating it through a copper cooling coil wound around the motor (see Dwg. 403 of Ref. 1). The original selection for this cooling coil was 1/4 in i.d. and 1/16 in wall copper tube. Erosion/corrosion in the copper cooling coil caused leaks resulting in two pump failures in the Buoy Series I experiments, one after 10.6 weeks and another after 20.3 weeks of operation. Later, design changes were made to use slightly larger diameter (0.175 in i.d.) copper tube of greater wall thickness (0.100 in.) to reduce the possibility of such failures.

Subsequent to the Buoy Series I experiments, a second series was begun on the submerged buoy at Keahole Point in September 1977. It was very soon aborted partly due to two pump failures. Both of these pump failures were related to poor performance of some of the materials of construction. Inside the pump housing, both at the inlet and the discharge end, clear Tygon tubing (of 1-1/4 in i.d. x 1/4 in wall) were used in the plumbing. (Refer to Dwg. D-403 of Ref. 1). In one of the pumps, the Tygon tubing ruptured, flooding the pump housing. Figure 6.4 shows this failure as it was found on disassembly. Also, reinforced (i.e., braided) Tygon tubing (1/2 in i.d. x 3/32 in wall) was used in the cooling coil loop. The second pump failure occurred due to failure in this braided Tygon tubing. In all subsequent work, Aeroquip hoses (two layers of rubber with fiber impregnation) replaced both the clear and reinforced Tygon tubing. This solved the problem of hose ruptures.

At Keahole Point, Hawaii, operator-controlled, "master" beach electronics and the remote, "slave" buoy electronics are interconnected by a 1,500 ft. long submarine cable. This cable carries power and control signals to the buoy from the beach, and brings data signals from the buoy to the beach. During the Buoy Series I experiments, problems of cross-talk arose. Control pulses to step the flow meter circuit and step the thermopile circuit are carried as differential signals in untwisted unshielded pairs. In close proximity to them is the conductor carrying ac power to the heater. Transients generated while the heater is switched on, caused transmission of sharp pulses down the above mentioned control lines. This sometimes resulted in unwanted switching of the thermopile circuitry and/or the flow meter circuitry. This was solved by incorporating a .01 μf capacitor after the line receiver, one each for the step flow meter circuitry and the step thermopile circuitry. The capacitor shunted the high frequency noise to the ground.

For each of the biofouling experiments, the flow velocity of seawater through the heat exchanger pipe was measured by a target-type flow meter (Mark V) by Ramapo Instrument Co. In the first application of this kind of flow meter (on board Noi'i), the flow meter body was made of SS 316 while the flow sensing part, namely target and lever arm, was of 17-PH. This led to severe galvanic and crevice corrosion underneath the teflon 'o' ring seal where the lever arm is coupled to the body of the flow meter. Luckily this didn't cause a water leak in the system. In later work, all SS 316 flow meters were used to avoid galvanic corrosion. As a further improvement, the PVC was selected for the body of the flow meter and Hastalloy C for the lever arm and the flow-sensing target. These changes have made the flow meters quite durable in seawater applications.

If macrofoulers attach to the target or the space around it, they can alter the calibration constant of the flow meter. The BA6 experiment is an example of this problem. At 11.4 weeks, flow stopped for a period of a few

days. The flow velocity monitored by the flow meter subsequently could not be interpreted uniquely as shown in Fig. 6.5. The flow meter on disassembly is shown in Fig. 7.6, where we see macrofoulers (barnacles) attached to the flow meter body. There is no evidence in all our work for the attachment and growth of macrofoulers as long as flow is maintained without long interruptions.

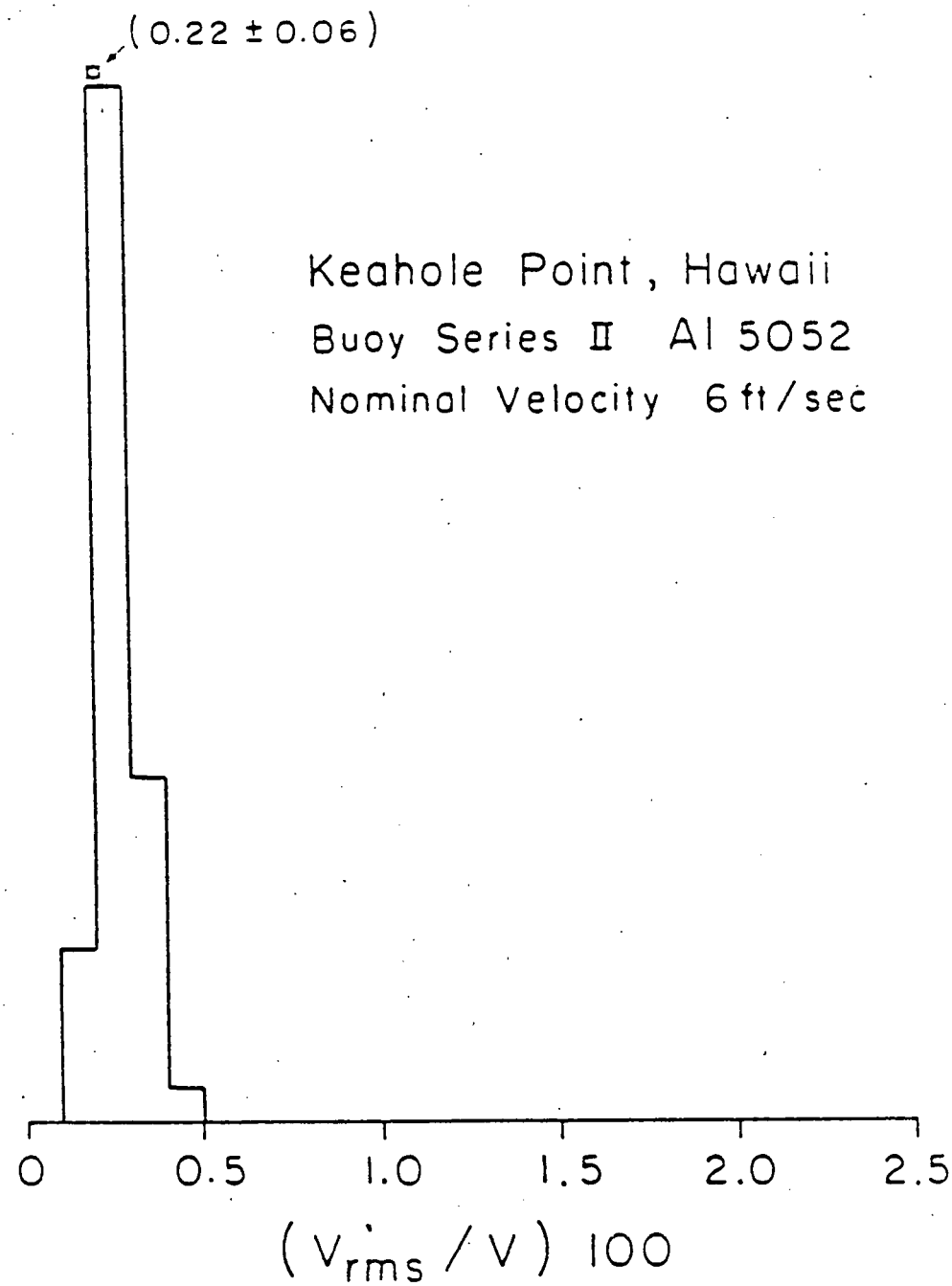

6.1 Histogram of velocity fluctuations for sub-surface operation: BA6 (Series II) experiment

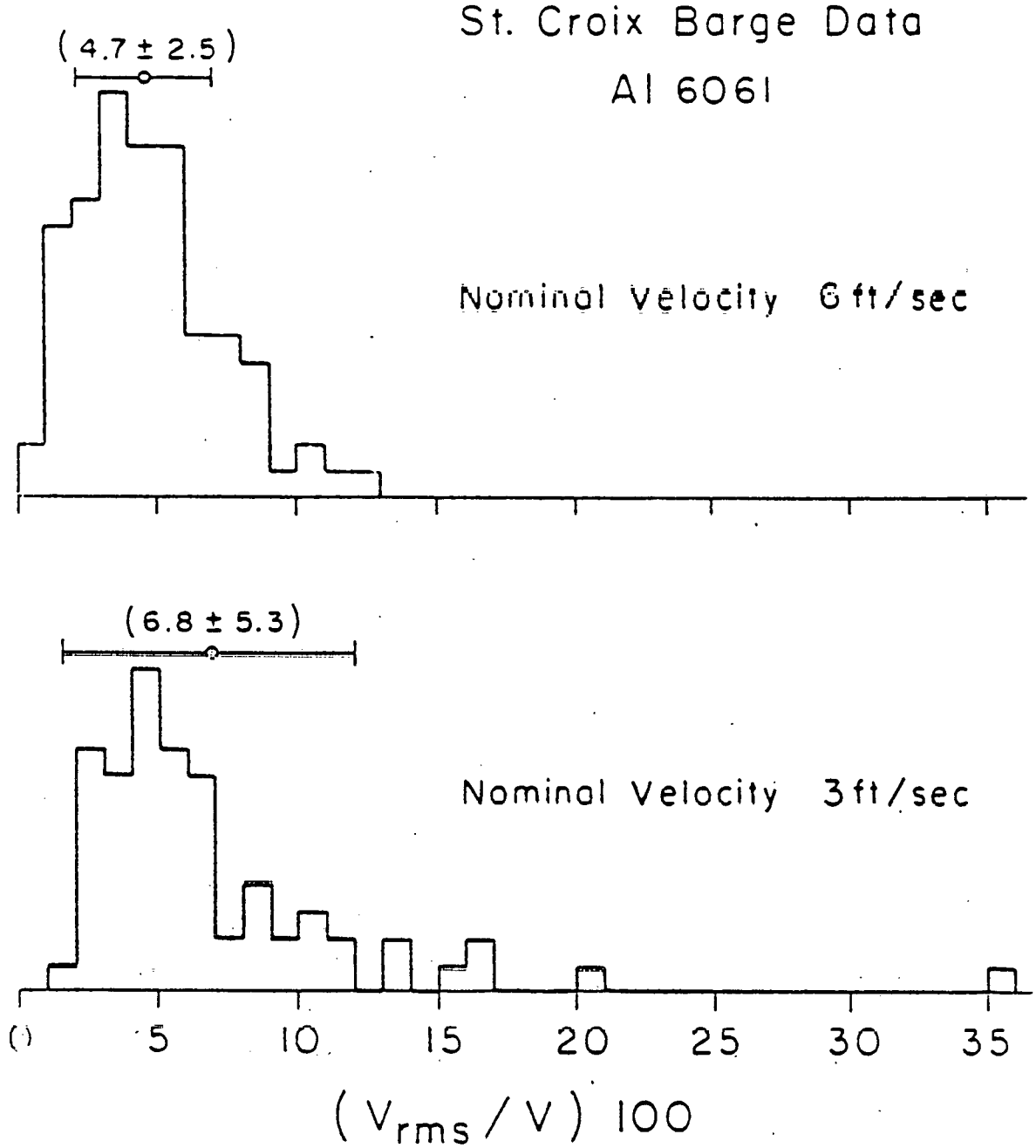

6.2 Histograms of velocity fluctuations for above-surface operation: SA3 and SA6 experiments

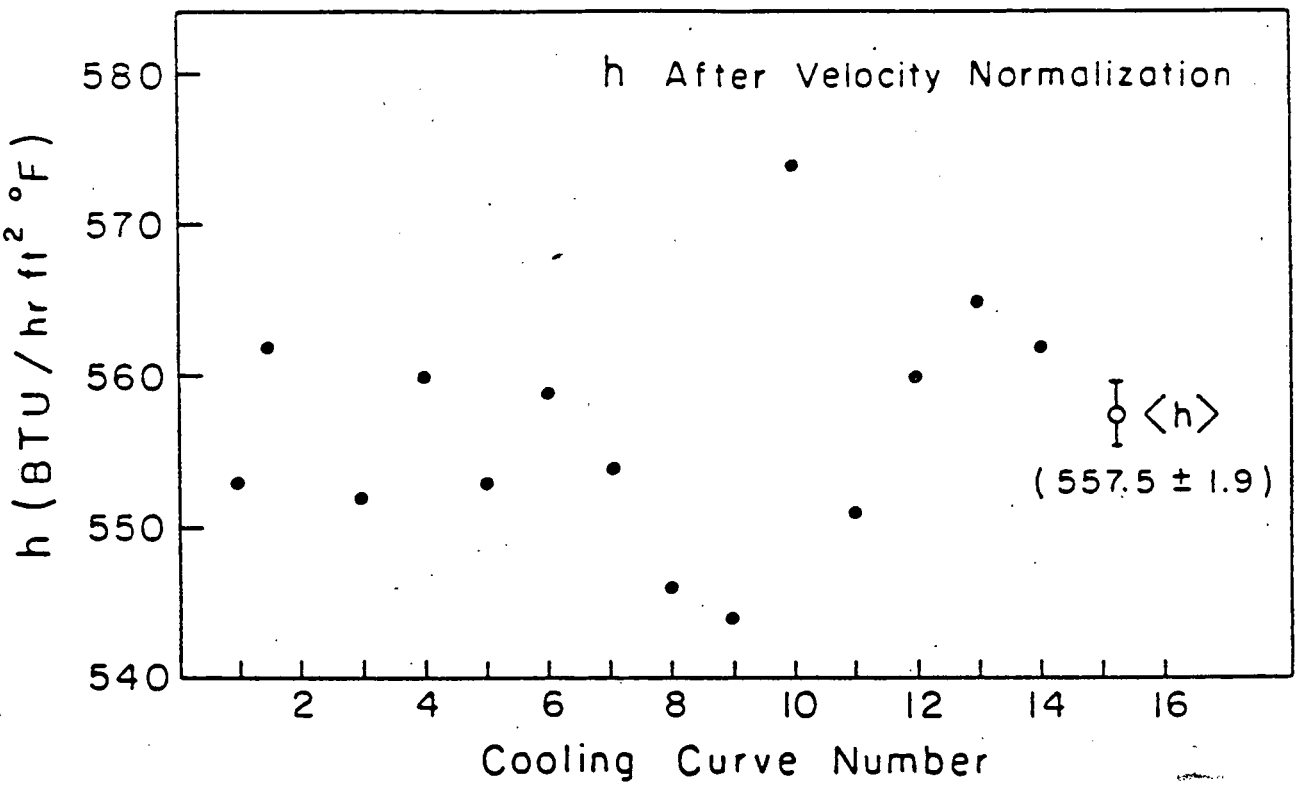

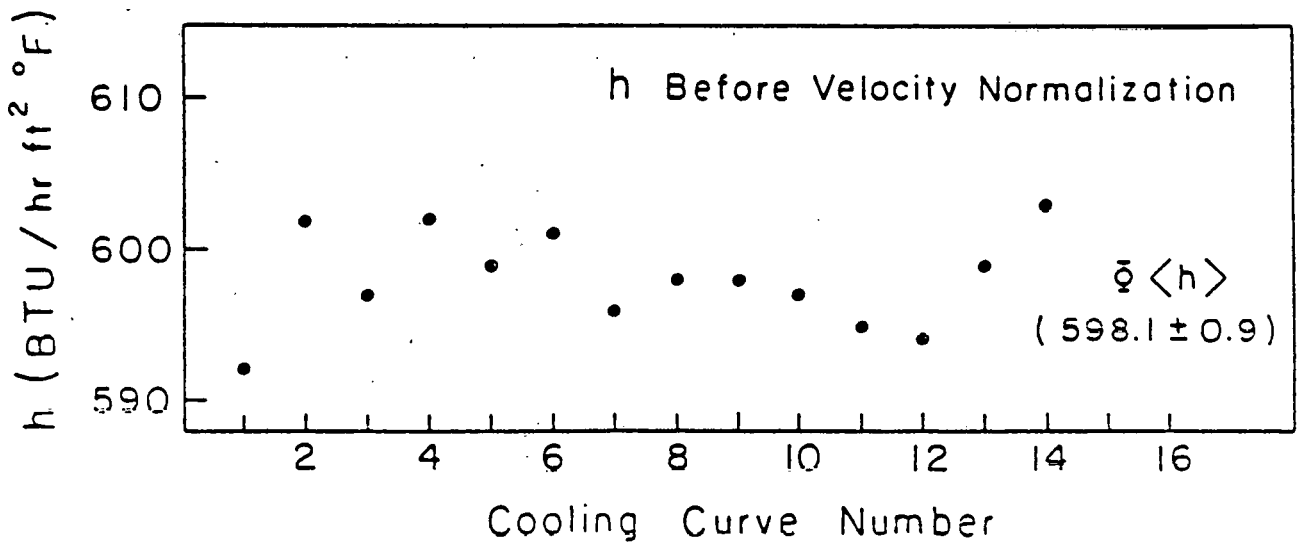

6.3 Scatter plots of h before and after velocity normalization: SA3 experiment

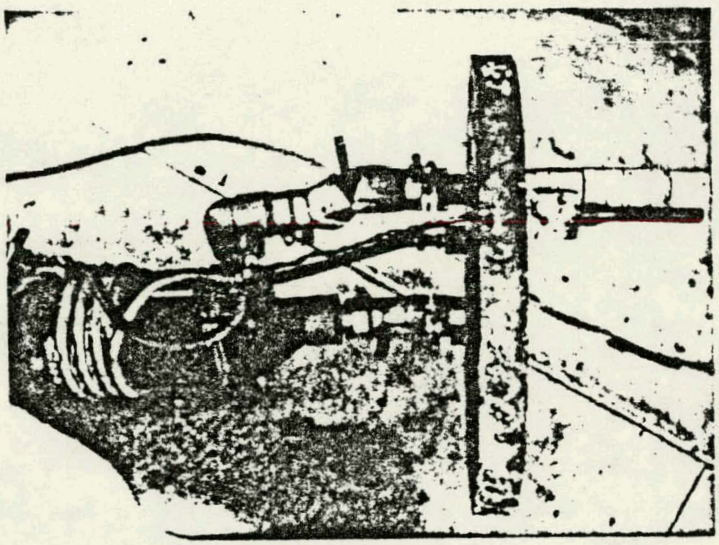

Figure 6.4 Pump failure due to failure of the clear Tygon tubing in the plumbing. Subsequently Tygon tubing has been replaced by Aeroquip hoses.

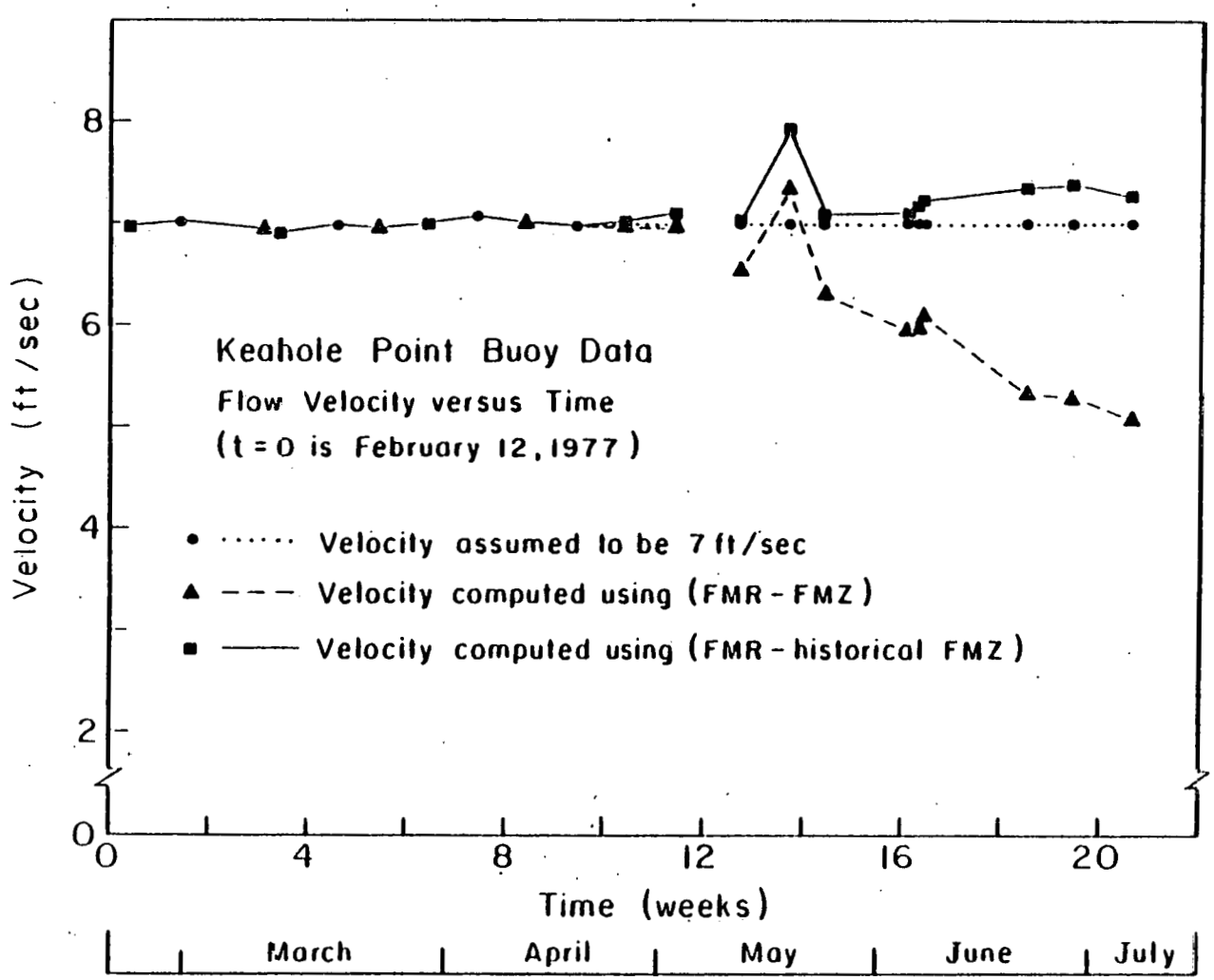

6.5 Water velocity vs. Time for the BA6 experiment with different assumptions about instrumentation. Unique interpretation of flow velocity was not possible subsequent to the long term flow stoppage that occurred at 11.4 weeks.

SECTION 6 REFERENCES

1. J. G. Fetkovich, C. W. Fette, R. W. Findley, G. N. Grannemann, L. M. Mahalingam, D. L. Meier and P. D. Runco, "A System for Measuring the Effect of Fouling and Corrosion on Heat Transfer Under Simulated OTEC Conditons," DOE Report No. COO-4041-10, (1976).

2. J. G. Fetkovich, C. W. Fette, R. W. Findley, G. N. Grannemann, L. M. Mahalingam, D. L. Meier and P. D. Runco, "A System for Measuring the Effect of Fouling and Corrosion on Heat Transfer Under Simulated OTEC Conditions," DOE Report No. COO-4041-10, (1976), pp. 21-27.

7. DISCUSSION

In the last two years of operation, the heat transfer monitoring device has been employed in the field under various conditions to measure the "biofouling" potential in the warm mixed layers of the ocean. In this section, we will first briefly enumerate some of the parameters that have been varied in the course of these experiments. Then, we will present the common features observed in the thermal data. Two different views are presented offering possible explanations for the origin and the nature of the "fouling layer." It is followed by some interesting observations that bear some importance in the design and operation of OTEC heat exchangers.

7.1. Parameters and Their Variations. Thermal measurements were conducted at two different geographical locations. Experiments on board the research vessel Noi'i and on the submerged buoy were off the coast of the Big Island of Hawaii at 19°N, 156°W in the Pacific Ocean (Fig. 2.1). Those aboard the moored barge at St. Croix were off the coast of the Virgin Islands at 18°N, 65°W in the Caribbean Sea (Fig. 3.1).

Both of these waters are generally classified as tropical. However, there are differences in their characteristics including their chemical nature and biological activity. The experiments at Keahole Point were about 1100 feet away from the seashore in about 150 feet of water. During the Noi'i experiments the water samples collected in that region indicated high biological activity with 20,000 bacteria/ml of water[1]. At this experimental site, the water is influenced in its character by the nearby land mass[2]. In contrast, the experimental site at St. Croix was seven miles north of the island (the nearest land mass) in about 12,000 feet of water. The water is more like open ocean and the biological activity of the water is lower than that at Keahole Point. During the St. Croix operation, the bacterial population was measured to be 10/ml of sea water[3].

The experiments were operated in two major modes — one above the sea surface and the other submerged in the ocean. In the Noi'i operation, two experimental units were mounted and operated on board the moored research vessel Noi'i. In the case of the St. Croix operation, two experiments were operated on board a moored barge. In both of these operations, warm water from the mixed layers of the ocean was brought to the experimental apparatus through flexible PVC hose. In the case of the buoy experiments, three heat transfer monitoring devices were attached to a submerged buoy and operated at a depth of about 40 feet. Seawater entered the heat exchanger pipe after passing through a fish screen. For each of these seven experiments, the pump was located on the downstream side and hence the viability of organisms was not impaired to any degree. But due to the plumbing arrangements, the organisms were subjected to different pressure drops before they reached the experimental section. The pressure drops were of the order of 35 feet of water for the Noi'i experiments, 70 feet of water for the St. Croix experiments and about 3 feet of water for the buoy experiments.

There have been seasonal variations during the course of operation of these experiments. Both the Noi'i and St. Croix experiments were carried out during the summer. The Buoy Series I experiments were started during early spring and continued through the middle of summer.

Two different heat exchanger pipe materials were employed. Most of the experiments (two on Noi'i, two on the buoy and both at St. Croix) were carried out with Al 6061-T6 alloy. One experiment on the buoy used titanium (grade 2).

The water-side surfaces of these pipes were prepared differently prior to the experiments. In one of the Noi'i experiments, the interior surface was swabbed with acetone to remove grease and dirt. For the other Noi'i experiment and for all three experiments in Buoy Series I, the pipes were cleaned with a nylon brush and household cleanser. Both St. Croix heat exchanger pipes

were treated by a much more aggressive process. Ten percent NaOH at ambient temperature was used as an etchant to strip the oxide layer from the Al 6061-T6 surfaces. This was followed by a thorough rinsing[4]. This method is believed to prepare a uniform oxide layer under controlled conditions.

The flow velocity has been varied too. One Noi'i, one buoy and one St. Croix experiment were run at a nominal flow of 3 ft/sec. One Noi'i, two buoy and one St. Croix experiment were at a nominal flow of 6 ft/sec.

Fluctuations in the flow velocity during short time spans (of the order of a thermal time constant of the unit) were lower for the subsurface than for the above-surface operations. At 6 ft/sec flow, the typical fluctuations were 0.2% for the buoy experiments (Fig. 6.1) and 5% for the St. Croix barge experiment (Fig. 6.2).

The overall water temperature at the buoy site was in the range of 24.2°C-26.6°C (Fig. 2.10). At the St. Croix site, the temperature was in the range of 28°C - 28.5°C (Fig. 3.3).

For a quick reference, Table 7.1 lists these parameters that have been varied in the biofouling experiments.

7.2. Common Features in the Thermal Data. To facilitate the discussion, the $R_f(t)$ data are reproduced from previous sections in Figures 7.1 through 7.3. Figure 7.1 features the $R_f(t)$ data for the two experiments of Noi'i. The $R_f(t)$ data for each of the three experiments of Buoy Series I are in Figures 7.2a, 7.2b and 7.2c. The same data for all three experiments on the buoy are featured in Figure 7.2d. Figure 7.3 displays the $R_f(t)$ data for the two St. Croix experiments.

7.3. Nature of the "Fouling Layer." Next, we would like to inquire about the nature of the material composition of the fouling and the phenomena that cause it. It is generally believed that the layer is composed of biological fouling (microfouling), chemical corrosion, and scale deposition. The thermal measure-

ments measure the overall effect of the fouling layer and cannot determine its origin. However, the thermal data, together with microscopic observations, help to construct a coherent picture.

On one extreme is the view that the "fouling layer" is mostly biological in nature. It is well known that a material surface exposed to biologically active water (such as the heat exchanger pipe in seawater) is coated with a slime layer in a few hours to a few days[5]. The slime layer consists of polysaccharides with low solubility in water. These are excretions by organisms such as bacteria. The thermal resistances for all seven curves shown in Figures 7.1 through 7.3 show only a small change in R_f's value in the first few days to few weeks. It is speculated that this "induction period" in the fouling curves corresponds to the initial conditioning of the heat exchanger surfaces by the deposition of non-living organic material. Subsequently there is a linear growth period.

Some quantitative biological studies were carried out by G. Harvey during the Noi'i operation (Appendix A). This study indicates that "there appear to be two layers, a scale layer possibly containing bacteria which may or may not be viable, and a layer over this composed of living organisms, their products, particulate inorganic material and inert biologically derived materials such as diatom frustules." A heat exchanger pipe sample from the Noi'i experiment (NA3 experiment) preserved in 2.5% glutaraldehyde solution was analyzed for its fouling layer deposits by collodion film. A value of about 23 μm measured by this technique may be compared with a value of 70 μm deduced from the thermal data. Deposits removed (using a collodion film) from preserved sections of the NA6 experiment (from the Noi'i operation) contained many bacteria and buried diatom frustules. Titanium pipe samples that were kept in the flow (~6 ft/sec) for a period of 5.4 weeks during the Noi'i experiments were also analyzed. The deposits contained many bacteria and some diatoms. Thickness

measurements of these deposits yielded values in the range of 1.7 to 8.5 μm. This thickness may be compared to that deduced as 9.5 μm from the thermal data for the Ti pipe during the buoy experiments (at the same site after 5.4 weeks of operation.

More elaborate and quantitative biology work was conducted by Barry Taylor et al. on heat exchanger samples from the St. Croix operation. Based on a preliminary study, they state that the live biological contribution to the "fouling layer" is about 1 μm[6]. This may be compared with a value in the range of 30-50 μm expected from the thermal data. However, the biologists working on the St. Croix samples caution that "an extremely expanded film of live organisms could trap and bind a considerable volume of water." If such were the case, a thin film of biological material could yield a thermal resistance that is many times more than that deduced from the biological contents alone.

On the other extreme is the view that the thermal resistance is mostly due to processes that are non-biological in nature and in fact is due to scaling and chemical corrosion. This suggestion is based on the analysis of heat exchanger pipe samples from Noi'i, Buoy Series I and St. Croix experiments. Metallurgical techniques such as optical microscopy, scanning electron microscopy, x-ray spectroscopy, secondary ion mass spectroscopy, and x-ray diffraction were employed in this study. A brief account of this study is described in Section 4 and the details are given in Appendix B. These studies indicate that in the case of Al heat exchanger pipes, the major components of the "fouling layer" are Al and Ca. Thus the metallurgical studies suggest that corrosion and scaling may be major phenomena in the formation of the "fouling layer" for Al heat exchanger pipes.

The various methods for determining the nature of the fouling layer do not lead to a consistent picture. Even the thickness determinations vary widely depending on method. It is possible that a very low-density or spongy organic fouling layer which traps stagnant water is the cause of the measured R_f.

Depending on the method of preservation of the samples, such a material could show up as a very thin organic layer upon later examination.

7.4. Flow Stoppages. In the St. Croix experiments, there were no flow interruptions, while the NOII experiments suffered many "short term" stoppages (i.e., less than ~2 hrs. each). The effects of these short-term interruptions are being studied further and will be reported on in the future.

The Buoy I experiments suffered long-term flow interruptions (at least a day). These evidently allow macrofoulers to attach sufficiently firmly so that they are not washed away when the flow is restarted. Figures 7.5 and 7.6 show such macrofoulers after disassembly of the BA3 and BA6 experimental units.

7.5. Cleaning the Fouled Heat Exchanger Surfaces. For the continued operation of the heat exchangers in an actual OTEC plant, the thermal resistance due to the "fouling layer" needs to be kept below a certain acceptable level. Thus during their lifetime, the OTEC heat exchangers must be cleaned periodically. The first cleaning experiments were conducted on two Al heat exchanger pipes as already described in Section 2.1.3. After 16.1 weeks of operation, it was found that cleaning the fouled heat exchanger pipes was relatively easy. Figures 7.2a and 7.2b display the results of cleaning experiments.

It is relevant to ask how often one should clean the heat exchanger surfaces and to ask if there is any answer to this question to be found in the $R_f(t)$ data. Indeed the slope of the linear portion of the fouling curve will play an important role in arriving at a cleaning schedule. At this point, we will make a distinction between "new pipe" and "cleaned pipe."

A "new pipe" will go through the initial conditioning of its surface as seen by the "induction period" in each of the fouling curves. An aggressive cleaning process may take the pipe surface back to the "new pipe" condition. However, such a cleaning process may remove a significant amount of the pipe material over the life of the pipe as an OTEC heat exchanger surface. A less

aggressive cleaning technique, such as the one tested in our cleaning experiments, would leave the pipe surface in a status close to that after the initial "induction period." Thus cleaning methods that would be used in the OTEC program are more likely to leave the pipe in a "cleaned pipe" condition, and OTEC heat exchangers will always be fouling along the linear portion of the fouling curve.

Using an average value of 6.4×10^{-5} hr ft^2 $^\circ$F/BTU week for the slope of the linear portion of the fouling curve, we can determine the cleaning schedule. For example, if the design attempts to keep $R_f \leq 10 \times 10^{-5}$ hr ft^2 $^\circ$F/BTU, the heat exchanger surfaces must be cleaned once in 1.6 weeks or every 7.8 weeks to keep $R_f \leq 50 \times 10^{-5}$ hr ft^2 $^\circ$F/BTU.

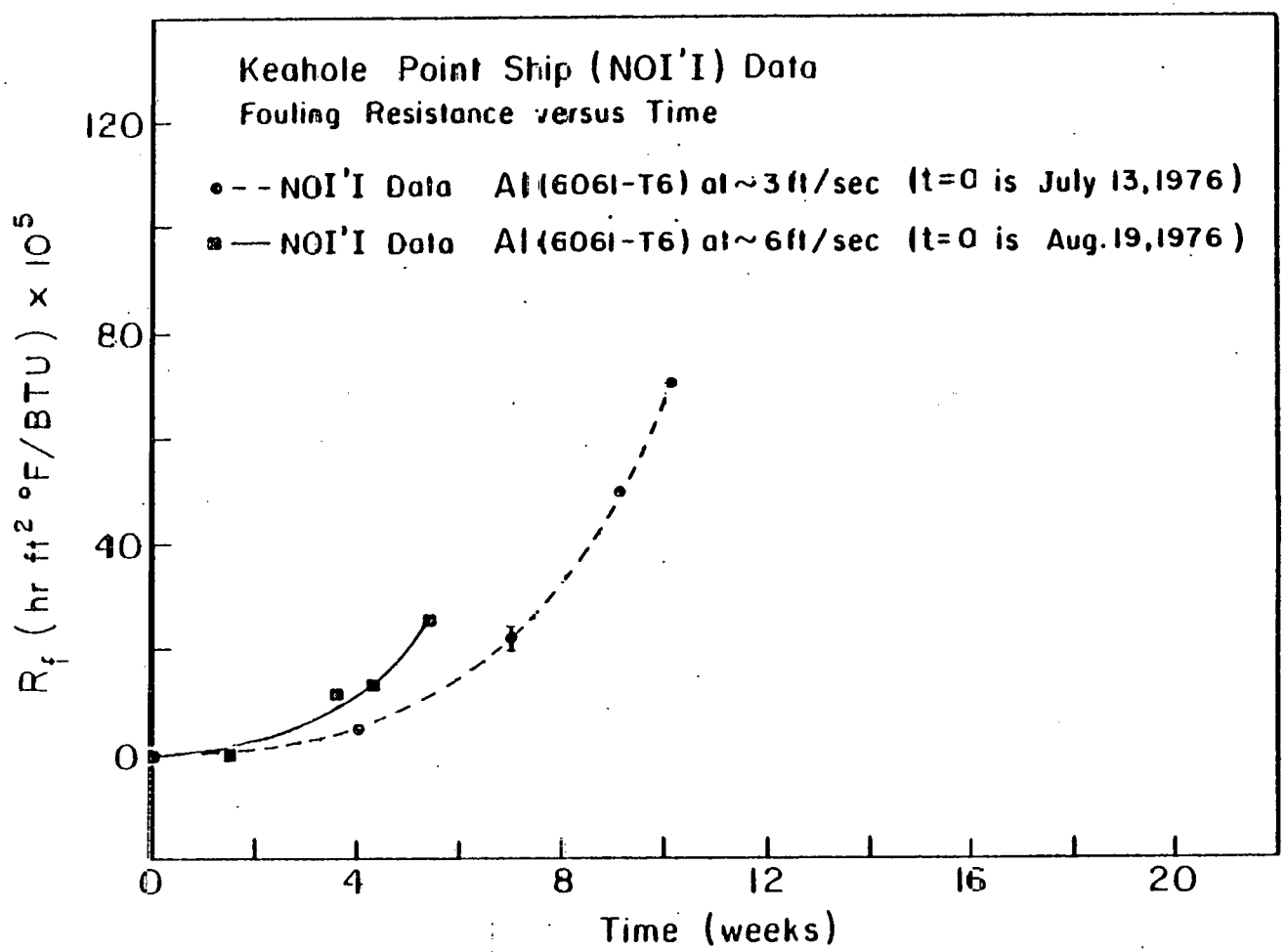

7.1 Thermal Resistance (R_f) vs. Time for Noi'i experiments at Keahole Point

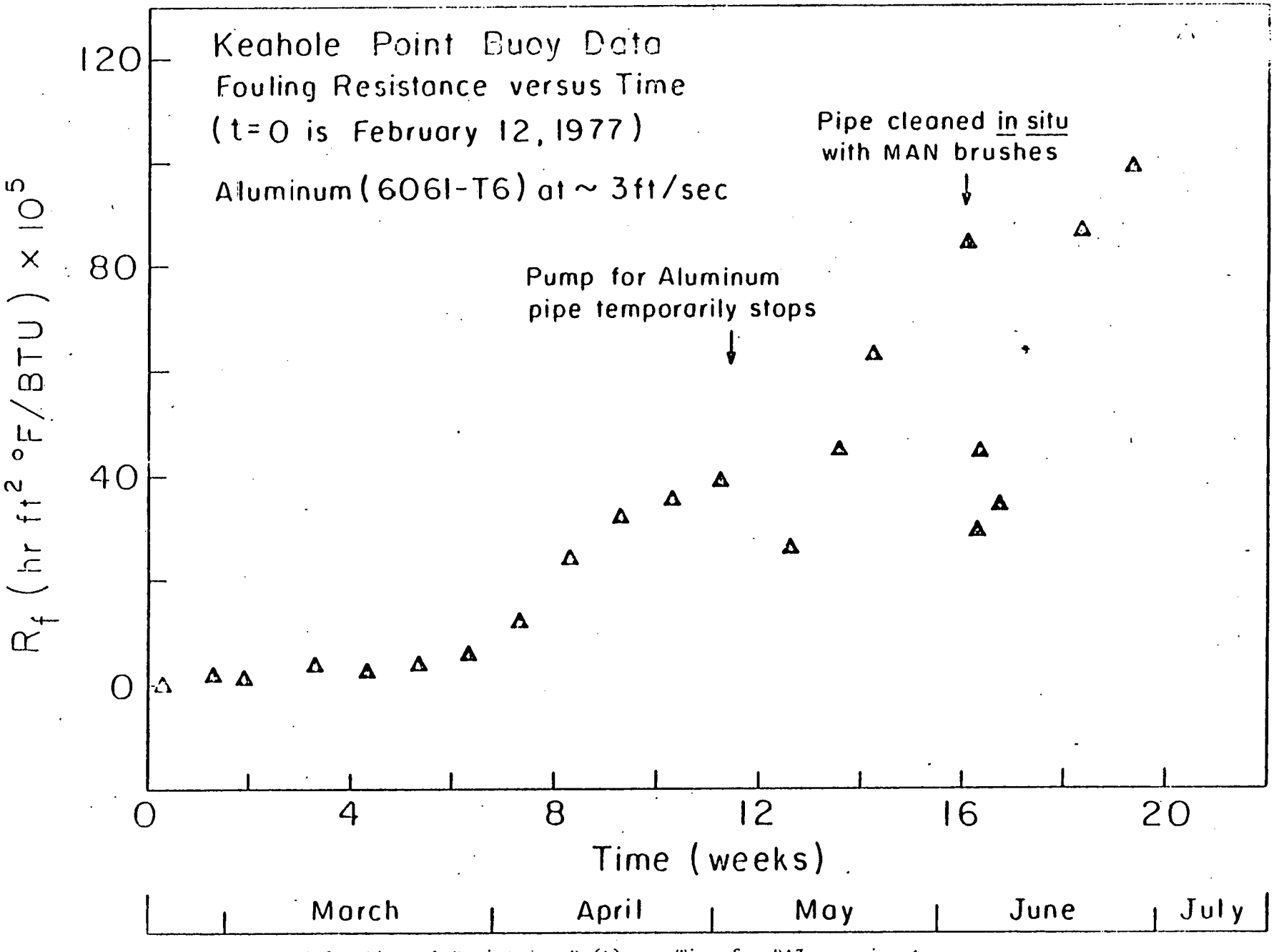

7.2a Thermal Resistance $R_f(t)$ vs. Time for BA3 experiment

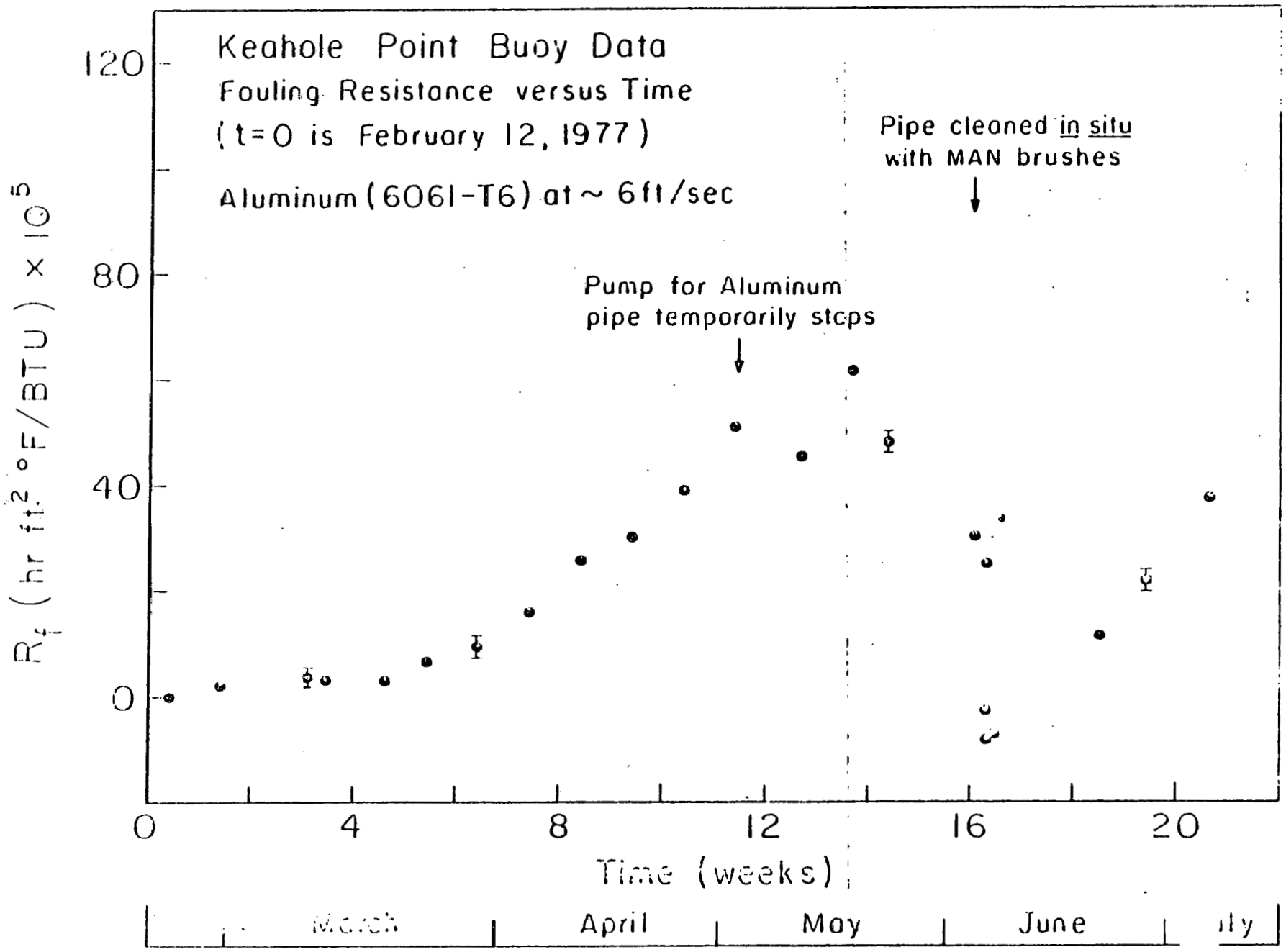
Keahole Point Buoy Data
Fouling Resistance versus Time
(t=0 is February 12, 1977)
Aluminum (6061-T6) at ~ 6ft/sec
Pipe cleaned in situ with MAN brushes
Pump for Aluminum pipe temporarily stops
R_f (hr ft.^{2} °F/BTU) × 10^5
120
80
40
0
0
4
8
12
16
20
Time (weeks)
March
April
May
June

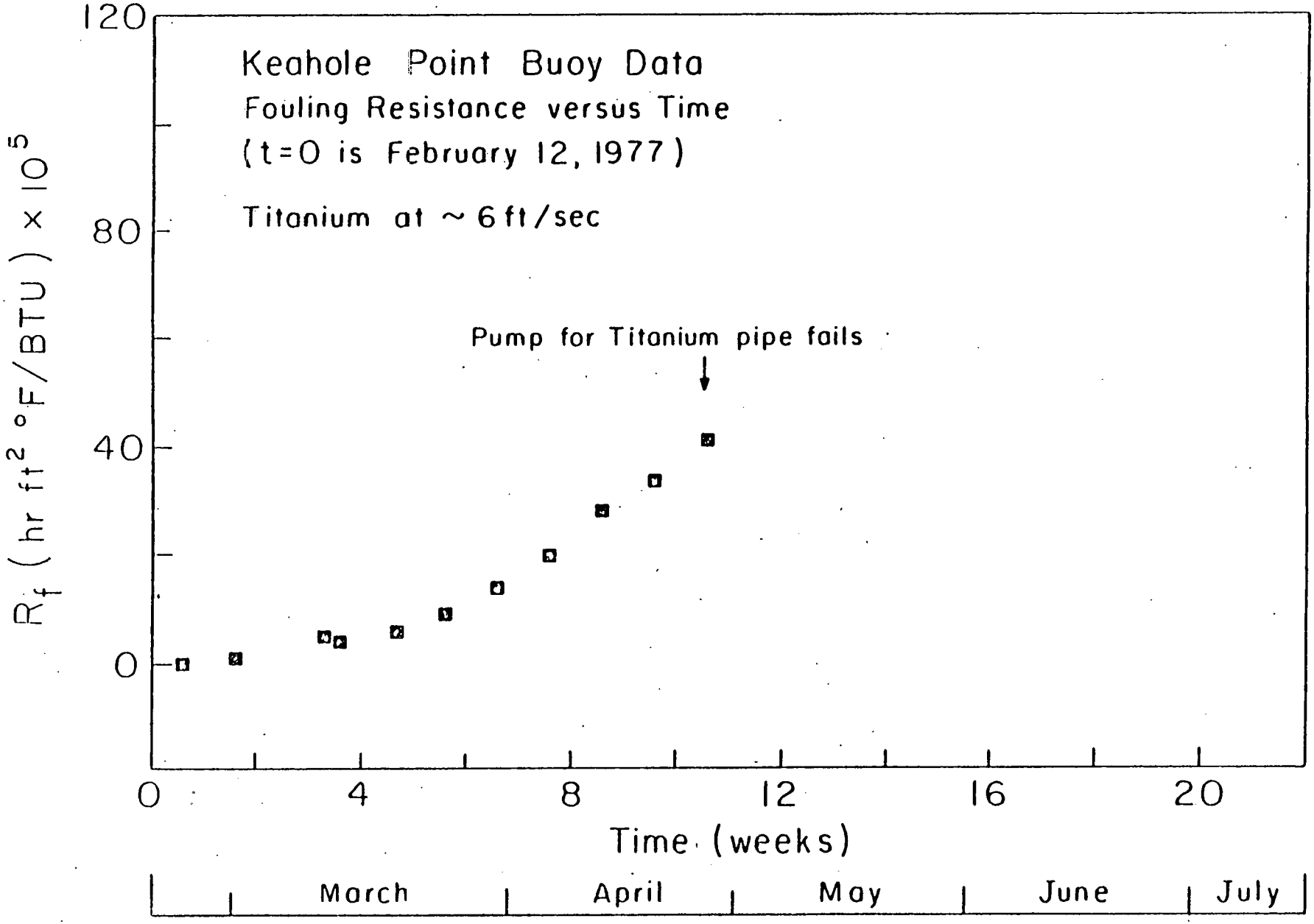

7.2c Thermal Resistance $R_f(t)$ vs. Time for BT6 experiment

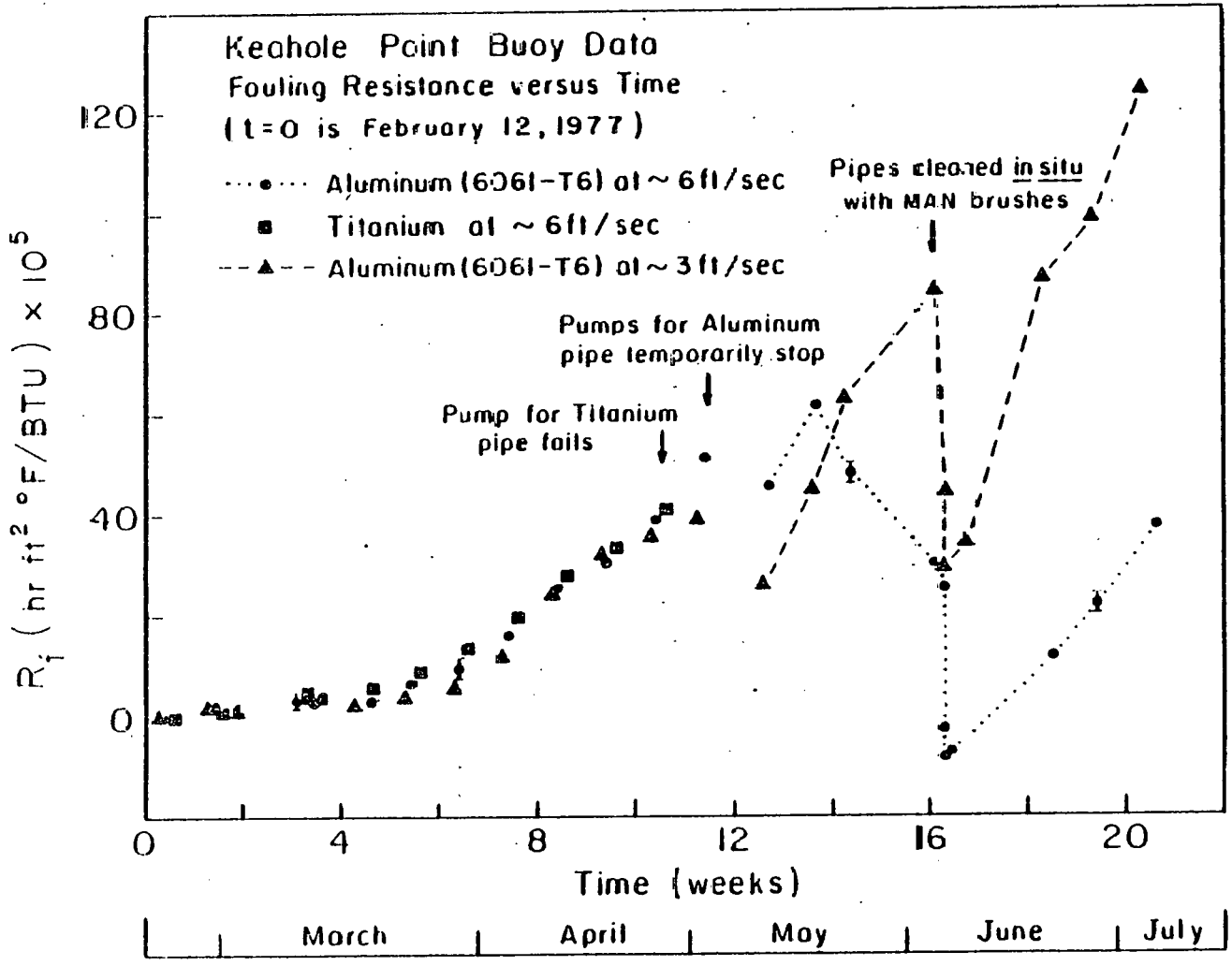

7.24 Thermal Resistance $R_f(t)$ vs. Time for the Buoy Series I experiments

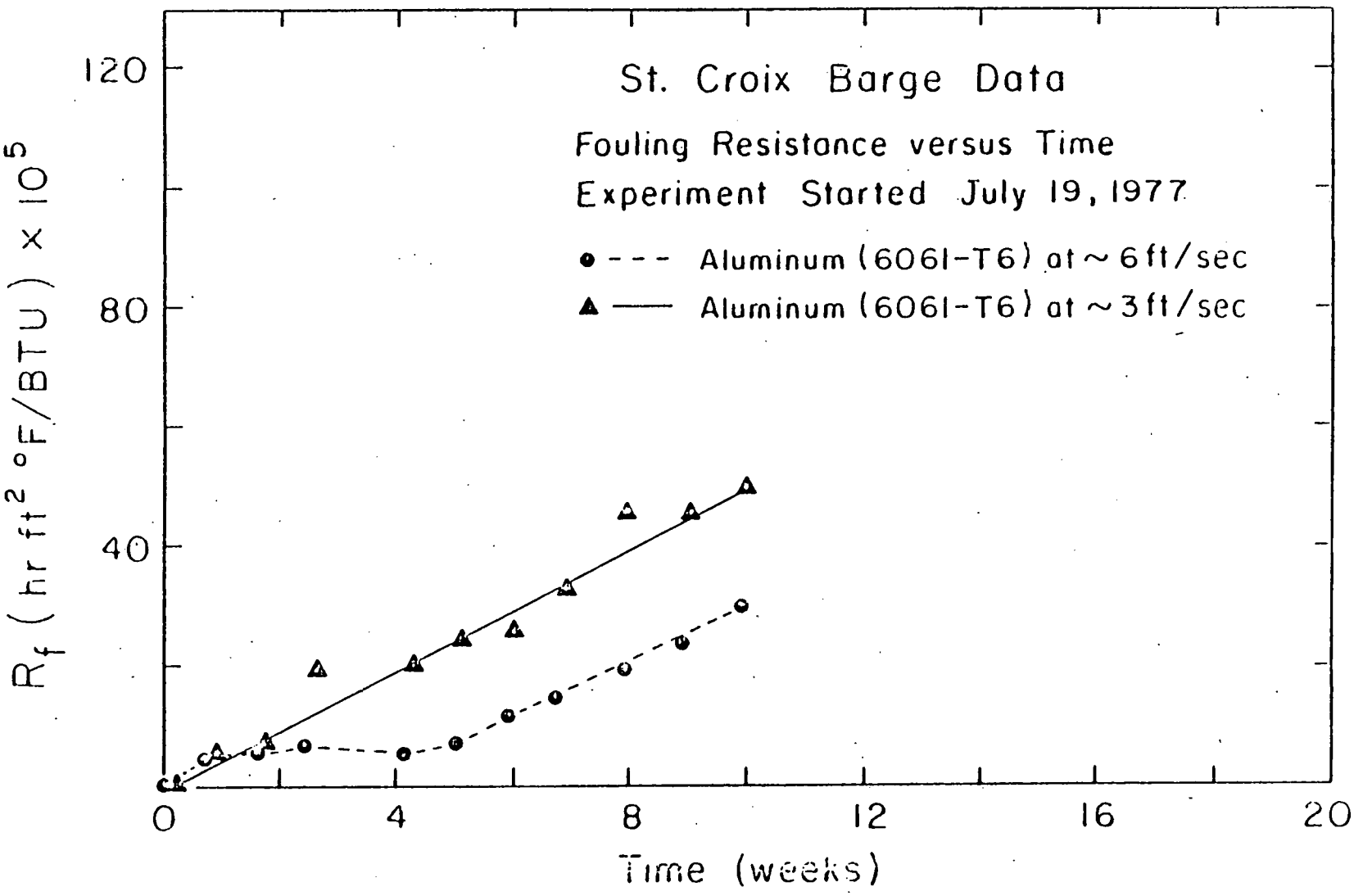

7.3 Thermal Resistance (R_f) vs. Time for St. Croix experiments

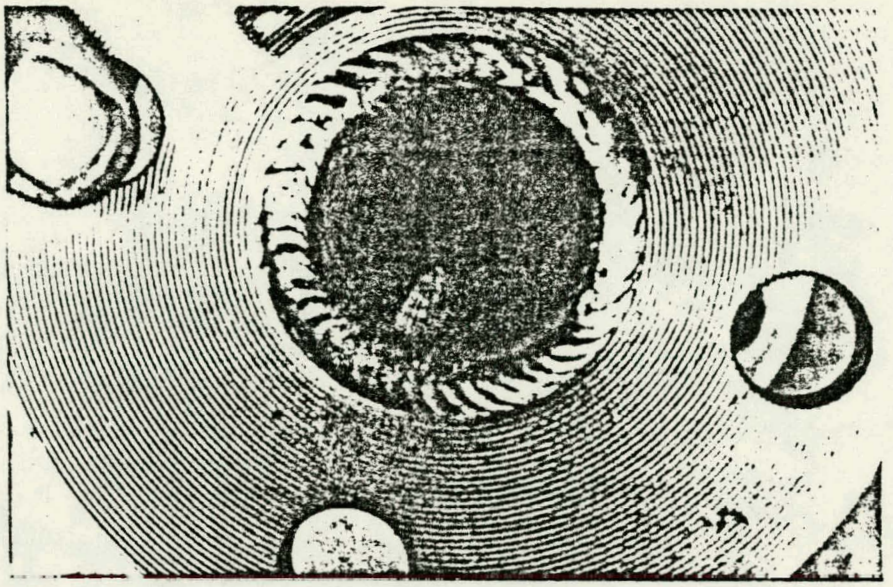

Figure 7.5 Macrofouler (barnacle) attached to the body of the flow meter on the downstream side, from the BA3 experiment.

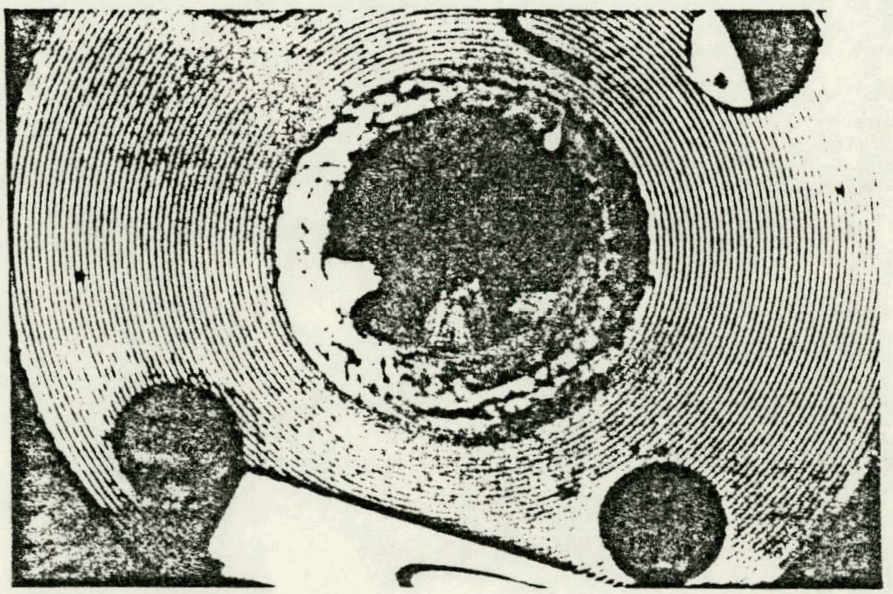

Figure 7.6 Macrofoulers (barnacles) attached to the body of the flow meter on the upstream side, from the BA6 experiment.

TABLE 7.1
PARAMETERS OF CMU OTEC BIOFOULING EXPERIMENTS

Geographical Location	Keahole Point, HI	Keahole Point, HI	Keahole Point, HI	Keahole Point, HI	Keahole Point, HI	St. Croix U.S.V.I.	St. Croix U.S.V.I.
Bacteria/ml of seawater at site	20,000*	20,000*	20,000**	20,000**	20,000**	10+	10+
Pressure change experienced by fouling organisms upstream of the test	35 ft of H_2O	35 ft of H_2O				75 ft of H_2O	75 ft of H_2O
Time of Year	July-Sept	Aug-Sept	Feb-July	Feb-July	Feb-April	July-Sept	July-Sept
Pipe Material	Al 6061-T6	Al 6061-T6	Al 6061-T6	Al 6061-T6	Ti Grade 2	Al 6061-T6	Al 6061-T6
Surface Preparation	cleanser-nylon bristle brush 100 strokes	swabbed with rag and acetone	cleanser-nylon bristle brush 100 strokes	cleanser-nylon bristle brush 100	cleanser-nylon bristle brush 100 strokes	NaOH 10% solution rinse and swab with rag & detergent	NaOH 10% solution rinse and swab with rag & detergent
Nominal Flow Velocity (ft/sec)	3	6	3	6	6	3	6
Water (^{o}C) Temperature	23.2-26.9	22.2-29.1	24.2-26.6	24.2-26.6	24.2-25.8	28.0-28.5	28.0-28.5
Length of Intake Hose (ft)	40	40	0	0	0		
Depth Water Is Taken From To Be Pumped Through Pipe (ft)	20	20	40	40	40	60	60
Section of This Report Describing This Experiment	2.1.1	2.1.1	2.1.2	2.1.2	2.1.2	3	3

* Appendix A of this report.

** No measurements were reported for the period of the experiments, but we expect it to be similar to the count obtained during the Nov'd experiments.

\+ Section 3, Reference 1.

TABLE 7.2

CHARACTERISTICS OF THERMAL RESISTANCE CURVES FOR

CMU OTEC BIOFOULING EXPERIMENTS

Expt.	Conditioning Period (weeks)	Slope of linear portion $\left(\frac{\text{hr ft}^2\ ^\circ\text{F}}{\text{BTU week}}\right) \times 10^5$
NA3	~ 6	20.7[+] ± 2
NA6	> 5	[++]
BA3	~ 6	6.5 ± 1.1
BA6	~ 6	8.4 ± 0.7
BT6	~ 6	6.5 ± 0.3
SA3	< 1	5.9 ± 1.2
SA6	~ 4	4.5 ± 0.3

+ During the course of this experiment there were more short term flow stoppages than other experiments. Further, there was an iron foot valve at the water intake.

++ Experiment did not run long enough to determine a slope.

SECTION 7 REFERENCES

1. Appendix A of this report.

2. K. H. Bathen, R. M. Kamins, D. Kornreich and J. E. T. Moncur of University of Hawaii, "An Evaluation of Oceanographic and Socio-Economic Aspects of a Nearshore Ocean Thermal Energy Conversion Pilot Plant in Subtropical Hawaiian Waters," submitted to National Science Foundation - RANN (April 1975), p. 3.1-23.

3. J. Hirshman, D. L. Meier, R. S. C. Munier and B. F. Taylor, "Introduction to the St. Croix Biofouling and Corrosion Study," Proceedings of the Ocean Thermal Energy Conversion (OTEC) Biofouling and Corrosion Symposium, edited by R. H. Gray (Pacific Northwest Laboratory, Seattle, WA, 1978), p. 387.

4. H. L. Craig, Jr., J. Nelson and R. S. C. Munier, "Cleaning Procedures for Aluminum Pipe and Tubing for Biofouling and Corrosion Experiments," Proceedings of the Ocean Thermal Energy Conversion (OTEC) Biofouling and Corrosion Symposium, edited by R. H. Gray (Pacific Northwest Laboratory, Seattle, WA, 1978), pp. 277-286.

5A. K. C. Marshall, "Mechanism of Adhesion of Marine Bacteria to Surfaces," Proceedings of the Third International Congress on Marine Corrosion and Fouling, edited by R. F. Acker, B. F. Brown, J. R. DePalma and W. P. Iverson (Northwestern University Press, Evanston, IL, 1973), pp. 625-632.

5B. W. A. Corpe, "Periphytic Marine Bacteria and the Formation of Microbial Films on Solid Surfaces," Effect of the Ocean Environment on Microbial Activity, edited by R. Colwell and R. Morita (University Park Press, Baltimore, MD, 1974), pp. 397-417.

5C. W. A. Corpe, "Primary Bacterial Films and Marine Microfouling," Proceedings of the Fourth International Congress on Marine Corrosion and Fouling (Juan-les-Pins, Antibes, France, 1976), pp. 105-108.

5D. K. C. Marshall, R. Stout, and R. Mitchell, "Mechanism of the Initial Events in the Sorption of Marine Bacteria to Surfaces," J. General Microbiology 68, 337-348 (1971).

6. R. P. Aftring, D. G. Capone, L. Duguay, J. W. Fell, I. M. Master and B. F. Taylor, "Biofouling and Site Characterization Studies in an Ocean Thermal Energy Conversion (OTEC) Experiment at St. Croix, U.S. Virgin Islands," Proceedings of: The Fifth Ocean Thermal Energy Conversion Conference, edited by A. Lavi and T. N. Veziroglu (Clean Energy Research Institute, University of Miami, Miami, FL, 1978), pp. VIII-45-VIII-72.

8. MISCELLANEOUS

During this contract period, a good deal of our effort and time were directed toward tasks such as preparing and disseminating information about the heat transfer measurements, producing, testing and deploying equipment for different field operations, consulting and training personnel of other interested research groups and drawing up plans for improvements in the biofouling research. Many of these activities do not conveniently fall under the previous sections. We briefly discuss them in here.

8.1. Design Document and Industry Standard Drawings. As already mentioned, our research group developed this technique of high precision heat transfer measurement suitable for assessing the biofouling potential and accumulated considerable expertise in constructing, testing, and operating this device and in analyzing, interpreting, and correlating the data.

In an attempt to make available this expertise to the OTEC community, we prepared an extensive design document in late 1976 (Ref. 2.4). This document describes in detail the theory, mechanical, electrical and electronics design, assembly, testing and operating procedures, data analysis programs, and some laboratory and field results.

8.2. Equipment. During the contract period, we constructed and tested various items of equipment required for the performance of the experiments reported herein. These included the heat transfer monitoring devices for all the experiments. Both for the Noi'i and the buoy operation, we also constructed the hardware necessary for the pumping. The manual data acquisition systems used with Noi'i experiments, Buoy Series I experiments and the St. Croix experiments were designed and constructed by us as well as a microprocessor-based automated data acquisition system for the buoy operation.

All the hardware pieces produced for field experiments were subjected to appropriate tests before deployment. For example, equipment constructed for the sub-surface application were subjected to extensive tests for any possible leaks using test procedures such as He^4 leak testing, inflation testing and water pressure testing. Each of the heat transfer units deployed during this period also underwent extensive Wilson plot tests to assure their integrity.

8.3. Information Dissemination, Consultation and Training. Another important activity during the contract period was to help diffuse the technology and expertise accumulated within our groups, as directed by the Project Office, through technical discussions, letters, and telephone consultations. In particular, we expended considerable effort in training groups at the Pacific Northwest Laboratories of Battelle, the David Taylor Naval Ship Research and Development Center of the U.S. Navy, the National Data Buoy Office of NOAA and the Natural Energy Laboratory of the University of Hawaii.

8.4. Plans for Greater Automation. The initial biofouling experiments were done with a data acquisition system requiring manual control. The experimental procedure involved a great deal of repetitious work by the operator. This has a tendency to degrade the quality of the data, due to operator mistakes. As already described in Section 2.2.3, we designed and deployed a microprocessor-based data acquisition system which relieves the operator of this burden. This facility also reduced the volume of the raw data.

In 1977, we drew up plans for total automation. The proposed system was based on a DEC (Digital Equipment Corporation) LSI 11/03 with floppy disk facility. Each installation operating many biofouling experiments would have one of these computers. Controlling and running the experiments would be done under software control. The acquired raw data would be stored on diskettes. Such

diskettes would be sent to a central computer which would again be an LSI 11/03 with greater features for software development than the field computer.

Such an approach will have many advantages. Since the field and central computer will be basically identical, any software developed in the central computer could be easily implemented in the field computer. Thus any new control features needed for the field experiments could be developed and implemented easily. The central computer could specialize in developing software features to reduce, analyze and interpret the data. It would make it worthwhile to develop certain sophisticated data analysis procedures and correlation studies. Such features would improve the quality of the acquired information and would make possible better use of it. Further, if there is a need to upgrade a field computer to the status of a stand-alone facility, it would be straightforward to transfer the software developed for the central facility to the field computer.

Our efforts toward these plans included a detailed layout of various system components, a market search for cost and availability of various hardware and software components, and firm quotations on these items. We submitted these plans during April of 1977 to Battelle, the Project Office, who later took part of our proposed plans and asked NSRDC of the U.S. Navy to implement it in connection with planned cleaning tests.

SECTION 8 REFERENCES

1. J. G. Fetkovich, C. W. Fette, R. W. Findley, G. N. Grannemann, L. M. Mahalingam, D. L. Meier, and P. D. Runco, "A System for Measuring the Effect of Fouling and Corrosion on Heat Transfer Under Simulated OTEC Conditions," DOE Report No. C00-4041-10, (1976).

9. CONCLUSIONS AND RECOMMENDATIONS

At the beginning of the contract period, the Biofouling Research Group at CMU had developed and tested a method to measure the heat transfer coefficient under a low temperature differential (~1°C) with a very high precision (better than 1%). This device was approved as suitable for studying the severity of biofouling in OTEC heat exchangers. During the contract period covered by this report, the group successfully applied this technique in three different field experiments, two at Hawaii and one at St. Croix, to evaluate the performance of heat transfer surfaces in the warm seawater. Experiments were conducted with various combinations of relevant parameters such as geographical location, biological and chemical characteristics of the water, season, heat exchanger pipe material, surface preparation, flow velocity, ambient water temperature, and mode of operation with the consequent pressure drop. Before these experiments, it was generally assumed that heat exchanger fouling would be a complex function of all the above (and other) parameters.

On the contrary, the thermal resistance due to the fouling layer seems to have a simple and predictable pattern. A newly deployed heat transfer surface area first passes through the initial conditioning period. This may last a few days to a few weeks, until the thermal resistance grows to about 20×10^{-5} hr ft^2 °F/BTU. Subsequently, the fouling curve is linear. The rate of change of the thermal resistance during this period does not seem to be a function of any of the parameters previously mentioned.

We also carried out the first cleaning experiments (using M.A.N. brushes). The cleaning experiments were encouraging in that the fouling layer could be cleaned relatively easily. The cleaned surfaces then refoul along a linear curve without again passing through a conditioning period. These results, which form the core of the thermal data available to date, have direct relevance to the design of the evaporator of an OTEC power plant.

The simple structure of the fouling curves suggests the possibility that the phenomena causing the thermal resistance may also be simple. To understand these phenomena would be of great use to the OTEC program. It will enable solutions for the biofouling problem in OTEC heat exchangers to be found at lesser costs and in a shorter time. Macroscopic measurements such as the measurement of the thermal resistance of the fouling layer cannot reveal the microscopic structure (the nature) of the fouling layer. To accomplish the tasks of identifying the composition of the fouling film, of understanding the processes responsible for it and of correlating these with the observed thermal data, more detailed thermal, biological and metallurgical studies must be done with coordination.

To date, all the biofouling experiments conducted are of direct relevance to the evaporator of an OTEC plant. It is usually presumed that the condensers will be affected to a much lesser degree. However, it is possible that the condensers may have a severe scaling problem. Furthermore, the biofouling may be equally serious. Thus there is an urgent need to begin fouling experiments with deep cold ocean water, as we have often recommended.

Our experience with the heat transfer monitor is that the flowmeter limits its precision. Also, the target-type flowmeter used is susceptible to macrofouler attachment during long-term flow stoppages. It would be useful to replace this flowmeter by a more precise non-contact type, if possible.

The preparation of the simulated heat exchanger tube has varied in these experiments. The most vigorous cleaning procedure was that used in the St. Croix run, which included immersion in an etching solution. Since this is unlikely to be done with actual OTEC heat exchangers, a more realistic procedure probably should be devised.

We strongly recommend against attempts to "tune" the heater and reference cylinders to equal time constants by means of varying the applied torque on the

clamping bolts. This is likely to lead to more serious problems than the one being solved. It is much simpler and safer merely to reject data affected by large seawater temperature fluctuations by means of the criteria discussed in this report. We have found the loss of precision by such rejections to be negligible.

APPENDIX A

BIOFOULING EXPERIMENTS AT KEAHOLE POINT, HAWAII, 1976

BIOLOGICAL STUDIES PROGRESS REPORT

George W. Harvey
Pan Pacific Laboratories *
and
Department of Zoology, University of Hawaii
Honolulu, Hawaii
December 23, 1976

* Pan Pacific Laboratories was hired by the University of Hawaii to do the biological studies. The University of Hawaii was a subcontractor to Carnegie-Mellon University at that time.

BIOFOULING EXPERIMENTS AT KEAHOLE POINT, HAWAII, 1976

BIOLOGICAL STUDIES PROGRESS REPORT

George W. Harvey
Pan Pacific Laboratories
and
Department of Zoology, University of Hawaii
Honolulu, Hawaii

December 23, 1976

INTRODUCTION

These studies are related to a broad area of marine microbiology involving hundreds of species that were involved in biofouling during the Keahole Point experiment, but are concerned here with direct observations of microorganisms found in the flow system and in the seawater near the experiment intake region. The organisms observed within the flow system include those in deposits on the interior of system pipes, on glass surfaces inserted in the flow within a 1 1/4-inch PVC pipe, and on short sections of aluminum and titanium pipe inserted in the flow within a similar pipe.

The organsims ranged in size from 0.1 micrometer to somewhat more than 100 micrometers. The most numerous, of course, were the bacteria; as time progressed, a substantial biomass composed of larger organisms developed on the exposed surfaces.

It has been known for at least 45 years that bacterial activity in seawater is greatest at surfaces, and that clean glass rapidly becomes covered with a variety of bacteria and other kinds of particulate material, and finally with fouling organisms easily visible to the eye (ZoBell 1933; 1935). The materials deposited by bacteria on surfaces submerged in seawater have been called bacterial slimes, but these materials, as distinct from the organisms included with them, are probably better thought of as bacterial polysaccharides. It has been thought that bacterial populations and the films that they form by means of extracellular products may be necessary precursors of heavy fouling growths of larger organisms, but no definitive tests of this hypothesis have been conducted. There is substantial evidence that such precursors are not necessary (Wood 1967).

Many investigators have observed bacterial growth on carefully prepared glass microscope slides immersed in seawater for various lengths of time, and there is general agreement, based upon work carried out at various nearshore locations,

that significant numbers of bacteria usually attach to glass surfaces within just a few hours (Corpe 1974).

The development of "bacterial slimes" on several types of test surfaces has been studied in some detail by Waksman and others (1940; 1941) in work that was not published. It was found that bacterial populations doubled in about four hours, and that within 30 days the dry weight of the organic material in "slime films" reached as much as 500 micrograms per square centimeter in the summer season. The insoluble mineral materials in the film reached as much as 2000 micrograms per square centimeter. ZoBell (1939) found that the primary film in water near La Jolla, California was made up mainly of bacteria. Wood (1950) found that in other localities diatoms could make up a large portion of the primary film, along with other organisms, and they were resistant to copper and copper salts. Some marine algal flagellates can live in seawater that is practically saturated with copper, and since they are closely related to some bacteria-consuming flagellates, it seems possible that copper tolerance may also exist in that group, and that they could be involved in biofouling communities on metals. Corpe (1974) and Sieburth et al (1974) have recently studied details of primary marine fouling and microbial film formation in waters rich in bacterial nutrients. Firm attachment of bacteria to glass surfaces occurred within 6 to 12 hours. Many bacteria form substantial quantities of polysaccharides and related materials that are deposited on surfaces immersed in seawater. A wide range of bacteria is involved in primary fouling, including very small cocci and large stalked forms.

Sechler and Gundersen (1972) studied the formation of primary films on glass, plexiglass, stainless steel, aluminum, monel, and phosphor bronze, held in glass racks immersed in Kaneohe Bay, Hawaii at a depth of 3 meters. The populations of bacteria and diatoms on metals were generally in proportion to galvanic activity. Aluminum was the most galvanically active metal among those tested, and by the fifth day of immersion had extremely large colonies of microorganisms.

The effects of velocity on fouling of surfaces by marine diatoms was studied by Wood (1967), who found that diatoms would form "felts" about 1 centimeter thick at flow velocities of 5.7 meters per second, and that these offered protection to organisms as large as skeleton shrimps at these velocities. Conventional power plant condenser velocities lie in the range of 1.5 to 2.5 meters per second, while naval designs go as high as 4.5 meters per second. Diatom populations undoubtedly harbor large numbers of bacteria in flowing systems, but details of

the relationships involved have not been worked out.

Corrosion of metals in seawater is strongly influenced by microbial populations. These populations can raise the pH during the day time in volumes of seawater exposed to light, and can reduce it at night, producing variations that have often been observed to vary between pH 9 and pH 7.6. Lower pH values can be produced locally on surfaces by bacterial populations. Redox values can also be altered by bacterial populations so that ordinary solubilities of metals do not apply in areas heavily populated. Marine bacteria can corrode iron by the formation of sulfides or other sulfur compounds, and aluminum can be corroded in the same way except that aluminum hydroxide is formed instead of a sulfide (Wood 1967). It is common knowledge that metals can also be precipitated in seawater in the form of oxides, as for example ferrous and manganous oxides that have been oxidized by bacteria to the ferric and manganic oxides.

METHODS AND MATERIALS

Sections of 1-inch aluminum pipe, 33.58 mm O.D. X 26.24 I.D., removed from the flow experiment units II and III at the end of the tests at Keahole Point were sawed into convenient pieces for examination. The interior surfaces were examined without further preparation, after biological staining, after mounting in glycerine jelly, and after removal of surface deposits by film stripping and by scraping. These surface deposits, after removal, were mounted for microscopy using No. 1 Corning coverglasses. These treatments were applied to two sets of pipes, one that had been air-dried immediately upon removal from the experiment, and one that had been preserved in glutaraldehyde-seawater 2.5% solution.

Sections of the same kind of aluminum pipe, 37 mm long, with the O.D. reduced for clearance, were placed in a PVC 1 1/4-inch pipe which was inserted into the experiment flow system. These sections were removed at different times, and preserved in 2.5% glutaraldehyde-seawater solution except for one that was air-dried immediately upon removal. These were treated and observed in the same way as were the other pipe sections.

A section of titanium pipe, 26.4 mm I.D., 32 mm long, with the O.D. reduced for clearance was inserted in the 1 1/4-inch PVC pipe along with the 37 mm long aluminum pipe sections, at the end of the string, so that it could be left in place until the end of the experiment. This section was preserved in 2.5% glutaraldehyde-seawater solution, and treated in the same way as the aluminum sections except that deposits were not scraped off because there were practically none left after film stripping.

Eight microscope slides, 25 mm X 75 mm X 1 mm (Corning No. 2948), were placed in the flow within a 1 1/4-inch PVC pipe. These were cemented with narrow strips of silicone rubber cement at each end, four slides on either side, to a stainless steel strip running down the center of the PVC pipe. The slides were removed after different lengths of time in the flow, and immediately preserved in 2.5% glutaraldehyde-seawater solution. They were then stained and mounted for microscopy using Corning No. 1 coverglasses.

Forty paired microscope slides, 25 mm X 75 mm X 1 mm (Corning No. 2948), were placed in Wheaton glass staining trays, which were in turn held in groups in a polymethylmethylmethacrylate frame that was submerged at approximately the depth of the experiment intake. Slides were removed at various times and immediately preserved in 2.5% glutaraldehyde-seawater solution. These were subsequently stained and mounted for microscopy using No. 1 Corning coverglasses.

Seawater samples were collected by means of a hose and bellows assembly, or by means of a Van Dorn sampler, from the experiment intake depth and from other depths, and immediately preserved by adding glutaraldehyde to make a 2.5% solution. These were filtered through membrane filters which were then stained and mounted for microscopy using No. 1 Corning coverglasses.

The pipe inner surfaces, glass slides, membrane filters, preserved seawater samples, and surface deposits on the pipe surfaces were examined by means of microscopes that included a Bausch and Lonb metallographic microscope, a Leitz dissecting microscope (8 X to 216 X), and a Leitz inverted phase contrast microscope with 0.65 NA and 1.32 NA objectives. Photomicrographs were taken with a Microflex unit. To simplify enumeration, bacteria with dimensions below 1 micrometer were grouped under "small bacteria"; those above 1 micrometer were classed as "large bacteria". For each visually observed microscopic field, many image planes were utilized so that the smallest bacteria could be detected.

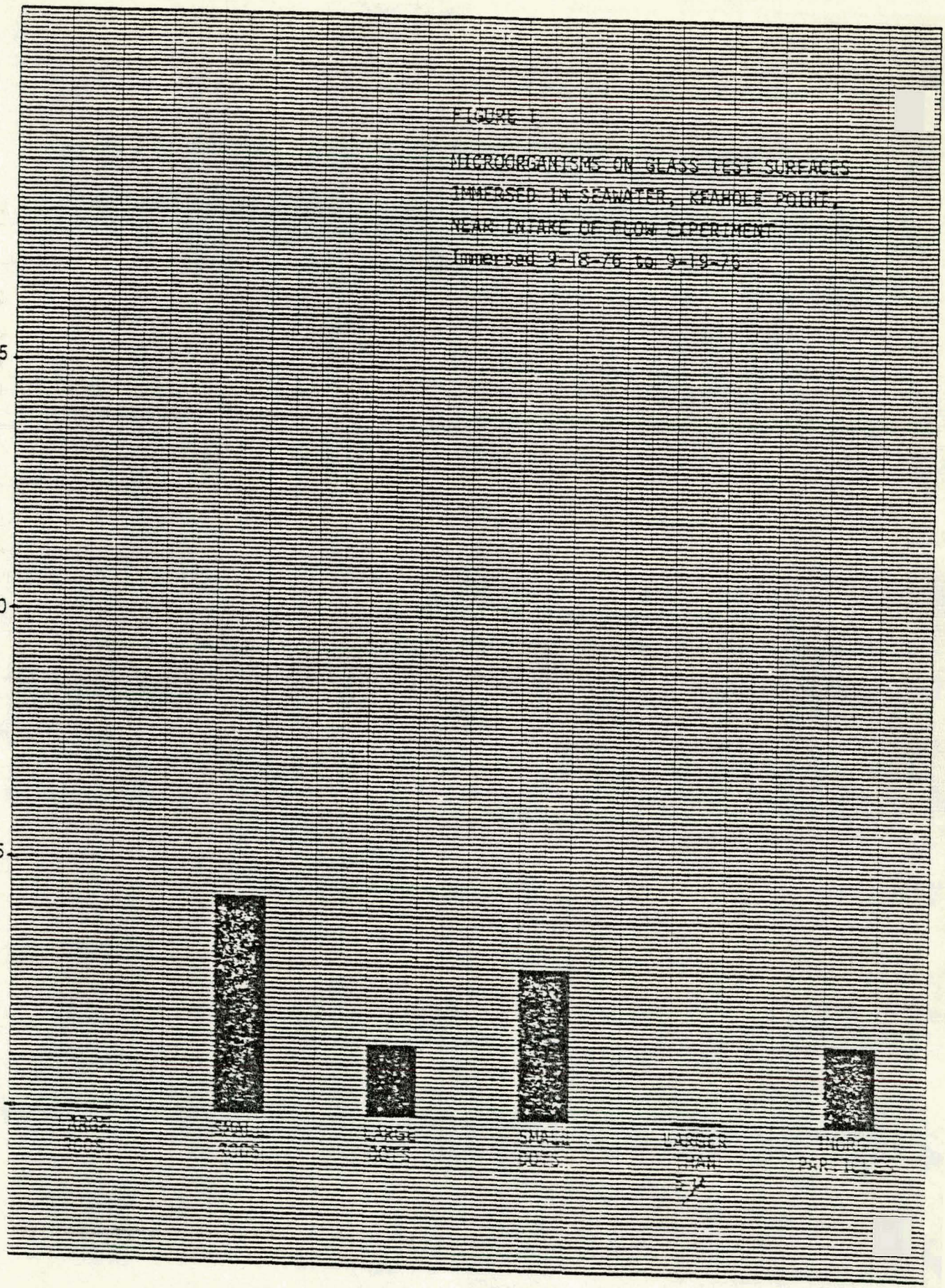
FIGURE 1
MICROORGANISMS ON GLASS TEST SURFACES
IMMERSED IN SEAWATER, KEAHOLE POINT,
NEAR INTAKE OF FLOW EXPERIMENT
Immersed 9-18-76 to 9-19-76
15
10
5
0
X 10⁴/cm²
SMALL RODS
LARGE RODS
SMALL BUDS
LARGER BUDS
PARTICLES

RESULTS

Examination of glass surfaces immersed near experiment intake

The particulate material found on the glass slides with the shortest immersion time (1 day) was composed mostly of small bacteria, as shown in Figure 1. There were no large particles, although a very few glass flakes and mineral grains approaching 5 micrometers in size were present. No organisms larger than bacteria were found, although a more extended observation of glass surfaces immersed for one day or less probably would disclose diatoms.

Slides with a 4-day immersion time had increased numbers of small rod bacteria, a few large rod bacteria, fewer inorganic particles than the 1-day slides, and considerable numbers of large diatoms. The numbers of the various types of organisms are shown in Figure 2. Although all the organisms in the larger than 5 micrometers category are large pennate diatoms, illustrated as being present in numbers of 10,000 per square centimeter, a more extensive study of this material would probably show far fewer of these along with other kinds of organisms not indicated in the illustration. Large numbers of diatoms often accumulate in localities with very few individuals outside the groups. Many pennate diatoms can "crawl" rapidly over surfaces, and can adhere quite firmly either while at rest or while moving. Those found on 4-day slides are shown in Figure 5.

Slides with an eight-day immersion time were still more heavily populated by small rod bacteria (Figure 3). The numbers of large dot bacteria and small dot bacteria had increased, as had diatoms. The species composition of the diatom population was different from that of the 4-day slides, being made up mostly of Nitzschia, many of which were dividing (Figure 6 a). In some areas on these slides, there were clusters of the same large diatoms as found on the 4-day slides, but with other species of diatoms and additional small particles and organisms included in the diatom clusters (Figure 6 b, Figure 6 c). Flagellates smaller than 6 or 7 micrometers were also present, but in smaller numbers than the diatoms. Inorganic particles were fewer than on the earlier slides.

The numbers of marine bacteria populating these slides were far lower than those

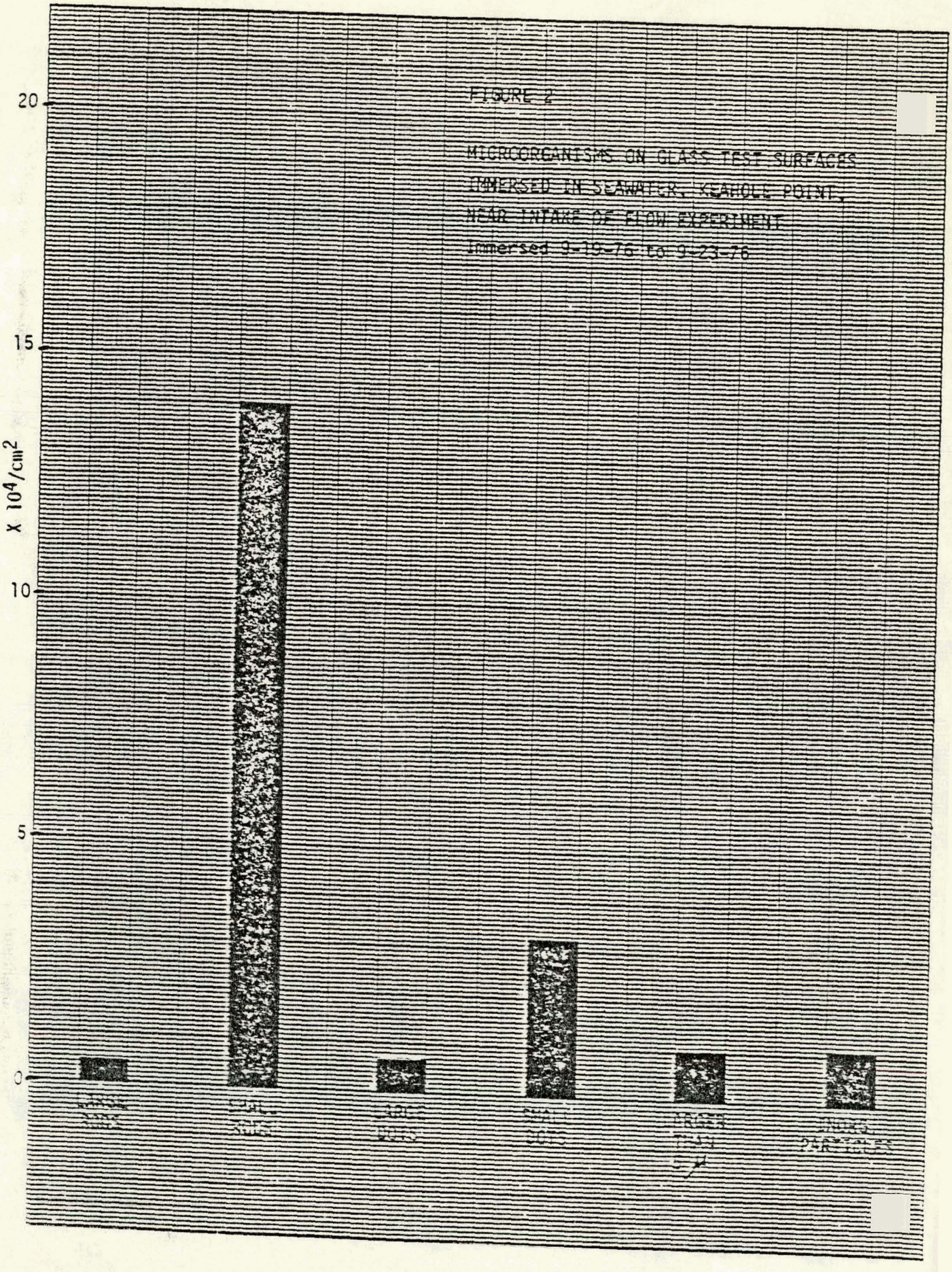
FIGURE 2
MICROORGANISMS ON GLASS TEST SURFACES
IMMERSED IN SEAWATER, KEAHOLE POINT,
NEAR INTAKE OF FLOW EXPERIMENT
Immersed 9-19-76 to 9-23-76
20
15
10
5
0
X 10⁴/CM²

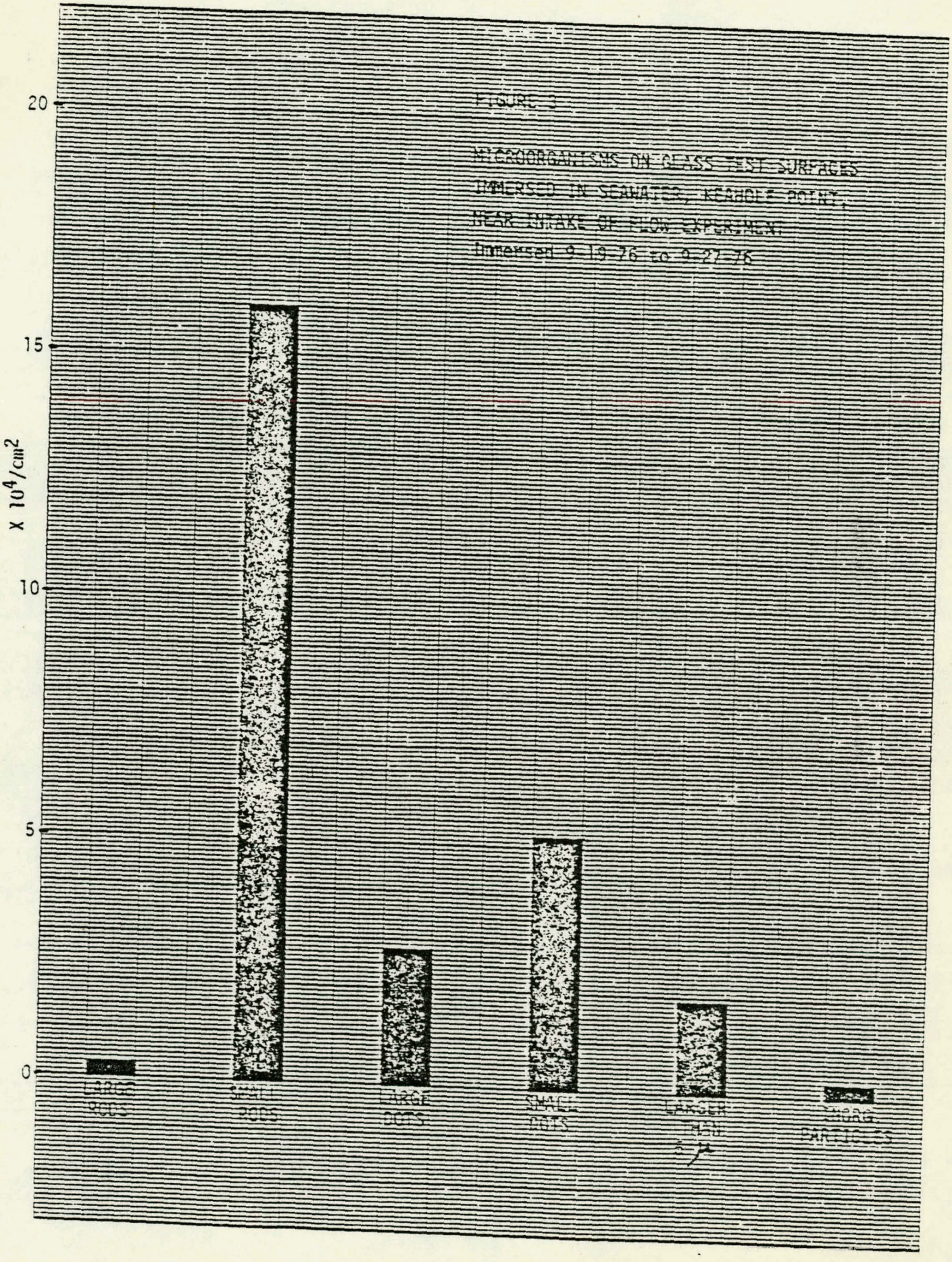
FIGURE 3
MICROORGANISMS ON GLASS TEST SURFACES
IMMERSED IN SEAWATER, KEAHOLE POINT,
NEAR INTAKE OF FLOW EXPERIMENT
Immersed 9-19-76 to 9-27-76
X 10^4/cm^2
20
15
10
5
0
LARGE RODS
SMALL RODS
LARGE DOTS
SMALL DOTS
LARGER THAN 5 µm
CHARG. PARTICLES

FIGURE 4

NUMBERS OF MARINE BACTERIA PER SQUARE CENTIMETER ATTACHING TO GLASS SLIDES IMMERSED IN SEAWATER AT SCRIPPS INSTITUTION OF OCEANOGRAPHY PIER

Data from Corpe 1974

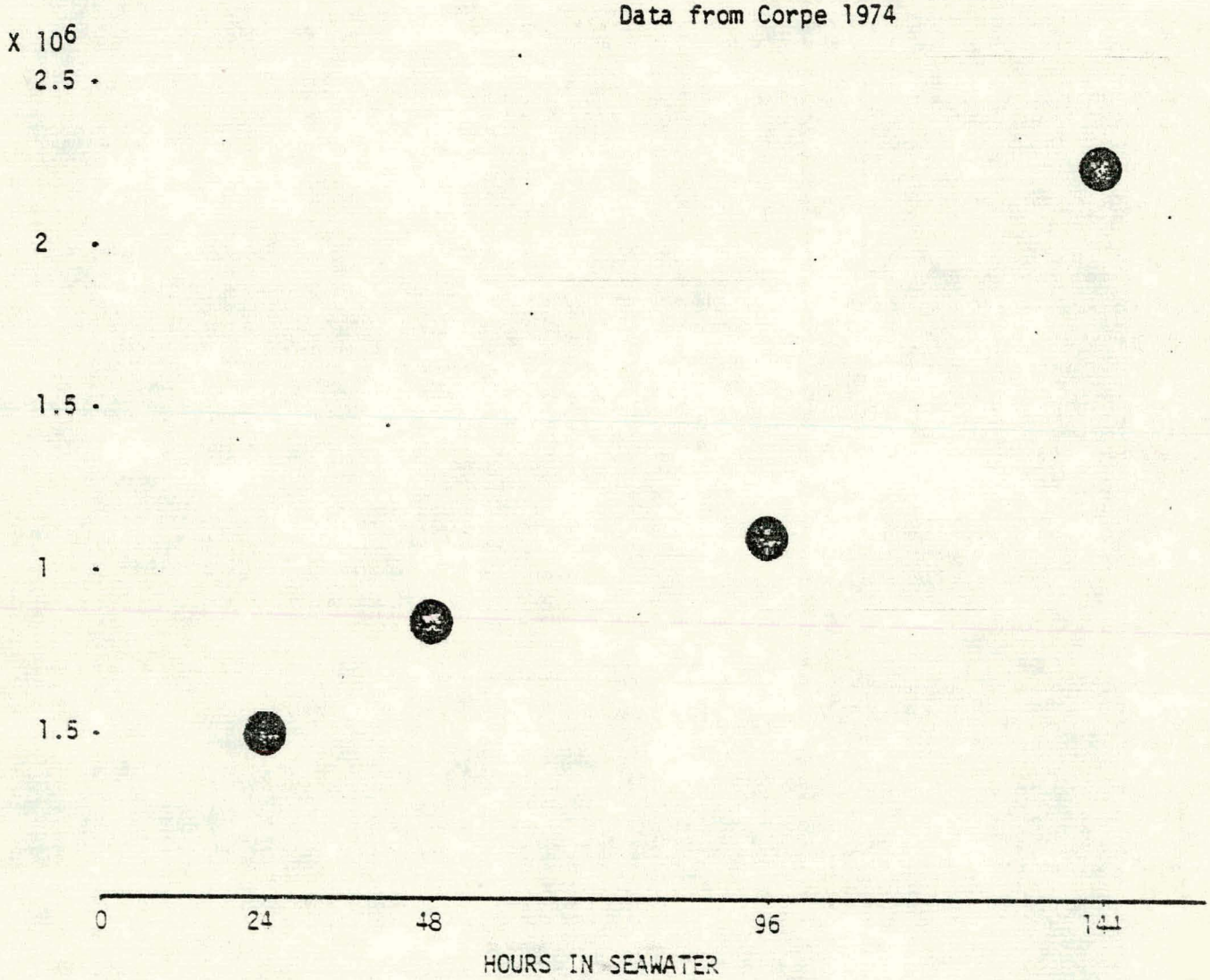

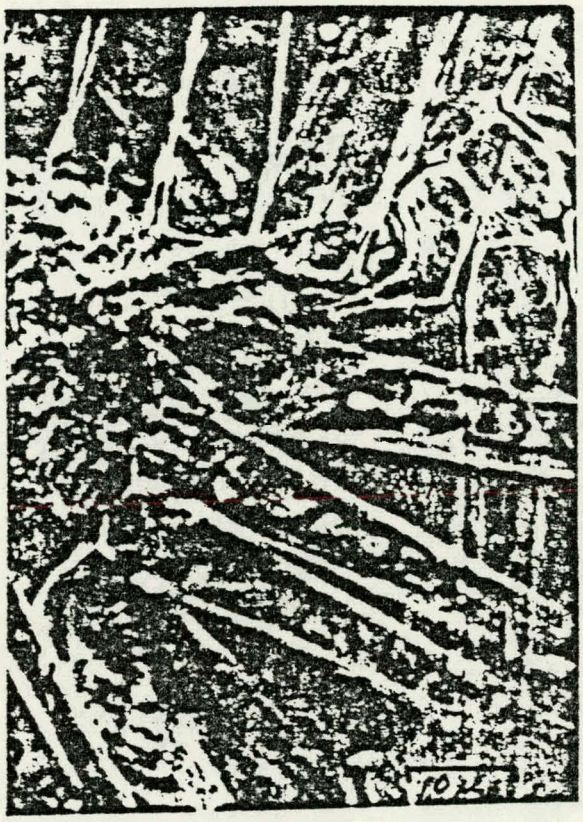

FIGURE 5. Cluster of large pennate diatoms found on glass slide immersed for 4 days in seawater near experiment intake.

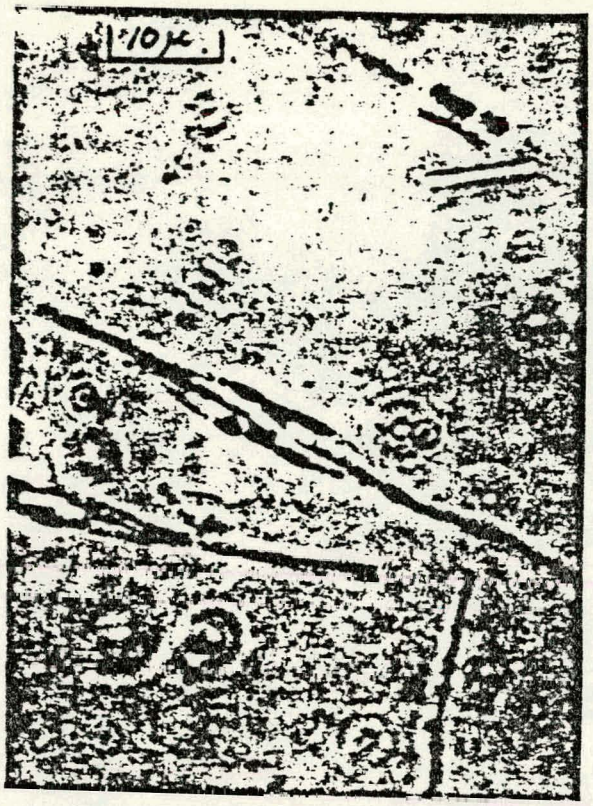

a

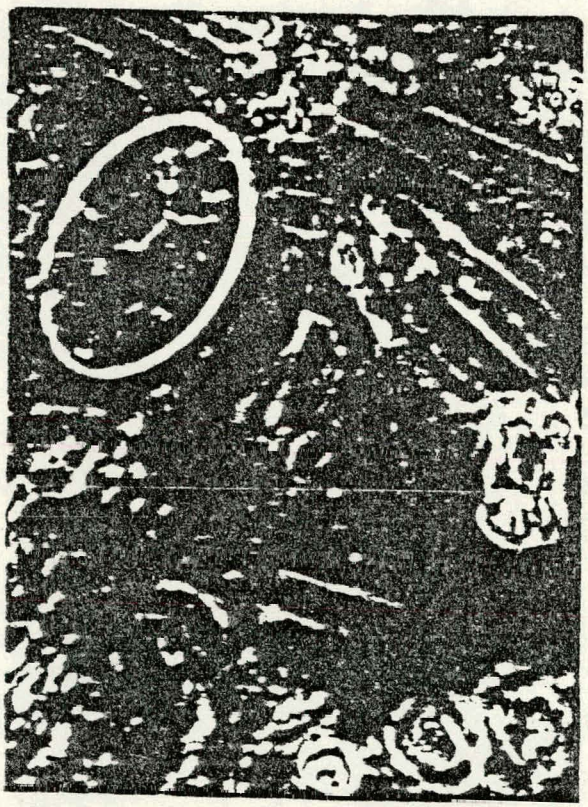

b

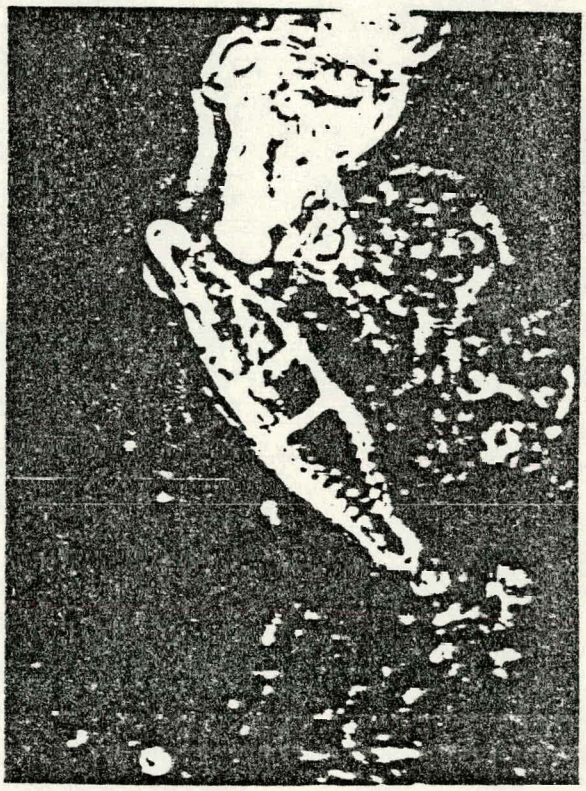

c

FIGURE 6. Diatoms found on glass slides immersed for 8 days in seawater near experiment intake. a, pennate diatoms (Nitzschia) in process of division. These are typical of the many found on the slides. b, and c, Clusters of pennate diatoms with an accumulation of other organisms and particles.

found attaching to glass slides in nearshore water at La Jolla, California in a study carried out by Corpe (1974). The numbers found at different times ranging from 24 to 144 hours of immersion are shown in Figure 4. The water at this location is turbid, with a very high bacterial population accompanied by bacterial viruses and bacteria-consuming protozoa in large numbers, and contains a high level of bacterial nutrients. Primary fouling film formation cannot be directly compared at La Jolla and at Keahole Point although similar glass surfaces and immersion times were employed at both locations. The differences in water quality and temperatures are far too great to allow a detailed prediction based on one locality to be used for the other.

Examination of glass surfaces exposed to flow in pipes

Slide exposed to flow for 6 days: There were very few particles or organisms on the slide, but widely scattered groups of bacteria were present. The numbers of bacteria and other particles are shown in Figure 7. There were also significant numbers of flattened nucleated cells 15 micrometers across. These very thin cells were not encountered on the other slides.

Slides exposed to the flow for 32 days presented a very different appearance from the earlier slides. At low magnifications, the most striking feature was a strongly developed pattern aligned with the pipe axis. This pattern was due to strings of bacteria, various filamentous organisms, and a variety of particulate material that included glass flakes and fibers. Several kinds of diatoms were present. There was a strong development of amebas, probably ameboid flagellates. The surface of the glass was covered, entirely, by a well developed film containing much fine and ultrafine granular material. This film was very dense, and contained various kinds of bacteria including filamentous types. Some of the filamentous organisms are shown in Figure 8 a, which also shows the dense film. In the area photographed, the film varied from 1 micrometer to about 2.5 micrometers in thickness, and is representative of the film on this slide as well as on the others with similar exposure times. Typical amebas found on this group of slides are shown in Figure 8 b and c.

One of the 32-day slides was extensively covered by a colonial hydrozoan, shown in Figure 9. This colony grew on the surface of the primary fouling film, and was

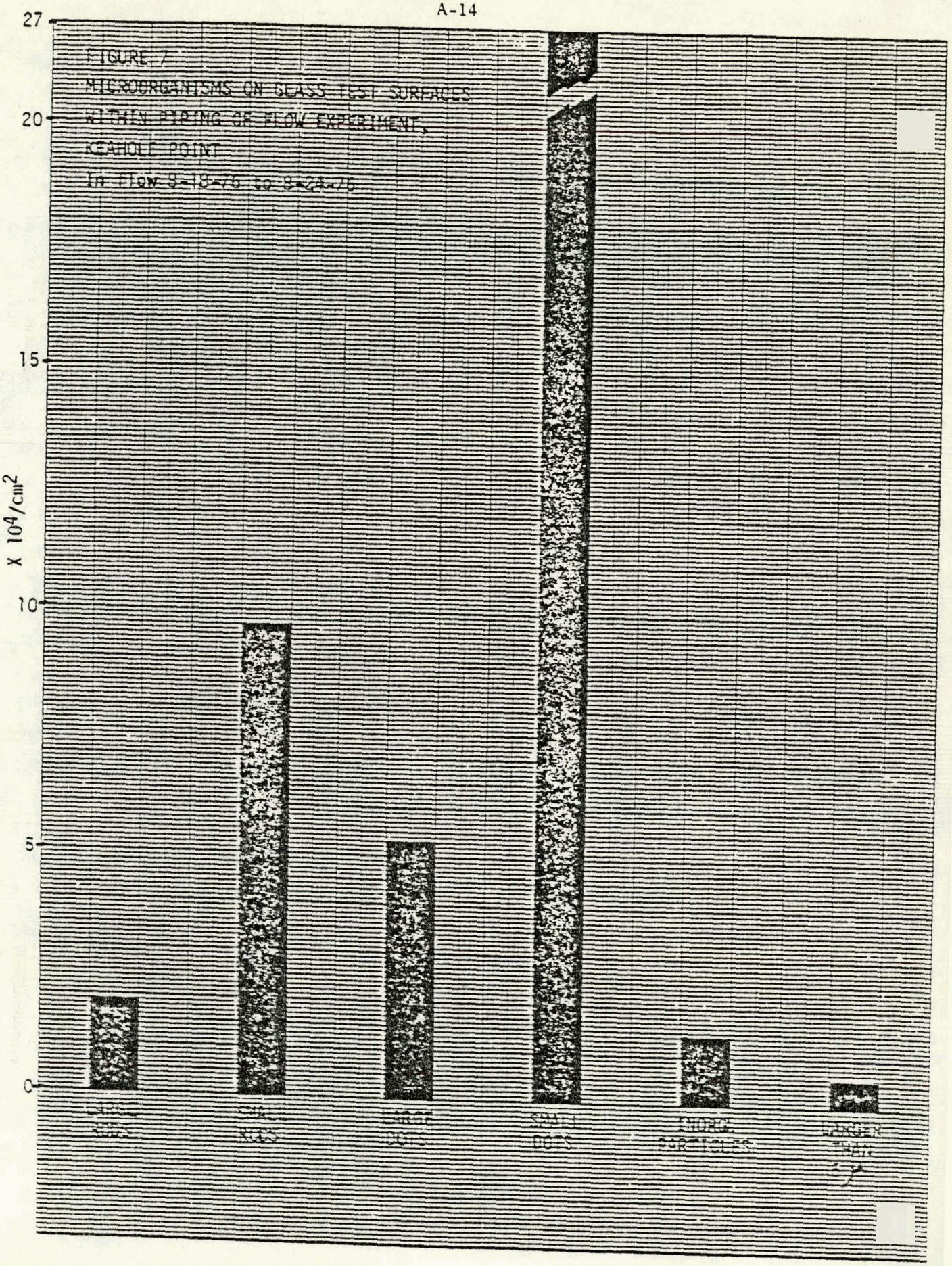
FIGURE 7
MICROORGANISMS ON GLASS TEST SURFACES
WITHIN PIPING OF FLOW EXPERIMENT,
KEAHOLE POINT
IN FLOW 8-18-76 TO 8-24-76
X 10⁴/cm²
27
20
15
10
5
0
SMALL RODS
COIL RODS
LARGE RODS
SMALL DOTS
INORG. PARTICLES
LARGER THAN

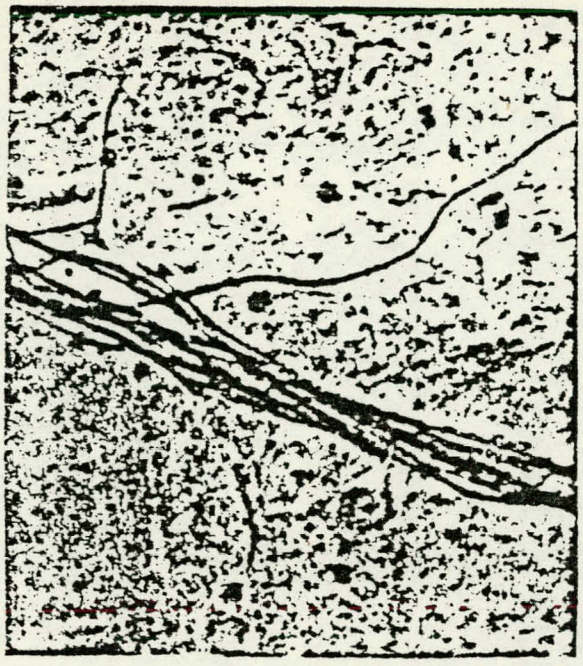

a

FIGURE 8. Primary fouling film and filamentous organisms (a), and amebas (b, c) found on glass surfaces exposed to flow for 32 days

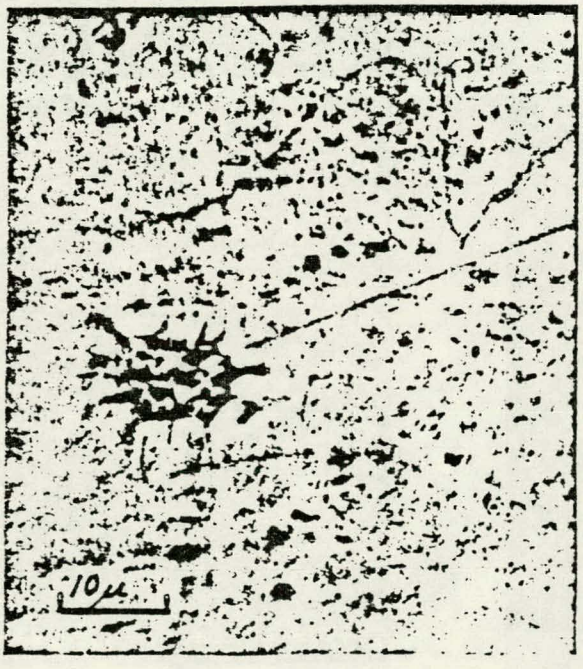

b

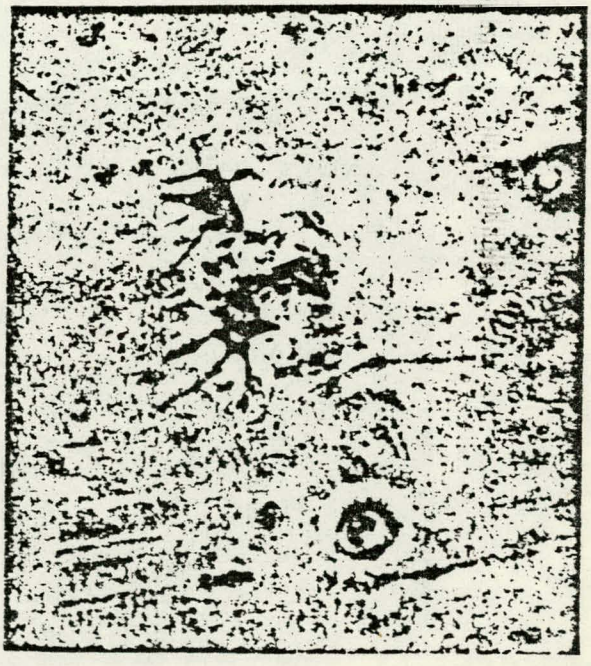

c

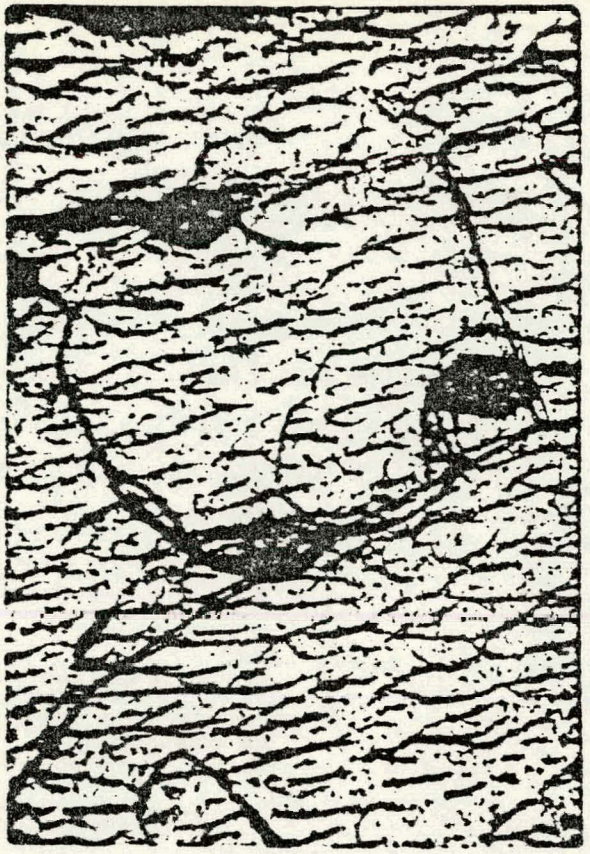

a

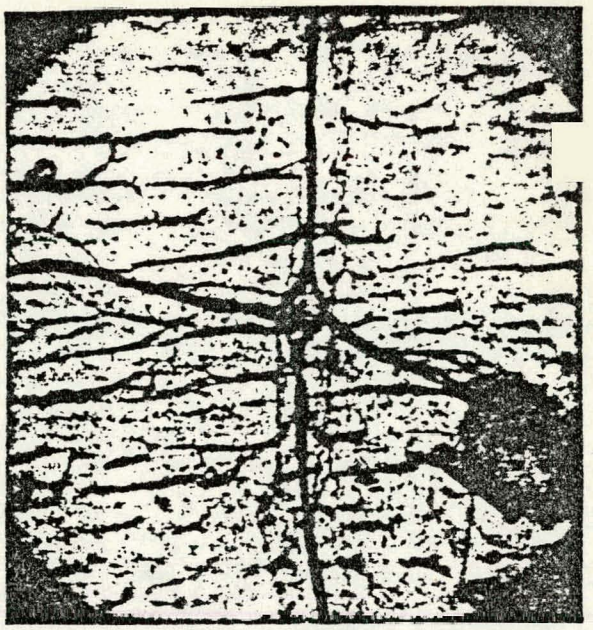

b

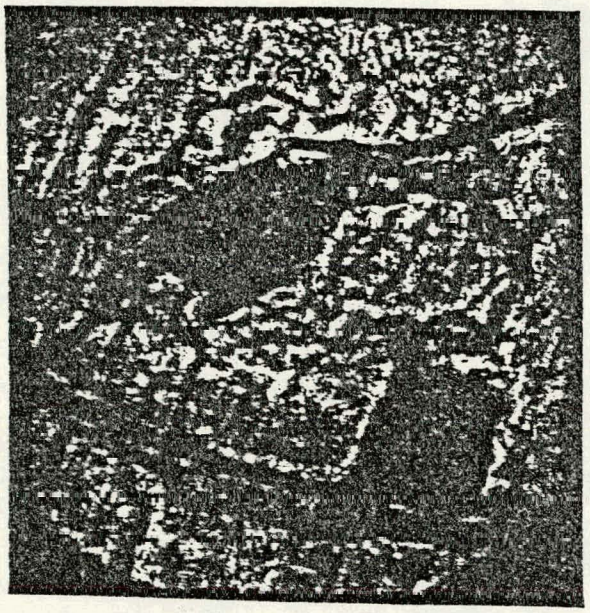

c

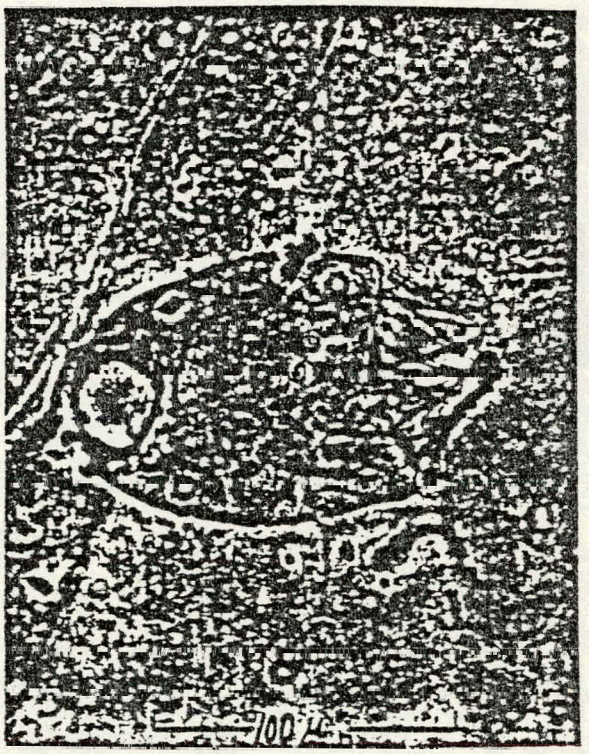

d

Figure 9. Colonial hydroid extending over a large area of a glass slide exposed to flow for 32 days. a, b, c, portions of branching colony growing on primary fouling film. d, chitinous hydrotheca and perisarc of individual zooid. The pattern induced by flow and resulting microbial growth lies beneath hydroid colony.

in the process of budding when removed from the flow. Many of the zooids had accumulations of large pennate diatoms around them. In Figure 9 a and 9 b, the pattern of bacteria, filamentous organisms, and other particles, induced by the flow, can be clearly seen beneath the hydroid colony. Figure 9 d shows the chitinous hydrotheca and perisarc of an individual zooid. Although some very long diatoms are present (length about 230 micrometers), the organisms largest in volume are the hydroids.

Examination of seawater samples

The seawater samples collected near the experiment intake, and at "New Site" and "Buoy Site" after completion of the flow experiment were examined qualitatively. Quantitative determinations of bacteria, protozoa, phytoplankton, and inorganic particulate materials were not carried out because of the necessity to economize. By far the most numerous organisms were bacteria, with small rod and coccus forms predominating. Small diatoms (Nitzschia), small heterotrophic flagellates, and dinoflagellates of several species were common, but all combined made up only 1/100th of the numbers of total bacteria. There 14 times as many bacteria as there were particles of debris and inorganic materials.

In some seawater samples there were relatively large quantities of plant fibers that may have originated in runoff from land, or from sewage.

In many of the seawater samples there were glass fibers typical of "glass wool" or "rock wool", as well as fragments of glass in the form of chips. There were also small spheres of various sizes that appeared to be of glass. The glass fibers could form a significant portion of deposits on surfaces in the seawater because of entrapment by biological materials. Typical glass fibers are shown in Figure 10, a and b.

Total bacteria in many of the seawater samples were on the order of 20,000 per milliter of seawater, with small rod bacteria making up about 43%, small cocci making up about 39%, and large rods and large cocci contributing equally to the remainder.

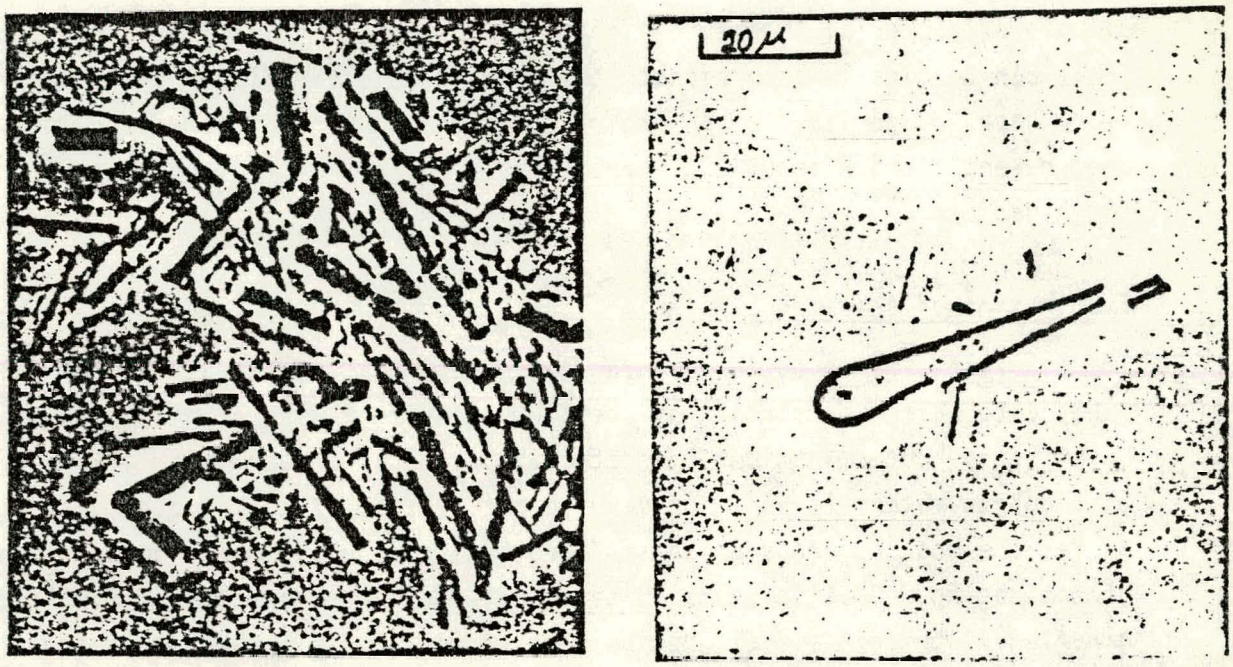

a b

FIGURE 10. Glass fibers typical of those found in seawater samples and on surfaces in flow

Examination of pipes

Aluminum pipe labeled II-F was removed at the end of the experiment at Keahole Point; there were two sets of these pipes, one that had been air dried immediately upon removal, and one that had been preserved in 2.5% glutaraldehyde-seawater solution. These 1-inch schedule 40 pipes were of Type AL 6061 T6, 33.58 mm O.D. X 26.24 mm I.D.

The inner surface of the dried section was covered with an orange-yellow colored deposit that had a fibrous, ropy appearance under the microscope. The major features of the deposit paralleled the axis of the pipe, but other ran at an angle to the axis. The surface of the fouling layer was very irregular, with many ridges and mounds, as shown in the photographs in Figure 11. Some whitish aluminum corrosion products can be seen in the photographs. There were a few mounds outside of the area photographed that were a brick red color. The rough-structured surface of the deposit could be smeared without breaking, and could be scraped off with heavy pressure from a fingernail, leaving a denser, smoother "pavement" on the aluminum surface which had a cracked and checked appearance. This in turn, could be scraped off with a boar's tusk; it was very brittle and easily broken up with a steel probe. Some of the scale was carefully scraped off the aluminum surface, and mounted for microscopy. The inclusions in this scale, and the brittle fracture are shown in the photomicrographs in Figure 12. A few small pits were found under the deposits.

The inner surfaces of the preserved portions of the aluminum pipes were very similar in appearance to those of the dried ones, but more detail could be observed. In order to facilitate measurement of deposit thickness and observation of particulate materials within the deposit, the entire deposit was removed by means of collodion films and mounted for observation with high resolution optics. The average height of the deposits, from 10 measurements at random. was 22.9 micrometers. The thickest of these was in a "ridge" area, and measured 34.8 micrometers. There were occasional portions of the deposits that were much thicker—up to 87 micrometers high.

Many bacteria and pennate diatoms were present in this material. Most of the larger diatoms (some measuring 3.5 X 60 micrometers) were approximately parallel to the flow, as were the ridges and crevices of the deposit. The interior surface of the pipe had longitudinal crevices and ridges that probably initiated the general pattern of the deposit, and definitely was responsible for inclusion of parallel

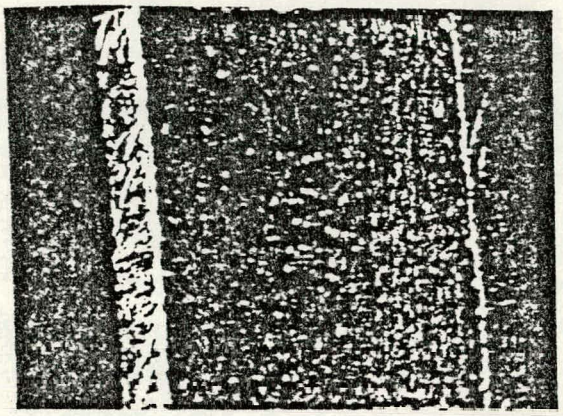

FIGURE 11. Inner surfaces of aluminum pipe II-F, air dried after removal from flow. The white spots are aluminum corrosion products. The metal particles, which could not be removed without disturbing the rest of the material, are from the saw cuts.

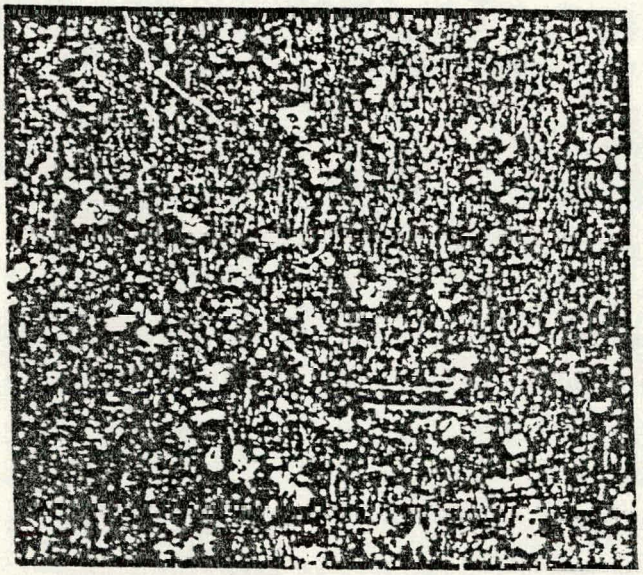

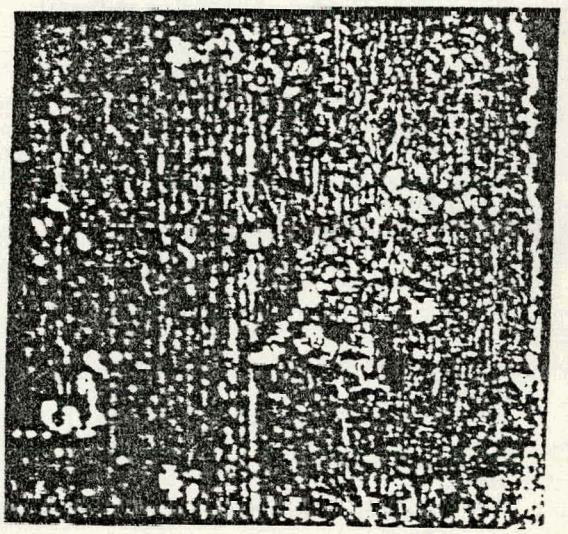

a

FIGURE 12. Scale material scraped from inner surface of aluminum pipe II-F. a, b, and c are under different phase contrast conditions to show inclusions and brittle fracture.

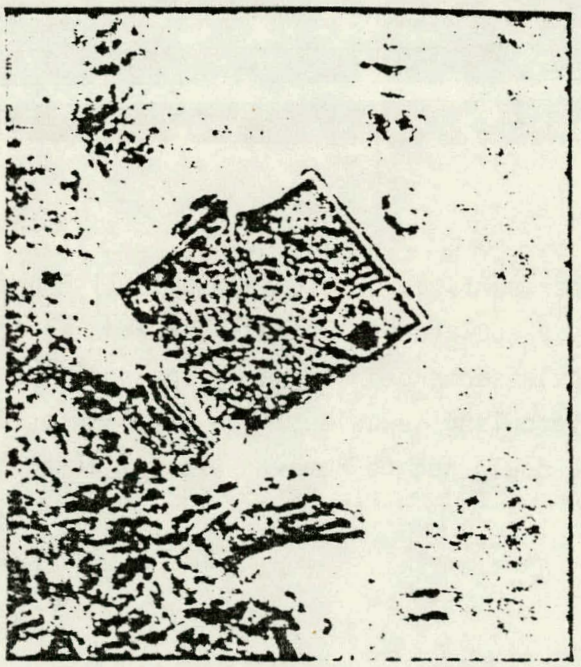

b

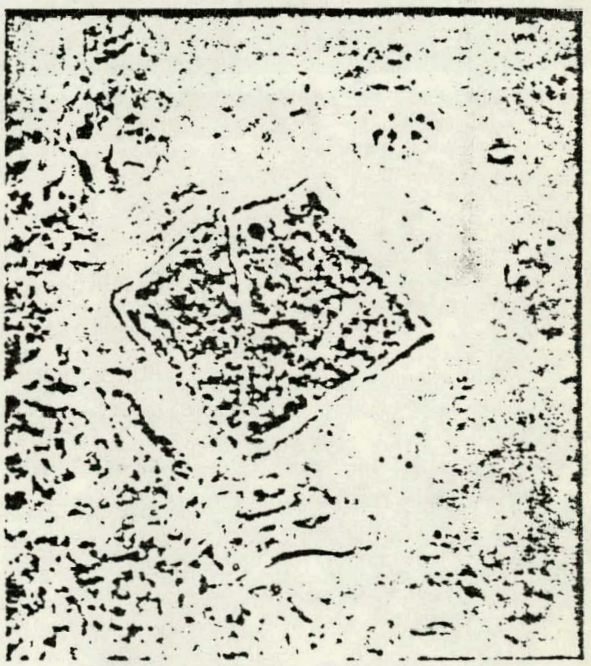

c

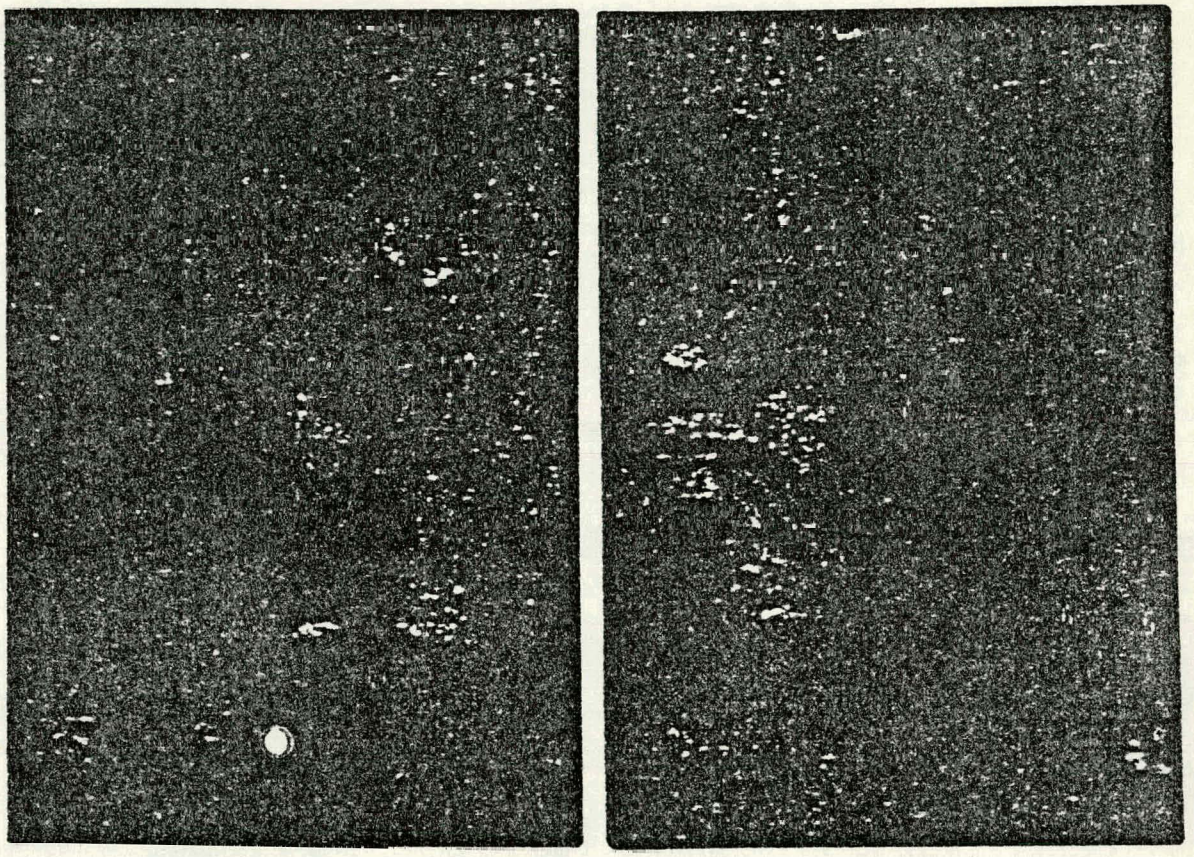

FIGURE 13. Inner surfaces of aluminum pipe II-F preserved in glutaraldehyde-seawater solution after removal from flow. Photographed while submerged in preserving solution to show typical biofouling deposits. The metal chips from sawing the pipe could not be removed without disturbing the deposit.

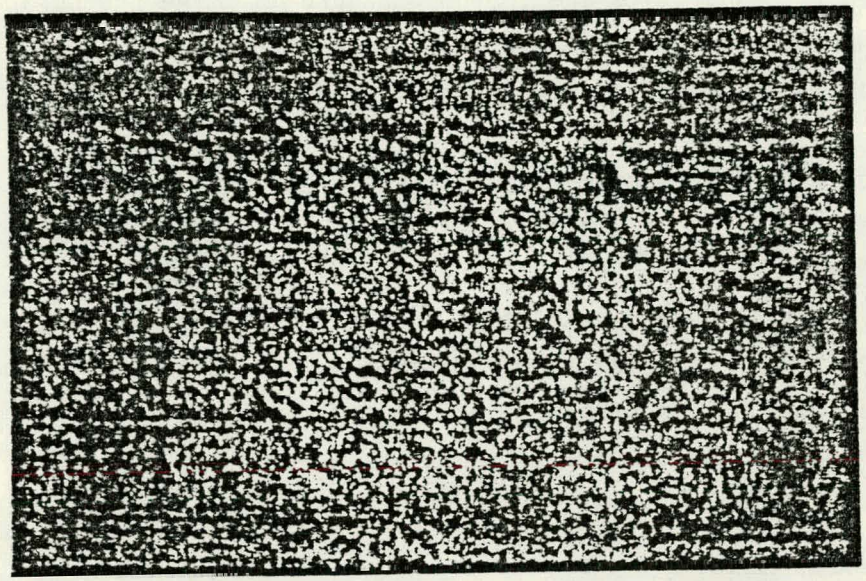

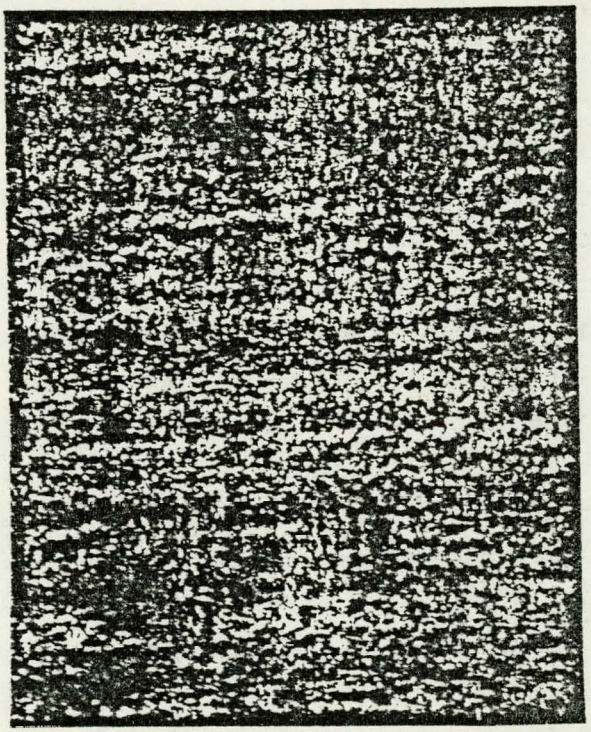

FIGURE 14. Same as in Figure 13 but illuminated from a different angle to show ridges in the aluminum

strings and filaments of bacteria and some of the pennate diatoms. Typical portions of the deposits are shown in Figure 13. The photographs in Figure 14 were taken with illumination at an angle different from that used in the photographs in Figure 13 in order to show the underlying ridges in the aluminum pipe.

A portion of the preserved pipe was washed and dried, and the deposit removed from it by careful scraping. Microscopic examination of this deposit showed the thickness to be from 6.5 micrometers to 24 micrometers within the small area observed. This material contained pennate diatoms, glass fibers, and other filamentous material. A portion of the deposit was orange colored and contained filaments, but individual bacteria could not be resolved because of the density of the material. A colorless portion appeared to be full of bacteria, but many of these particles could be other than bacteria since they were not tested by characteristic staining properties.

Aluminum pipe labeled III-F, with the same dimensions and treatments as pipe II-F, was removed at the end of the experiment and observed in a fashion similar to that employed for II-F.

Figure 15 shows air dried inner surfaces of pipes II-F and III-F together for comparison. Figure 16 shows the inner surface of pipe III-F that had been preserved in glutaraldehyde immediately after removal from the flow. The inner surface was grayish, with a faint yellowish tinge, in contrast to the II-F section with an orange colored deposit. The deposits were uneven, in streaks, but the thickness when examined over a wide area appeared to be rather uniform. A stained and dried layer when examined in place had the cracked and checked appearance noticed in the layer of scale on the II-F section. Some of this material, scraped from the aluminum and mounted for microscopic observation, was examined for thickness. The thicknesses of 10 fragments were nearly the same, varying from 9.9 to 10.2 micrometers.

Deposits removed from the preserved sections by means of collodion films, and stained, contained many stalked and branching bacteria (Figure 17) many filamentous bacteria (Figure 18), and buried diatom frustules. Some of this deposit did not stain; the color was slightly yellowish, the appearance finely granular. These unstained portions contained many angular, opaque, black or brown inclusions 1 to 3 micrometers across, and many small particles in the 0.1-micrometer size range in which shape and color could not be distinguished.

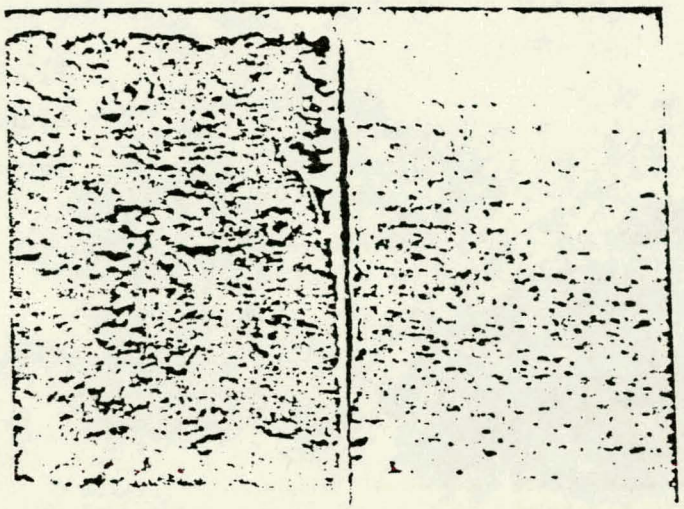

FIGURE 15. Comparison of inner surfaces of air dried aluminum pipes II-F (left) and III-F (right).

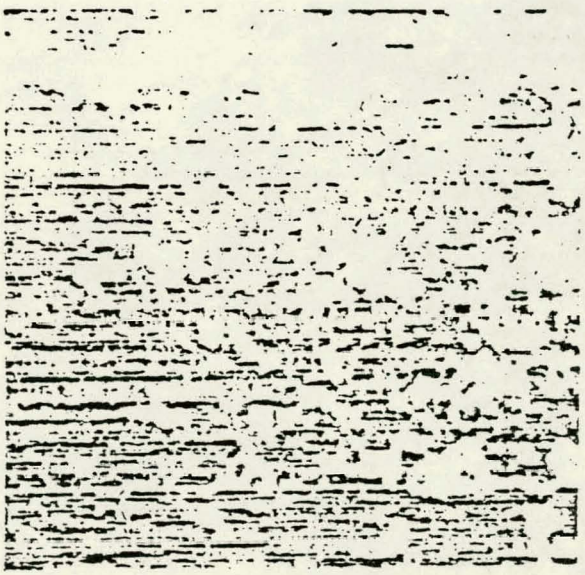

FIGURE 16. Inner surface of aluminum pipe III-F preserved in glutaraldehyde-seawater solution after removal from flow. Photographed while submerged in the preserving solution.

FIGURE 17. Portion of stained biofouling layer removed from inne surface of aluminum pipe III-F-Top that had been preserved in glutar- aldehyde-seawater solution after removal from flow. Dense bacteria mass with numerous stalked bacteri

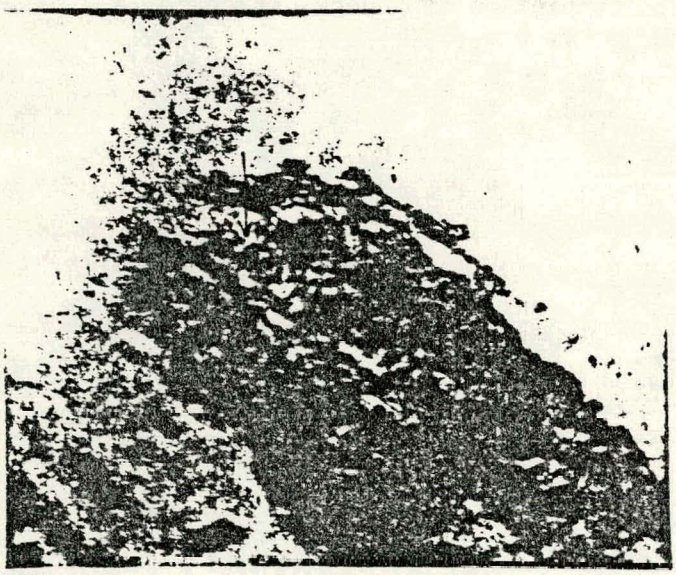

Figure 18. Same layer as in Figur 17. Bacterial mass containing many branching bacteria and long, filamentous bacteria.

Titanium pipe, 26.4 mm I.D. removed from 1 1/4-inch PVC pipe at the end of the experiment.

The deposit on the interior surface was yellowish orange, very similar in color to that of the deposit in aluminum pipe II-F, but thinner. The greatest difference between this section and similar aluminum pipe sections in the PVC pipe is that there was no layer of colorless material about 10 micrometers thick underlying the colored material. Because of this, the titanium section appeared bright. However, at the end next to the aluminum pipe section which preceded it, there was a small amount of the same white amorphous material as found on the aluminum surface in pits beneath deposits of organic material. This seems likely to be aluminum hydroxide. Figure 19 shows the deposits in the titanium section under different conditions of illumination. It was difficult to measure the thicknesses of these irregular deposits with the metallographic microscope because of diffraction from raised crystal surfaces in the metal, but a few points gave the following measurements: 5.5 micrometers; 13 micrometers; 2.6 micrometers; 7.8 micrometers. In order to provide additional measurements, thicknesses were determined at 10 points in a "peeled" deposit using the inverted microscope. These varied from 1.7 to 8.5 micrometers, with an average of 4.0 micrometers. Living in the deposit were many branching bacteria and some diatoms, including large Nitzschia that measured 4.5 X 112 micrometers.

The heaviest of the colorless deposits removed by collodion films were made up predominantly of bacteria and their extracellular products, with scattered naviculoid diatoms in the size range 7 micrometers X 60 micrometers. The biofouling deposit could be scraped from the titanium with a fingernail using as much pressure as possible.

Small bits of material washed from portions of the metal surface contained many bacteria of large and medium sizes, including some filamentous forms (Figures 20 and 21). In these loose portions of the deposit, there were pieces of yellowish orange material containing more or less parallel filaments of small diameter and considerable length which closely resembled those in the deposits found in the aluminum pipes. Some diatoms were present (naviculoids). There were no stalked bacteria and no Nitzschia. A few glass fragments and fibers were present.

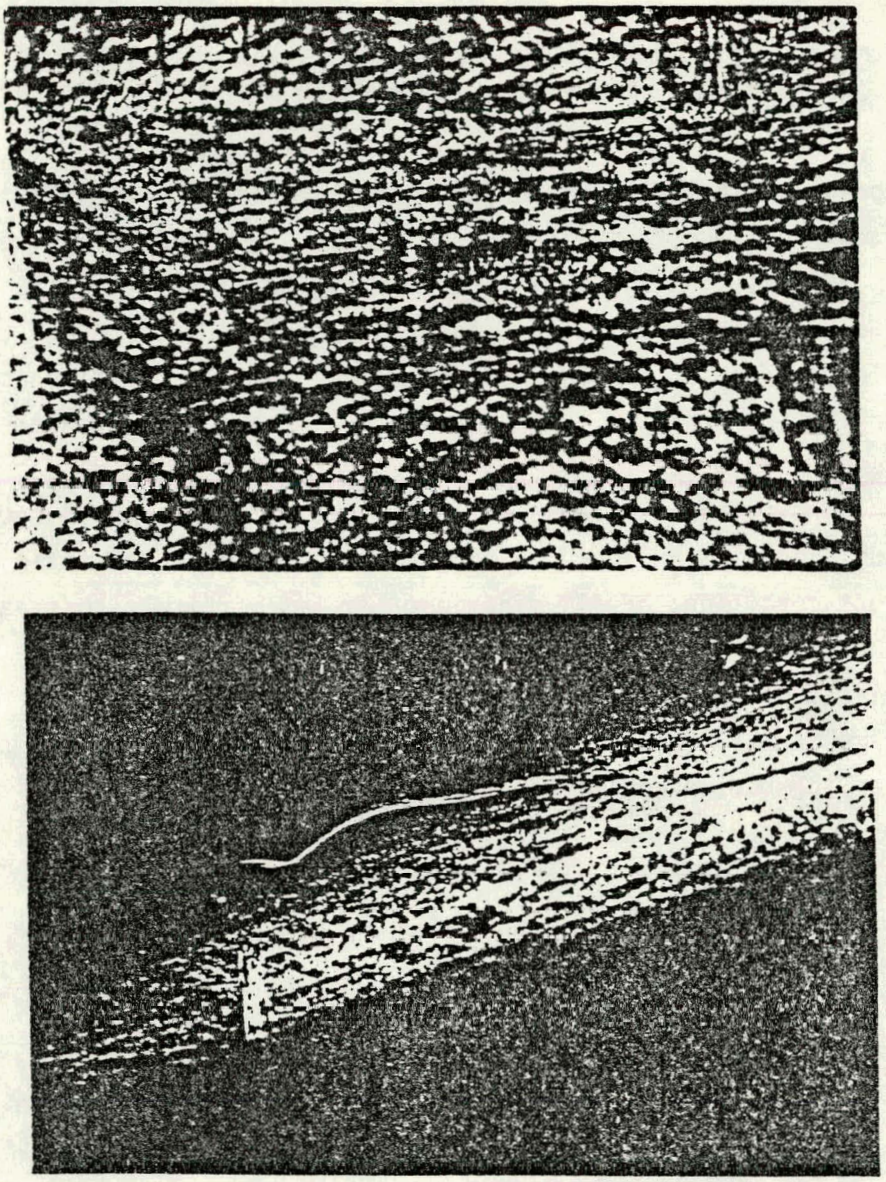

FIGURE 19. Inner surfaces of titanium pipe section preserved in glutaraldehyde-seawater solution after removal from flow. Photographed with illumination from different directions while submerged in preserving solution to show typical biofouling deposits.

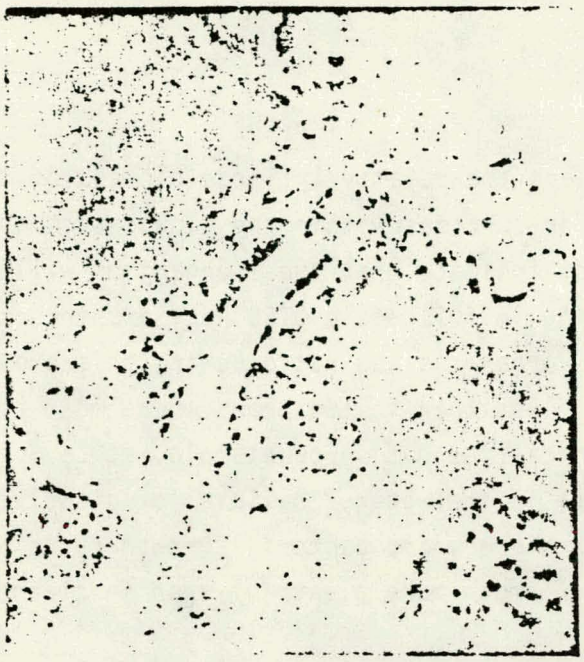

FIGURE 20. Material washed from titanium pipe section during handling. Loose aggregates attached to fiber contain many bacteria, only a few of which are in focus in a single image plane. Several kinds of bacteria are present in the mass.

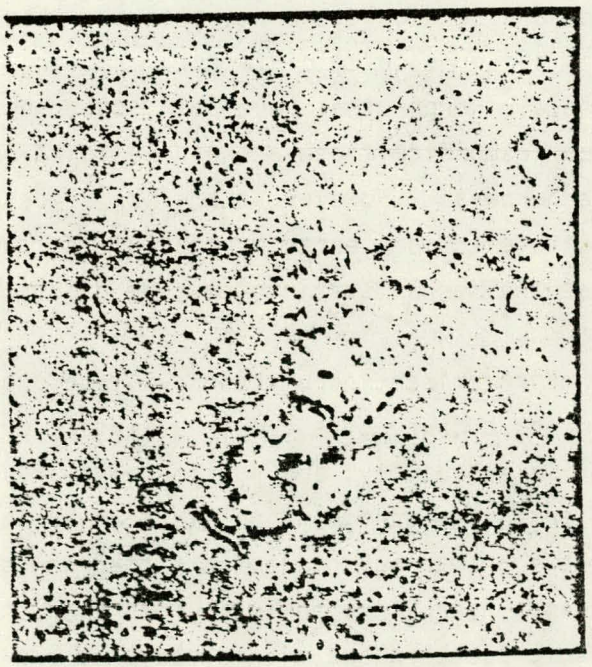

Figure 21. Material washed from titanium pipe section during handling. The small, loose aggregates of organic material containing bacteria are typical of the portion of the deposit extending away from the surface.

DISCUSSION

The large numbers of bacteria and the relatively large biomass of diatoms that developed within a short time on surfaces within the flow system and on the immersed glass slides in this experiment indicate that these organisms will be substantial early contributors to biofouling in full scale OTEC heat exchangers. Although growth of populations of these organisms was rapid during this experiment, the growth rates were considerably less than in locations where most previous work on primary biofouling has been carried out. For example, at La Jolla the numbers of bacteria and other organisms in the water, the level of dissolved and micro-particulate nutrients was much higher, and bacterial growth rates were higher; organisms such as bryozoans were much more plentiful than in clean ocean water around Hawaii.

The test at Keahole Point is the first to be carried out as a biofouling study in relatively clean seawater; the tests of Sechler and Gundersen were carried out in Kaneohe Bay where the nutrient and particulate content of the water was higher than at Keahole Point, and the flow patterns quite different. Fouling studies such as those in Pearl Harbor and Honolulu Harbor that have been concerned with the larger fouling organisms would not correspond to those at Keahole Point because of the far higher pollution in these harbors. However, the glass slides used in this study provide information that is to some extent comparable to that obtained in several other studies, because the mechanisms involved are practically the same.

In biological communities, the predominant populations will be those of species that have developed large numbers because of a growth advantage over other forms. Where favorable temperatures, water quality, and nutrients are readily available, very many different kinds of organisms can grow, but as soon as nutrients become limiting, those organisms with a growth advantage, no matter how slight, will grow the fastest and eventually predominate. Another principle that strictly controls the growth rates of most oceanic bacteria and microalgae that are free living is that of nutrient transfer from water to organism which is roughly proportionate to the flow of water past the surfaces of the organisms (otherwise stated as sinking rate). Bacteria fixed to surfaces can attain faster flow rates in open ocean water because larger particles have faster sinking rates. The same advantage applies bacteria and to larger organisms such as diatoms and barnacles fixed to surfaces of pipes. In a continuously flowing system, such attached organisms have a great

advantage over unattached forms because the supply of nutrients is "unlimited" in the sense that over long periods of time tons of nutrients will pass by and thus be made available to fixed organisms that can extract them.

Diatoms are usually thought of in simple terms as organisms that require light because they are plants. However, some species grow quite well in the dark when supplied with adequate nutrients, and can become significant in heterogeneous populations of fouling organisms. Those species best adapted to the specific conditions prevailing in a given environment will become dominant, the time required for domination depending upon a number of factors including competition for nutrients and space. As population species ratios change in an assemblage of organisms, conditions favor different species so that there is usually a succession of species during buildup of populations of fouling organisms. The surface area available to microorganisms in conditions such as those in the present experiment becomes greater very rapidly as the initial surface is covered with irregular projecting deposits of organisms, their extracellular products, and other materials trapped in the resulting matrix. This results in a potential increase in the fouling rate, and in the diversity of species and sizes of organisms in the fouling community.

As was mentioned in the introduction, diatoms can adhere to surfaces immersed in seawater flowing at velocities of more than 5 meters per second, and can protect larger organisms from flow effects so that sooner or later large fouling organisms may become a part of the fouling population. Since standard industrial practice is to limit flow velocities to 0.6 to 2.5 meters per second in order to decrease impingement attack by particulate materials to practical levels, there is no hope of eliminating all possible diatom attachment by increasing velocities when conventional heat exchanger materials are employed. In the case of aluminum, which is very sensitive to this type of attack, to pitting and crevice corrosion, and to cavitation, flow velocities in seawater would have to be kept in the low range even for relatively short periods of service. Thus, both bacteria and diatoms can be expected to rapidly build up primary fouling films that in turn will lead to growth of larger organisms such as the hydroids that grew in the flow system in the present experiment.

These tests did not provide the resolution necessary to determine either short or long term rates of buildup of fouling layers in the piping, so that they can not be used to predict the relative importance of scale deposits as distinct from biofouling deposits in regard to possible effects on heat exchanger performance. However, the tests did establish the order of magnitude of fouling rates and the general types of organisms involved in primary biofouling in nearshore waters at Keahole Point.

There is no industrial experience with aluminum pipes of the type used in this experiment for heat exchangers in seawater. The closest comparison that could be made would be that of operating installations where 25 mm diameter aluminum bronze tubes with a wall thickness of 1.06 mm, and 1.3 m support centers were used. With these materials, which have a Brinell hardness of about 82, there is usually a continued scale buildup from corrosion products in seawater so that this deposit alone can be responsible for about 50 percent of the total resistance to heat flow. Biological processes can increase the rate of buildup of this layer, and contribute additionally to a complex layer that seriously impedes the flow of heat. After cleaning, the heat flow resistance due to fouling may drop to only about 3 percent of that prior to cleaning. Harder materials would allow higher flow velocities to be used, with less overall fouling, but aluminum will not withstand high velocities.

In the case of the bronze pipe from the initial flow experiment at Makapuu Point that was briefly examined earlier, the extensive calcareous and other biological products deposited on the inner surface were underlain by a scale that looked very much like that within the aluminum pipe sections in this experiment. The most apparent difference was that is the case of the bronze pipe small areas of the scale and the overlying deposit had become detached, and a new growth of microorganisms had begun to cover the freshly exposed metal surface. The few pits observed were shallow and relatively broad. The growth of microorganisms on the surfaces of the two kinds of pipes cannot be compared due to the quite different conditions of exposure. However, it could be guessed that the scale observed on both the aluminum pipes and on the bronze pipe would contribute resistances to the flow of heat that would be of the same order of magnitude.

The predominantly microbial deposits found in the aluminum pipe II-F were sufficiently thick and irregular that they could contribute significantly on a microscale to the stagnant layer near the pipe surface, and thus to the total restance to heat flow. There appear to be two layers, a scale layer possibly containing bacteria which may or may not be viable, and a layer over this composed of living organisms, their products, particulate inorganic material, and inert biologically derived materials such as diatom frustules. Included in these deposits was also an apparently significant amount of glass fragments and glass fibers, presumably from local volcanic activity, either undersea or on land, along with what appear to be glass spheres of similar origin. When attempts were made to scrape the deposit from the pipes with a nylon scraper, some of these hard particulate materials left new scratches on the surface of the aluminum. These would accelerate the wear produced by cleaning systems such as the Amertap system. In view of the hard scale in the aluminum pipes, and the softness of the aluminum beneath (Brinell hardness of 95), the Amertap system would possibly not be able to maintain satisfactory surfaces on heat exchanger tubes even though these materials posed no problem, as they perhaps would not due to their small quantities.

Because there has been little experience with aluminum in industrial heat exchangers used with seawater, it was desirable to include a standard reference material, titanium, which has been for the past twenty years the material of choice for flowing seawater systems. Aluminum is one of the poorest metals in regard to corrosion resistance under biofouling deposits in seawater, as well as to erosion and cavitation, and will vary tremendously in attack rates in response to biological and other variations. Titanium, on the other hand, does not pit and has complete resistance to corrosion under biofouling deposits, and is one of the most unchanging metals when exposed to seawater at ordinary temperatures. Like aluminum, titanium readily becomes covered with fouling organisms in the usual seawater environments. In quiet water, where fouling is worst, it does not appear to accumulate fouling organisms as rapidly as aluminum, but in this respect it is far inferior to 90/10 cupronickel, and is a little worse than aluminum bronze. In fast-flow conditions, titanium is relatively free from fouling problems, and is highly resistant to abrasion, partly due to its hardness (215 Brinell). Titanium immersed in seawater for 20 years shows no measurable corrosion, and long experience with industrial heat exchangers employing seawater with 25 mm tubes having a wall thickness of 0.76 mm (using standard designs but replacing aluminum bronze tubes 25 mm O.D. X 1.06 mm wall thickness) and involving well over 3 million meters of tubing, indicates that

titanium should remain serviceable for at least 15 years.

The titanium reference pipe section used in this test showed no change on the surface of the metal except for the accumulation of the biofouling layer. The surface deposits were rather loose except for the portions made up primarily of bacteria adhering to the metal surface. There was no scale as on the aluminum and bronze pipes. This would be an excellent material for use in developing antifouling measures of several types.

Biofouling in flowing seawater systems such as will be used in OTEC systems can not be avoided, but there appears to be a good possibility of preventing excessive early buildup of microfouling layers. Even this early stage fouling appears to be capable of interfering with heat flow in heat exchangers to an important degree. Because of the excellent potential of ocean thermal energy, a substantial emphasis should be placed on prevention and control of primary marine biofouling. The very early development of strongly adherent bacterial deposits observed during the 1976 Keahole Point experiments indicates the possible advantages of applying antifouling measures before extensive buildup of thicker deposits has occurred.

REFERENCES

Corpe, W. A., 1974. Periphytic marine bacteria and the formation of microbial films on solid surfaces. Pages 397-417 in R. R. Colwell and R. Y. Morita, eds., Effect of the ocean environment on microbial activities. University Park Press, Baltimore.

Sechler, G. E. and K. Gundersen, 1972. Role of surface chemical composition on the microbial contribution to primary films. Proc. Internat. Corrosion and Fouling Congr., 2-6 Oct. 1972, National Bureau of Standards, Gaithersburg, Maryland. P. 610-616.

Sieburth, J. McN., R. D. Brooks, R.V. Gessner, C. D. Thomas, and J. L. Tootle, 1974. Microbial colonization of marine plant surfaces as observed by scanning electron microscopy. Pages 418-432 in R. R. Colwell and R. Y. Morita, eds., Effect of the ocean environment on microbial activities. University Park Press, Baltimore.

Wood, E. J. F., 1950. The role of bacteria in the early stages of fouling. Australian J. Marine Freshwater Res., 1:85-91.

Wood, E. J. F., 1967. Microbiology of oceans and estuaries. Elsevier, Amsterdam. 319 p.

ZoBell, Claude E. and E. C. Allen, 1933. Attachment of marine bacteria to submerged slides. Proc. Soc. Exper. Biol. Med. 30:1409-1411.

ZoBell, Claude E. and E. C. Allen, 1935. The significance of marine bacteria in the fouling of submerged surfaces. J. Bacteriol. 29:239-251.

ZoBell, Claude E., 1939. The role of bacteria in the fouling of submerged surfaces. Biol. Bull. 77:302.

APPENDIX

ADDITIONAL REFERENCES

The following references do not represent a comprehensive bibliography, but were selected for initial consultation during the biofouling studies at Keahole Point. The emphasis in these studies has been on the primary fouling layer and on the layers immediately following it because of their additive effects, which can significantly increase thermal resistance. Another important aspect is that of fouling prevention and removal, which must be accomplished during relatively early stages of fouling development if satisfactory efficiency of OTEC heat exchangers is to be maintained.

Most of the references are concerned with the organisms that are in the size range of the bryozoans and hydroids to the smaller bacteria; these colonize new surfaces very rapidly and have long been known to be important in the development of biofouling, but have not been investigated as thoroughly as have the larger forms. There is a need for additional investigations of primary biofouling and its prevention; the additional references are intended as an aid in these studies.

SUPPLEMENTARY BIOFOULING REFERENCES

Allen, F. E., and E. J. F. Wood, 1950. Investigations of underwater fouling. II. The biology of fouling in Australia. Results of a year's research. Aust. J. Mar. Freshwater Res., 2:92-105.

Baier, R. E., 1972. Influence of the initial surface condition of materials on bioadhesion. Proc. 3rd. Internat. Congr. Marine Corrosion and Fouling, 2-6 Oct. 1972. Gaithersburg, Md., P. 633-639.

Barnes, H., and H. T. Powell, 1950. The development, general morphology and subsequent elimination of barnacle populations, Balanus crenatus and B. balanoides, after a heavy initial settlement. J. Anim. Ecol., 19:175-179.

Booth, G. H., and A. K. Tiller, 1968. Some special features of the anaerobic corrosion of steel by organisms of estuarine origin. Congr. Internat. de la Corrosion Marine et des Salissures, 2d, Athens 1968. P. 361-363.

Brisou, J., G. Valensi, H. Constant, and T. Guillaume, 1968. Participation des bacteries aerobies aux processus de corrosion du cuivre et du nickel. Congr. Internat. de la Corrosion Marine et des Salissures, 2d, Athens 1968. P. 355-359.

Coe, W. R., and W. E. Allen. 1937. Growth of sedentary marine organisms on experimental blocks and plates for nine successive years at the pier of the Scripps Institution of Oceanography. Bull. Scripps Inst. Oceanogr. Tech. Ser., 4:101-136.

Corpe, W. A., 1970. An acid polysaccharide produced by a primary film forming marine bacterium. Develop. Ind. Microbiol., 11:402-412.

_____, 1970. Attachment of marine bacteria to solid surfaces. Pages 73-87 in R. S. Manley, ed., Adhesions in Biological Systems. Academic Press, N.Y.

_____, 1972. Microfouling: The role of primary film forming marine bacteria. Proc. 3rd. Internat. Congr. Marine Corrosion and Fouling. 2-6 Oct. 1972. Gaithersburg, Md., P. 633-639.

_____, 1972. The attachment of microorganisms to glass slides submerged in San Diego Bay, with special reference to a colonial protozoan. U.S. National Technical Information Service. Government Reports Announcements, 72:55

Crisp, D. J., and J. S. Ryland, 1960. Influence of filming and of surface texture on the settlement of marine organisms. Nature, Lond., 185:119-121.

Cole, H. A., and E. W. Knight Jones, 1939. Some observations and experiments on the settling behavior of larvae of Ostrea edulis. J. Cons. Perm. Int. Explor. Mer, 14:86-105.

Daniel, A., 1960. The primary film as a factor in the settlement of marine foulers. J. Madras Univ., 26:189-212.

Depalma, J. R., 1968. A study of deep-ocean fouling. Congr. Internat. de la Corrosion Marine et des Salissures, 2d, Athens 1968. P. 595-600.

Eiben, R., 1976. Einfluss von Benetzungsspannung und Ionen auf die Substratbesiedlung un das Einsetzen der Metamorphose bei Bryozoenlarven (Bowerbankia gracilis). Mar. Biol., 37:249-254.

Grave, B. H., 1930. The natural history of Bugula flabellata at Woods Hole, Massachusetts, including the behavior and attachment of the larva. J. Morph., 49:355-383.

Haug, A., and S. Myklestad, 1976. Polysaccharides of marine diatoms with special reference to Chaetoceros species. Mar. Biol., 34:217-222.

Horbund, H. M., and A. Freiberger, 1970. Slime films and their role in marine fouling: A review. Ocean Engineering. 1: 631.

Jebram, D. 1975. Dauerknospen ("Hibernacula") bei den Bryozoa Ctenostomata in mesohalinen und vollmarinen Gewassern. Mar. Biol., 31:129-138.

Jensen, A., B. Rystad, and S. Melsom, 1976. Heavy metal tolerance of marine phytoplankton, II. Copper tolerance of three species in dialysis and batch cultures. J. Exp. Mar. Biol. Ecol., 22:249-256.

Karande, A. A., 1968. Studies on marine fouling and boring organisms in Bombay Harbor. Congr. Internat. de la Corrosion Marine et des Salissures, 2d, Athens 1968. P. 563-569.

Lewin, J., and J. A. Hellebust, 1976. Heterotrophic nutrition of the marine pennate diatom Nitzschia angularis var. affinis. Mar. Biol., 37:313-320.

Marshall, K. C., R. Stout, and R. Mitchell. 1971. Selective sorption of bacteria from seawater. Can. J. Microbiol., 17:1413-1416.

_____, _____, and _____, 1971. Mechanisms of the initial events in the sorption of marine bacteria to surfaces. J. Gen. Microbiol. 68:337-348.

Marshall, K. C., 1972. Mechanism of adhesion of marine bacteria to surfaces. Proc. 3rd. Internat. Congr. Marine Corrosion and Fouling, 2-6 Oct. 1972. Gaithersburg, Md., P. 625-632.

Mawatari, S., 1952. On Watersipora cucullata (Busk). Misc. Rep. Res. Inst. Nat. Resources, Tokyo, 28:17-27.

Menon, N. R., and N. B. Nair, 1971. Ecology of fouling bryozoans in cochin waters. Marine Biology, 8:280-307.

Pomerat, C. M., and M. Weiss. 1946. The influence of texture and composition of surface on the attachment of sedentary marine organisms. Biol. Bull. 91:57-65.

Pyefinch, K. A., and F. S. Downing, 1949. Notes on the general biology of Tubularia larynx Ellis and Sollander. J. Mar. Biol. Ass. U.K., 28:21-44.

Relini, G., 1975. Preliminary results of fouling investigations carried out at a depth of 200 m in the Ligurian Sea. Rapp. P. -V. Reun. Cons. Int. Explor. Mer Mediterranee, 23:105-107.

Saroyan, J. R., E. Lindner, and C. A. Dooley, 1968. Attachment Mechanism of Barnacles. Congr. Internat. de la Corrosion Marine et des Salissures, 2d, Athens 1968. P. 495-512.

Scheer, B. T., 1945. The development of marine fouling communities. Biol. Bull. 80:103-121.

Stebbing, A. R. D., 1971. Growth of Flustra Foliacea (Bryozoa). Mar. Biol. 9: 267-272.

_____, 1976. The effects of low metal levels on a clonal hydroid. J. Mar. Biol. Ass. U. K., 56:977-994.

Willey, J. D., 1975. Reactions which remove dissolved alumina from seawater. Mar. Chemistry, 3:227-240.

Wisely, B., 1958. The settling and some experimental reactions of bryozoan larvae Watersipora cucullata (Busk). Ann. Inst. Océanogr., Monaco, 27:362-371.

Wood, E. J. F., 1950. Investigations on underwater fouling. 1. The role of bateria in the early stages of fouling. Aust. J. Mar. Freshwater Res., 2: 85-91.

ZoBell, Claude E., 1937. The influence of solid surface upon the physiological Activities of Bacteria in sea water. J. Bacteriol. 33:86.

_____, and C. B. Feltham, 1938. Bacteria as food for certain marine invertebrates. J. Mar. Res., 1:312-327.

_____, 1938. The sequence of events in the fouling of submerged surfaces. Official Digest Fed. Paint & Varnish Production Clubs, 178:379-385.

APPENDIX B

CHARACTERIZATION OF HEAT EXCHANGER PIPES AND THEIR BIO-MASS DEPOSITS

Lawrence F. Vassamillet
Department of Metallurgy
and Matierals Science
Carnegie-Mellon University

April, 1978

Table of Contents

I. INTRODUCTION

Four sets of heat exchanger pipe samples are to be reported on in this investigation. The purpose of the study is to characterize the deposit layer and its effect on the inner surface of the pipe. To do this it will be necessary to measure the thickness of the layer, establish its composition and inspect the layer-metal interface. Not included in the investigation is a measure of the loss of metal by corrosion except as might be inferred by a measurement of the pipe wall dimension.

The pipes are of two materials: Al 6061-T6 and Ti; from three locations: the ship Noi'i at Keahole Point, Hawaii, Buoy Series I (submerged) at Keahole Point and the barge at St. Croix in the Caribbean Sea. Runs were taken at two operating water flow velocities: 3 ft/sec and 6 ft/sec. The samples are identified by the following code:

Letter for location	N for Noi'i, B for Buoy and S for St. Croix
Letter for Material	A for Aluminum and T for Titanium
Number for water flow velocity	3 for 3 ft/sec and 6 for 6 ft/sec
Letter for section of pipe	A, B, C...

More detailed history of the heat exchanger pipes is given in Appendix B.1.

II. TYPES OF ANALYSES, MEASUREMENTS AND INVESTIGATIONS

A. Metallographic

Much of the information sought in this investigation can be obtained by an optical examination of a cross-section of the heat exchanger pipe. To this end a slice from the pipe must be mounted in mounting media in such a way that the deposit layer and the exposed edges of the metal are protected during the grinding and polishing operations.

Under the microscope the mean wall thickness and its variance and the mean deposit thickness and its variance can be measured. The extent of corrosion and the depth of corrosion pits can be observed and measured.

Since it is anticipated that corrosion of the surface may be related to the grains in the aluminum metal, an etchant which develops the grain boundary structure provides a mechanism for investigating grain boundaries and grain size.

B. Scanning Electron Microscopy (SEM)

The SEM can be used to observe, over a wide range of magnifications, the appearance of the exposed surface of the deposited material. The large depth of field that is an inherent property of a focused electron beam provides excellent imaging of rough surfaces. Although study of the appearance of the deposit is not a primary purpose of this investigation, any significant differences between the various deposits are readily identifiable.

Qualitative information on the composition of the deposits is provided by the energy-dispersive X-ray analyses. Elements in the periodic table above oxygen are detectable. This X-ray spectrographic analysis is extremely useful when combined with X-ray diffraction results since the chemical information it provides, albeit qualitative, is usually adequate to provide positive identification of the crystalline compounds present.

C. X-Ray Diffraction

X-ray diffraction analysis of the deposit material indicates the presence and relative amount of crystalline phases. Successful pattern interpretation provides identification of the compounds present. Whether the pattern can be successfully analyzed depends on the quality of the pattern and the experience of the diffractionist.

D. Other Analyses

Auger Electron Spectroscopy (AES) is frequently capable of providing quantitative information on the chemical composition of the surface layer of a sample. This technique has better sensitivity for the lighter elements of the periodic table. In order to obtain suitable spectra, the sample must be able to conduct electrons to a degree. Practically speaking the sample must not be an insulator, but have resistances in the range associated with semi-conductors.

Secondary Ion Mass Spectroscopy (SIMS) is a second technique designed to establish the chemical composition of a surface. In addition, since it can measure the mass of molecular fragments, many organic materials are identifiable.

III. SAMPLE PREPARATION PROCEDURES

From each sample pipe two sections were cut to thicknesses of .25 in. and .40 in. These were cut using a parting tool and lathe without lubrication so as to avoid in so far as possible any contamination or disturbance of the deposited films.

The .25 in. rings were placed in a vacuum coating facility where a "thick" layer of Au - 10% Pd alloy was deposited on them. This procedure is identical to that given to specimens that require a conducting surface before examination in the scanning electron microscope (SEM) except that the amount of metal used in the deposition was about twice that used for routine SEM sample coatings. It is estimated that the thickness of the "Au" film is of the order of 400 Å ± 100 Å. The purpose of this step was to provide an electrically conducting surface so that electro deposition of nickel on top of the deposit layer could take place.

The mounting, grinding, and polishing operation on seven aluminum samples were done by Mr. R. M. Slepian of Westinghouse Research Laboratories. The steps carried out in his laboratory were:

1. Nickel deposition at room temperature using a nickel sufanate bath, run at 20 volts and 2 amperes for approximately 18 hours.
2. Mounting the rings in Technovit 4000. This is a relatively new mounting medium developed and sold by Kulzer and Co., Bereich Technik, D638 Bad Homburg, Germany. It is a three component resin with exceptionally good molding, adhesion and polishing characteristics.
3. Grinding through six papers using water as lubrication.
4. Automet polishing with 3 μm diamond paste and oil base lubricant.
5. Automet polishing with .06 μm cerium oxide and water as lubricant.

After the first set of metallographic measurements were carried out on these samples, they were etched using a warm solution of 5 parts HF (48%), 10 parts H_2SO_4, 85 parts H_2O from 30 secs. to 3 min.

The polished surfaces were given a nominal (100-200Å) Au-Pd coating for SEM examination.

The .40 in. ring was converted to a regular hexagon using a milling machine. It was then divided into six segments. One segment from each sample was coated with Au-Pd for SEM examination of the top of the deposit layer. Another segment was subjected to ultrasonic cleaning or enzyme attack and ultrasonic cleaning before Au-Pd coating for SEM examination of the metal-deposit layer interface.

Two segments were designated for Auger Electron Spectroscopy (AES) but were not used for this purpose because successful spectra could not be obtained from the deposit layer.

The samples submitted for X-ray diffraction examination by Materials Consultants and Laboratories (MCL) were the rings remaining from the original pieces. The X-ray examination was of the deposit layers only. These were "...removed by carefully scraping with a toothpick under a low power stereo light microscope." Some of this deposit material was mounted on "... high purity graphite wafers with Duco cement, coated with approximately 200 Å of carbon" for examination in the SEM.

IV. RESULTS

A. Thickness Measurements

1. Wall Thickness

Thickness measurements were performed on the specimens prepared by R. M. Slepian, Westinghouse Research Laboratories. They were measured in the "as polished" state. They were measured on a measuring microscope with the samples being mounted in a holder devised to accommodate the mounted specimen. The reproducibility of the measurement using this system is slightly better than 0.01 mm when performed on an unexposed piece of tubing at a single position. Thus the standard deviations on the measured wall thickness represent variations due to out-of-roundness of the cross-section or to differing amounts of corrosion around the section. Three measurements were made at each of eight locations around the section to determine wall thickness. The results are tabulated in columns 1 and 2 of Table B.1.

TABLE B.1

Tubing Wall Thickness and Scale Thickness in mm.

	1	2	3	4	5	6	7	8
Sample *	Wall Thick-ness	Std. Dev.	Scale Thick-ness 1st Run	Std. Dev.	Scale Thick-ness from micro-graph	Scale plus Ni layer from micro-graph	Scale Thick-ness 2nd Run	Std. Dev.
A.A.	3.471	0.059						
NA3I	3.438	0.069	.098	.016	.010-.015	.080-.090	.036	.018
NA6G	3.488	0.059	.038	.009	.030-.035	.05 -.055	.038	.011
BA3D	3.218	0.093	.075	.018	.035-.055	.05 -.065	.036	.014
BA6D	3.188	0.027	.040	.006	.035-.04	.05 -.06	.050	.020
SA3H	3.251	0.184	.050	.012	.015-.020	.040-.045	.029	.022
SA6H	3.157	0.204	.087	.023	.035-.040	.07-0.10	.029	.013

2. Scale Thickness

Scale thickness measurements were performed twice, first in the "as polished" state, and later after the sample surface had been etched and repolished. In the first measure of scale thickness, seven readings were taken around the inside diameter. These results are listed in Table B.1, columns 3 and 4 for the average thickness and standard deviation respectively.

A photographic record of the scale thickness was made of each sample at a magnification of 140 X. Measurements of the average thickness of the deposit layer taken from the photographs are listed in column 5 of Table B.1. Because these measurements are not in very good agreement with those in column 3, the width of the deposit plus the nickel coating has also been estimated, and these values are listed in column 6. After etching, the samples were repolished and remeasured. Approximately 25 readings were made around the rings. The average thickness and the standard deviation are listed in Table B.1 in columns 7 and 8 respectively. When the depoist layers were remeasured after etching and repolishing of the samples, the average deposit thicknesses were not in very good agreement with the original values. However, it was observed under a higher power microscope that in many places, for some of the samples, the deposit layer had been pulled away from the pipe wall creating the appearance of a thicker deposit layer. Therefore, the values in column 7 most properly represent an upper limit to the deposit thickness. The values of deposit layer thickness listed in column 5 are the most probable measurements. It should be pointed out that the photographs from which these values have been obtained were not taken for the purpose of obtaining these measurements, but rather to show irregularities in the appearance of the deposit

layer as seen in cross-section. They do serve, however, to recall the appearance of the samples, and estimates of "average" deposit thicknesses can be deduced from them.

B. Optical Microscopic Survey

All samples were immersed in an etching solution of 5 parts HF (48%), 10 parts H_2SO_4 and 85 parts H_2O, for times of 30 seconds to 3 minutes, to develop the grain boundary structure. This was done to determine the extent to which pitting relates to the grain boundaries. The first result of this part of the investigation was the observation that there was considerable difference in sample response to the etchant. Some samples etched quickly and easily, showing a clear grain boundary structure. Others did not. The details for each specimen are listed below along with other observations about the microstructure as well as the nature of the pitting. The differences in etching behavior are most probably related to variations in pipe composition and thermal history. Although all the pipes undoubtedly meet the standard specifications for 6061-T6 piping, plant procedures may vary in annealing temperatures and times and cooling rates so as to produce different inclusion distributions. The amount and distribution of impurities in grain boundaries will be affected by these thermal treatments and obviously have a marked effect on corrosion behavior as well as etching behavior.

1. NA3I

This sample shows a well developed grain boundary pattern after 30 secs. etch. Some texture variation among the grains. The etching is along grain boundaries. Considerable grain size variation observed from inside to outside of pipe. Grain size decreases with distance from inside surface except that some very small grains are seen at inside edge.

Corrosion appears to be along grain boundaries with loss of smaller grains at inner surface. Penetration is small, usually only one grain. Pitting is frequent and more or less uniform in distribution.

2. NA6G.

Shows poorly developed grain boundary pattern after 40 secs. etch in heated etching solution. Extensive pitting at what appears to be inclusions, although they are not always observable. One type of inclusion does not etch!! Variation of grain size across pipe section hard to establish. May have larger grain sizes near inner surface as above.

Almost negligible corrosion, and apparently little to no grain boundary attack. Occasional very small grain missing along surface.

3. SA3H

Moderate grain boundary pattern after 40 secs. etch. Some attack at inclusion locations. Well developed inclusion distribution. Grain size more or less uniform with larger size distribution towards inner surface.

Moderate corrosion more or less uniformly distributed along surface. Some clear examples of grain boundary attack, usually with one or more "grains" missing. Not all the pits have appearance of attack via grain boundaries. This sample shows most extensive pitting.

4. SA6H

Good grain boundary pattern revealed by variation of etching rates of grains, not by grain boundary attack. Attack around inclusions selective. Same grain size variation as for SA3H.

Corrosion behavior not related to grain boundaries. Only a few moderately deep pits. No reason evident for pit formation at these sites. General, shallow type, pitting is slight, but not negligible.

5. BA3D

Good grain boundary pattern, but not all grain boundaries etched equally. Some boundaries revealed by precipitates and some by differences in etching rates. Some boundaries are hardly visible. General heavy pitting on etched surface, primarily at inclusions. Most inclusions etch to some extent. Does not look like a double population, one that pits and one non-pitting.

Corrosion attack is moderately extensive, localized, of varying severity and not grain boundary induced. Yet much of this surface shows no evidence of attack.

6. BA6D

Grain boundary contrast is poor with many boundaries not evident at all. No contrast due to differential etching rates. Many boundaries evident by decorating precipitates: Surface pitting varies from region to region.

Corrosion is infrequent. Some small pits developed. Grain boundary process not particularly evident, but can not be excluded. Two large pits are present. Most of surface (edge) shows uniform type of attack, possibly related to presence of inclusions which are both numerous and uniformly distributed.

The preceeding observations are not based on the micrographs taken of the etched surfaces but on extended study of the entire surface of each sample at a variety of magnifications and lighting conditions. The optical micrographs were taken as examples of both etching behavior and inside surface attack.

C. SEM Results

The SEM study was conducted by Martin Haller using a JEOL JSM-II scanning microscope equipped with an EDAX solid state energy dispersive X-ray detection system. All samples were coated with a thin (100-200 Å) layer of Au-Pd before introduction into the microscope. In the report the samples are identified by numbers 1 through 6. The relation to the numbering system being used here is as follows:

1 NA3E	4 - SA6H
2 - SA3H	5 - BA3D
3 - NA6G	6 - BA6D

The various SEM micrographs are identified by a number-letter combination. Table B.2 lists the micrographs, identifies the subject and gives the magnification.

The following generalizations were made:

NA3E: Sample contained many crystals, parallel ridges and inclusions.

SA3H: Sample contains no crystals, few inclusions (~ 2%/area)

NA6G: Same matrix as SA3H, many crystals on surface, a few Al/Cl particles.

SA6H: Mostly cracked matrix with a few large inclusions (<1%)

BA3D: Same matrix as others, heavily covered with stringy material (~50%)

BA6D: Matrix has thinner, larger chips. Few inclusions.

The following comments by Mr. Haller are observations of both appearance and composition.

All samples are typified as having a cracked, loosely adherent coating (identified as matrix) of large (>10u) thickness. This material looks as though it might be an amorphous electro-deposited salt layer which grows

TABLE B.2

List of SEM Photo Micrographs

Sample No.	Film No.	Subject	Magnification
NA3E	1A	Large, non-typical inclusion	100 X
NA3E	1B	Typical area, no large inclusions	100 X
NA3E	1C	Typical area, no large inclusions	1000 X
NA3E	1D	Typical area, salt crystals	3000 X
NA3E	1E	Lath type crystals (?)	1000 X
NA3E	1F	Material in ridges on surface	1000 X
NA3E	1G	Typical ridge on amorphous background	600 X
NA3E	1H	Al X-ray map of 1G	600 X
SA3H	2A	Typical area containing an inclusion group	100 X
SA3H	2B	Inclusions	1000 X
SA3H	2C	Typical area with spalled matrix	100 X
SA3H	2D	Detail in spalled region	1000 X
SA3H	2E	Matrix detail	1000 X
SA3H	2F	Matrix detail	3000 X
NA6G	3A	Typical matrix area	100 X
NA6G	3B	Detail of matrix	1000 X
NA6G	3C	Crystals	1000 X
NA6G	3D	Details of debris, crystals and non crystals	600 X
SA6H	4A	Typical matrix area	100 X
SA6H	4B	Typical matrix area	3000 X
SA6H	4C	Inclusion (dendritic crystal growth)	300 X
SA6H	4D	Inclusion (dendritic crystal growth detail)	1000 X
BA3D	5A	Typical matrix structure plus attached material	100 X
BA3D	5B	Typical matrix structure	1000 X
BA3D	5C	Diatom	3000 X
BA3D	5D	Diatom	3000 X
BA3D	5E	Bio-mass attachment	100 X
BA3D	5F	Bio-mass attachment detail	300 X
BA3D	5G	Ca oxide skeletons (*)	3000 X
BA3D	5H	Bi-valve mollusk shell	600 X
BA6D	6A	Typical matrix area	100 X
BA6D	6B	Matrix detail	1000 X
BA6D	6C	Reverse side of detached matrix flake	100 X
BA6D	6D	Detail of 6C,	300 X
BA6D	6E	Substrate revealed by flake removal	1000 X
BA6D	6F	Detail of 6C, detached flake	1000 X

(*) Ca seems associated with biological material, probably in the form of internal skeletal structure of which the triangles, etc. are the exposed skeletons. Diatoms seem to be composed of SiO_2 only. Biological material appears to be strongly attached to matrix.

on the pipe surface. Measurements with the EDAX unit show a very high Al content for this phase strongly indicating chemical interaction between this layer and the pipe surface. In addition, an excrescence or growth (2-A and 2-B typical) is seen in all samples, consisting of Al and Cl, this is probably a direct corrosion product. In frequency, about 1% of the areas examined consist of this phase. Further evidence of corrosion and electro-chemical deposition are seen in sample 6. Here, several chips of the matrix material have spalled off, revealing the matrix/metal interface (6-E). The reverse side of one of these chips (6-C, D, F) faithfully replicates the interface, showing what appear to be etched grains of Al covered with a coating of alumina (probably not α-alumina). For these reasons, it is tentatively concluded that the coatings shown are not biological (i.e. organic), but are electro-deposited inorganic salts and corrosion products.

Only two of the six samples examined had identifiable biological material. The stringy material seen in 1-A and 1-F (about 20% of the total sample area), and the diatoms, mollusk shells, and stringy amorphous material in sample 6 are typical. This material looks to be anchored onto (not below) the matrix coating, as can be clearly seen in 5-E and 5-F. These materials are highest in Si, Ca, and Cl, due at least in part to the inclusion of fragments of diatom, shells, etc. The author speculates then that, based on these samples the biological material has grown on (or attached itself to) a previously existing salt layer.

X-ray spectra were obtained on the matrix and other features for all six samples. Table B.3 identifies each spectrum. The spectra are presented as a photograph of the counts recorded in the EDAX multichannel analyser.

TABLE B.3

List of EDAX SPECTRA

Sample No.	Spectrum No.	Subject
NA3E	1- AM	Amorphous background material
SA3H	2- M	Matrix
SA3H	2- I	Inclusion
NA6G	3- M	Matrix
NA6G	3- C	Crystal
SA6H	4- E	Matrix
SA6H	4- A incl.	Inclusion
BA3D	5-	Bio-mass
BA3D	5-	Matrix
BA3D	5- Ca oxide	Inclusion
BA6D	6- M	Matrix
BA6D	6- Chip R	Reverse side of chip
BA6D	6- Substrate	After chip removal

TABLE B.4

Sample	Element	Na	Mg	Al	Si	P	S	Cl	K	Ca	Fe	Location
1.	NA3E		722	20295			1471	13583		22	313	Inclusion on micro 1A
	NA3E	922	737	5000	240	81	1205	7868	101	747	3350	Matrix-spot made
	NA3E		1098	54356	167	21					819	Metal substrate, edge of sample
	NA3E		623	2350	1285	170	4778	4424	200	3626	4670	Lath type crystals, micro 1E
	NA3E	170	686	5451	51	151	1026	3223	181	302	3252	Matrix-amorphous background material
	NA3E	972	552	1584	2025	515	2407	6338	126	2234	9250	Material in surface ridges, micro 1F
2.	SA3H	337	2794	5304	32		2105	3738	147	696	369	Matrix
	SA3H	114	1076	17068		22	556	11882		97	366	Inclusion, micro 2B
3.	NA6G	612	2459	8562	358	207	2022	3555	48	648	714	Matrix
	NA6G	4959	141	838	10	31	751	37512			337	Crystals, micro 3C
4.	SA6H	314	3903	4121	17	2	1747	5446	96	424	292	Matrix
	SA6H	45	378	9083			772	5257			37	Inclusion, micro 4C
5.	BA3D	122	2639	10537	604	165	1346	29		818	288	Matrix
	BA3D		135	963	344	15	138			4130	490	Bio-mass, micros 5A, 5C, 5F
	BA3D	60	669	477	127	137				31205	233	Inclusions, micros 5G, 5H
6.	BA6D	71	1260	5486	319	145	1385			663	122	Matrix
	BA6D	274	1365	67270	296	27	38			18	280	Substrate, micro 6C, 6E
	BA6D		2708	13733	1325	130	1195		6	789	341	Overturned chip, micro 6C, 6D

Many more spectra were obtained than were recorded in photographic form. These measurements are listed in Table B.4, which presents the number of counts obtained for fixed incident beam current and fixed counting times for each of ten elements. These results can be considered as qualitative only, since topography and electrical conductivity play an important role in controlling X-ray generation and detection. The major constituents in the deposits, including crystals, inclusions, etc. are Al, Cl, and Ca. Minor amounts of Na, Mg, Si, & S are present. The presence of a large amount of Fe in NA3 sample is known to be due to the experimental set-up. There are also trace amounts of P and K as well as others not specifically identified. These results agree reasonably well with a similar study by Materials Consultants (MCL).

D. AES Results

This part of the study was not possible due to excessive charging by the samples. The deposited layers appeared as infinitely thick to the incident electron beam, with very high resistance. No spectra could be obtained.

E. MCL Results

For the report from MCL, see Appendix B.2. In their study, three techniques were used: X-ray diffraction (XRD), scanning electron microscopy (SEM) with EDAX analysis and secondary ion mass spectroscopy (SIMS).

Not all samples were analyzed in this study. The following had deposits removed for XRD: BA6D (two types of deposit), BA3D, SA3H and BT6D. In all cases the amount of crystalline material was a small part of the deposit and the degree of crystallinity was poor. In some cases compound

identification was marginal and only possible because the major elements present were known. Table B.5 lists the samples and the compounds identified.

The SEM studies were not as extensive as those performed by M. Haller. The results were not significantly different.

The SIMS study confirmed the presence of organic materials. The sample studied was BA6D, two separate areas. The operators reported, based on their experience that the organic content was estimated to be 5% in one area and 10% in the other. This technique established the presence of oxygen, as expected, but also showed some fluorine, an element not identified in the EDAX studies.

In conclusion these studies attribute the composition of the average deposit as being:

Major $CaCO_3$ and $Al(OH)_3$

Minor $Al_2(SO_4)_3$ H_2O, $CaMg$ CO_3 and organic matter

SiO_2 and NaCl

Obviously in some other samples, such as NA6G, NaCl would be a major constituent.

TABLE B.5

Results of MCL X-Ray Study

Sample			
BA6D	White isolated material	$Al(OH)_3$	$Al_2(SO_4)_3 \cdot H_2O$
	Yellowish matrix	$Al(OH)_3$	$Al_2(SO_4)_3 \cdot H_2O$
		$CaCO_3$	SiO_2
			$CaMgCO_3$
BA3D	Matrix	$CaCO_3$	$CaMgCO_3$
			SiO_2
SA3H	Matrix	Al	NaCl
BT6D	Matrix	no crystalline pattern	

V. STATE OF THE ALUMINUM PIPES

The appearance of the etched cross-sections of the aluminum pipes shows that important differences exist from one pipe to another in terms of composition and/or age hardening treatment. The 6061 alloy is not one where composition is carefully-controlled. It is frequently used in many melt shops as the alloy to use up extra amounts of scrap. That may significantly change the amount of some trace elements such as Cr or Cu. The age hardening elements in 6061 are Mg and Si. So the concentrations of these are carefully controlled. The T-6 temper is achievable by several heating and age hardening programs. However the precipitation distribution and concentration of impurity elements in the grain boundaries may vary considerably as a result. Since corrosion by seawater and the bio-mass is a process rather similar to etching, it is important that for the purposes of a study of this kind the starting pipes all be identical. As a consequence it is not useful to try to interpret the results of the metallographic investigation of the deposit-metal pipe interface as seen in cross-section. The differences in the corrosion behavior as described in IV B may be just as likely due to differences in the metal as to differences in the deposit-seawater environment.

VI. CONCLUSIONS AND RECOMMENDATIONS

These investigations have shown that run of the mill 6061-T6 aluminum alloy pipes are not suitable for a study of this kind as it is not a well enough controlled material in terms of its resistance to chemical attack. There are other aluminum alloys of equal or better resistance to salt water corrosion.

It was not possible to estimate the rate of metal loss due to corrosion in these studies. For this to be done, a measurement of wall thickness of a section adjacent to the test piece would have to be possible. The variation in average wall thickness from 3.19 mm to 3.49 mm more probably represents variations in starting wall thickness than it does in loss of metal through corrosion. This program was started before the necessity of controlling initial wall thickness was established.

The sample mounting procedure used for the metallographic study can be improved by inserting a metal disc approximately an inch in diameter inside each pipe section during mounting in the mounting compound. While the mounting medium used in this study (Technovit 4000) is very low in shrinkage during curing, it is not negligible. A reduction in the amount of mounting m dium by a metal plug will certainly eliminate any shrinkage problem.

The measurement of the thickness of the deposited layer involved some subjectivity. A photographic approach looks to be more prudent than the one originally chosen here, using a relatively low power traveling microscope. If samples are repolished and remeasured, and if more than one person makes the measurements, meaningful comparisons may then be possible. In this investigation, the photographs that were taken to show exceptional features along the deposit-metal interface played a significant role in establishing the deposit layer thickness. It should be noted that the effect of grinding and polishing of the pipe section on the thickness of the deposit was not clearly established. That is, no reproducibility studies were performed to show that the mechanical processes did not alter the

appearance and hence the thickness of the deposited scale. To the extent that scale thickness is a crucial parameter in these studies, such reproducibility tests should be performed. Finally it should be noted that there was clear agreement between the metallographic measurements of scale thickness and estimates of the same from the scanning electron microscopist. Deposit thickness on these samples are in the range of 10 to 50 microns, primarily. Significant variations around these numbers are possible, especially to larger values, when larger biological entities were located or extensive corrosion took place.

The problem of establishing the maximum rate of etch pit penetration has not been dealt with in this study. No sampling procedure based on arbitrarily selected cross-sections can locate the "deepest" pit. This part of the study must of necessity consist of at least two stages. The first would be to find out, if possible, the corrosion mechanisms. The second to measure the frequency of the exceptional mechanisms. The critical question to answer is whether a fast corrosion (or etch) rate is determined by a unique local surface chemistry, or a particular surface defect, or the chance combination of both. The results of the study to date has not cast any light on this problem.

NA3E 1A 100 x

Large, non-typical inclusion

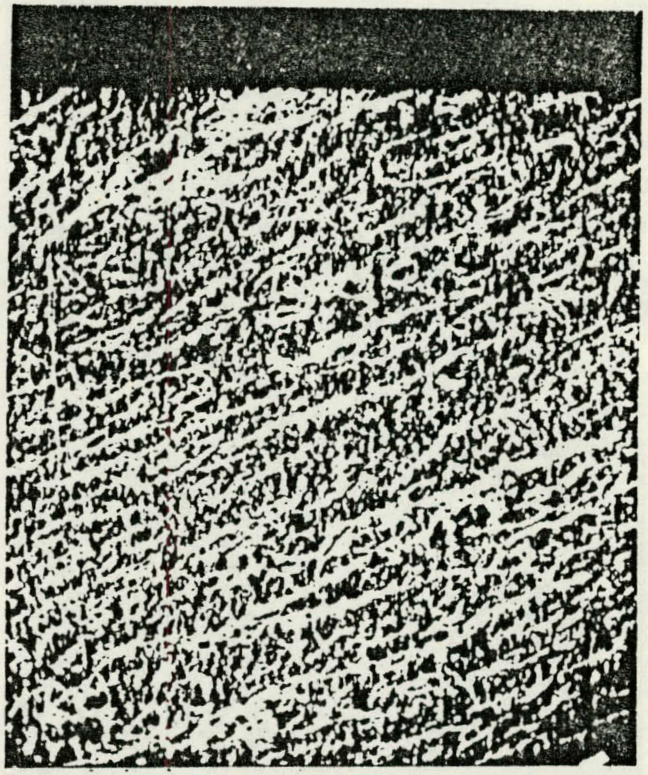

NA3E 1B 100 x

Typical area, no large inclusions

NA3E 1C 1,000 x
Typical area, no large inclusions

NA3E 1D 3,000 x
Typical area, salt crystals

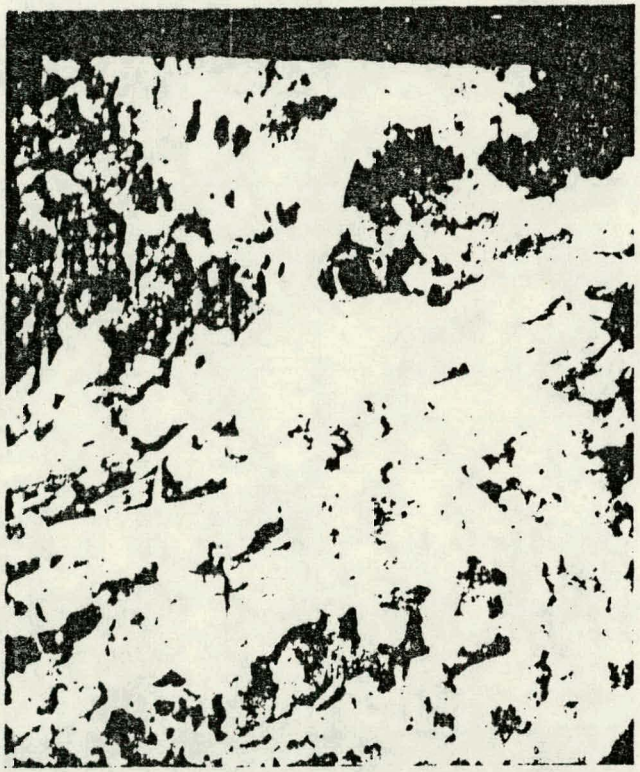

NA3E 1E 1,000 x

Lath type crystals (?)

NA3E 1F 1,000 x

Material in ridges on surface

NA3E 1G 600 x

Typical ridge on amorphous background

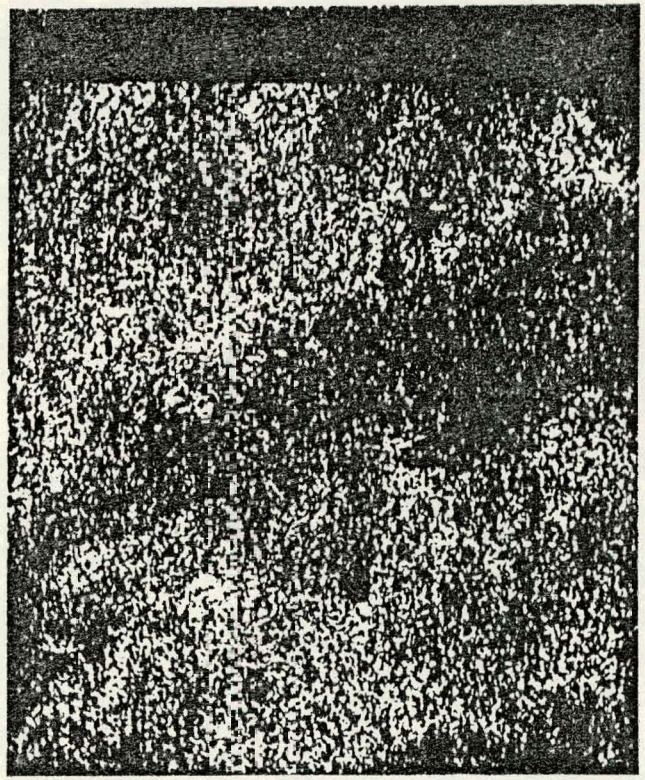

NA3E 1H 600 x

Al X-ray map of 1G

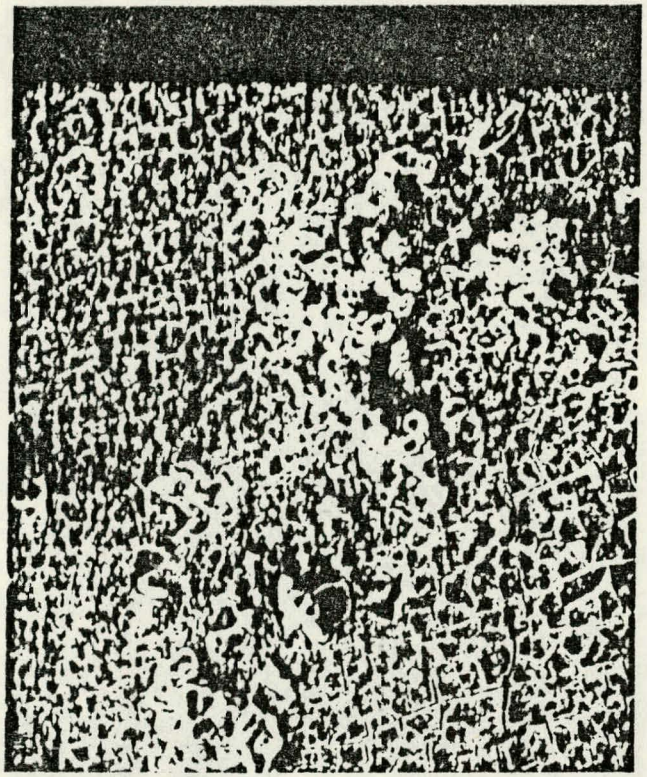

SA3H 2A 100 x

Typical area containing an inclusion group

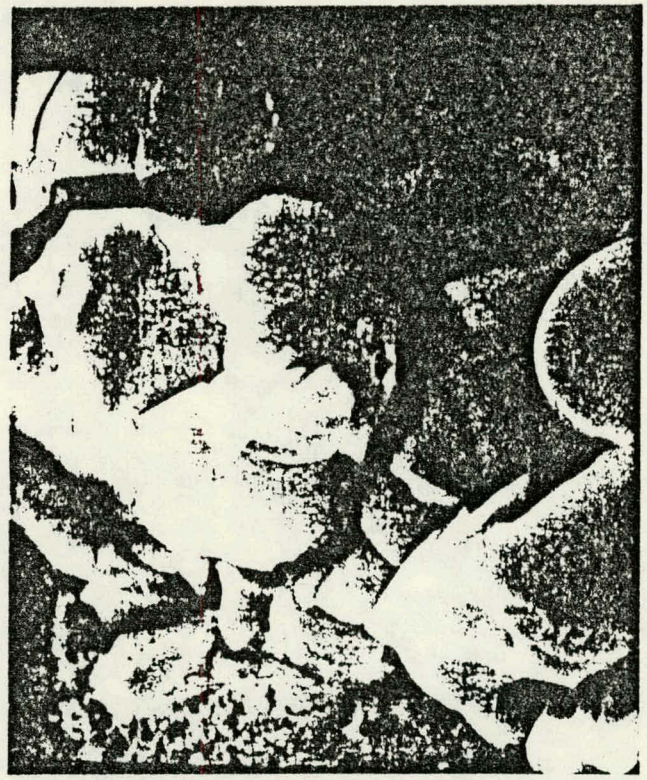

SA 3H 2B 1,000 x

Inclusions

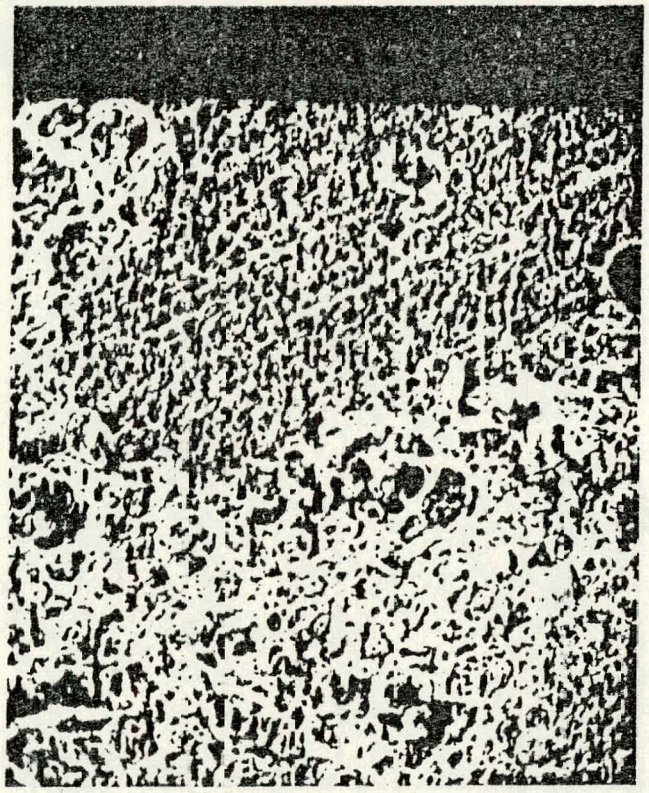

SA3H 2C 100 x

Typical area with spalled matrix

SA3H 2D 1,000 x

Detail in spalled region

SA3H 2E 1,000 x
Matrix detail

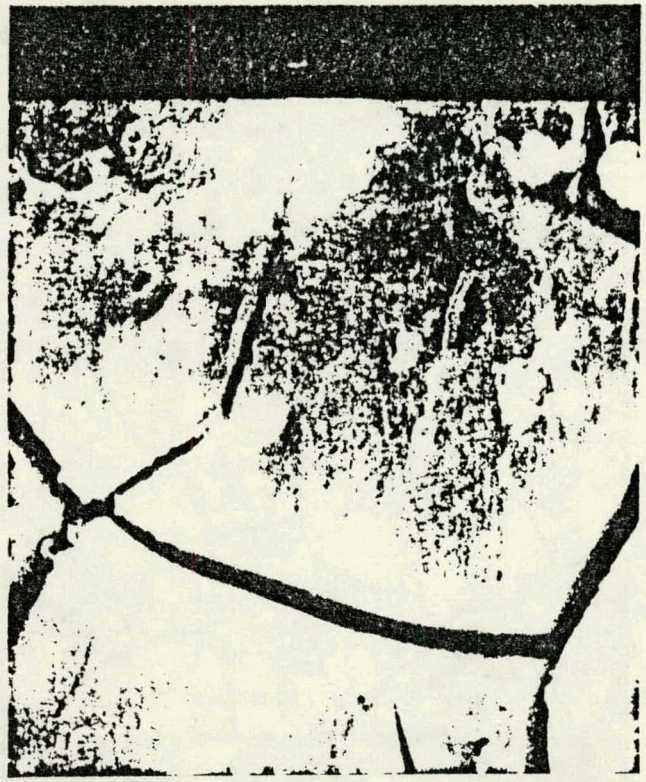

SA3H 2F 3,000 x
Matrix detail

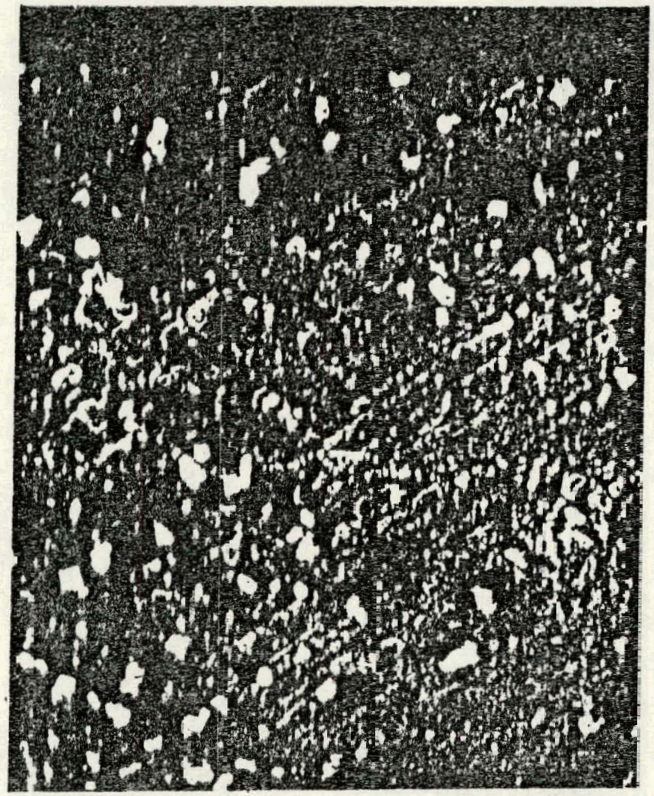

NA6G 3A 100 x

Typical matrix area

NA6G 3B 1,000 x

Detail of matrix

NA6G 3C 1,000 x
Crystals

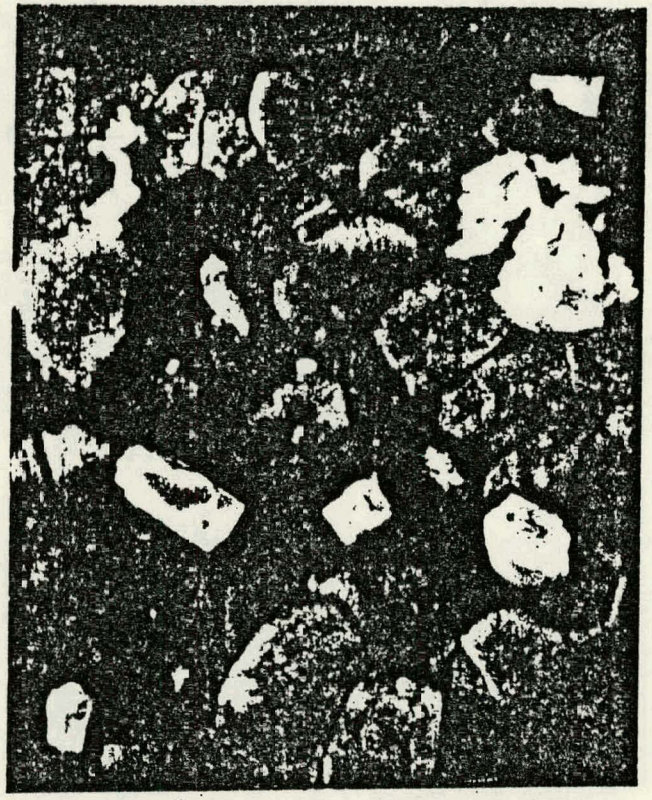

NA6G 3D 600 x
Details of debris, crystals and non crystals

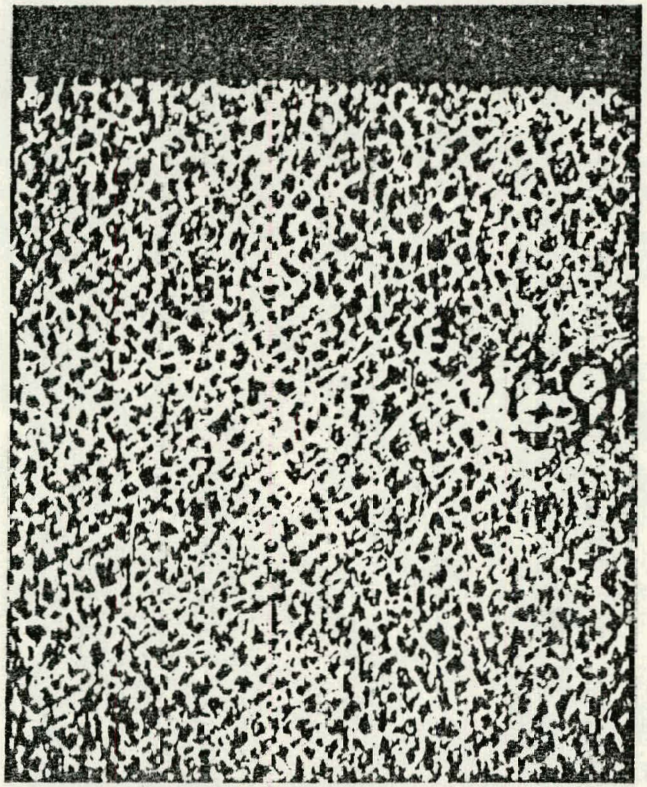

SA6H 4A 100 x

Typical matrix area

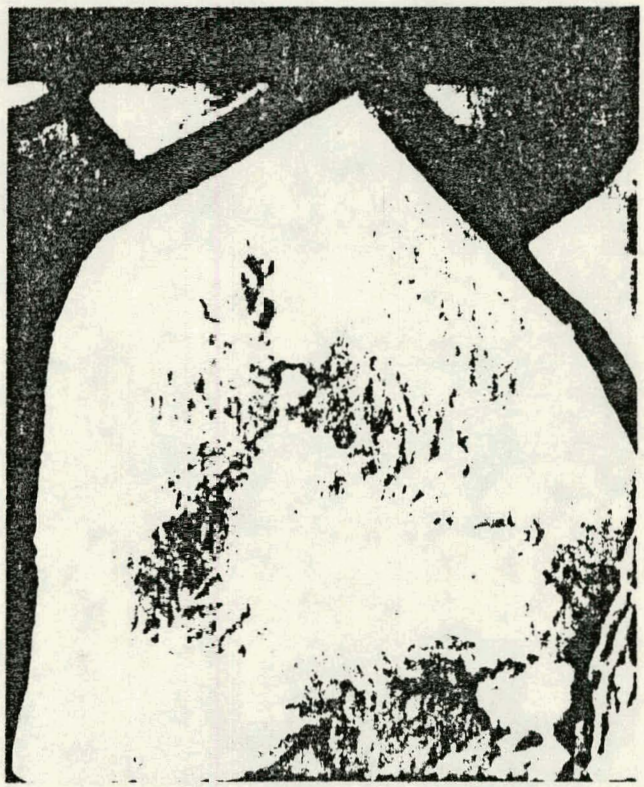

SA6H 4B 3,000 x

Typical matrix area

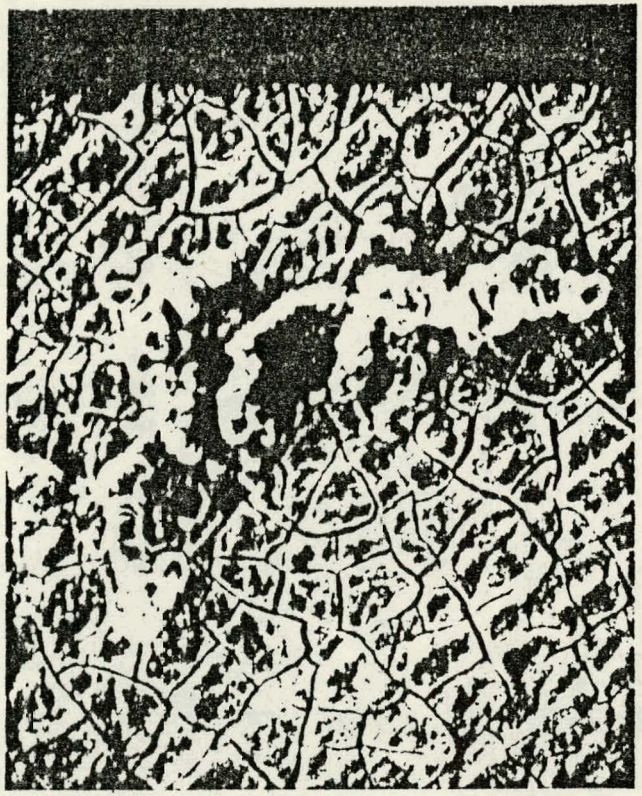

SA6H 4C 300 x

Inclusion (dendritic crystal growth)

SA6H 4D 1,000 x

Inclusion (dendritic crystal growth detail)

BA3D 5A 100 x

Typical matrix structure plus attached material

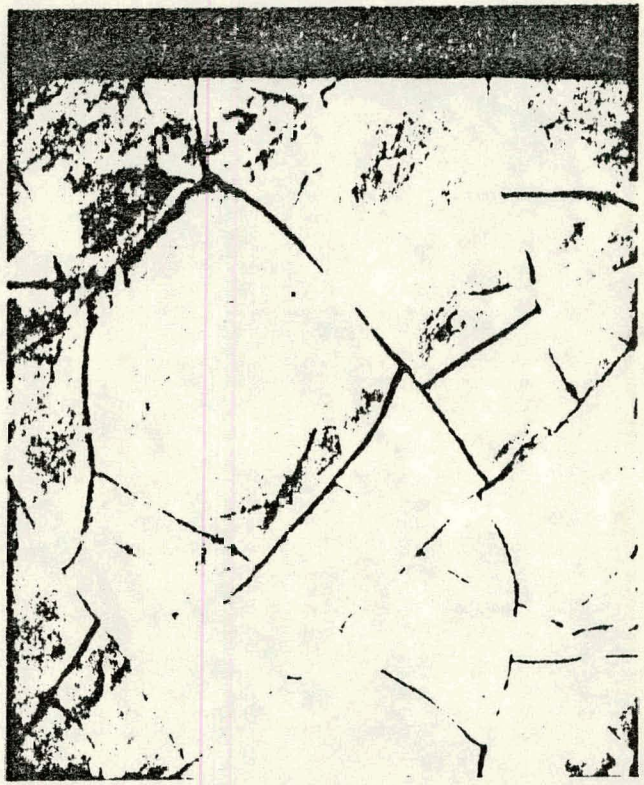

BA3D 5B 1,000 x

Typical matrix structure

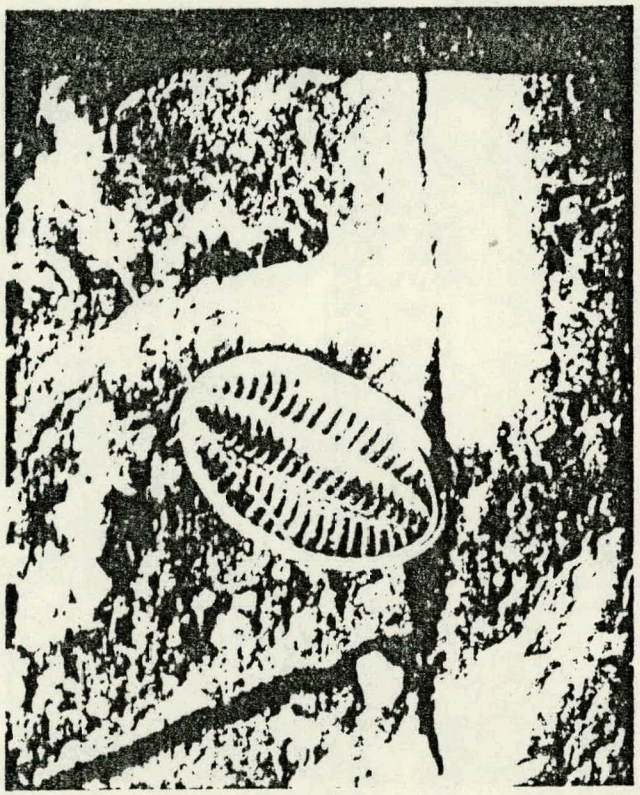

BA3D 5C 3,000 x
Diatom

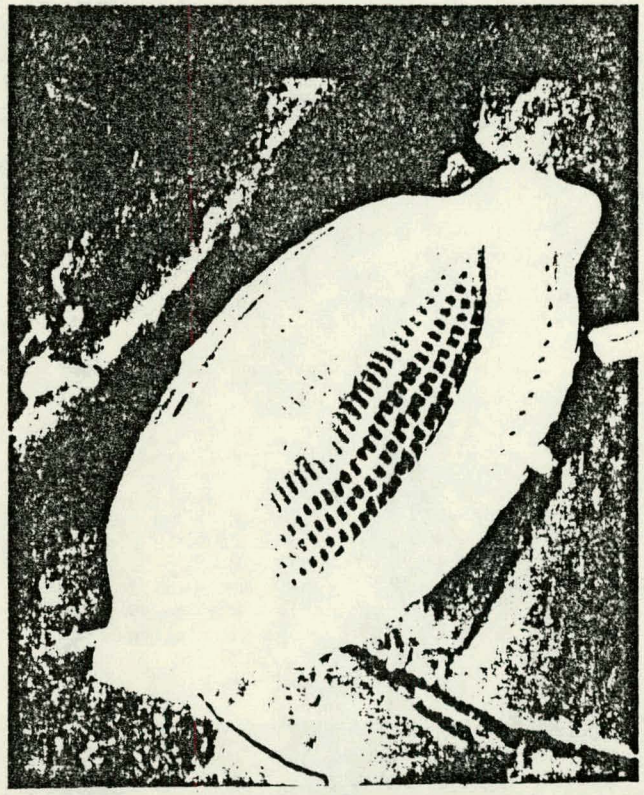

BA3D 5D 3,000 x
Diatom

BA3D 5E 100 x

Bio-mass attachment

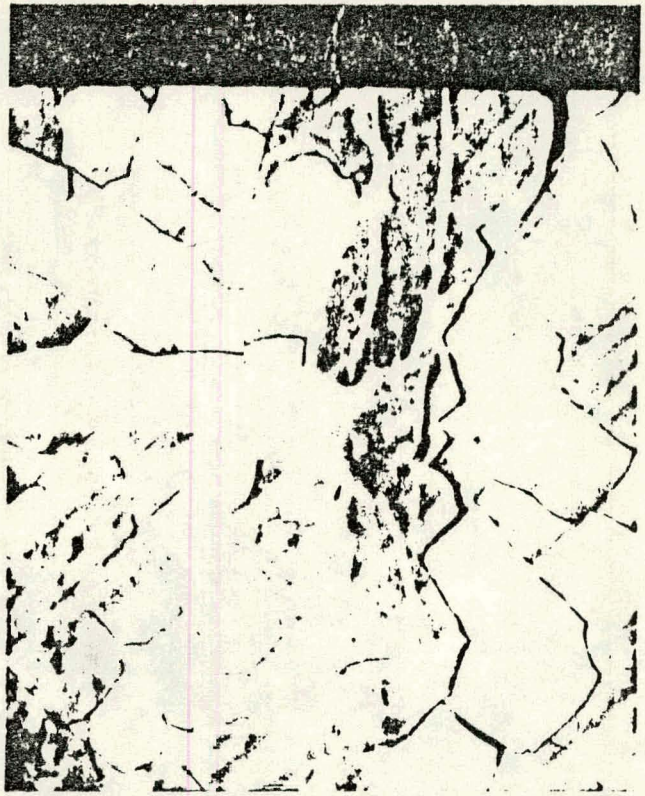

BA3D 5F 300 x

Bio-mass attachment detail

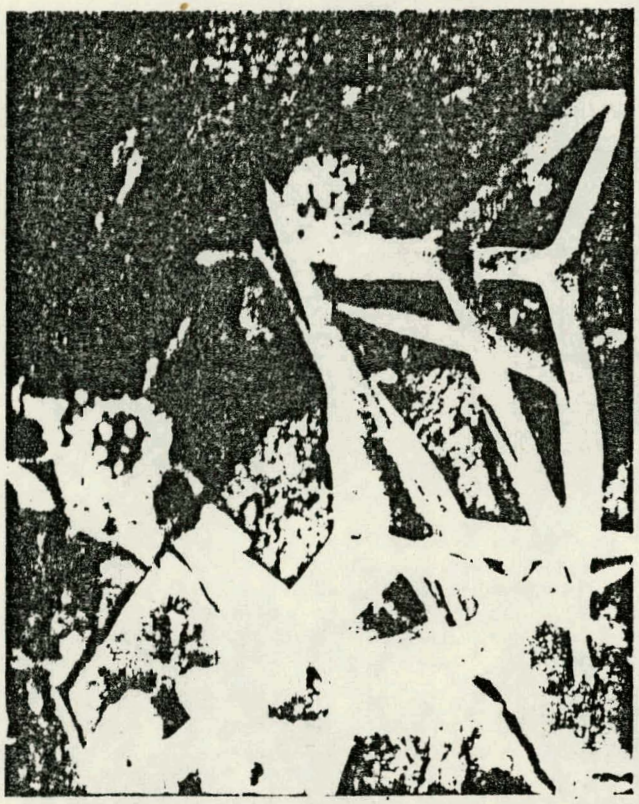

BA3D 5G 3,000 x

Ca oxide skeletons (*)

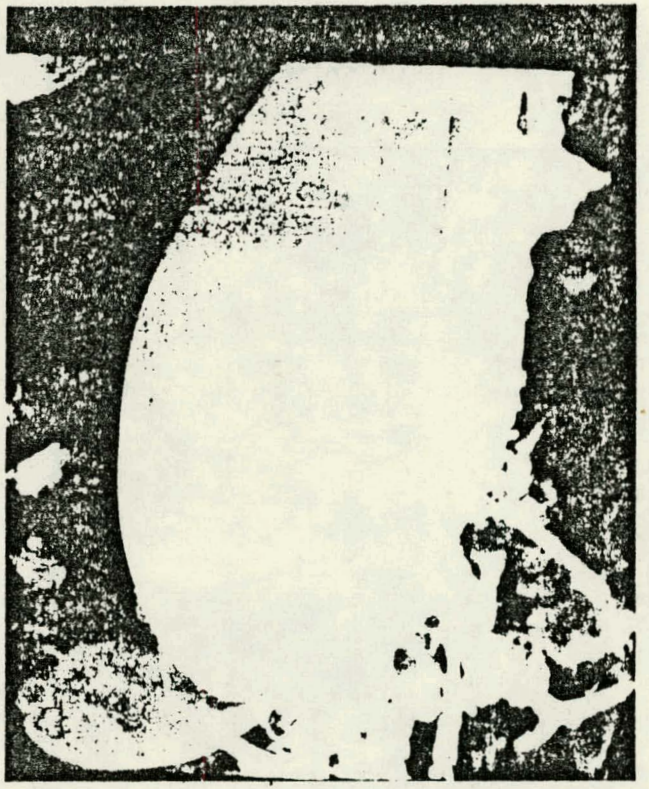

BA3D 5H 600 x

Bi-valve mollusk shell

(*) Ca seems associated with biological material, probably in the form of internal skeletal structure of which the triangles, etc. are the exposed skeletons. Diatoms seem to be composed of SiO_2 only. Biological material appears to be strongly attached to matrix.

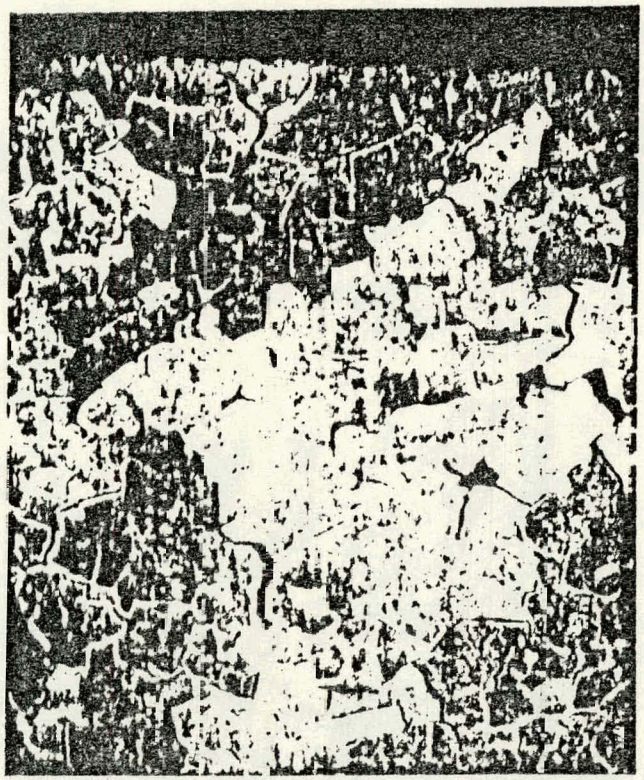

BA6D 6A 100 x

Typical matrix area

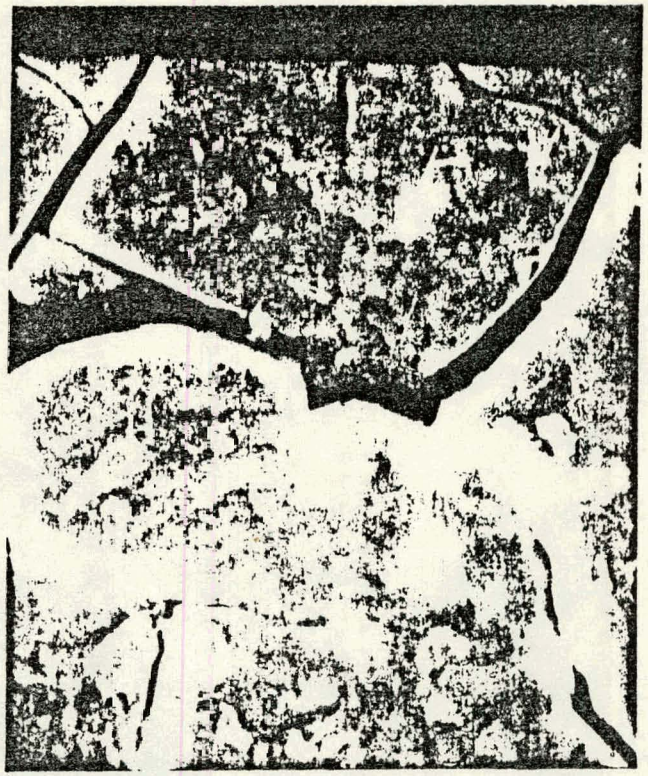

BA6D 6B 1,000 x

Matrix detail

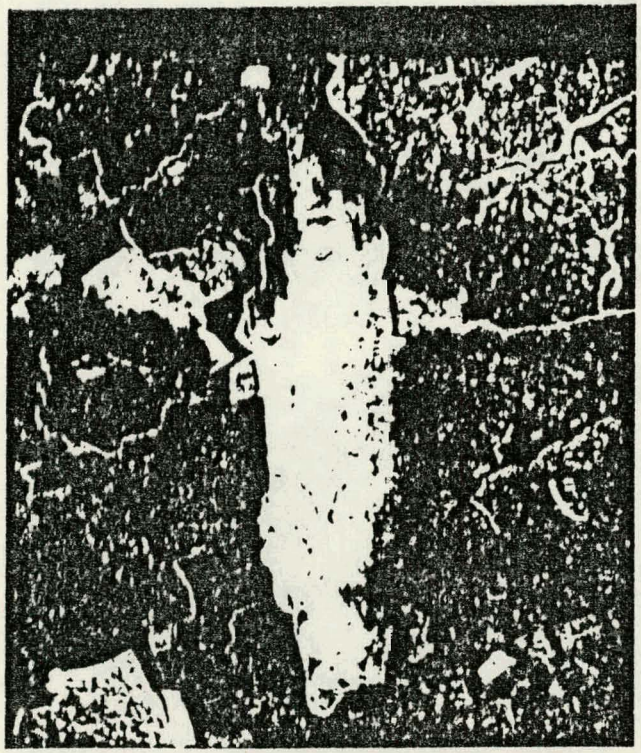

BA6D 6C 100 x

Reverse side of detached matrix flake

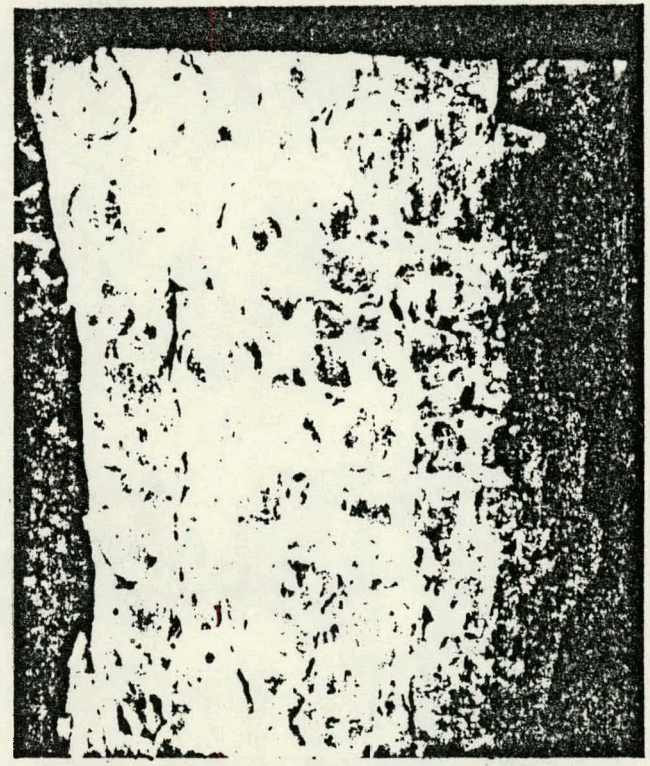

BA6D 6D 300 x

Detail of 6C

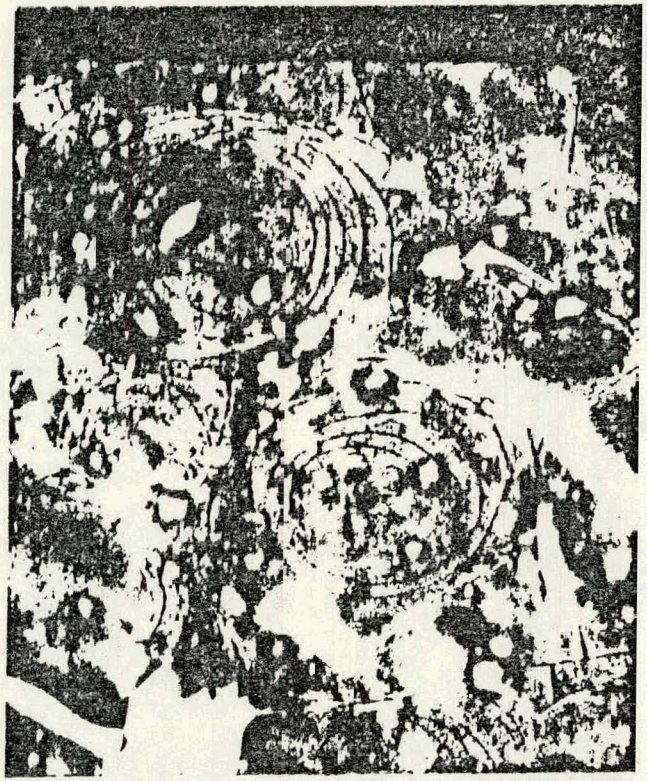

BA6D 6E 1,000 x

Substrate revealed by flake removal

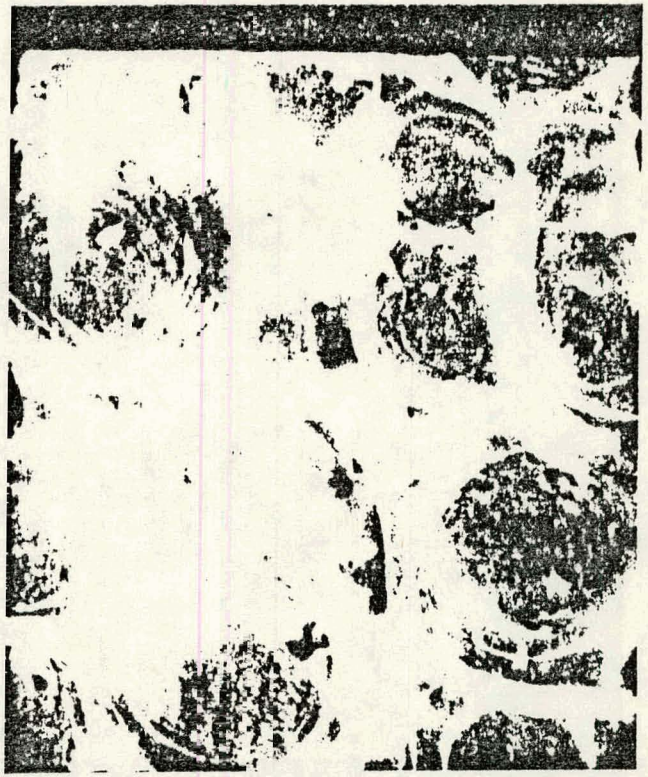

BA6D 6F 1,000 x

Detail of 6C detached flake

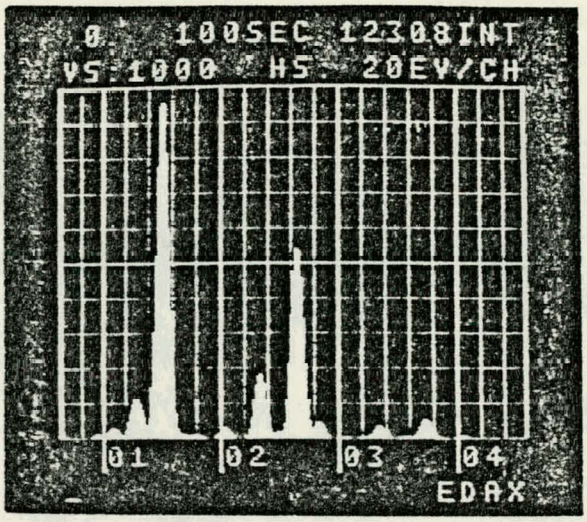

NA3E 1-AM

Amorphous background material

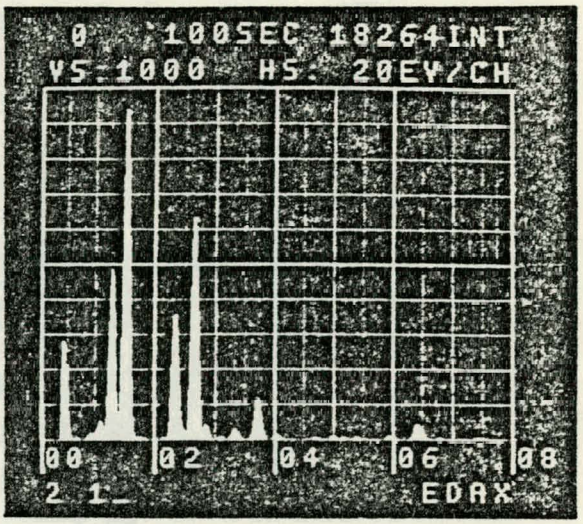

SA3H 2-M

Matrix

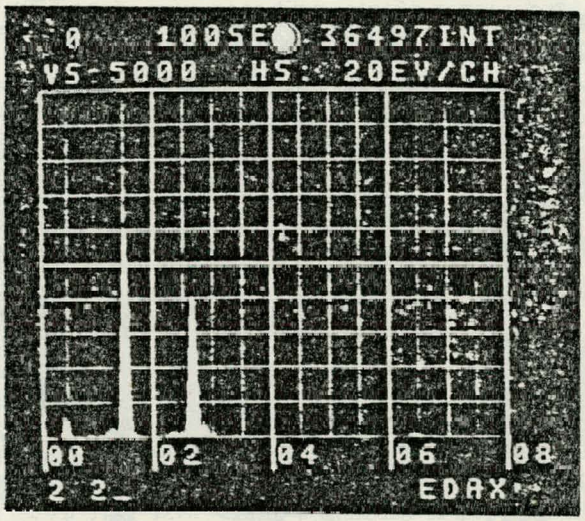

SA3H 2-I

Inclusion

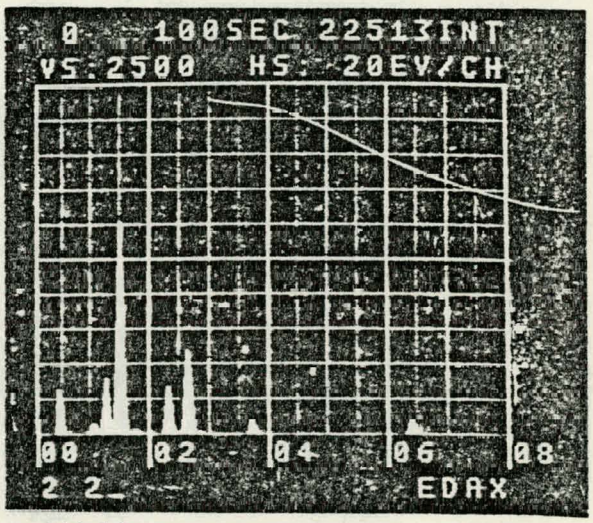

NA6G 3-M

Matrix

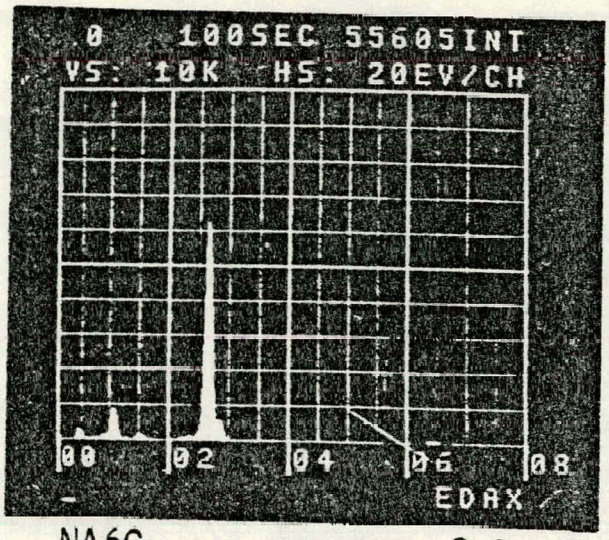

NA6G 3-C

Crystal

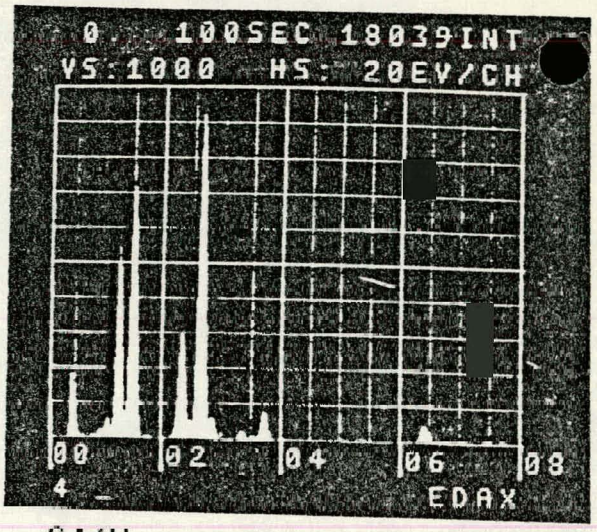

SA6H 4-E

Matrix

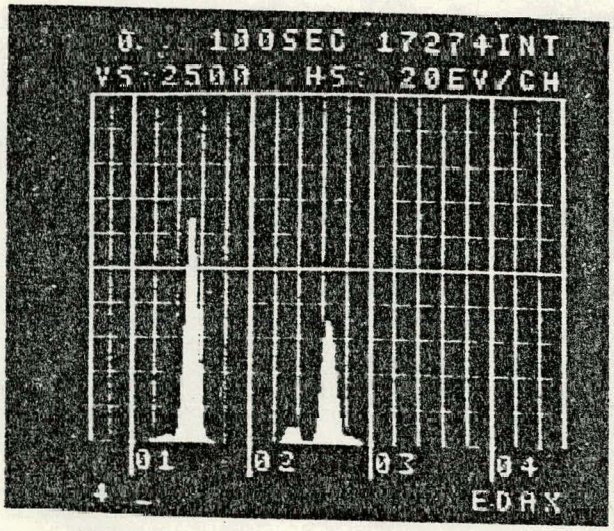

SA6H 4-A incl.

Inclusion

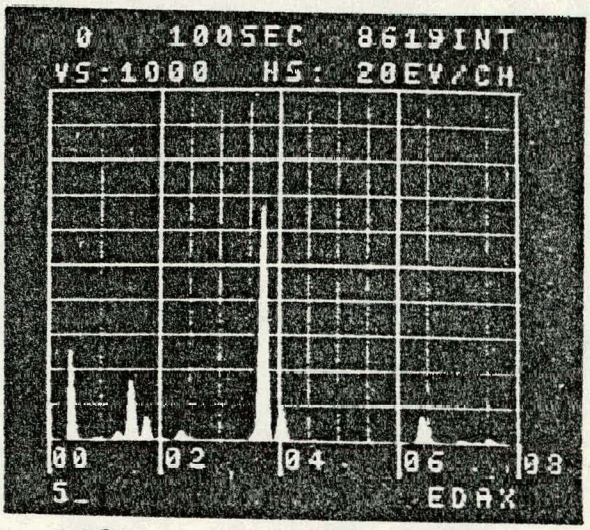

BA3D 5-

Bio-mass

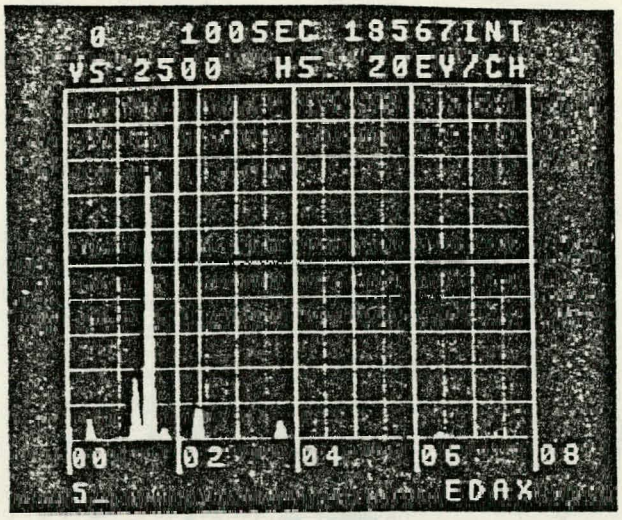

BA3D 5-Matrix

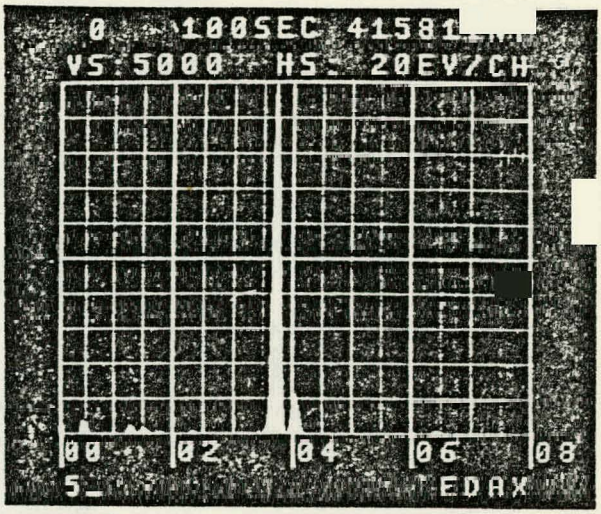

BA3D 5-Calo Inclusion

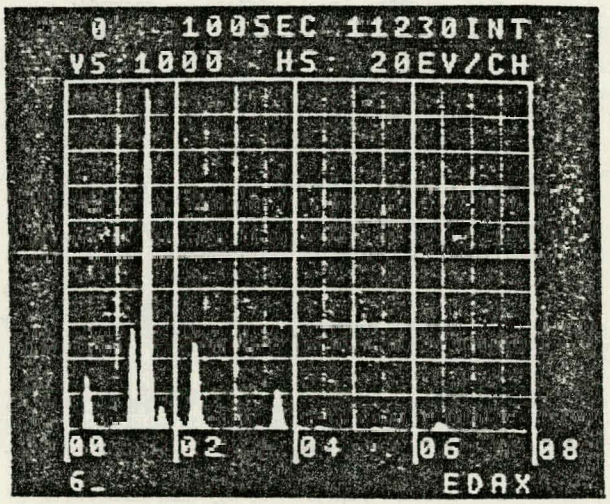

BA6D 6-M Matrix

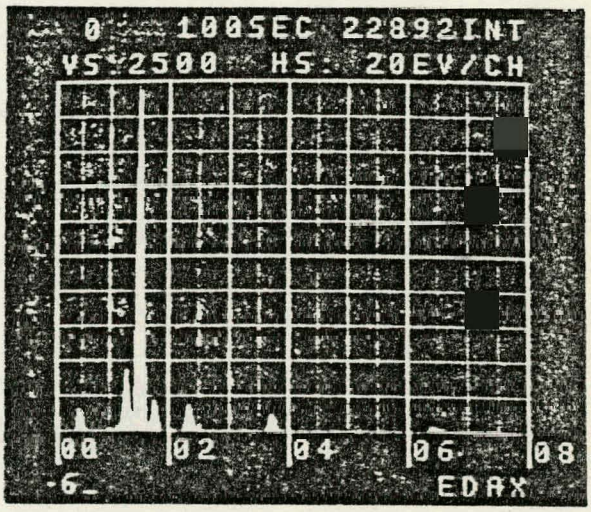

BA6D 6-Chip R Reverse side of chip

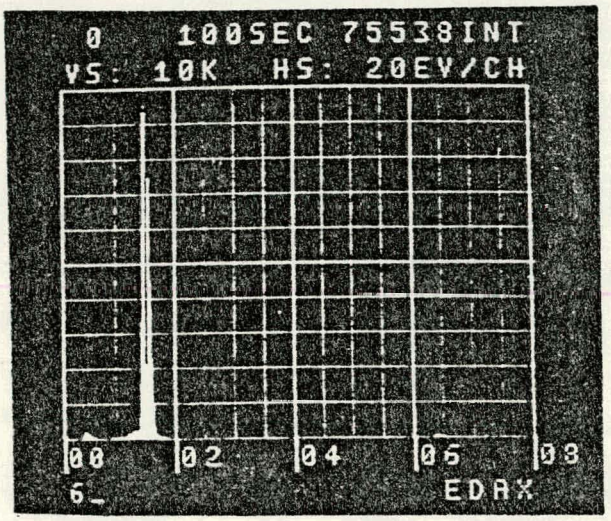

BA6D 6-Substrate
After chip removal

APPENDIX B.1

HISTORY OF HEAT EXCHANGER PIPE SAMPLES

NOI'I Samples:

Two Al 6061-T6 pipes (nominal 1 in. id) were run on board the ship NOI'I during July-September 1976 at Keahole Point, Hawaii. One unit was operated at a flow velocity of ~3 ft/sec and the other at ~6 ft/sec. Water was taken from depths of 20 ft using flexible PVC pipe as feed line.

The two heat exchanger pipes were prepared prior to the experiment in the following way. The inside of the pipe that was operated at 6 ft/sec, was cleaned by a clean rag wet in acetone. The pipe that was operated at 3 ft/sec, was cleaned by cleanser (household Ajax) and bottle brush (nylon bristle - 1 in size). The brush was passed 100 times through the pipe.

During the experimental period, flow stoppage occurred only during flow meter zero measurements and oil change for the ship's generator.

The 3 ft/sec unit had an iron foot value in its flow path which caused a rusty coloration on the pipe's inner surface.

At the end of the experimental period, the heat exchanger pipes were drained off seawater and let dry in air.

We have a supply of three ~1 in. long sections (taken from various locations along the 8-1/2 ft. length) from each unit.

Buoy Samples:

Two Al 6061-T6 and one Ti heat exchanger pipes were operated at Keahole Point, Hawaii. The units were submerged at a depth of 50 ft and operated during the period February-July 1977.

Both Al pipes and the Ti pipe were prepared by the cleanser brush method prior to the experiment.

Al 6061-T6: One unit was run at a flow velocity of ∿3 ft/sec and the other at ∿6 ft/sec.

Short duration flow stoppage occurred during flow meter zero measurements.

Pumps failed during May 6-11 and the pipes were in stagnant water during this time. Pumps were restarted on May 11.

On June 6, the thermal resistance layer (due to biofouling, corrosion and scaling) was cleaned fully for the 6 ft/sec unit and partially for the 3 ft/sec unit by M.A. N. brush (nylon bristle brush traversing up and down the pipe).

Both pipes continued to operate till July 11, 1977. From July 11 till July 16 the pipes remained in stagnant water. On July 16 the pipes were removed, drained off their seawater and let dry.

Between July 17 and August 1, 1977, the pipes were exposed to fresh water for flow meter calibration. This fresh water bathing was intermittent in nature.

Again the pipes were drained off fresh water and let dry in air.

Ti: The unit was operated from February till April 27. It remained in stagnant water from April 27 till June 6.

On June 6, it was pulled out, drained off seawater and let dry. Between July 17 and August 1, it was exposed to fresh water as were the Al pipes.

For each of the above three heat exchanger pipes, a sample length was cut while the pipes were still submerged in the sea; these samples were stored in Glutaraldehyde solution for biological work and are with Dr. Harvey of Hawaii.

St. Croix Samples:

Two Al 6061-T6 heat exchanger pipes were run in the Caribbean Sea in the period of July-September 1977. They were mounted on board a barge in the open ocean. Seawater was taken from a depth of 60 ft with flexible PVC pipe as feedline. One unit was operated at ~3 ft/sec and the other at 6 ft/sec.

Both Al pipes were prepared prior to the experiment by the following procedure. Interior of the pipes were treated with 10% (by weight) NaOH solution at ambient temperature. The reaction being exothermic the pipe becomes hot and reaches a temperature of ~150°F during this procedure. Subsequently, the pipes were rinsed with fresh water; then swabbed (~40 times) by a clean rag (wet in dishwashing liquid solution) to remove any residue.

At the end of the experimental period, the pipes were drained off the seawater and let dry in air.

We have five 1 in pieces from each experimental pipe taken from various locations along the 8-1/2 ft length.

APPENDIX B.2

MCL
X-Ray Diffraction—Scanning & Transmission Electron Microscopy

December 30, 1977
JOB NO 7712055

SUBJECT: Scanning electron microscopy (SEM), Electron-excited, energy-dispersive x-ray analysis (E/EDAX), X-ray diffraction (XRD) and Secondary Ion Mass Spectroscopy (SIMS) analyses of the deposits forming on the interior surfaces of several aluminum tubes and one titanium tube through which salt water had been pumped, for the purpose of chemically and structurally characterizing the deposits.

EXPERIMENTAL PROCEDURES AND RESULTS

Sample Preparation - The deposits from the interiors of the tubing were removed by carefully scraping with a toothpick under a low power stereo light microscope. The SIMS sample was sectioned from tubing #BA6D and was examined in the as-received condition.

SEM and E/EDAX - The deposit samples were mounted on high purity graphite wafers with Duco cement, coated with approximately 200Å of carbon and examined in the SEM using a 20 KV accelerating voltage and a tilt angle of approximately 45°. (The carbon coating provides an "invisible" electrically conducting surface which is necessary for efficient SEM examination, and does not interfere with the SEM or E/EDAX results. The samples were examined using both secondary and back-scattered electron emission.

All elements with atomic numbers greater than eight (oxygen) are detected simultaneously with E/EDAX; elements with lower atomic numbers are not detected. This enables the detection of elements not necessarily expected concurrently with the elements of principal interest.

The E/EDAX results are summarized in the enclosed table.

XRD (Debye Scherrer) - The deposit samples were mounted on glass fibers with Canadian Balsam and exposed to nickel-filtered, copper K-alpha radiation in 114.6 mm diameter Debye Scherrer cameras for 8 hours. The resulting patterns were very diffused indicating that the samples were not well crystallized. The Bragg reflections were compatible with the following structures:

BA6D (white isolated material)

major - $Al(OH)_3$ #7-324

minor - $Al\text{-}SO_4\text{-}H_2O$ #11-475

BA6D (yellowish continuous film)

major - $Al(OH)_3$ #7-324
$CaCO_3$ #5-586

minor - $Al\text{-}SO_4\text{-}H_2O$ #11-475
SiO_2 #5-490
$CaMgCO_3$ #11-78

BA3D

major - $CaCO_3$ #5-586

minor - $CaMgCO_3$ #11-78
SiO_2 #5-490

SA3H

major - Al #4-787 (from substrate)

minor - NaCl #5-628

BT6D

no crystalline pattern

The levels of the crystalline fraction shown above were estimated from the intensities of the principal Bragg reflections. It should be emphasized that because of the low degree of crystallinity of the material the $CaCO_3$, $CaMgCO_3$ and SiO_2 phases are considered conclusive identifications, the others are probable but not conclusive.

SIMS - The SIMS surface analysis was conducted on areas A and B of micrograph #5468 with a 3M Secondary Ion Mass Spectrometer equipped with an ion imaging package, charge neutralization system and a raster-gating system to reduce background levels. The SIMS quadrapole mass analyzer is mounted on a Cambridge Mark IIA Stereoscan scanning electron microscope which enables a detailed three-dimensional examination of the sample and the surface area selected for analysis.

Positive and negative SIMS spectra were generated from the surfaces by bombarding them with an inert beam, approximately 0.5 mm in diameter, of 2.5 KV argon ions for 300 seconds. The removal rate of surface atoms was approximately 20Å/minute (ion current density = 100 micro amps/cm^2). The raster area was 2x2 mm. Scans were taken over 0-100 and 100-200 atomic mass units (amu) for positive ions and 0-50 amu for negative ions. The results may be summarized as follows:

- Organics were detected in both areas A and B. We estimate (from ion yield values) the organic content of area A to be about 5% and area B to be about 10% of the total deposit present.

- Area A contains principally calcium and oxygen with intermediate levels of sodium, fluorine, magnesium, sulfur, chlorine and aluminum while area B contains principally sodium and oxygen with intermediate levels of fluorine, sulfur, chlorine, aluminum and potassium.

- Area A also contains minor levels of potassium, iron and carbon, trace levels of silicon and area B contains minor levels of magnesium, iron and carbon and trace levels of silicon.

CONCLUSIONS

Because of the very poor crystallinity of the material the XRD patterns were very difficult to index. However, with the aid of the E/EDAX and SIMS data the XRD results were determined. The following is a synthesized composition representing an average of all of the data taken for the aluminum tubing deposit.

Average deposit - Aluminum tubing

major	$CaCO_3$
	$Al(OH)_3$
minor	$Al\text{-}SO_4\text{-}H_2O$
	$CaMgCO_3$
	organic component
trace	SiO_2
	NaCl

E/EDAX Results of Tubing Deposits

	BA6D (wt matl)	BA6D (yw film)	BA3D	SA3H	BT6D*
Mg	Tr	Tr	Tr	Tr	--
Al	Ma	Ma	Tr	Ma	--
Si	Tr	Tr	Int	--	Ma
S	Mi-Int	Mi	Tr-Mi	Mi	Mi
Cl	Tr	Tr	Tr	Int	Mi
K	Tr	Tr	Tr	Tr	Mi
Ca	Mi	Ma	Ma	Tr+	Int
Ti	--	--	--	--	Tr+
Fe	--	Tr	Tr	Tr	Mi
Cu	--	Tr	--	--	Tr
Zn	--	Tr	Tr	--	Tr

Tr=Trace

Mi=Minor

Int=Intermediate

Ma=Major

*very high organic component

E/EDAX-Exposed metal surface

Area A in #5468

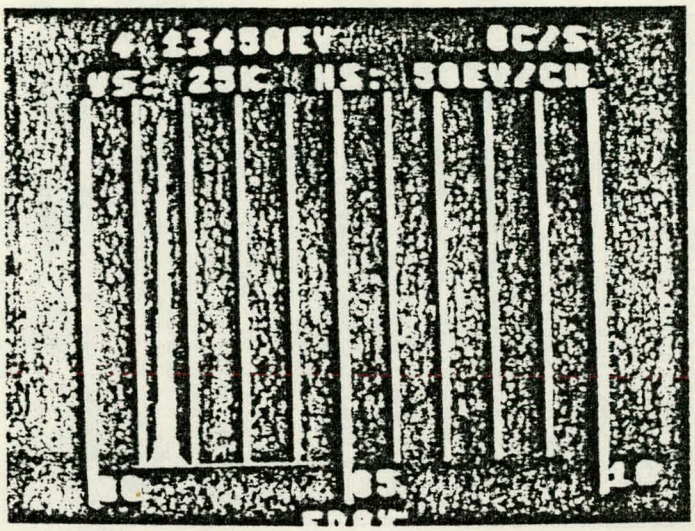

Al

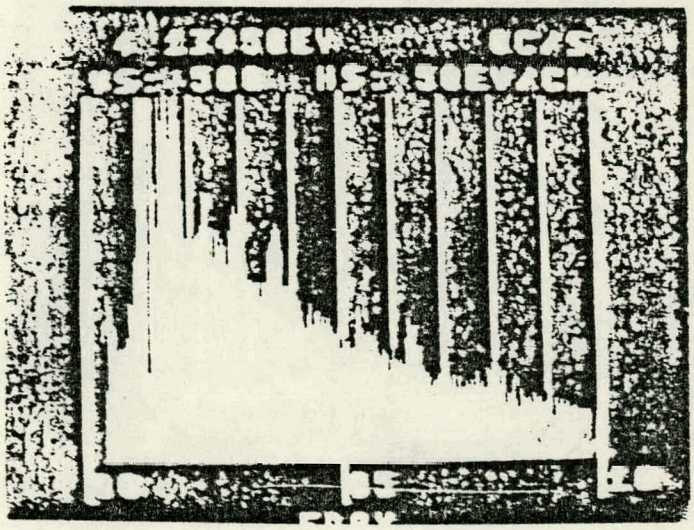

Expanded
Vertical
Scale

Al S Ar* KCa Cr Fe Cu

*Ar - From ion implantation during SIMS analysis.

E/EDAX of corroded surface

Area B in #5468

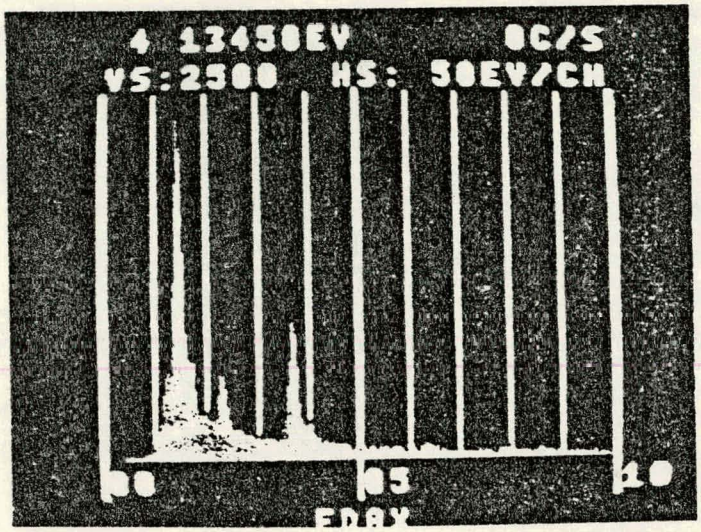

Mg Al Si S Ca Fe

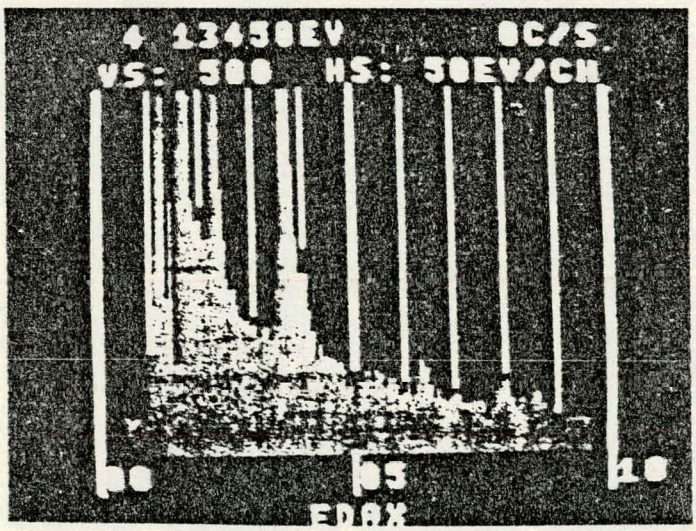

Al Si S Cl Ca Fe Cu Zn

Expanded Vertical Scale

Areas analyzed by SIMS

BA6D Section

#5468

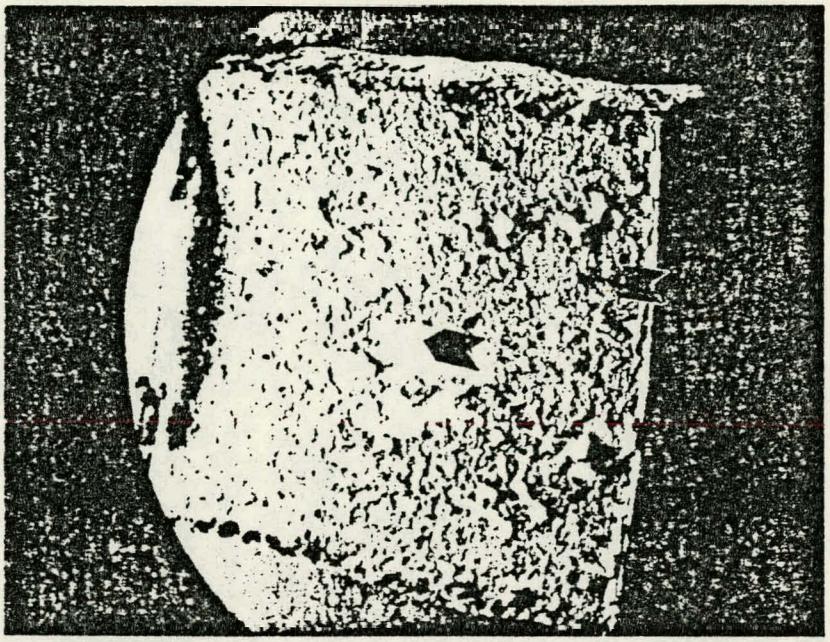

8x

#5469

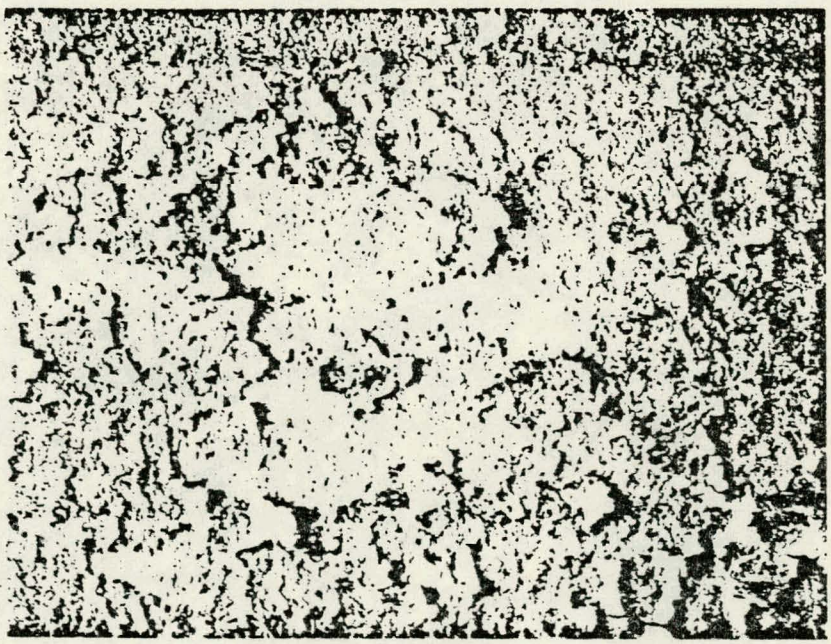

26x

SEM MICROGRAPHS OF SAMPLE BA6D (YELLOW MATERIAL)

#543

100X

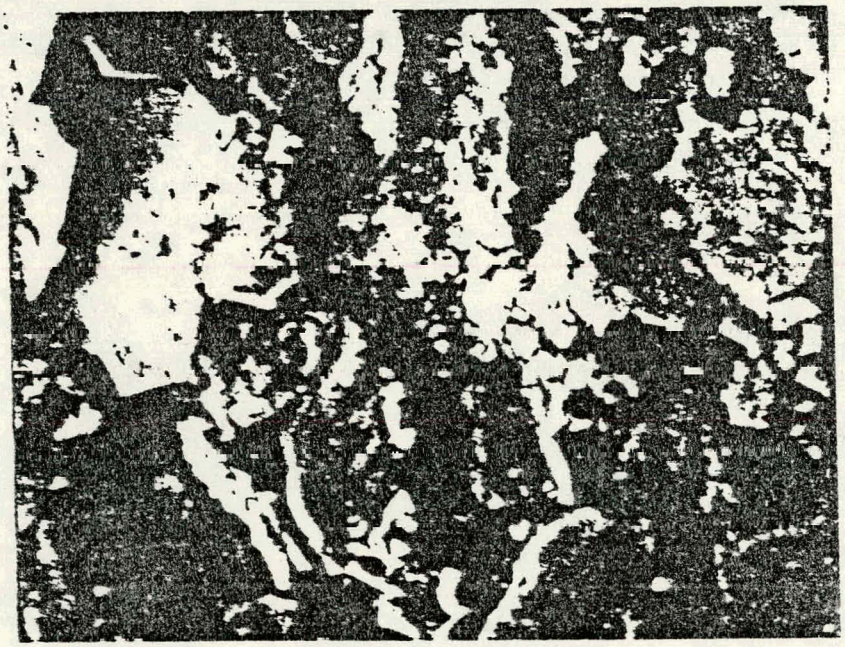

#5440

400X

SEM MICROGRAPHS OS SAMPLE BA6D (WHITE MATERIAL)

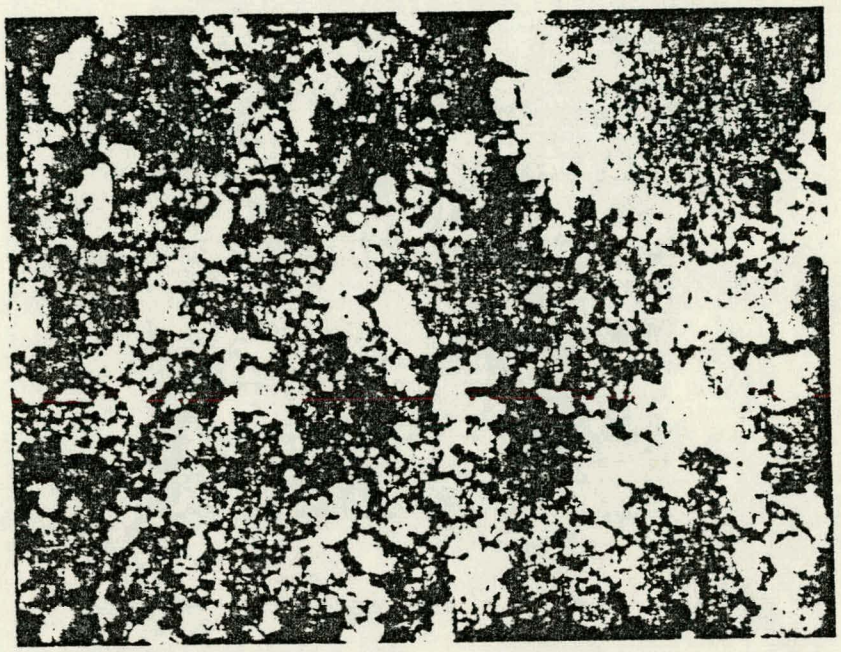

#5437

1200X

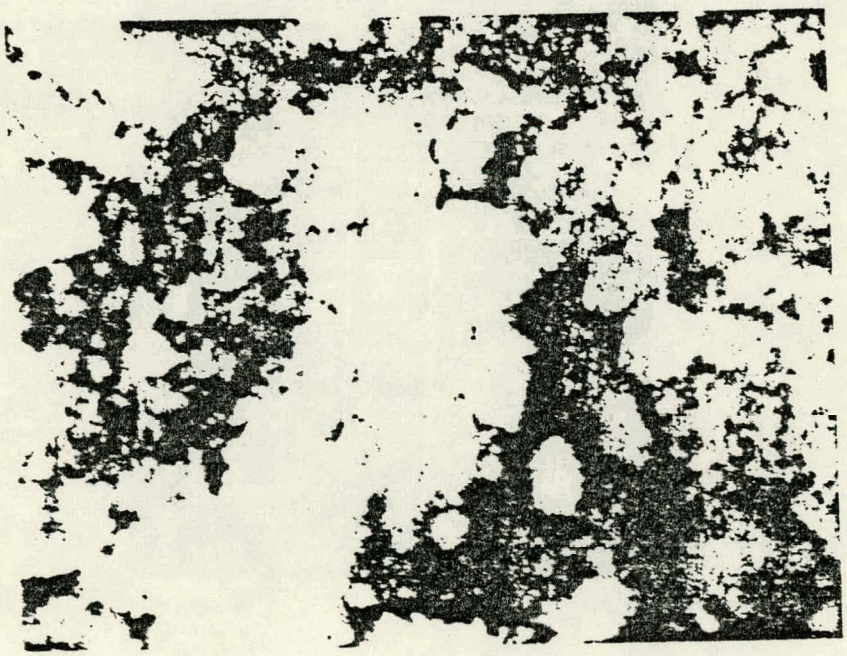

#5438

4000X

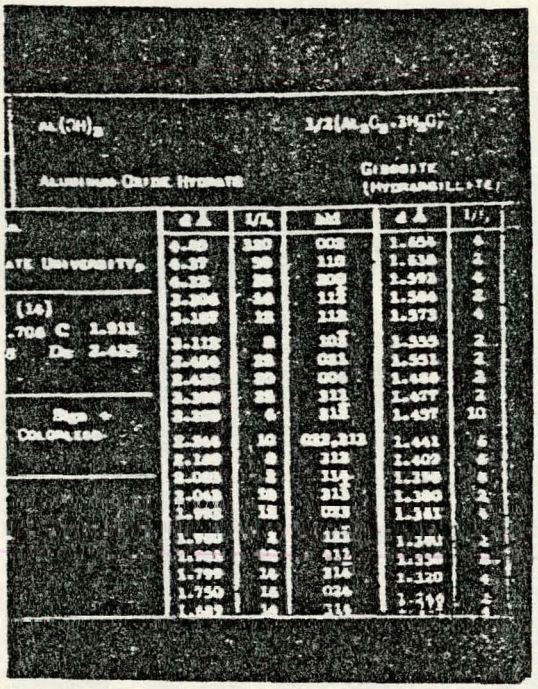

Al(OH)$_3$
#7-324

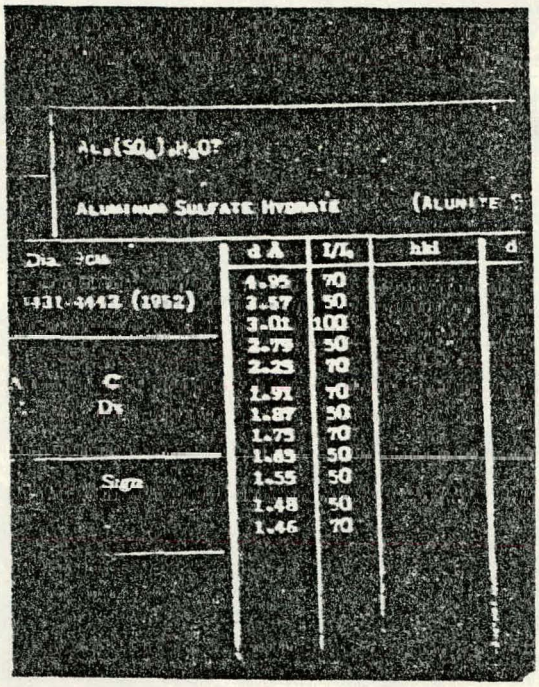

Al$_2$(SO$_4$)$_3$.H$_2$O
#11-445

Crystallographic Data

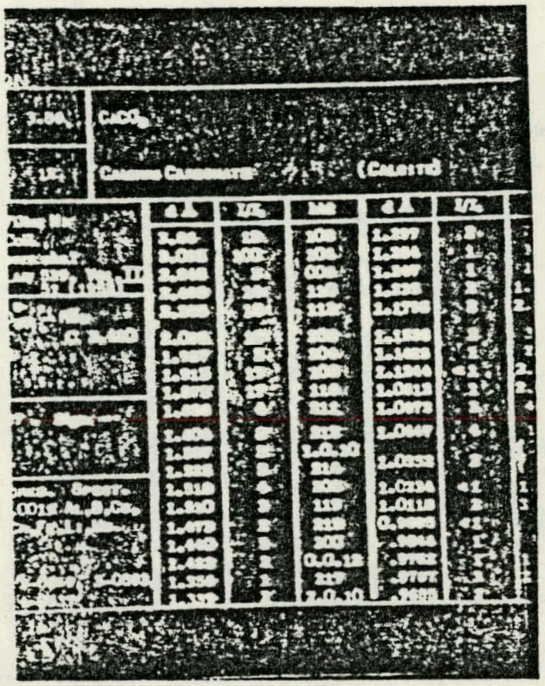

$CaCO_3$
#5-586

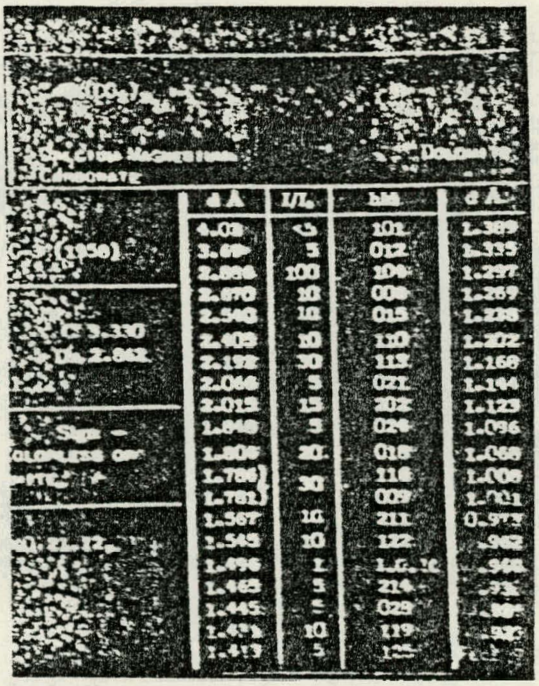

$CaMgCO_3$
#11-78

E/EDAX OF SAMPLE BA6D (WHITE MATERIAL)

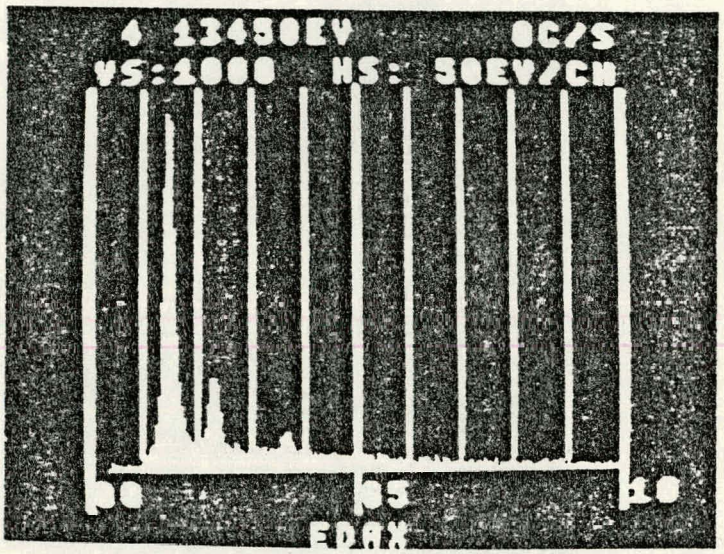

Al S Cl Ca

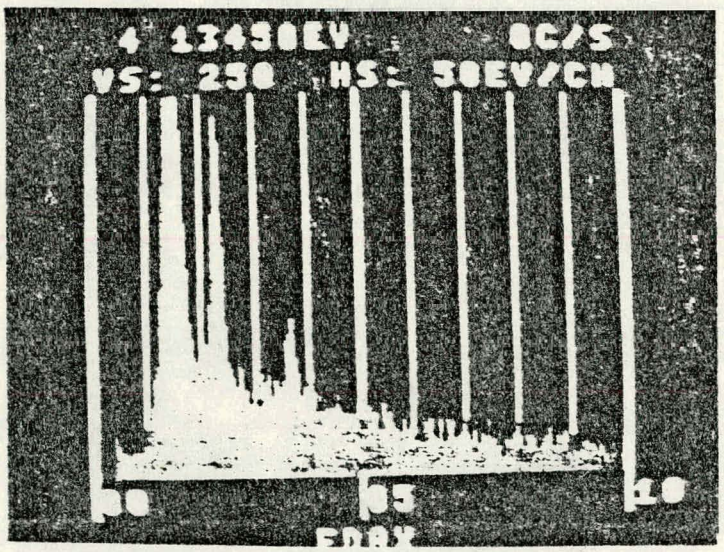

Expanded Vertical Scale

Al S Cl Ca

SEM MICROGRAPHS OF SAMPLE BT6D

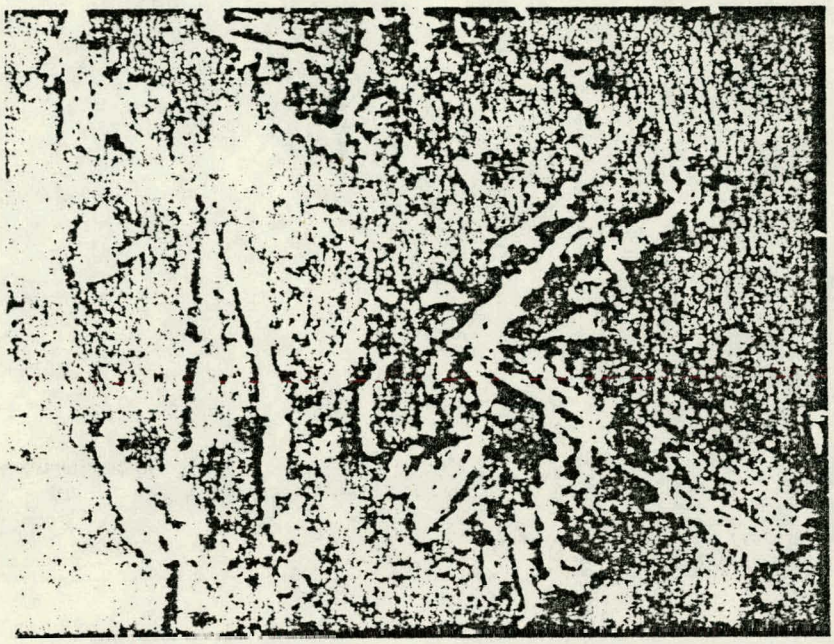

#5445

300X

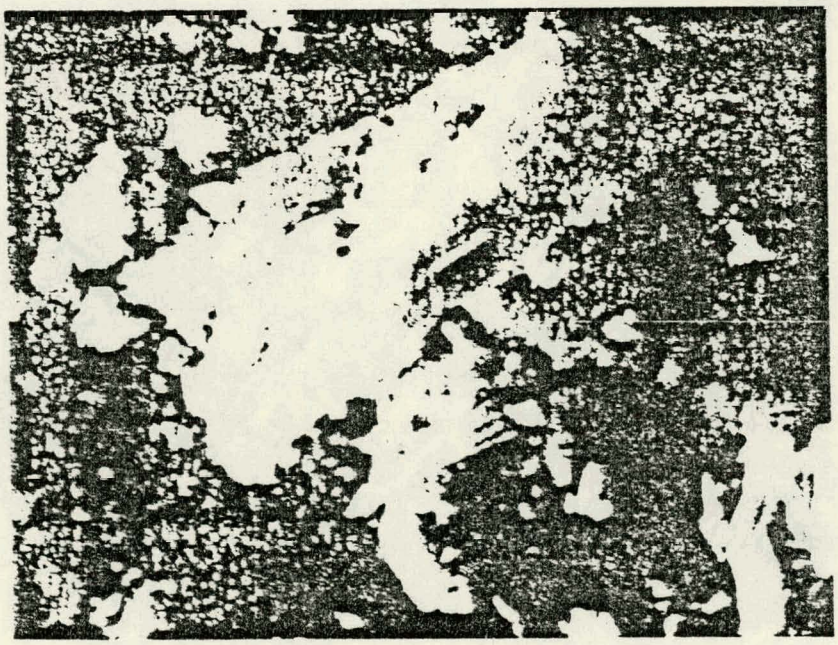

#5446

1300X

SEM MICROGRAPHS OF SAMPLE SA3H

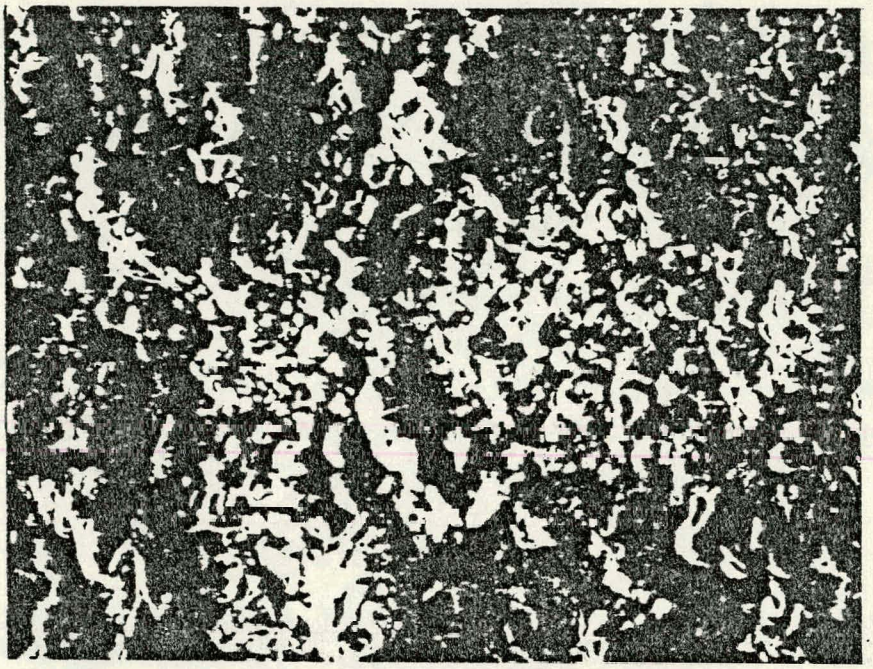

#5443

175X

#5444

700X

SEM MICROGRAPHS OF SAMPLE BA3D

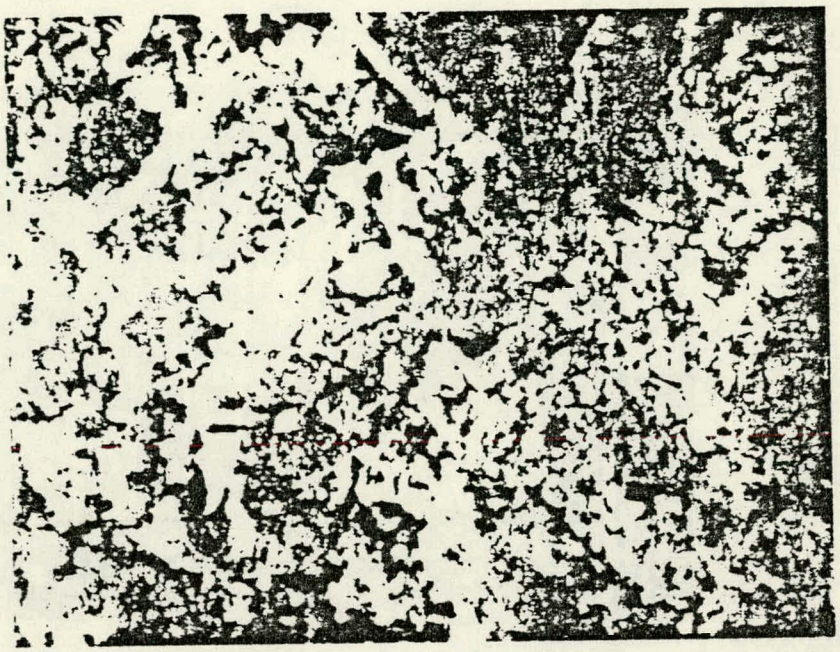

#5441

500X

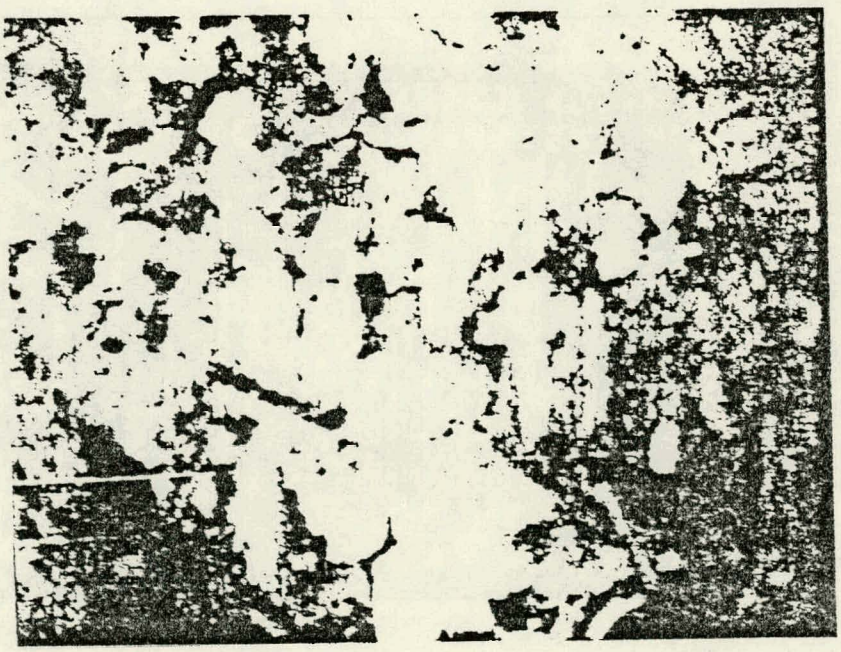

#5442

2000X

E/EDAX OF SAMPLE BT6D

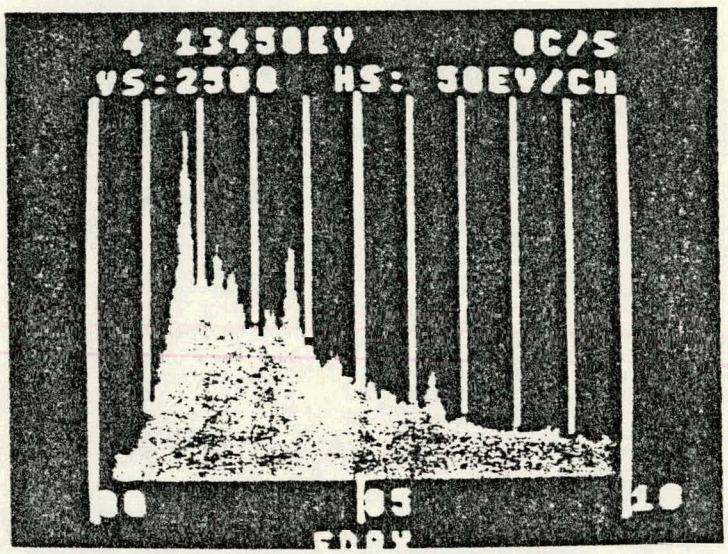

Mg Al Si S Cl K Ca Ti Fe Zn

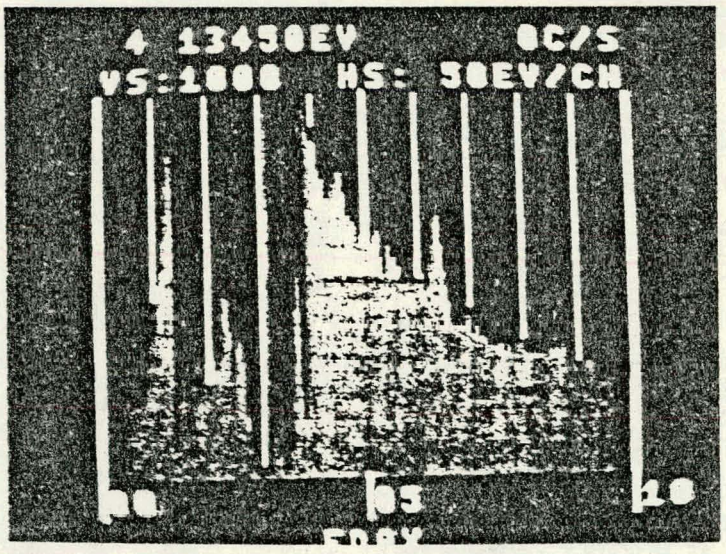

Expanded Vertic
Scale

Fe Cu Zn

E/EDAX OF SAMPLE SA3H

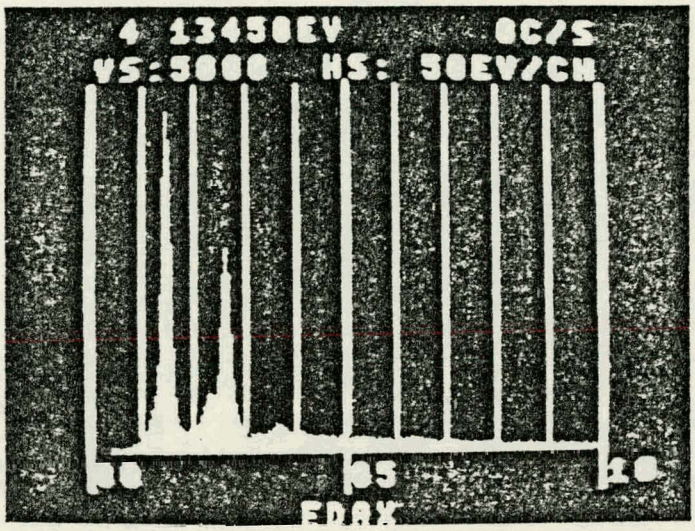

Al S Cl Ca

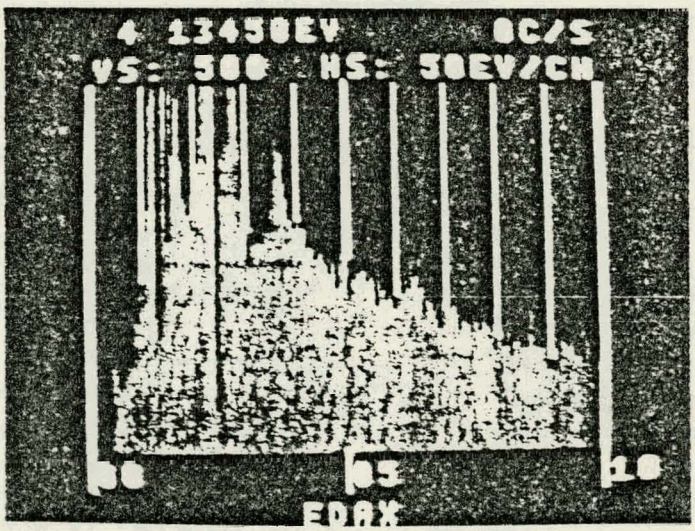

Expanded Vertical Scale

Al S Cl Ca Fe

E/EDAX OF SAMPLE BA3D

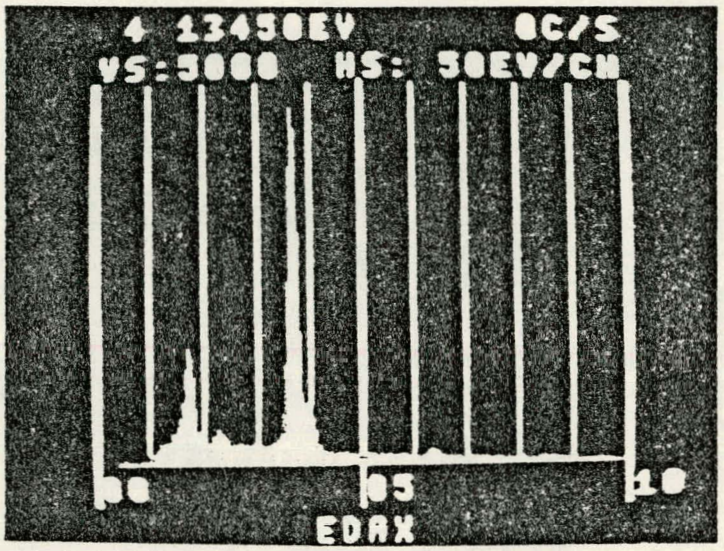

Mg Al Si S Ca Fe

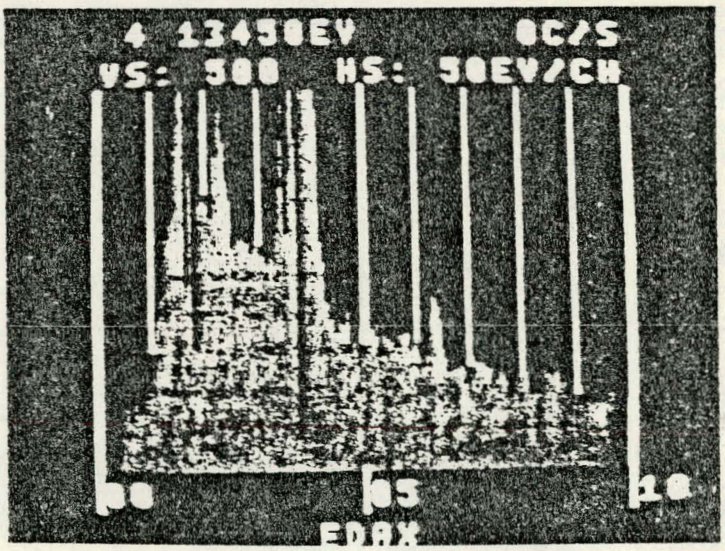

Expanded Vertical Scale

Mg Al Si S Cl Ca Fe Zn

E/EDAX OF SAMPLE BA6D (YELLOW MATERIAL)

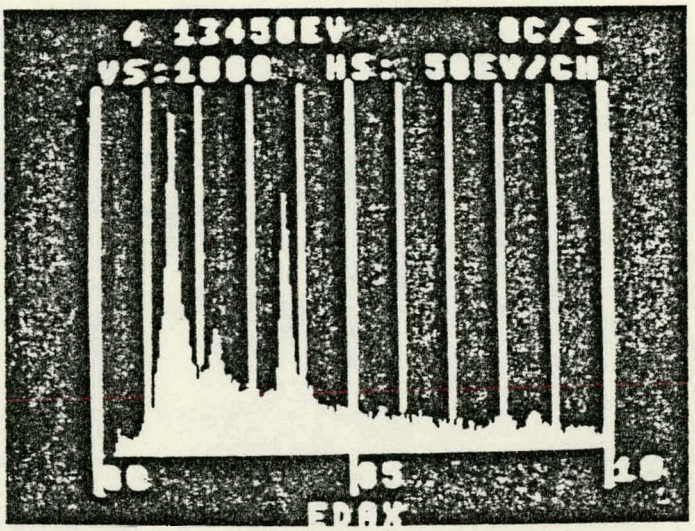

Al S Ca Cu Zn

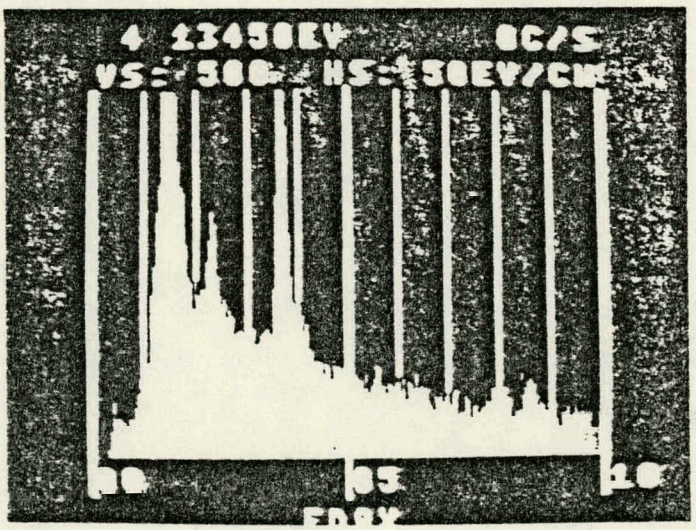

Expanded Vertical Scale

Al S Ca Cu Zn